Final Report
Version 2
September 2012

Evaluation of Diesel Particulate Filter Systems at Stobie Mine

Diesel
Emissions
Evaluation
Program

VALE

Principal Investigator: Jozef Stachulak
Report Prepared by: Bruce R. Conard
Edited by: George Schnakenberg

Contributions from:
Greg Nault
George Schnakenberg
Alexandar Bugarski
Gilles Bedard
Andreas Mayer
Rick Mayotte
Robert Coupal
Mahe Gangal

Preface

Vale Canada's (Vale's) Stobie project to test diesel particulate filter systems on operating equipment underground was truly a team effort. Many people with a variety of skills, knowledge, and expertise contributed to the success of the project by giving their interest, enthusiasm, energy and skills to this important effort. Most of these people are listed below.

Dr. Bruce Conard prepared this report by working collaboratively over several months with the principal investigator (PI), the project team, and primary consultants. He was tasked with the organization and presentation of their efforts, the selection of tables and figures, and the writing of the text which were reviewed by the team. Dr. George Schnakenberg, working collaboratively with the author and the PI, reviewed and edited the completed draft report to its final version.

The project was led by Dr. Jozef Stachulak, the principal investigator, who provided guidance and insight throughout the process and provided the final review of these efforts.

When the project started, Stobie mine was operated by Inco Limited. Inco was purchased by CVRD (Vale) in 2006. Thus, in this report, the name "Vale" also refers to the former Inco company.

The stakeholders of DEEP
The DEEP Management Board
The DEEP Technical Committee
The Ontario Workers Safety and Insurance Board
The United Steelworkers of America

Technical Assistance

Dr. George Schnakenberg	Dr. Aleksandar Bugarski	Dr. Mahe Gangal	Brent Rubeli	Dr. Andreas Mayer
Paul Nöthiger	David Young	Vince Feres	Don Dainty	Michel Grenier
Mike Kingston	Bill Howell	Dr. Addy Majewski	Charles Graham	

Vale Ontario Division administration

Ron Aelick	Alistair Ross	Scott MacDonald	Alex Henderson
Mark Cutifani	Michael Winship	Brian Maynard	
Mike Sylvestre	John O'Shaughnessy	Steve Wood	

Stobie Mine Operations

Keith Boyle	Larry Lauzon	Joe Loring	Mike MacFarlane
Bob Steinke			

Stobie central team and support

Lindy Agnello	Gilles Bedard	Tim Beres	Bob Coupal	Dan Dubuc
Mike Dupuis	Dave Fram	John Huggins	Denis Lafebvre	Mike Leclair
Ernie Leduc	Rick Mayotte	Don McGraw	Greg Nault	Simon Nickson
Rick Nelson	Doug O'Connor	Don Peloquin	Gilles Pilon	Ron Pilon
Jim Rouselle	Jim Sharpe	Dan Stefanczyk	Terry Turcotte	Ken Zayette

Trainers

Tracy Cardinal	Mike Doniec	Fred Goulet	Denis Lefrancois	Gary McGee	Tony McGuire
Lynn Mitchell	Mike Palkovits	John Whitehead			

Operators

L. Albrechtas	R. Anand	A. Anger	D. Archambault	R. Audet	A. Barrette
J Beaudin	W. Beckerleg	G. Bergeron	R. Bernard	P.Boucher	K. Brouse
R. Brunette	K. Castonguay	J. Chenier	P. Christine	J. Conrad	D.Corriveau
J. Daoust	D. Decker	M. Demore	D. Drake	K.Eadie	B. Falkner
F. Fournier	P. Fournier	G. Foy	R. Gagnon	R. Gauvin	G.Gillis

M. Gionet	E. Girard	R. Godin	D.Hansen	E. Hearty	K.Hill
T. Jaculak	J. Larocque	P. Lasalle	M. Lavallee	R. Leblanc	G. Macmillan
L. MacNamatra	R. Mathieu	A. McGuire	R. Melcher	R.Niemelainen	D.Noel
R. Pancel	D. Plante	M.Plante	E. Poisson	R. Proulx	K. Raby
S. Rayner	K. Renaud	R. Rodden-Aubut	J. Rollins	L. Samuels	R. Savoie
R.Schneider	D. Sikatowsky	J. Sioni	D. Smith	J. Smith	R.Stevens
C. St.Georges	B. St.Pierre	H. Suchit	T. Thompson	D. Vergunst	J. Villeneuve
Y. Villeneuve	B. Walker	D. Yentha	D. Yantha	B. Young	

Maintenance, Electrical

M. Bruno	S. Campbell	R. Currie	A. Baronette	G. Bergeron	P. Brouillard
S. Campbell	R.Campeau	J.Charbonneau	D. Coffin	R. Condie	R. Connie
D. Cormier	P. Cranford	R. Currie	J. Dajczak	G.Dumont	J. Dajczak
G.Favot	R.Gareau	T. Giambattista	A.Gregoire	M. Gregoire	S. Heikkila
K. Hill	R. Imbeau	D. Jones	D. Lamoureux	P. Lance	J. Lawrence
M. Leclair	K. Maciborka	B. Mercer	J.Mercier	S. Michaud	R. Moncion
G. Moratz	C. Parent	G. Pilon	S. Powers	E. Ross	D.Ryan
K. Schutt	C. Theriault	C.VanDenBrock			

Engine and vehicle manufacturers

Cast:	Myles Bruce
Detroit Diesel	Mike Meadows, Brian Gillespie, George Hedge
Deutz	Jamie Sauerteig, Peter Prince, John Stimson, Joe Unseth
Kubota:	Brad Oliver
Truck and Wheels:	Conrad Houle

Control equipment, fuel suppliers, and measuring equipment manufacturers

3M:	Kevin Manuel
Arvin-Meritor:	Ed Kinnaird, John Barley, Brooke Huntington, Prasad Tumati
Clean Diesel Tech:	Mark Hildebrandt, J. Valentine
DCL:	Steve Finnemore, George Swiatek, Paul Terpin, Joe Aleixo
Deutz:	H. Breuer
ECOM:	Drue Wilson
ECS:	Edward Richards, Ted Tadrous, Don Malgast, Cesar Baumann, Rocky Karim, Tom Levander
Engelhard:	Aleksander Gorel, J. Kusan, A. Mullen
Finnkatalyst:	Arno Amberla, P. Wiklund
Greentop:	Marcel Lees
HUSS:	H. Rembor
Levitt Safety:	Dan Menard
Matter Eng.:	Dr. Ulrich Matter, Dr. Markus Kasper
Oberland-Mangold:	Bernard Kahlert, Hicham Agna, John Stekar
Johnson Matthey:	Peter Werth, Joe Stevenson, Marco Conrad, Dr.Richard O'Sullivan
Rhodia Catalysts:	Matthew Quigley, Steven Deutsch
Sandvik Mining:	Bill Maki, Wayne O'Link

International interests

Australia:	G. Fawcett
Austria:	R. Antretter
Germany:	Dr. Henrik Soenksen, Dr. Dirk Dahmann, Wolfgang Ruether, Dr. Paul Zelenka
Japan:	Hiroshi Matuoka, Toru Saito
Sweden:	Karl-Erik Ranman, Lennart Mukka, Tommy Eriksson, Bodil Melbloom, Dr. Par Jones, Lars Hergart
Switzerland:	Dr Jan Czerwinski
USA:	Edward Thimons, Bob Timko, Dr. Win Watts, Dr. Bruce Cantrell, Bob Waytulonis, Dr. David Kittelson, Dr. Susan Bagley, Bob Haney, Bill Pomroy, Dr. James Noll, Darrick Zarling, Dr. Richard Martin, Mukaram Syed, George Sassen

Vale Technical Services Limited (Sheridan Park)

Scott Price	Dawn Greville

Table of Contents

Appendices (on CD)

A: Duty cycle review session of Nov 2000
B: Workshop on technology transfer of Stobie results of July 2004
C: Cleaned data files and statistical information
D: Post-testing evaluations (CANMET report)
E: NIOSH Special Tests of Emissions Reports, July 2001, May 2002, and June 2004

Executive Summary

Project context:

Testing the long-term effectiveness of diesel particulate filter (DPF) systems that reduce the concentration of diesel particulate matter (DPM) of a vehicle's exhaust and thus in underground environments was conducted under the auspices of the Diesel Emissions Evaluation Program (DEEP) at Vales' (at that time, Inco's) Stobie mine from April 2000 to December 2004. Of particular concern was the ability of DPF systems to sustain long-term filtration efficiencies under the often harsh physical environment that exists for equipment operating in underground mining service.

Previous use of DPFs by the mining industry several decades ago had yielded mixed results, and technology at that time was considered impractical for routine use on underground diesel equipment. The primary cause of the past DPF failures in mining was the improper matching of a DPF to the vehicle on which it was expected to perform. Specifically, sufficient knowledge was lacking on sizing of the DPF to the soot emission rate of the engine and of the critical relationship between the engine duty cycle and the exhaust temperatures needed to burn off the soot collected by the filter medium (regeneration) during normal vehicle operation The objective of this project at Stobie was to show how to optimize the matching of a DPF system to a vehicle by using duty cycle monitoring prior to and during DPF installation and to demonstrate the effectiveness and ruggedness of those commercially available DPFs selected when subjected to the demands of production service.

Stobie Mine and Project Management:

Vale's Stobie mine is located on the south rim of the Sudbury ore basin. It started operations in 1886 and is currently an important mine in Vale's Sudbury nickel-copper ore mining. It uses a diesel fleet that is typical of hard-rock mining across the Canadian mining industry.

A team of Stobie personnel was gathered to work on the Stobie project in addition to their normal duties. The team was led by Dr. J. Stachulak, with outside technical advice being received from Dr. A. Mayer (European diesel DPF experience in tunnel construction), Drs. A Bugarski and G. Schnakenberg (U.S. NIOSH), and the DEEP Technical Committee. The team was responsible for all aspects of the testing and for interacting with Stobie operations. This latter aspect was critical because the vehicles selected for DPF testing were employed in routine production throughout the testing period.

Diesel vehicles used for the Project:

Five heavy duty load haul dump (LHD) vehicles were selected as representing the primary heavy duty workhorse in underground mining. One of these units had a dual exhaust

Deutz engine and the other four had Detroit Diesel DDEC 60 engines. The engines spanned a range of age and work cycles. Four Kubota tractors were selected as being representative of light duty vehicles, which are increasingly being used in transporting underground personnel. The use of DPF systems on underground light duty vehicles had not been studied anywhere at the time the Stobie project was started. Both DEEP and Vale considered their inclusion in the Stobie testing to be important because the proportion of light duty vehicles in use in underground mining was steadily increasing relative to heavy duty vehicles. As a consequence of this increase and the anticipated use of DPFs to reduce DPM from heavy-duty vehicles, the reduction of the DPM from light duty vehicles became an essential component to the overall strategy to improve the quality of underground air.

Duty cycle monitoring:

The duty cycles of the selected vehicles were monitored for six months prior to selecting the DPF systems for testing. Data loggers were mounted on these vehicles and collected exhaust temperature and backpressure at one-second intervals at the intended location of the DPF. These data loggers and their associated hardware had been used with success by a European consortium investigating DPF application in tunnel construction. Training of over fifty Stobie personnel in the operation and maintenance of this equipment was a key component of their successful use at Stobie.

The data obtained for each vehicle were analyzed to produce exhaust temperature and pressure history, temperature and pressure histograms, and more importantly for regeneration assessment, the dwell times of temperature as a function of temperature. This latter result is important, since a sustained (rather than a short excursion of) exhaust temperature above a certain minimum is a critical parameter in selecting the optimum DPF system (and its regeneration method) for a particular vehicle and its particular duty cycle.

Results clearly and surprisingly showed that heavy duty vehicles did not routinely achieve high enough exhaust temperatures for long enough periods during normal service to adequately regenerate the untreated or “bare” DPFs. In some cases the use of a “passive” regenerating DPF that uses a catalyst to lower the ignition temperature of the collected soot would possibly be adequate to achieve regeneration during normal operation of the vehicle. The catalysts are either wash-coated onto the filter element or added to the fuel by a dosing system. In the remaining cases the addition of heat would be required to achieve regeneration. These “active” systems usually involve periodic application of an electric heater while the vehicle is out of service, or an automatic in-service operation system using a fuel burner. Data on light duty vehicles clearly showed the need for “active” regeneration. The data on all vehicles indicated that exhaust backpressure would be an important diagnostic tool for monitoring the status (soot loading) of the DPFs.

Selected DPF systems:

For heavy duty vehicles, the LHDs:

•Two different passive DPF systems were selected.

The **Oberland-Mangold** DPF system used a deep bed filter element made of knitted glass fiber and a fuel-borne catalyst (FBC).

The **Engelhard** DPF had a ceramic wall-flow filter made of cordierite, the internal surfaces of which had been coated with a noble metal catalyst.

• Three active DPF systems were selected.

Two DPF systems were the **ECS** Combifilter which had a ceramic wall-flow filter made from silicon carbide (SiC), integral electric heating elements and off-board control system for regeneration while the vehicle was off duty.

The third DPF was from **Arvin Meritor**, and used a ceramic wall-flow filter element made of cordierite and an integral fuel burner to increase exhaust temperatures during vehicle operation to ensure filter regeneration.

• One DPF system was a hybrid of both passive and active regeneration methods.

The **Johnson Matthey** system used wall-flow filter elements made from either SiC or cordierite. Passive regeneration was achieved by using a FBC to reduce the minimum temperature for soot ignition; active regeneration was achieved, if and when required, by activating an integral electric heater when the vehicle was off duty or being serviced. Two of these DPF systems, acting independently, were installed on each exhaust of the dual exhaust Deutz engine.

For light duty tractors:

• Three active DPF systems were tested.

ECS/3M Omega used a ceramic fiber filter medium and an on-board electrical heater, activated when the vehicle was off duty.

ECS Combifilter used a SiC wall-flow filter element and an on-board electrical heater activated when the vehicle was off duty**.**

DCL used a SiC wall-flow filter element in a quick disconnect canister which was exchanged for a clean filter and regenerated in an off-board electric oven.

Fuel and lubrication oil:

The fuel used for all diesel units was Shell's Low-sulfur Diesel Fuel CP-34 containing 350 ppm sulfur. The lubrication oil used for all engines was Esso's XD-3™ Extra.

Methods for testing DPF system performance:

Exhaust emission tests on the DPFs were incorporated into routine maintenance and conducted every 250 hours of vehicle operation for heavy duty machines and monthly for light duty machines. An ECOM™ exhaust gas analyzer was used to measure exhaust concentrations of NO, NO_2, CO, CO_2 and O_2 and the Bacharach smoke numbers in the exhaust system upstream (engine side) and downstream (outlet) of the DPF.

Three additional comprehensive tests on all DPFs were conducted by Stobie personnel and NIOSH scientists in the summer of 2001, 2002, and 2004. These tests used three reproducible steady state engine conditions and measured the following upstream and downstream of the DPF: gases and smoke numbers, particulate concentrations using a photoelectric aerosol analyzer, particle size distributions using a Scanning Mobility Particle Sizer, and exhaust opacity.

Industrial Hygiene (IH) Measurements:

Even though the test vehicles were operating in normal production mode with the potential for other non-filtered vehicles to be operating nearby, the project team decided to conduct IH measurements before and after installation of some of the DPFs. Each test consisted of taking ten air samples: three for RCD analysis and three for elemental carbon (EC) analysis at a location just behind the driver of test vehicle, two for EC of the air into the area of operation and two for EC of the air exiting the area. Airflow measurements were also taken for each sampling period. The results showed a reduction in EC in the mine air when vehicles with DPFs were being used, but quantitative conclusions cannot be made because the with-DPF and without-DPF measurements were usually conducted while the vehicle was doing different kinds of work, and the airflow to the area of its operation varied depending on the working location of the vehicle.

DPF system-specific Results:

Engelhard DPF on an LHD: This DPF system had low complexity and required little special attention. Filtration efficiency for DPM (soot) was in excess of 98% throughout its 2221 hours of operation. Smoke numbers were reduced to an average of 0.6 downstream from 7.1 upstream. The system showed considerable robustness when it survived an accident with the LHD during which mud entered the discharge side of the DPF. The system was removed from testing when the engine's turbo failed, spewing lubrication oil into the hot exhaust and DPF resulting in oil fire. It is not clear what role (continued elevated exhaust backpressures) the DPF may have played in the turbo failure.

ECS Combifilter DPF system on two LHDs: Two of these systems were tested. The first one had marginal filtration efficiencies of 92-94% after about 300 hours of service, and concerns were raised about whether the required active electric regeneration was being routinely practiced by the vehicle operators. Data logging records showed that backpressures were fairly high and were not returning to normal after a shift when the DPFs should have been regenerated. After a total of 940 hours, the filter element was observed to have physical cracks and holes in the honeycomb structure. This was surmised as being the result of inattention to regeneration. As a result, the DPF was removed from the first LHD. The Stobie team then undertook renewed training of operators stressing the importance of their need to regenerate the DPF after every shift. Additionally, changes were made to facilitate easier access to the regeneration control station. On the second LHD, two new ECS Combifilter DPFs, connected in parallel to provide additional filtration capacity, were installed and performed well. This system achieved more than 98% filtration efficiency over 1.5 years of service. Tailpipe smoke numbers averaged 1.0 downstream of the DPF compared with 7.1 upstream, and opacity was excellent at 0.4%. IH sampling after normalization to 50000 CFM showed EC levels of 0.01 mg/m^3 with the DPF installed compared to 0.07 mg/m^3 without the DPF. The system had to be removed from the vehicle following an accident in which a muck pile collapsed and buried part of the LHD, resulting in significant damage to the vehicle. CANMET performed laboratory tests on each of these DPFs after the Stobie tests were completed. Results over a standard 8-mode test showed a 93-99.8% reduction of DPM for one DPF and a 56-85% reduction by the other DPF. The reduction ranges vary depending on whether DPM mass, the number of particles, or elemental carbon (EC) was being measured. Inspection of the filters showed some loss of ceramic cement used to join the SiC honeycomb blocks. Some evidence of soot was seen on the outlet side of the filters. Borescope images of individual filter channels showed the existence of a few cracks.

Johnson Matthey on an LHD: Two identical DPF systems were used because of the need to filter each side of the dual exhaust from the Deutz engine. Relatively higher than desired backpressures were experienced with this system which indicated that the dosing level of FBC was insufficient to achieve passive regeneration. Also, the continued high backpressures indicated that routine active regeneration was not being practiced by the vehicle operators. Filtration efficiencies remained fairly good ranging from 84% to >99%. IH sampling after normalization to 50000 CFM showed a reduction of EC to 0.04 mg/m^3 with the DPF compared to an average of 0.16 mg/m^3 without the DPF. After 2057 hours of operation one of the SiC filter elements (driver's side) showed excessive separation between it and its canister. As a consequence, DPM filtration efficiencies decreased and smoke numbers increased. A new DPF with a cordierite filter element was installed as a replacement which accumulated an additional 173 hours of operation before the project ended. One of the DPFs was sent to CANMET for testing. A large dent was observed on the outside shell of the filter canister, but the inside canister at this location was undamaged. The mat holding the ceramic filter element in place in the canister was severely degraded, and this was likely the cause of the filter being able to move within the canister. Where the filter had separated from the canister, there was evidence of soot. The filter had efficiencies of 89% (DPM mass), 98.4% (DPM particles) and 72.6 % (EC component of DPM).

Arvin Meritor on an LHD: This system was complex and required significant pre-installation fail-safe testing before it was permitted underground because of the existence of the

diesel fuel burner as the central component for regeneration. After only 116 hours of operation, the smoke numbers downstream were seen to be increasing to 3 compared to the upstream numbers ranging 5-7. The problems encountered with the control software for this system, combined with the indication of soot filter leakage, caused the testing to be terminated.

Oberland-Mangold on an LHD: This DPF system used a knitted glass fiber filter element and was complex due to the controls needed to regulate pumping the fuel-borne catalyst into the vehicle's fuel tank to maintain proper concentrations during refueling. Despite considerable team resources being used to install the system according to the manufacturer's criteria, and despite an intensive week of training of two Stobie mechanics in Germany, the system showed very inefficient filtration of soot, ranging from 3-70% and downstream smoke numbers of 5.5 compared to 7.0 upstream. The system was deemed to have failed with essentially zero hours of operation.

ECS Combifilter on a tractor: This DPF system successfully achieved 577 hours of operation over nearly three years. Excellent soot filtration efficiencies of >99% were measured with concomitant very low opacity and downstream smoke numbers. NO_2 decreased across the DPF due to conversion of NO_2 to NO by reaction with the collected soot. The ash left after burning the soot was collected from this DPF. Great care was required to avoid excessive contamination of the ash with unburned soot. The best ash sample obtained was analyzed by scanning electron microscope x-ray spectra of specific particles. The sample contained complex phosphates and sulfates of calcium and iron with some presence of iron oxides and zinc oxide. Owing to presence of other vehicles and after normalizing the ventilation rates, IH sampling at the vehicle showed no discernable difference in EC levels with and without DPF. Nonetheless, this system appears to be a good candidate for light duty vehicle service. CANMET tests showed the filtration efficiencies to be 94% (DPM mass), 99.9% (DPM particles) and 82% (EC component). The DPF was physically sound except for broken welds on the spider support.

DCL Titan on a tractor: This DPF system successfully operated for nearly three years achieving 864 hours of operation. Two DPFs were used alternately: one DPF was in use while the other was regenerated off the vehicle. Both DPFs maintained excellent soot filtration efficiencies of about 99%. The quick disconnect fittings made swapping the DPFs very easy. IH sampling, after normalization of ventilation rates, with the DPF installed showed EC at about 0.04 mg/m^3 compared to 0.09 mg/m^3 without the DPF. This system appears to be a good candidate for light duty service. One of the DPFs was examined by CANMET after completion of the testing. The filtration efficiencies were 95% (DPM mass), 97.8% (DPM particles) and 89% (EC component). The outlet side of the filter element showed evidence of soot over a small area. Borescope images confirmed very small microcracks in some of the filter channels.

ECS/3M Omega on a tractor: The system accumulated 453 hours of operation with marginally acceptable soot filtration efficiency ranging from 77% to 94%. Relatively high smoke numbers of 3.5 were measured downstream compared to 9.0 upstream. Opacity was marginal at 5%. The system was removed from the testing because 3M announced its cessation of manufacturing the glass fibers employed as the filter medium.

Ash Samples:

Samples of ash were collected from several filters after multiple regeneration cycles. These were prepared and analyzed using ICP-MS. Low magnification optical images and scanning electron microscope images were also obtained. Sampling of the ash turned out to be a difficult matter because unburned soot contaminated most samples. A special sampling of the ash from the ECS filter (from tractor #3013) was done by sampling dust from the regeneration oven itself. X-ray diffraction of this dust identified possible phases as calcium phosphate, calcium iron phosphate, anhydrite (calcium sulfate) and hematite (iron oxide). X-ray spectra of selected particles were obtained using an electron microscope. The x-ray spectra showed the presence of calcium, phosphorus, iron, sulfur and oxygen (in agreement with the diffraction results) and also zinc (as a zinc oxide or phosphate).

General conclusions:

(1) Both heavy duty and light duty vehicles in underground mining operations can be retrofitted with DPF systems that are highly efficient in removing DPM from diesel engine exhaust. However, all of the systems tested in the Stobie project required closer attention than was desired, although the amount of attention needed varied widely. Ideally, a DPF system would be invisible to the vehicle operator and almost invisible to the maintenance department. That is, people would go about their jobs in a conventional manner and would not need to pay attention to the DPF or its regeneration. This ideal was clearly NOT the case for any of the DPFs being tested in the Stobie project. However, and most importantly, this ideal remains a critical issue for a successful program of retrofitting DPFs or for installing DPFs in new equipment.

(2) Taking care to make the effort to correctly match the vehicle duty cycle with an appropriate DPF system is essential for a retrofit program to be successful.
   a. This matching must size the DPF correctly for the engine soot emission rate, exhaust gas volume, and collection/regeneration interval. Too small a DPF will result in premature loading the filter, excessive exhaust backpressures and frequent regeneration, all of which will negatively affect vehicle productivity. Too large a filter will result in cramped space for the unit on the vehicle; this could negatively impact safe use of the vehicle and impair ease of maintenance and inefficiency in utilizing exhaust heat to create sufficient temperature for passive regeneration.
   b. This matching must be done to obtain the optimum method of regeneration of the filter. The optimum method of regeneration must take into account issues such as the complexity of the regeneration system, the time needed for regeneration, maintenance of the regeneration system components, ease of installation and use, and cost.

(3) Proper training of and communication with vehicle operators is essential. The presence of a DPF system will increase the exhaust backpressure for the engine. Operators must be attentive to the additional alerts and alarms indicating high backpressure or else serious harm could be done to the engine and/or DPF.

(4) Simple, but effective, dashboard signals are needed in order to give information to the vehicle operator of the DPF's status.

(5) The increased emission of noxious gases often can result with some catalysts that are used to promote DPF regeneration; but this can be known in advance of selection and use.These emissions, particularly NO_2, must be watched carefully. While there are ways to control such emissions, they add to system complexity and cost.

(6) An emissions-based maintenance component of an overall vehicle/engine maintenance program is essential. Proper functioning of a DPF should be evaluated as part of routine maintenance. Training maintenance personnel to make and interpret tailpipe emissions and to understand the specifics of each DPF system is essential to successful implementation.

Additional information

The Diesel Evaluation Emissions Project's Stobie mine project had a final report issued in March 2006. (version 1). Some additional analyses of data collected and additional editing of that report has resulted in the current October 2011 report (version 2). This new version supersedes the earlier report.

During the intervening years between these reports a team at Vale's Creighton mine continued the DPF testing work under Vale's (Inco's) sponsorship. This has resulted in significant progress being made over what was learned during the DEEP Stobie project. Readers are encouraged to read the papers included in the references under the title "Additional references not specifically cited in the Report, but relevant to the Stobie project and to current state-of-the-art technologies", which give a good picture of current performances of diesel particulate filter systems being subjected to on-going testing at Vale's Creighton mine.

List of Tables

Vehicles

DPF Selection

DPF Performances

Oberland-Mangold on LHD #445

ECS/3M Omega on Tractor #2180

ECS/Unikat Combifilter on Tractors #2180 and #3013

DCL Titan on Tractors #621 and #017

Post-Testing Efficiencies and Analyses

List of Figures

Background on diesel exhaust and Stobie Project

Vehicles Tested

Data Logging Equipment and Procedures

Installation of DPF Systems

ECS Combifilter DPF on LHD #213

Arvin Meritor DPF on LHD #111

Instruments for Measuring DPF Performance

Data Treatment

Major Project Events

DPF Performances

ECS/Unikat Combifilter on Tractors #2180 and #3013

DCL Titan on Tractors #621 and #017

ECS/Unikat Combifilter on LHD #213

Engelhard on LHD #362

Industrial Hygiene Measurements

Ash Residue Analyses

Post-Testing Efficiencies and Analyses

Glossary

ACRONYMS and TERMS

3M	Minnesota Mining and Manufacturing Inc.
A/D	Analog to Digital Conversion
ACGIH	American Conference of Governmental Industrial Hygienists
ASCII	American Standard Code for Information Interchange
CANMET	Natural Resources Canada Laboratories in Ottawa
DCL	Diesel Control Limited
DDEC	Detroit Diesel Electronically Controlled, a modern diesel engine
DEEP	Diesel Emission Evaluation Program
DPF	Diesel Particulate Filter, a filtering element contained within a canister
ECS	Engine Control Systems
HEI	Health Effects Institute
HI	High idle, an engine test condition
IARC	International Agency for Research on Cancer
IH	Industrial Hygiene, here meaning sampling of airborne contaminants, RCD or EC
ISO	International Standards Organization
JM	Johnson Matthey
LHD	Load, Haul, Dump, a class of heavy duty vehicle used underground
LI	Low idle, an engine test condition
MSHA	Mine Safety and Health Administration (United States)
NIOSH	National Institute for Occupational Safety and Health under Centers for Disease Control and Prevention (CDC), Department of Health and Human Services (DHHS), United States
OEL	Occupational Exposure Level
PILP	National Research Council's Program for Industrial/Laboratory Projects
RAM	Random Access Memory, a type of digital memory
RCD	Respirable Combustible Dust, the carbon content of airborne dust
TLV	Threshold Level Value, an 8-h exposure limit for air contaminant set by ACGIH
TCS	Torque Converter Stall, an engine test condition which loads the engine consistently using the transmission
VERT	Verminderung der Emissionen von Real-Dieselmotoren im Tunnelbau. Curtailment of diesel engine emissions at tunnel sites, a joint project Swiss and Austrian occupational health agencies, the Swiss and German environmental protection agencies, the German association of construction engineers, and several engine manufacturers and particulate filter system manufacturers
WHO	World Health Organization

UNITS

CFM	cubic feet per minute
h	hours
hp	horsepower
L	liters
nm	nm = 10^{-9} meters
µm	micrometer = 10^{-6} meters
mBar	millibars (1 Bar = atmospheric pressure)
mg/m^3	milligrams per cubic meter
ppm	parts per million
rpm	revolutions per minute
σ	"sigma" = one standard deviation
s	second
T	temperature

CHEMICALS (gases)

NO	nitrogen oxide
NO_2	nitrogen dioxide
NOx	total of NO and NO_2
PAH	polycyclic aromatic hydrocarbons
CO	carbon monoxide
CO_2	carbon dioxide
O_2	oxygen

CHEMICALS (solids/liquids)

DPM	Diesel Particulate Matter, total of all particles in engine exhaust or in mine air generally considered to be two components, EC and HC.
EC	Elemental Carbon, the pure solid carbon component of DPM
FBC	Fuel borne catalyst, usually an organometallic added in small quantities to the fuel to promote oxidation of soot (regeneration).
HC	hydrocarbons, substances -- solids, liquids or gases -- containing hydrogen and carbon, e.g., oils from pneumatic drills and a part of DPM

MISCELANEOUS TERMS

Active DPF	A DPF in which filter regeneration is attained by means other than exhaust temperatures alone
Passive DPF	A DPF in which filter regeneration is initiated and sustained by exhaust temperatures alone
Regeneration	The process of removing the soot from a DPF by burning (oxidation)
Backpressure	also exhaust pressure or pressure in context of engine exhaust. The pressure on the engine caused by the restriction of a muffler or DPF in the exhaust pipe.
Cordierite	A cream-colored porous ceramic material extruded as a cylindrical honeycomb
Smoke number	A scale ranging from white to black in ten steps that is used to measure soot content of diesel exhaust
SiC	Silicon Carbide, a gray porous ceramic material used to make honeycomb filter elements

Filter element The component that removes soot from the diesel exhaust. It is mounted within a stainless steel canister to form a DPF; can be made from various filter materials.

Wall-flow A class of DPF filter elements using a honeycomb structured porous material with alternate open ends plugged so that gases entering one end must flow through the walls of the honeycomb

1. Introduction

This document reports results of testing the effectiveness and suitability of several types of diesel particulate filter (DPF) systems that are candidates for reducing the concentration of diesel particulate matter in underground air by reducing the DPM emissions from diesel powered vehicles. The tests were conducted at Vale's Stobie Mine from April 2000 to December 2004 as part of the Diesel Emission Evaluation Program (DEEP).

1.1 The Use of Diesels in Underground Mining

Since their introduction into underground mining operations in the mid-1960s, diesel-powered equipment has become increasingly employed and recognized as the workhorse in mining. Diesel engines are easier to maintain and generally have lower operating costs than their gasoline-fuelled internal combustion counterpart. In addition, diesel engines are more robust than most other engines and therefore have shown the ability to sustain high performance in a physically harsh environment.

In terms of safety, diesel engines have several advantages over gasoline engines. First, diesels operate in a lean fuel to air ratio and produce very low levels of carbon monoxide (CO) in their exhaust. Second, the diesel fuel itself has a fairly high flash point which reduces the possibility of unwanted fuel ignition and fires underground.

Vale employs about 800 diesel-powered units at its Ontario mining operations in the Sudbury basin. While the use of alternative power (e.g., electricity, fuel cells) is being explored, Vale and most other Canadian deep-rock mining companies realize that diesel engines will continue to be a very important component of a working fleet of vehicles for many years to come. In view of this, it is imperative to lessen diesels' undesirable features such as noxious substances in its exhaust.

1.2 Characteristics of diesel exhaust

Diesel exhaust is a mixture of a large number of distinct and complex substances (in solid, liquid and gaseous phases). The gaseous phase includes CO, carbon dioxide (CO_2), sulfur dioxide and sulfur trioxide from the sulfur in the fuel, nitrogen oxides (NO and NO_2, together termed NOx), and a number of low molecular weight hydrocarbons (HC) such as simple aldehydes.

The liquid phase includes condensed hydrocarbons of varying molecular structures (e.g. polycyclic aromatic hydrocarbons, PAHs). Sulfuric acid, formed by the combination of sulfur trioxide with water, can also be present.

The solid phase, often referred to as soot, is predominantly elemental carbon (EC) that arises from unburned fuel. It contains extremely small particles of carbon (15-40 nm equivalent

diameter, termed "primary particles") with some of these accumulating into somewhat larger particles (60-100 nm in what is called the accumulation mode) and some relatively coarse particles (100-1000 nm). Virtually all of these diesel-produced particles are respirable (that is, less than 10 µm). Due to the small particle sizes, EC particles have large surface areas which readily adsorb gaseous and liquid hydrocarbons. In addition to EC, the solid phase also contains metal oxides and sulfates. The small amount of metals contained in these compounds may arise from impurities in the fuel, engine wear, and engine oil. Metal additives are often introduced to the fuel to act as catalysts to enhance DPF regeneration, but they are effectively removed by the DPF. Metal sulfates result from the reaction of metal oxides with sulfur dioxide and water in the exhaust system.

A schematic of the components of diesel exhaust is shown in Figure 1, their typical proportions are shown in a pie chart in Figure 2. A typical particle size distribution summed over the operating modes of a diesel engine is shown in Figure 3.

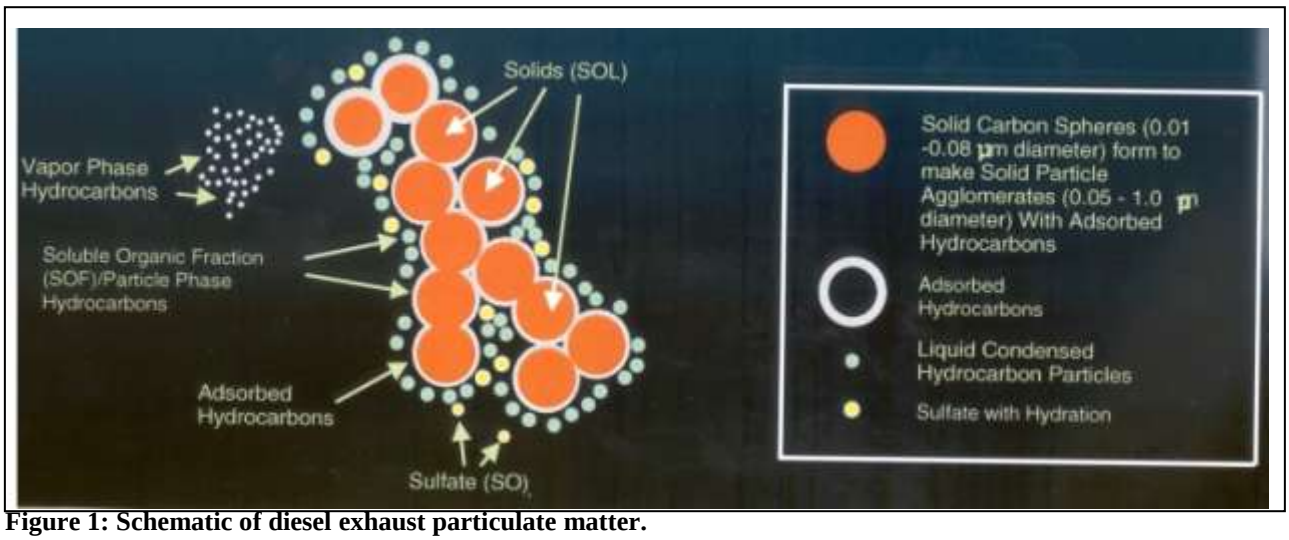

Figure 1: Schematic of diesel exhaust particulate matter.

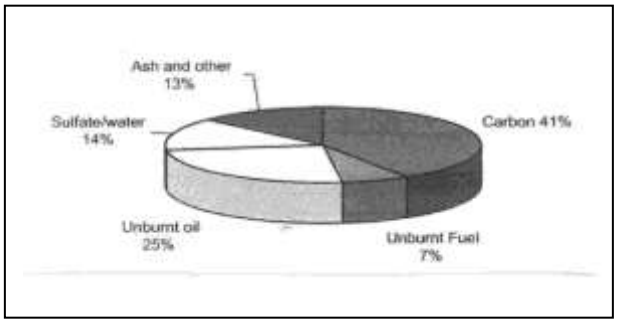

Figure 2: Typical constitution of diesel exhaust (after Burtscher, 2005).

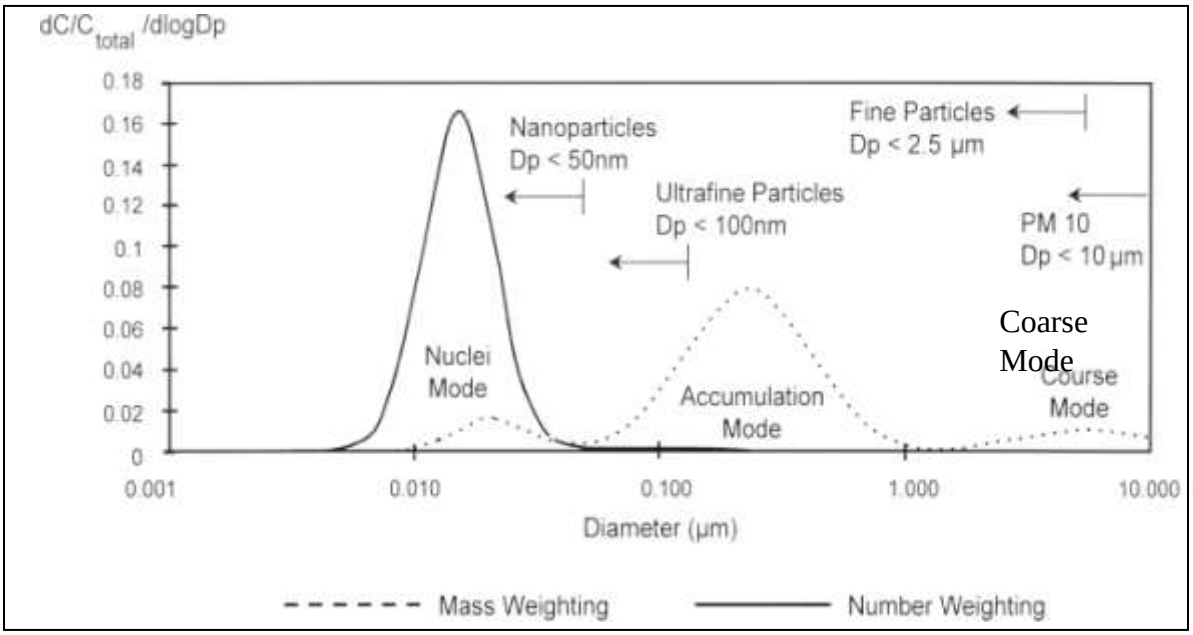

Figure 3: Typical particle size distribution of DPM (after Kittelson, 1998)

The specific composition and size distribution of a diesel engine's exhaust varies with the type and purity of the fuel, age of the engine, engine design, engine maintenance, fuel/air control, the work being performed by the engine, the operator of the vehicle, and conditions in the working environment (e.g. humidity). It is important to recognize that certain trade-offs exist in trying to minimize potentially harmful substances present in diesel exhaust. For example, improvements in burning efficiency by altering engine design and fuel injection will likely result in decreasing the mass of EC in the exhaust, but will also probably result in increasing the proportion of extremely fine carbon particles, which may be more harmful if inhaled (see below). Another example is improving the combustion of fuel by increasing the air to fuel ratio, which will decrease the mass of EC in the exhaust, but will simultaneously increase the concentration of NO_2.

While many exhaust treatment technologies can assist in reducing unwanted substances, their successful implementation is technically and operationally challenging (Schnakenberg and Bugarski, 2002; Bugarski et al., 2006a and 2006b). The general approach in minimizing the toxic properties of the exhaust includes (a) having engines in good working condition, (b) controlling the formation of certain noxious compounds during combustion (for example, using low sulfur fuels to decrease sulfate formation and using lean air/fuel mixtures to limit NOx formation), (c) balancing EC formation against NOx formation during combustion, and (d) installing devices to remove or to chemically alter substances prior to their release from the tailpipe.

1.3 Health Concerns

Concern within the underground mining industry and elsewhere on the toxicity of whole diesel exhaust and with certain components within the exhaust is a result of a number of occupational epidemiological and animal studies conducted over the past several decades. The

solid phase of diesel exhaust, termed diesel particulate matter (DPM), has been of particular concern because of its very small size and its ability to adsorb very complex and potentially toxic HCs and deliver them deep into the alveolar region of the lungs of workers. There exist several toxic effects due to DPM. For example, mucous membrane inflammation of the eyes is known to occur upon prolonged exposure to modest concentrations of diesel exhaust. In the lungs, tissue inflammation and chronic bronchitis may occur. Due to the presence of HCs known to be carcinogenic at high concentrations, there is concern about the possibility of respiratory tract cancers.

The Health Effects Institute (HEI, 1995) and the World Health Organization (WHO, 1996) issued comprehensive reports on knowledge about the health consequences of diesel exhaust, but were unable to set quantitative cancer risks. The International Agency for Research on Cancer (IARC, 1989) has determined that diesel exhaust is "probably carcinogenic" and the U.S. National Institute for Occupational Safety and Health (NIOSH, 1988) has stated that diesel exhaust is "a potential occupational carcinogen." While it is not clear whether the EC particles themselves (without the adsorbed substances) are carcinogenic, it is clear that these small particles are able to carry other noxious substances deep into the lungs. There has also been increasing concern by public health officials about the deleterious effects of nanoparticles in ambient air, due to a link seen in urban studies between respirable particle concentrations and hospitalization frequency or death rate in the general population. Research about nanoparticles in underground air is generally absent, but health concerns for workers mirror the concerns that exist for the general population.

There is little doubt that reducing miners' exposure to the noxious components of diesel exhaust, particularly DPM, would have a positive influence on sustaining their good health.

1.4 Regulatory initiatives

The American Conference of Governmental Industrial Hygienists (ACGIH) is the body that establishes recommendations for threshold limit values (TLVs) for workplace exposures. In 1995 the ACGIH notified stakeholders that it intended to adopt a TLV for DPM of 0.15 mg/m^3 with a classification of "suspected carcinogen" (ACGIH, 1995).[1] While the ACGIH does not have a regulatory mandate, governmental agencies with regulatory authority usually use the TLV of a substance as the starting point for setting an Occupational Exposure Limit (OEL).

The Mine Safety and Health Administration (MSHA, 2005) in the United States has recently used the ACGIH information, together with practical considerations, to establish a metal/non-metal mining OEL for the EC portion of DPM. It is clear that other jurisdictions world-wide have already adopted or are considering such regulations (USA – 0.16 mg/m^3 TC).

Some years ago many provinces in Canada, in consultation with the mining industry, adopted a target of 1.5 mg/m^3 for the respirable combustible dust (RCD) concentration in

[1] It should be noted that the ACGIH did not adopt the 0.15 mg/m^3 value, but notified stakeholders that it intended to adopt an even lower value of 0.05 mg/m^3 and then subsequently announced a lower value of 0.02 mg/m^3. Most recently, the ACGIH has withdrawn its notice for DPM entirely. It is likely that a new notification will come forward with improved designations of exactly what is meant by DPM.

underground mines. At the time of this project, most mines operated well below this target at 0.5-0.8 mg RCD/m^3. Experience in mines having a combination of diesel equipment and pneumatic drills has indicated that two-thirds of the RCD is DPM with the remainder being a combination of oil mist and carbon containing mineral dust. This means that the target DPM in most Canadian mines at the time of the project was about 1.0 mg/m^3. Note: Effective January 2012, the Occupational Health and Safety Act, Regulation 854, Mines and Mining Plants for Ontario, Section 183.1 (5) will limit TWA worker exposure to total carbon (or elemental carbon times 1.3) to not more than 0.4 mg/m^3.

Indeed, the mining industry in Canada became concerned (a) with the technology for sampling and analyzing DPM at extremely low levels and (b) about proven technology that would reduce the DPM emissions from diesels so that these flexible and robust engines could continue to be used to great advantage without causing adverse health outcomes in miners.

1.5 Formation of DEEP

In April 1997 several mining companies joined with several unions, Canadian government departments (both provincial and federal), diesel engine manufacturers, emission control equipment manufacturers and fuel suppliers to form the Diesel Emission Evaluation Program (DEEP). The objectives of DEEP were to (a) prove the feasibility of reducing miners' exposure to DPM in a reliable and effective manner using existing technology and (b) to establish the ability of measuring DPM underground with needed precision and accuracy at the desired targeted very low levels of DPM.

The work of DEEP initially focused on using alternative fuels to reduce DPM, and then evolved into improving engine maintenance programs and comparing analytical methods for DPM. Information about DEEP's research can be obtained at www.deep.org.

While some benefits in decreasing DPM emissions from diesel engines were found during DEEP's projects, it became apparent that fuel, maintenance, engine design improvements and operational and ventilation optimization would accomplish only a fraction of the targeted 90% reduction in DPM. It became apparent that removal of DPM from the exhaust stream prior to its release from the tailpipe was likely to be an integral part of any dramatic reduction in DPM emissions. DEEP therefore initiated two projects on Diesel Particulate Filter (DPF) Systems, one hosted by Noranda's Brunswick mine (McGinn, 2004) and the other hosted by Vale's Stobie mine. These companion projects aimed to test commercially available DPF system technologies in operating mines in order to determine if these systems were able to operate with effectiveness over a prolonged period in often harsh physical environments.

2. Particulate Filter Systems

2.1 General comments

The term “system” is used in conjunction with DPFs in this report to emphasize that a successful reduction of DPM relies upon several components working together. One component is the filtration medium itself. Another component is the instrumentation that may be necessary to monitor and log engine and or exhaust parameters. Yet another component may be a control system that would initiate certain actions (e.g., indicator lights or turn on a fuel burner) depending on pre-determined values of monitored parameters. Finally, there may be components such as electrical heaters (on-board as well as off-board) and their control systems or fuel burners that are used to ignite the soot collected on the filter element and thus “regenerate” the filter for continued effective performance. The term “system” refers to the integration of all the necessary components into a working partnership for effective and prolonged filtration efficiency.

Filtration media used in DPFs vary in chemical composition and morphology. All media must be able to withstand the relatively high exhaust temperatures that may occur during normal diesel engine operation. DPFs can employ differing filter media ranging from porous ceramic structures such as cordierite and silicon carbide (SiC), woven glass or metal fibers, sintered metal and metal foams. A variety of effective pore sizes are available and, accordingly, filters vary in their filtration efficiencies as a function of particle size of the DPM. Filter media also vary in the mechanism of filtration with many essentially being wall-flow filters, described below, and others being deep bed filters. In either case, the filtration is achieved by having a porous structure which allows transmission of the gas phase of the diesel exhaust, but effectively captures solid and liquid components of the exhaust.

The most common filter media are the ceramics — cordierite (magnesium aluminum silicate) and silicon carbide. Both are produced as honeycomb structures made by extrusion. Filtration is accomplished by plugging the alternate ends of neighboring channels of the honeycomb, as shown in the schematic in Figure 4. The soot-laden exhaust enters the open ends of the channels, and because the other end is plugged, is forced to flow through the porous walls, which trap the DPM particles, into the adjacent channels where it flows out and exits the filter though the open end of the channels. Because the exhaust flows through the wall that separates the honeycomb channels, it is termed a wall-flow filter.

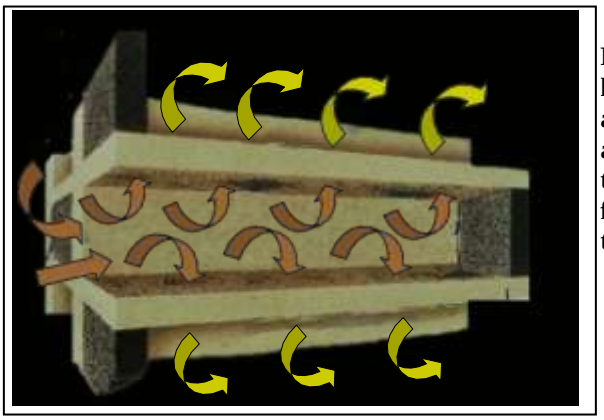

Figure 4: Representative view of the magnified honeycomb structure with adjacent channels blocked at alternate ends to create a wall-flow filter. Brown arrows show incoming exhaust containing soot entering the open channel on the left. The yellow arrows show filtered exhaust which can only flow to the right to exit the filter. (DCL International, with permission)

2.2 Past experience in underground service

The first DPF developed for use in underground diesels used a cordierite wall-flow filter element developed by Corning Glass in collaboration with Natural Resources Canada (CANMET) scientists. The cordierite substrate was primarily used in flow through catalysts for automotive (gasoline engine) exhaust. Plugging the alternate ends of the honeycomb channels created an effective wall-flow DPM filter. In the early 1980s prototype DPFs were laboratory-tested and then taken underground for field trials (McKinnon, 1989). Vale was involved in testing a prototype at Little Stobie Mine and in implementing what was then considered to be a successful technology via the National Research Council's Program for Industry/Laboratory Projects (PILP) run under the auspices of the Collaborative Diesel Research Advisory Panel.

However, the success was not uniform. While all filters appeared to work when first installed, many were found to plug rapidly with soot, resulting in unacceptable exhaust backpressures. Since excessive backpressures would invalidate engine warranties, the vehicles had to be pulled out of production and attended to which severely affected the ability of miners to conduct their work efficiently. As a result, many of these newly installed DPFs were discarded by vehicle operators. Mine management, as well as workers, became skeptical of most DPF systems. Since the late 1980s DPM filtration of engine exhaust has been done on a very limited basis at Vale.

Some DPFs worked well on certain equipment. It is now recognized that the performance of a DPF is intimately associated with frequent complete removal (burning off) of soot collected within the filter element. Likely the early implementation of filters on underground equipment relied on this removal being done by the heat in the engine exhaust itself and, as now realized, this was not achieved for many DPFs because of a combination of lower than expected exhaust temperatures and/or a lack of sufficient time at high exhaust temperature to completely burn all or mostly all of the collected soot. Exhaust temperatures in modern engines are lower than those encountered in the early tests making spontaneous burning off of soot even less likely to occur.

2.3 Methods of filter regeneration

The successful filtration of diesel exhaust by any medium will result in a build up of soot on the engine side of the filter resulting in increasing exhaust backpressure. In order to lower the backpressure to acceptable values, the soot must be removed. The trapped or collected mass of soot, the DPM, because it is almost entirely comprised of carbon and carbon containing compounds, can be burned off, a process termed **regeneration** or it can be removed by mechanical means as described below. DPF regeneration can be further categorized as happening **passively** or **actively.**

(a) **Passive regenerating** DPFs rely entire on the heat supplied by sufficiently high exhaust temperature to ignite and burn all or mostly all of the collected soot. Depending upon exhaust temperature, which depends upon the work being done by the engine, the soot can build up and be burned or burned off as it is collected. Since in modern diesel engines, it is unusual for the exhaust temperatures to get high enough to ignite the soot, catalysts in various forms and formulations are used to lower ignition temperature of the

soot resulting in regeneration at lower exhaust temperatures. Catalysts, usually a metal-containing substance, can be deposited onto the filter substrate (as a "wash coat"), and/or mixed with the diesel fuel in required proportions. Fuel borne catalysts (FBC) are organometallic compounds that produce a catalytic ash that is continuously deposited in the filter with the soot. Depending upon the catalyst, ignition temperatures of the soot can be substantially lowered. On-board automatic FBC dosing systems have been developed which add proper amounts of FBC to the fuel during vehicle operation. It is essential for the selection and success of a passive DPF that the exhaust temperatures are well characterized, **prior to DPF selection**, because they determine catalyst selection and ultimately whether passive regeneration can occur at all.

(b) **Active regenerating** DPFs are those which are not able to regenerate using prevailing vehicle exhaust temperatures. Either some means of exhaust temperature enhancement needs to be provided during the normal work cycle, or the DPFs are regenerated by some means when the vehicle is off-service. In some DPF systems, a fuel burner, intermittently activated during the production cycle when exhaust backpressure reaches a threshold, is used to add heat to the exhaust immediately before the filter element. Other systems use an electric heating coil positioned close to the filter element, an air supply, and control system, to perform regeneration while the engine is not running, i.e., when the vehicle is out of service. The electric heating element is an integral part of the DPF. Alternatively, the DPF can be removed from the vehicle and placed in a specially designed system which may employ a reverse flow of air to remove soot and ash and an electric heater to burn off the remaining soot under controlled conditions.

(c) DPFs can be cleaned by **mechanical** processes such as blowing out the collected soot and ash using compressed air jet played on the outlet face of the filter element. Care must be taken to either collect the escaping soot or otherwise avoid dispersing where it can be a hazard to others. This is not a practical solution as a substitute for regeneration, both because of the labour involved and the removal of the vehicle from productive use. However, every DPF will eventually accumulate enough ash from the trace metal particles in the exhaust (including those from a FBC) to require mechanical cleaning using compressed air or a vacuum system. Commercial regeneration/cleaning systems are available and were used in this project.

Operating personnel usually favor passive systems because they require little attention when working properly. However, to be successful, such systems must be matched to the duty cycle of the vehicle whose exhaust must sustain high enough temperatures for a sufficient time. If such matching is not done, then the operator risks ineffective regeneration, which will lead to increased frequencies of productivity interruptions due to high exhaust backpressure and ultimately to the rejection of the DPF.

2.4 Recent DPF experience in Europe

European workers have continued to experiment with newer filtration systems with good success. For example, a multi-year project to examine diesel soot reduction in tunneling operations was initiated by the national accident insurance institutions of Germany, Austria and Switzerland, and the Swiss Environmental Protection Agency. Both laboratory testing and field evaluations were conducted by the program, termed VERT, between 1993 and 1998. Thus, just

as DEEP was considering its own projects for DPM reduction, VERT was completing its work. Discussions between DEEP and A. Mayer, VERT's technical director, assisted greatly in developing the Stobie project's scope of work. The knowledge gained by VERT in successfully matching engine-DPF characteristics was particularly valuable (VERT, 1997, 2000, 2004).

Sudwestdeutsche Salzwerke AG and Kali und Salz also had been conducting trials of DPFs on operating diesel equipment and had shown the necessity of obtaining good regeneration performance as a critical factor in DPF use underground. A technical cooperation agreement was signed between DEEP and Kali und Salz to share experience in diesel-related issues.

3. The Stobie DPF Testing Project

The prevailing explanation of the formation of the Sudbury area nickel-copper ore body is that a meteor impact occurred about 1.85 million years ago. The impact is estimated to have released heat with about 10,000 times the energy of the current supply of the world's nuclear bomb stockpiles. This heat caused melting of the earth's crust and an up-welling of underlying magma rich in nickel and copper sulfides. The resulting orebody is in the shape of an elongated bowl, shown in the diagram in Figure 5.

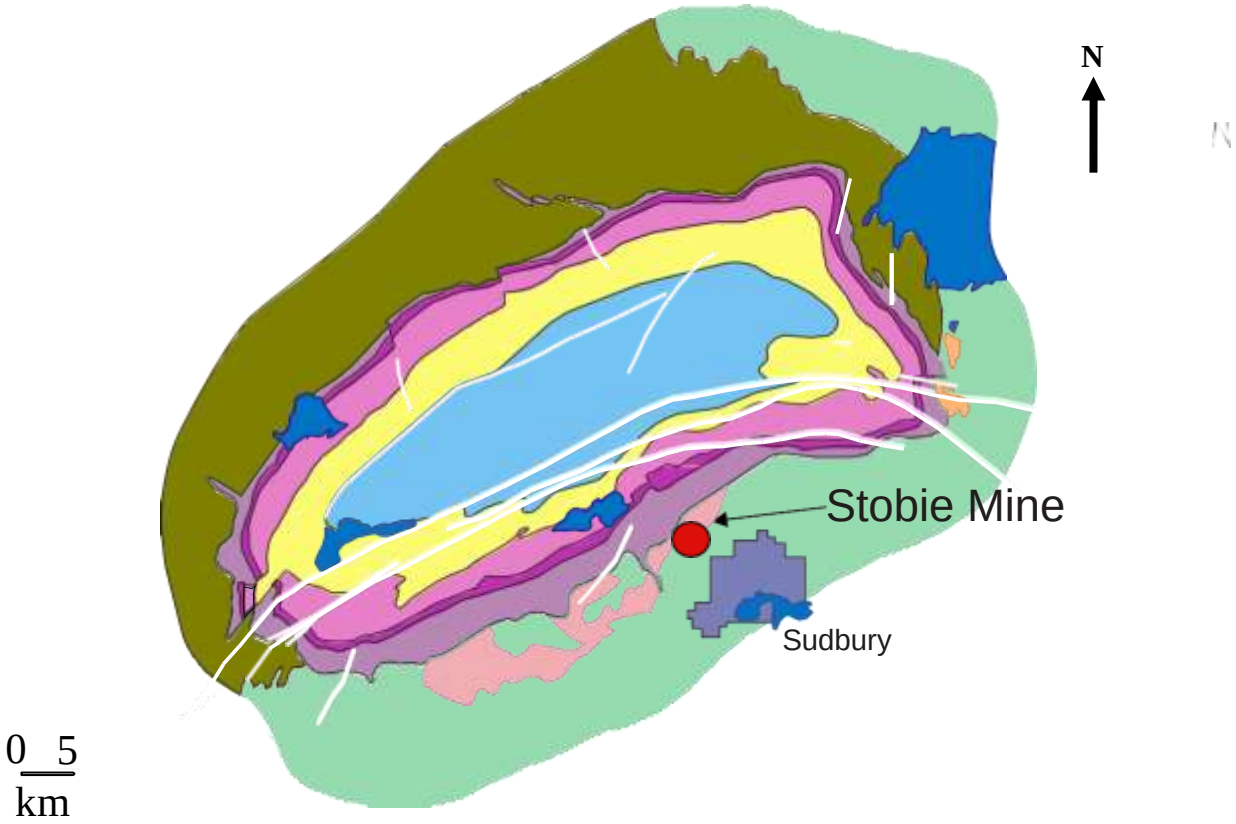

Figure 5: Schematic of Sudbury basin showing Ni-Cu ore in purple and pink colours in the shape of an elongated bowl. The white lines indicate faults. The City of Greater Sudbury is on the south side of the basin. Stobie Mine is just to the northwest of the urban centre of Sudbury.

Mining of ore started in this region in 1883. The Frood-Stobie complex was among the first workings. Since 1886 Stobie mine has produced about 250,000,000 tonnes of ore. The mine is located on Frood Road just to the north of the urban area of Sudbury.

3.1. Development of the Project

Writing a proposal for conducting DPF evaluations at Stobie started in early 1998. Many changes to the scope of work occurred over the following year with input from the DEEP Technical Committee and outside consultants. Partial funding was obtained from agencies outside the DEEP organization. The official approval by DEEP was given in mid-1999.

The scope of the project was to test six DPF systems on six vehicles doing production service in an operating Vale mine. In order to keep organizational issues minimized, one Vale mine, of the ten operating Vale mines in the Sudbury area, was approached by the Principal Investigator to host the project. Having one mine host the project avoided having to interact with multiple mine managers, superintendents and operating and maintenance personnel.

The acceptance by Vale's Stobie Mine to host the project was given with recognition of the urgency of testing the effectiveness of DPFs in order to meet potential regulatory actions. A concern of mine management was the amount of in-kind costs and potential loss of ore production that would occur by using production vehicles during the project. In balancing this concern, it was recognized that the education and training of personnel in technically sophisticated systems would serve the mine well in the years ahead and would enable the mine to implement successful systems in a more timely and efficient manner.

Originally planned to be conducted over roughly 2.5 years, the testing was extended until December 2004 primarily to enable reasonable operating hours to be accumulated on the DPF systems so that an evaluation of long-term ruggedness was possible. Project delays were chiefly associated with technical liaisons, with setting up operational agreements between the project team and DPF manufacturers, with training Vale personnel in new equipment and software, and with insufficient operating time of certain vehicles.

3.2 Objectives of the Stobie Project

The objectives of the Stobie tests were to:

- Develop methods for selecting DPF systems for mining vehicles, including the use of duty cycle monitoring and logging of relevant exhaust parameters with specialized data analysis for gaining information about DPF regeneration feasibility;

- Determine the ability of current DPF systems to reduce tailpipe DPM emissions without significantly increasing other noxious substances and to evaluate the long-term durability, reliability, and maintenance costs for such DPFs in a production mode;

- Develop Canadian expertise with DPF system technology and DPM measurement methods so that implementation of best-performing DPF systems in Canadian mines could be accomplished as efficiently as possible.

3.3 Team Organization

The primary personnel comprising the Stobie project team are shown in Figure 6. Dr. Jozef Stachulak, Vale's Manager - Strategic Ventilation, Canadian Operations, was the principal investigator responsible for all aspects of the project. He communicated with Vale management through Mike MacFarlane, who was the manager of Stobie mine at the time and later became Vice President-Mining and Milling, North Atlantic operations. J. Stachulak also communicated

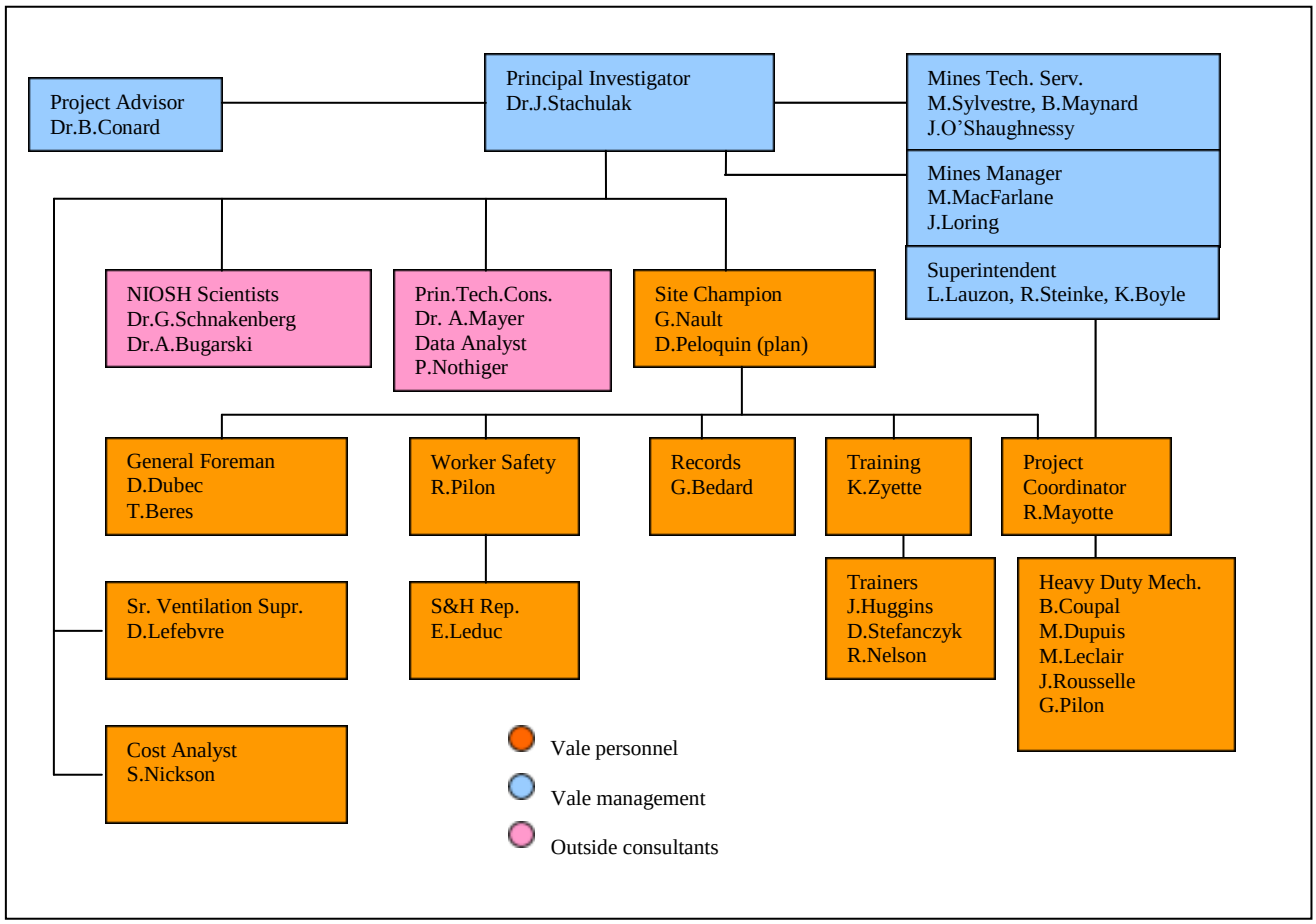

Figure 6: Stobie project team

with the DEEP Technical Committee (not shown). The outside consultants assisting the team reported to Stachulak and consisted of Dr. Andreas Mayer (past Director of the VERT program in Europe), Paul Nöthiger (data logger manufacturer and data analyst), Drs. George Schnakenberg and Aleksandar Bugarski (scientists at the U.S. National Institute for Safety and Health research center in Pittsburgh), and Dr. Bruce Conard (Vale's Vice President of Environmental and Health Sciences, retired in 2004).

The site champion for the project was Greg Nault, Superintendent of Maintenance, who was chiefly responsible for interfacing with Stobie mine personnel.. He communicated regularly with the Stobie Mine superintendent of operations, Larry Lauzon. Aspects of the project were split into five subjects. The work of the heavy duty mechanics assigned to assist the project in

equipment installation, maintenance and data logging were organized by Rick Mayotte, who reported to the Maintenance General Foreman.

Training of personnel (for example, the vehicle operators) was conducted by a team supervised by Ken Zayette.

Ventilation and industrial hygiene measurements were conducted and/or supervised by Denis Lefebvre.

Specific attention to worker safety issues was given by Ron Pilon and. Ernie Leduc.

All records pertaining to project business (for example, Minutes of all Stobie project team meetings over four years) were the responsibility of Gilles Bedard.

3.4 Stages of Work

Stage 1: Planning, site preparations and training

The core team from Stobie conducted weekly status meetings throughout the project life (meeting minutes are available for those interested). These meetings reviewed results, discussed problems, forecasted needed work, and adjusted schedules and staff accountabilities. Part of the planning was conducted through Vale's "Management of Change Methodology." The principal task in this method was to conduct hazard analyses of all new equipment being taken underground in order to reduce risks of fire, unwanted emissions, injuries to mining personnel, and equipment damage. (Minutes of these meetings are also available). Included in planning were discussions (negotiations) with engine manufacturers and equipment leasing companies regarding engine warranty criteria. Included in site preparation were fuel preparation areas (where needed) and off-board filter regeneration stations. The training of operators and maintenance personnel in new equipment was organized by Vale's Mines Training Department, assisted by agents from equipment manufacturers where desired. (Training manuals specific to this project were created and are available for those interested.)

Stage 2: Selection of candidate vehicles

Discussions were held with mine management to select vehicles most representative of heavy duty and light duty diesel vehicles used in underground mining. Consideration was given to maximizing the use of the vehicles in production service so that long-term testing of DPF system technologies could be obtained.

Stage 3: Duty cycle monitoring of vehicles

Initially data loggers and sensors were installed on the six selected vehicles to record exhaust temperature and pressure. Software for controlling the data loggers was provided by the data logger manufacturer. Training in logger hardware, operation, maintenance, and software was carried out by the manufacturer in association with Vale's Mine Training Department. The data, retrieved weekly from the loggers, was sent via e-mail to the Principal Technical Consultant (A. Mayer) for detailed analysis.

Stage 4: DPF selection

In a meeting at Stobie mine held in November 2000, the logged and analyzed data (duty cycle data) from each vehicle was reviewed by engine manufacturers, emission control equipment manufacturers, Vale and non-Vale technical personnel and consultants. The outcome of this meeting was the selection of the DPF systems individually matched to the six test vehicles. Details of this meeting are in Appendix A.

Stage 5: Installation of DPFs

With guidance supplied by the manufacturers and technical consultants, Vale project personnel installed each DPF system over the course of several months. Equipment manufacturers were invited to Stobie to assist in installation and to train maintenance personnel in specific requirements of each system.

Stage 6: Production use and regeneration logging

Vehicles were put into normal operation except that vehicle operators were trained to keep a log of operational performance for each shift. Each use of an active regeneration system was recorded in a log book.

Stage 7: Periodic monitoring by maintenance personnel

After every 250 hours of vehicle operation, a preventive maintenance procedure was carried out on the vehicle, its engine, its data logger and sensors, and its DPF system. Measurements of undiluted tailpipe gases and opacity/smoke were carried out by Vale maintenance personnel.

Stage 8: Industrial hygiene monitoring of mine air

Even though the vehicles being used were not in an isolated area of the mine away from non-DPF-equipped vehicles, attempts were made to determine if the air in the mine in the immediate area around the DPF test vehicle exhibited a lower DPM concentration as a result.

Stage 9: Detailed DPF efficiency measurements

Three times during the four-year project more comprehensive exhaust measurements were conducted in conjunction with NIOSH scientists. Most measurements were made upstream and downstream of the DPF so the effect (reduction efficiency) of the DPF on the measured exhaust components could be determined. These measurements included particulate concentrations, particle size distributions, gaseous components (NO, NO_2, CO, CO_2, and O_2), exhaust opacities, and smoke numbers.

Stage 10: DPF post-use analysis

At the end of the project the DPFs were removed and sent to Natural Resources Canada (CANMET) for detailed physical examination and laboratory testing of efficiency. Where possible, DPF manufacturers were invited to examine the internal state of their filters to determine either the mode of failure (for those that failed during the project) or to determine the internal status of a filter (for those exhibiting a good efficiency at the end of the project).

Stage 11: Integrate results and form conclusions

Stage 12: Technology Transfer

Near the end of the project, in July 2004, interested parties were invited to attend a workshop to review the results of the Stobie testing. A summary of this workshop is in Appendix B.

Stage 12: Write Final Report

4. Selection of Vehicles for DPF System Testing

4.1 Criteria for vehicle selection

Since the objective of the DEEP research was ultimately to explore methods that greatly reduce DPM in underground hard-rock mines, it follows that the Stobie project should be testing DPF systems on those vehicles that are the greatest contributors to DPM concentrations. Two classes of vehicles meet this criterion: heavy duty production vehicles, and increasingly numerous light duty utility vehicles. Heavy duty vehicles, typically the LHDs, use large horsepower engines which have significant quantities of exhaust. The light duty vehicles which use small engines, are quite numerous, run about throughout the mine, and emit a disproportionately higher fraction of DPM for their size.

The vehicles had to be in good condition and were to be neither the oldest nor the newest. Older vehicles were excluded because they were considered to be "on-the-way-out" and would not represent a significant portion of a fleet within a few years. While newer vehicles (and engines) might be perceived as being the best choice, the project did not want to use a vehicle that had not already put in some work and had its "newness" worked out so that it could be expected to log significant operating hours.

The selected vehicles had to have an expectation of heavy use so that the DPF systems being tested could incur a significant portion of their service life within the project duration. LHDs are used extensively in underground mining. The Atlas Copco Wagner ST8B scoop is commonly used throughout the mining industry to perform high load jobs such as mucking. A variety of engines may be used to power an LHD and in general both older and newer engines are found in a mine's production fleet. Thus the Stobie project selected LHDs which used an older Deutz engine and a newer electronically-controlled Detroit Diesel engine.

Haulage trucks are also common heavy duty vehicles and the project initially selected a 26 ton 4-wheel drive end-dump truck as being representative of such vehicles. Unfortunately, this truck was retired from service shortly after the project was started, and no substitute truck could be found.

The project also included light duty vehicles for DPF system testing because their contribution to the total underground horsepower (and DPM) was increasing, and because the companion DEEP project at Brunswick mine had not included such vehicles. The selection of individual light duty vehicles for DPF testing was not as critical as for the heavy duty vehicles because their exhaust temperatures precluded the use of passive DPFs. Therefore the detailed character of its duty cycle was not as relevant for DPF selection as it was for heavy duty vehicles. Tractors commonly used at Stobie for personnel transport were determined to be good light duty vehicles for the project.

The selected vehicles also had to be accessible for servicing that might be required. In the case of certain DPFs it was also necessary to ensure that the vehicle could be routinely returned to a certain place within the mine to receive active regeneration of its DPF.

A final criterion was that all vehicles chosen had to be able to be taken out of production for a week's time annually for special emission testing with NIOSH scientists.

4.2 Vehicles selected

Each vehicle used underground has a Vale vehicle number. The selected vehicles, Table 1, were all subjected to duty cycle monitoring required for DPF system selection.

Table 1: Vehicles selected for duty cycle monitoring

Vale #	Vehicle service class	Engine
820	LHD	Deutz (12 cyl)
445	LHD	DDEC 60
362	LHD	DDEC 60
735	Haulage truck	Deutz (12 cyl)
621	Kubota tractor	Kubota
2180	Kubota tractor	Kubota

Specifications of these vehicles are given below.

LHD #820: Atlas Copco Wagner Scooptram™ ST8B, shown in Figure 7 with specifications shown in Table 2.

Vehicle service:	heavy-duty, LHD
Engine:	Deutz F12L-413FW
Engine displacement:	19.14 L
Engine Type:	12 cylinders, V configuration, 4 stroke, mechanically controlled, turbocharged
Rated Power:	280 HP @ 2300 rpm
Transmission:	Automatic

Figure 7: Vehicle #820, Wagner ST8B scooptram with Deutz F12L-413FW engine.

Table 2: Specifications for #820 Wagner ST8B scooptram

WAGNER

TECHNICAL SPECIFICATION – STANDARD

ST-8B

Diesel Scooptram®

Capacity	kg	(lbs)
Breakout Force, Digging	22371	(49,327)
Tramming Capacity	13608	(30,000)

Bucket – S.A.E. Rating	m3	(yd3)
Nominal Heaped	6.5	(8.5)
Struck	5.4	(7.0)
Boom Raising Time	6.8 Seconds	
Boom Lowering Time	8.0 Seconds	
Bucket Dump Time	7.0 Seconds	

Vehicle Speeds – Loaded
Forward or Reverse with 3% Rolling Resistance

Gear	1st	2nd	3rd	4th
Speed in km/h	4.7	8.0	13.4	22.3
Speed in mph	2.9	5.0	8.3	13.9

Gradeability
Maximum ..... See Performance Curve

Engine
Deutz Diesel F12L-413FW
MSHA Power Rating @ 2,300 rpm ..... 207 kW (277 hp)
Maximum Torque @ 1,500 rpm ..... 975 Nm (719 ft-lbs)
Number of Cylinders ..... 12, In "V"
Displacement ..... 19.1 L (1,168 in3)
Cooling ..... Air
MSHA Ventilation ..... 679 m3/min (24,000 cfm)

Exhaust Conditioner
Catalytic Purifier Plus Exhaust Silencer

Electrical System
24 Volt Starting, 24 Volt Accessories

Torque Converter
Single Stage, Clark ..... C-8000 Series

Transmission
Modulated Power Shift, 4 Speeds Forward/Reverse
Clark ..... 5000 Series

Axles
Spiral Bevel Differential, Full Floating, Planetary Wheel End Drive
Rock Torque® ..... 508 Series

Standard Brakes
Service ..... SAHR®
Spring Applied Hydraulically Released; Fully Enclosed, Force-Cooled Multiple Wet Discs at Each Wheel End
Parking and Emergency ..... Same (SAHR)

Tires
Tubeless, Nylon, Smooth Tread Design, For Underground Mine Service, On Demountable Rims
Tire Size, Front & Rear ..... 26.5 x 25, 32 Ply, L-5S

Steering
Articulated Hydraulic Power Steering, Pilot Operated, Monostick Control
Turning Angle ..... 85° (42.5° each way)
System Pressure ..... 15.8 MPa (2,300 psi)

Hydraulic System
Dump and Hoist Control ..... Pilot Operated, Single Lever
Cylinders ..... Double Acting, Chrome Plated Stems
Steering Cylinders (2) Diameter ..... 152 mm (6.0 in)
Hoist Cylinders (2) Diameter ..... 228 mm (9.0 in)
Dump Cylinder (1) Diameter ..... 228 mm (9.0 in)
Pumps ..... Heavy Duty Gear Type
Dump/Hoist ..... 208+208 lpm (110 gpm) @ 2,200 rpm
Steering ..... 208 lpm (55 gpm) @ 2,200 rpm
Filtration ..... Pilot Flow: 10 Micron; Suction: 25 Micron
Dump/Hoist System Pressure ..... 13.8 MPa (2,000 psi)

Tank Capacities	liters	(gallons)
Fuel	380	(100)
Hydraulic	360	(95)

Oscillation
Rear Axle, Trunion Mounted, Synthane Bushings
Degree of Oscillation ..... Total 18°

Operator's Arrangement
Side Seating For Bi-Directional Operation and Maximum Visibility

Operating Weight	kg	(lbs)
Empty, Approximate	36750	(81,020)

Manufactured with an MSHA Title 30, Part 32, (Schedule 24) Certified Engine.
Under our policy of continuous improvement, we reserve the right to change specifications and designs without prior notice.

LHDs #362 and #445: Atlas Copco Wagner ST8B Scooptrams, shown in Figure 8 with specifications given in Table 3.

Vehicle service:	Heavy duty, LHD
Engine:	DDEC Series 60
Engine displacement:	11.1 L
Engine Type:	6 cylinders, in-line, turbocharged
Rated Power:	325 HP @ 2100 rpm (engines are derated to 285 HP)
Transmission:	Automatic

Figure 8: Vehicle #362 (left) and #445 (right) - Wagner Scooptrams with DDEC 60 engines.

Table 3: Wagner scooptram specifications for vehicle with DDEC 60 engine (derated to 285 HP).

Capacity	**kg**	**(lbs)**
Breakout Force, Digging	22371	(49,327)
Tramming Capacity	13608	(30,000)

Bucket – S.A.E. Rating	**m3**	**(yd3)**
Nominal Heaped	6.5	(8.5)
Struck	5.4	(7.0)
Boom Raising Time	6.8 Seconds	
Boom Lowering Time	8.0 Seconds	
Bucket Dump Time	7.0 Seconds	

Vehicle Speeds – Loaded

Forward or Reverse with 3% Rolling Resistance

Gear	**1st**	**2nd**	**3rd**	**4th**
Speed in km/h	5.3	9.0	15.1	24.6
Speed in mph	3.3	5.6	9.4	15.3

Gradeability

Maximum ..... See Performance Curve

Engine

Detroit Diesel ..... Series 60
MSHA Power Rating @ 2,100 rpm ..... 242 kW (325 hp)
Maximum Torque @ 1,200 rpm ..... 1559 Nm (1150 ft-lbs)
Number of Cylinders ..... 6 In Line
Displacement ..... 11.1 L (677 in3)
Cooling ..... Water
MSHA Ventilation ..... 992 m3/min (35,000 cfm)

Exhaust Conditioner

Catalytic Purifier Plus Exhaust Silencer

Electrical System

24 Volt Starting, 24 Volt Accessories

Torque Converter

Single Stage, Clark ..... C-8000 Series

Transmission

Modulated Power Shift, 4 Speeds Forward/Reverse
Clark ..... 5000 Series

Axles

Spiral Bevel Differential, Full Floating, Planetary Wheel End Drive
Rock Torque® ..... 508 Series

Standard Brakes

Service ..... SAHR®
Spring Applied Hydraulically Released; Fully Enclosed, Force-Cooled Multiple Wet Discs at Each Wheel End
Parking and Emergency ..... Same (SAHR)

Tires

Tubeless, Nylon, Smooth Tread Design, For Underground Mine Service, On Demountable Rims
Tire Size, Front & Rear ..... 26.5 x 25, 32 Ply, L-5S

Steering

Articulated Hydraulic Power Steering, Pilot Operated, Monostick Control
Turning Angle ..... 85° (42.5° each way)
System Pressure ..... 15.8 MPa (2,300 psi)

Hydraulic System

Dump and Hoist Control ..... Pilot Operated, Single Lever
Cylinders ..... Double Acting, Chrome Plated Stems
Steering Cylinders (2) Diameter ..... 152 mm (6.0 in)
Hoist Cylinders (2) Diameter ..... 228 mm (9.0 in)
Dump Cylinder (1) Diameter ..... 228 mm (9.0 in)
Pumps ..... Heavy Duty Gear Type
Dump/Hoist ..... 200+200 lpm (105 gpm) @ 2,100 rpm
Steering ..... 200 lpm (52 gpm) @ 2,100 rpm
Filtration ..... Pilot Flow: 10 Micron; Suction: 25 Micron
Dump/Hoist System Pressure ..... 13.8 MPa (2,000 psi)

Tank Capacities	**liters**	**(gallons)**
Fuel	379	(105)
Hydraulic	360	(95)

Oscillation

Rear Axle, Trunion Mounted, Synthane Bushings
Degree of Oscillation ..... Total 18°

Operator's Arrangement

Side Seating For Bi-Directional Operation and Maximum Visibility

Operating Weight	**kg**	**(lbs)**
Empty, Approximate	39474	(87,040)

Manufactured with an MSHA Title 30, Part 32, (Schedule 24) Certified Engine.
Under our policy of continuous improvement, we reserve the right to change specifications and designs without prior notice.

Tractors # 621 and #2180: Kubota Tractors (M-5400), shown in Figure 9 with specification given in Table 4.

Vehicle service:	light-duty, man and material transport
Engine:	Kubota Model F2803-B
Engine displacement:	2.7 L
Engine Type:	4 cylinder, in-line, 4 stroke, mechanically controlled, naturally aspirated
Rated power:	55.5 HP @ 2700 rpm
Transmission:	Manual

Figure 9: Vehicles #621 (left) and #2180 (right) - Kubota tractors

Table 4: Specifications for Kubota tractors

SPECIFICATIONS

Model			M4700		M5400	
			2WD	4WD	2WD	4WD
PTO power (Factory observed)			31.3 kW (42 HP, 2600 rpm)		37.3 kW (50 HP, 2700 rpm)	
Engine	Model		F2803-LA		F2803-A	
	Type		Vertical, water-cooled, 4-cycle diesel engine			
	Number of cylinders		3			
	Total displacement		2746 cm³ (167.6 cu.in.)			
	Bore and stroke		87 x 92.4 mm (3.4 x 3.6 in.)			
	Engine rated output		35.1 kW (47 HP)		40.3 kW (54 HP)	
	Rated revolution		2600 rpm		2700 rpm	
	Maximum torque		158 N·m (16.1 kgf·m, 116.5 ft-lbs)/ 1400 to 1600 rpm		175 N·m (17.9 kgf·m, 129 ft-lbs)/ 1400 to 1600 rpm	
	Battery		CCA 615 K, RC150 min (12 V)			
	Fuel		Diesel fuel No.1-D [below -40 °C (15 °F)] Diesel fuel No. 2-D [above -10 °C (15 °F)]			
	Fuel tank capacity		65 L (17.2 U.S.gal., 14.3 Imp.gal.)			
	Engine crankcase capacity		8.0 L (8.5 U.S.qts., 7.03 Imp.qts.)			
	Engine coolant capacity		6.2 L (6.6 U.S.qts., 5.7 Imp.qts.)		8.0 L (8.5 U.S.qts., 7.03 Imp.qts.)	
Dimensions	Overall length		3495 mm (137.6 in.)	3405 mm (134.1 in.)	3495 mm (137.6 in.)	3405 mm (134.1 in.)
	Overall width (Minimum tread)		1700 mm (66.9 in.)		1650 mm (65.0 in.)	
	Overall height (with ROPS)		2357 mm (93.0 in.)		2375 mm (93.5 in.)	
	Wheel base		2000 mm (78.7 in.)			
	Tread	Front	1420 to 1620 mm (55.9 to 71.7 in.)	1330 mm (52.4 in.) 1430 mm (56.3 in.)	1420 to 1620 mm (55.9 to 71.7 in.)	1330 mm (52.4 in.) 1430 mm (56.3 in.)
		Rear	1420 to 1720 mm (55.9 to 67.7 in.)			
	Minimum ground clearance		430 mm (16.9 in.) (BRACKET DRAWBAR)		460 mm (18.1 in.) (BRACKET DRAWBAR)	
Weight (with ROPS)			1650 kg (3637 lbs)	1800 kg (3968 lbs)	1730 kg (3813 lbs)	1850 kg (4078 lbs)
Traveling system	Standard tire size	Front	6.5-16	9.5-22	7.5-16	9.5-22
		Rear	14.9-28		16.9-28	
	Clutch		Dry, Single plate			
	Steering		Full hydrostatic power steering			
	Transmission		Shuttle synchromesh, 8 forward and 4 reverse			
	Brake	Travelling	Wet type, multiple discs (mechanical)			
		Parking	Connected with the travelling brake			
	Differential		Bevel gears (with differential lock)			
Hydraulic system	Hydraulic control system		Position, draft and mix control			
	Pump-up capacity		34.7 L (9.2 U.S.gal., 7.6 Imp.gal.)/min.		41.6 L (11.0 U.S.gal., 9.2 Imp.gal.)/min.	
	Three point hitch		Category I & II			
	Maximum lifting force		1900 kg (4189 lbs) at lower link end 1500 kg (3307 lbs) at 610 mm (24 in.) behind lifting point			
	System pressure		18.6 MPa (190 kgf/cm², 2702 psi)			
PTO	Independent clutch		Wet type, multiple discs			
	Live PTO	Direction of turning	Clockwise, viewed from tractor rear			
		PTO speed	540 rpm at 2295 engine rpm			
Traction system			Swing drawbar, adjustable in direction			

11790200040

Truck #735: Eimco Jarvis Clark 26 Ton Truck, with specifications shown in Figure 10.

Vehicle used as:	Heavy duty: Ore transport
Engine:	Deutz F12-413FW
Engine displacement:	19.1 L
Engine Type:	12 cylinder, V-configuration, air cooled, turbocharged
Rated power:	277 HP @ 2300 rpm
Transmission:	Automatic

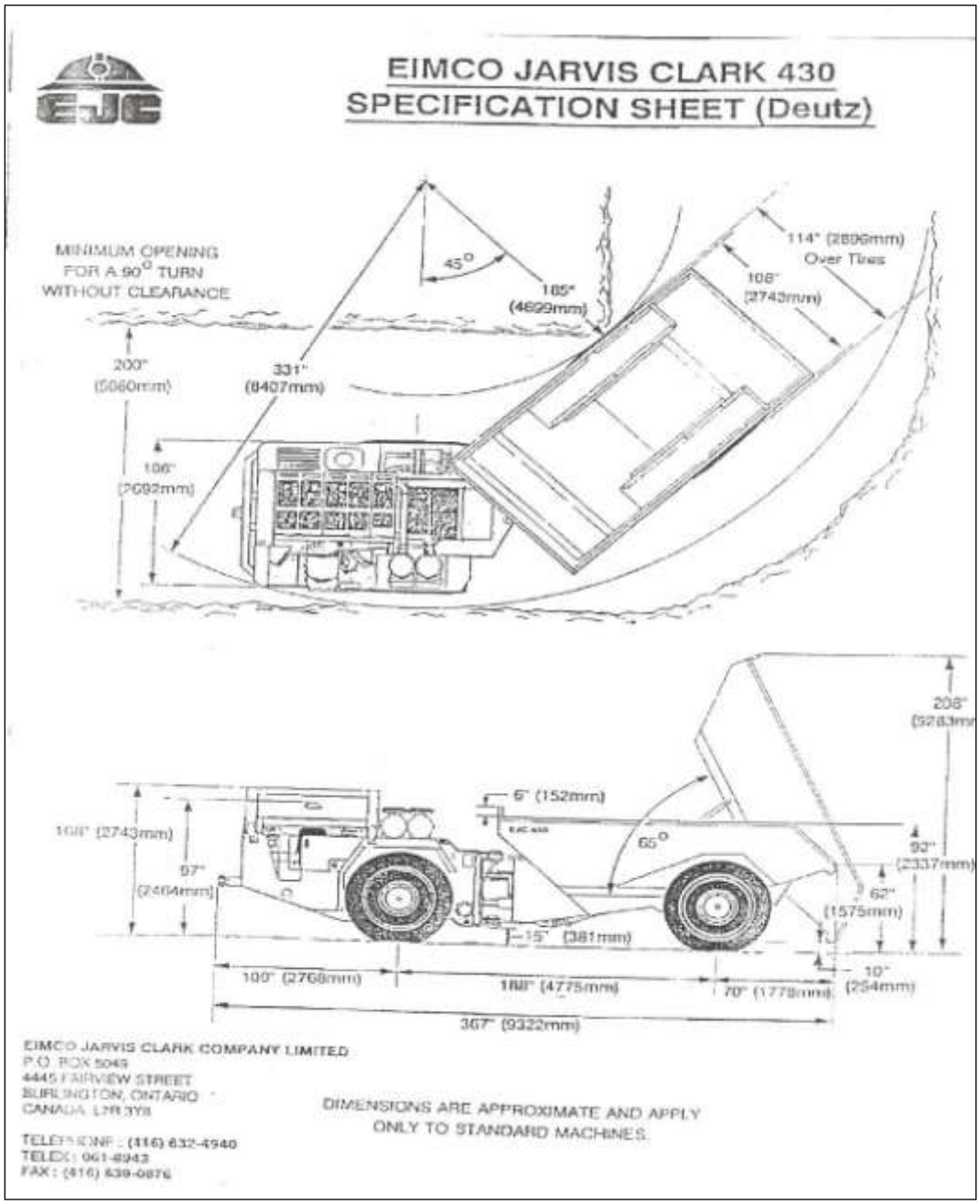

Figure 10: Vehicle #735 Eimco 26-Ton Truck

5. Duty Cycle Monitoring

5.1 Sensors and Data loggers

The European VERT Project had motivated the development of a new data logger with the ability to accept relevant measured diesel engine variables and with appropriate software for interactive, archival, and data presentation options. With extensive experience gained in working with VERT, Paul Nöthiger Electronic was contracted to supply the technology for the data loggers and sensors. Data were collected on two exhaust temperatures (before and after muffler or DPF once that was installed), exhaust backpressure before the muffler or DPF, and engine RPM.

5.1.1 Sensors

The temperature sensors, Figure 11 were Heraeus, type TS-200 EGTS, with a range of -40 to 1000 °C and an accuracy of ±1.5%. The sensor tip was placed into the center of the exhaust stream through a female stainless steel A 182-68 nut, welded to the exhaust pipe. The signal sensitivity was > 1mV per °C.

Figure 11: Temperature sensor

The temperature sensors were installed in the exhaust pipe at the muffler inlet and outlet (the DPF system was to be inserted in place of the muffler). The port for pressure sensing was installed on the engine side of the muffler (see Figure 12). The RPM signal was taken from the alternator.

The pressure sensor initially installed was a Series BT8000 from Sensor Technics. It had an operating pressure of 0-1 bar (relative to atmospheric pressure) and a response time of 1 millisecond. Limitations on its use were from -40^{o}C to 100^{o}C, 0-98% relative humidity, and 50 grams mechanical shock. The output signal was in the range 0-10 volts. Unfortunately, this sensor showed signal drift and possible adverse effects from vibration that could not be corrected by the U.S. manufacturer. Consequently, replacement pressure sensors were obtained from Keller/Winterthur. The pressure sensor was located inside the data logger box shown to the left of the green circuit board in

Figure 13 and was connected by a hose, a water drop-out trap, to the port on the exhaust pipe.

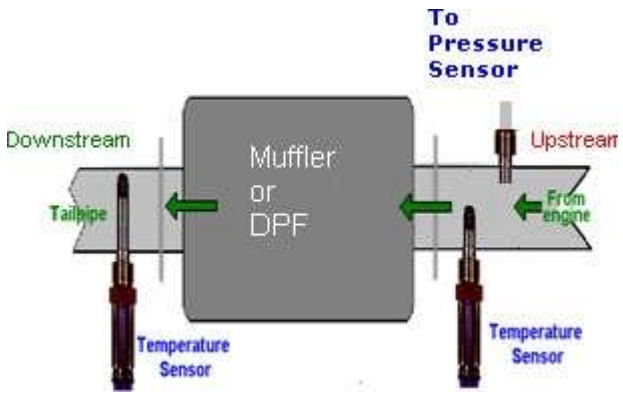

Figure 12: Positions of the sensors. The DPF replaces the original muffler and is installed to minimize the distance from the engine manifold.

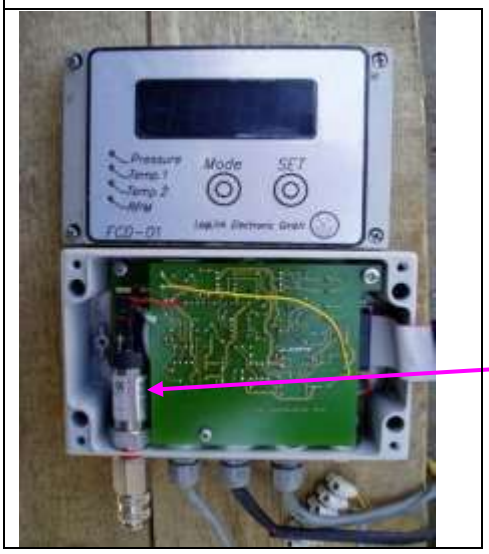

Figure 13: Pressure sensor located inside data logger housing at the lower left.

Pressure sensor

5.1.2 Data loggers

Model FCD-001 of the data logger from Paul Nöthiger Electronics is shown inside its protective case (made at Stobie) in Figure 14 and as received in Figure 15.

Figure 14: Data logger shown inside protective box with the cover off.

Figure 15: As-received data logger. The five I/O ports (left to right) are for pressure, two temperature sensors, engine rpm, power, and alarm outputs.

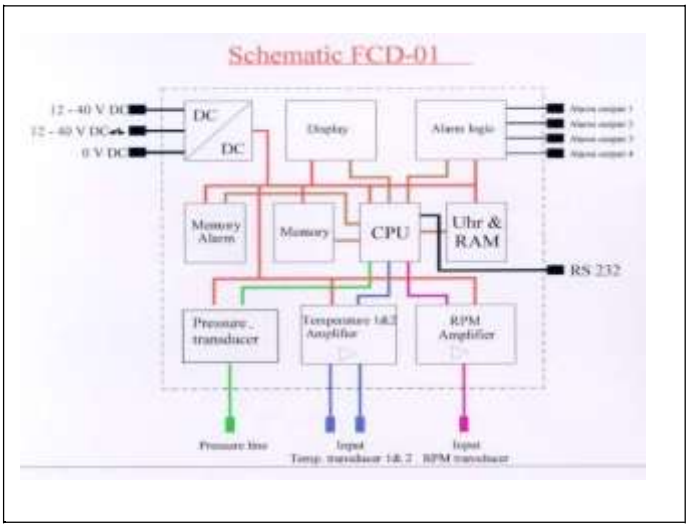

Figure 16: Schematic diagram of data logger.

The block component diagram for a data logger FCD-01 is shown in Figure **16.** Typically exhaust backpressure, temperature before and after muffler/DPF, and engine rpm were scanned by the logger approximately every second. The ranges of the parameters were 0-500 mBar backpressure, 0-750^{o}C temperature, and 0-8000 rpm. The values of each signal were stored in the working memory (RAM). One data channel could be viewed during real time data collection. The maximum values of the parameters were stored permanently in memory until reset by the user. An alarm module was used to compare the present value of a parameter to a pre-determined upper limit. The alarm could be used simply to alert the operator visually and/or audibly, and it could also be used to control the engine to prevent possible damage should excessive values occur for prolonged periods.

The data logger could be powered by 12-40 volts direct current. The vehicle batteries were used and power maintained when vehicle was shut down so that cool-down of the engine could be observed. Having the data loggers remain on when the vehicle was not operating also allowed examination of the possible shifts in signal stability with prolonged exposures to high humidity and other environmental factors. Once DPFs were installed, loggers only operated when vehicle was running.

Because of its development during the VERT project, the data logger had the following beneficial features:

- Extended data storage
- Intelligent alarm processing
- Remote data collection
- Temperature resistance
- Vibration resistance
- Anti-tampering devices

After being constructed in Switzerland, each data logger was vibration tested, subjected to temperature cycling, calibrated using high-precision standards, and its systems checked for data storage, downloading capability, and general software performance. Each data logger was also installed for 48 hours on an in-use heavy duty vehicle to ensure its ruggedness before being shipped to Stobie mine.

5.2 Software

The software used to retrieve and work with the FCD-01 data logger was supplied by Loglink Electronic GmbH. running under Windows 95/98. The main menu of the software included:

Logger:	Used for interacting with the data logger
Export:	Used to create data in an ASCII format
Graphic:	Used to display graphs of data
E-mail:	Used to send data via e-mail to other parties
Settings	Used to input or change data logger settings

An example of the sub-menu appearing when “Logger” was selected from the main menu:

Technical Data:	Showed collected data
Logger Read:	Extracted data from the logger
Logger Clear:	Deleted stored data
Alarm-Store Read:	Extracted alarm data
Alarm-Store Clear:	Deleted alarm data
Logger Configuration:	Allowed logger settings to be made
Real-time read:	Showed instantaneous values

The Graphics menu could display either direct LogLink data or ASCII data as a function of time. A zoom feature allowed closer inspection of information by reducing the time interval shown on the display. An example of graphical information is shown in Figure 17.

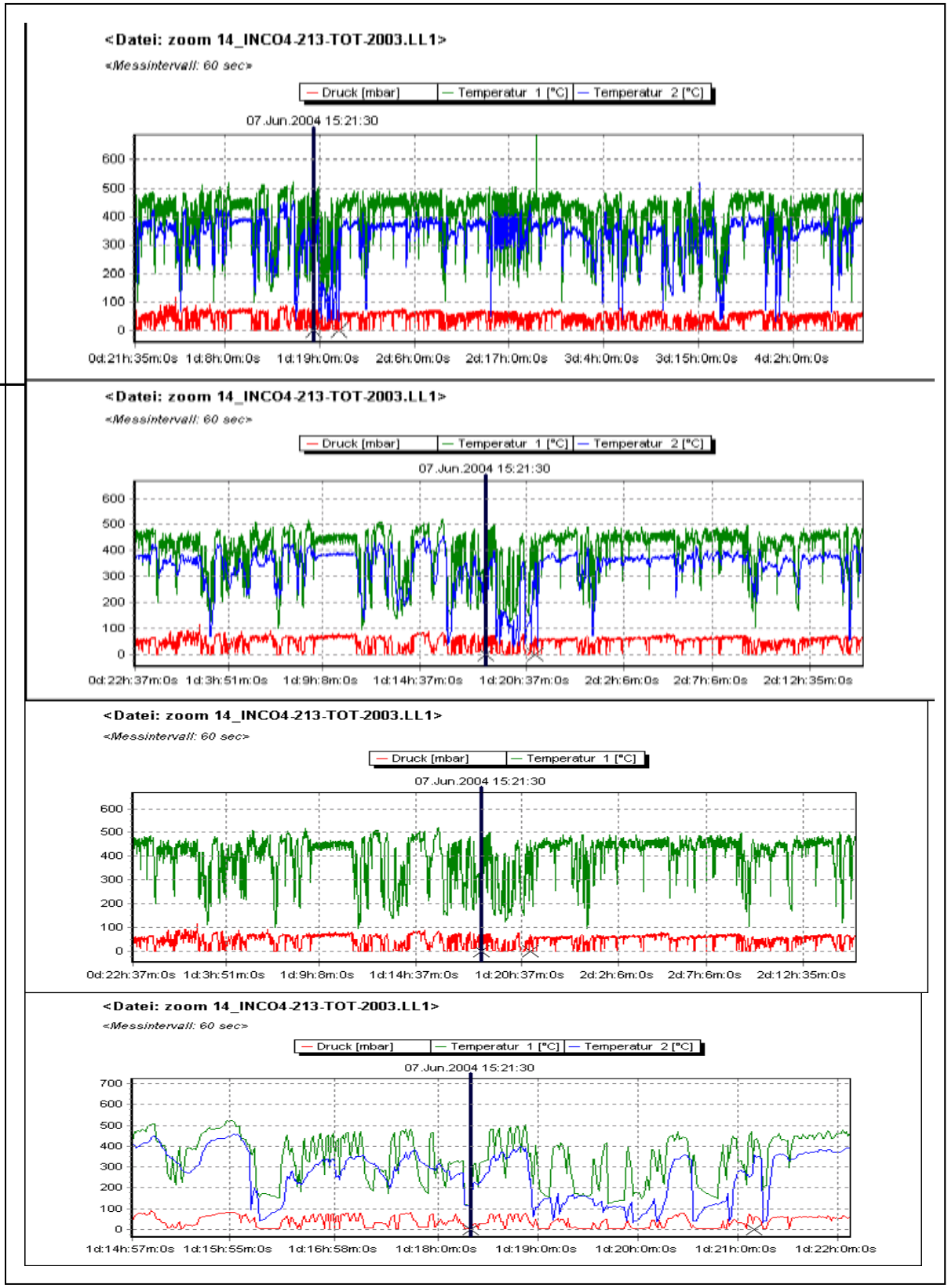

Figure 17: Data displays showing zoom capabilities. Each comes from LHD #213 (replaced #445) around 07 June 2004 and is centered about 15h:21m:30s shown in each display as a solid vertical black line. The exhaust data shown are inlet temperature (green), outlet temperature (blue) and backpressure (red).

5.3 Installation

Data logger installation was started in April 2000 during a visit to Stobie by P. Nöthiger and A Mayer. The data loggers were positioned on each vehicle to allow reasonably easy access while not interfering with normal duties of the vehicle operator. Examples of data logger installations are shown in Figure 18 and Figure 19.

Figure 18: Installation of data loggers on LHDs.

Figure 19: Installation of data logger just behind driver's seat on a Kubota tractor

5.4 Training

During the visit by P. Nöthiger and A. Mayer, significant time was spent with Vale's Training Department in order to write a Training Manual for the data loggers. This manual is the property of Vale and liability issues restrict its direct use by other parties. However, for the purposes of information, interested parties can obtain the manual on request.

Fifty-one people were put through a Vale training program on the data logger operation. These people were from departments such as ventilation, maintenance, operations, and management.

5.5 Data treatment

All data records were routinely downloaded by Stobie project personnel and were transmitted electronically to A. Mayer and P. Nöthiger in Switzerland. The following types of data treatment were performed by A. Mayer:

- Early in the data processing the temperature channels were switched during data transfer due to a loss of one byte of information during data downloading. This problem was quickly solved by a software repair; for the data already downloaded, the switched channels were re-assigned their correct labels in the transferred files.
- Often data spikes occurred due to stray voltage. These spikes were eliminated so that appropriate statistical parameters could be accurately calculated.
- Early in the data processing, sometimes the amount of data exceeded the pre-set limit. This was corrected in the software, and the data exceeding the limit were recovered.
- Data from engine "off" conditions were deleted from the data records in order to calculate proper statistics for the engine "on" conditions. Criteria for excluding engine "off" were that the exhaust temperature was <50 °C, and the exhaust backpressure was <5 mbar.
- The data logger converted the analog sensor voltages to digital values every second. Sometimes it was advantageous to set the data logger to log the data at less frequent intervals. In this case only the highest value of the 1-second digital values over the longer interval was logged. Selecting the highest/peak value ensured that the worst case data for backpressure was captured since backpressure was a critical parameter for DPF performance and status. [It is noted that it would be advantageous to have capability for selecting different values for different measured parameters. For example, being able to select the mean temperature, instead of the highest temperature, during the measuring period would have been preferred, but doing more than peak capture would involve more complex digital processing.]
- Statistical analyses were then performed on the data resulting from all of the above. Calculations for each parameter included: mean value, standard deviation of the mean, median value, range of values, and frequency distributions and frequency dwell times.

Examples of treated ("cleaned") data are shown in Figure 20, which contains the entire history (logged record) of the exhaust temperature upstream of the muffler for LHD #445 prior to installation of a DPF system. The data cover 21,313 min (335.2 hr) of monitoring. This record includes many shifts by many operators. The variations in temperature show the essential characteristic of the operation of the scoop, covering periods of full power and other periods of extensive idling. Included in this history are also differences in driving habits of different operators. Interestingly, the high peak temperatures expected for a fully loaded engine were not seen by the sensor despite the fact that this LHD was periodically operating under peak load conditions. The reason for the lower than expected temperatures are that the high loads lasted only a relatively short time and that the relatively small volumes of very hot gases produced are being cooled by the thermal inertia of the exhaust manifold and tailpipe before the muffler. The absence of high temperatures for a heavy duty LHD is extremely important in deciding whether passive DPF systems could work.

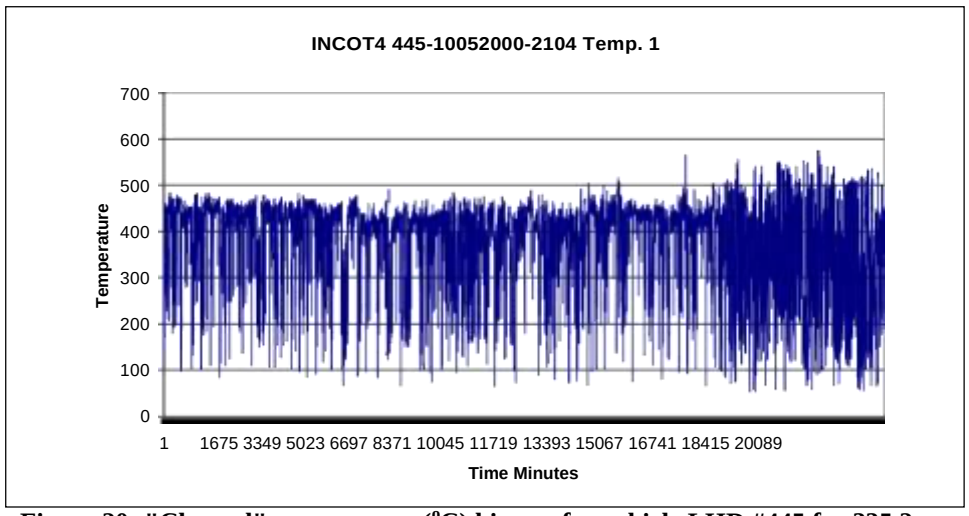

Figure 20: "Cleaned" temperature (°C) history for vehicle LHD #445 for 335.2 hours of duty cycle monitoring.

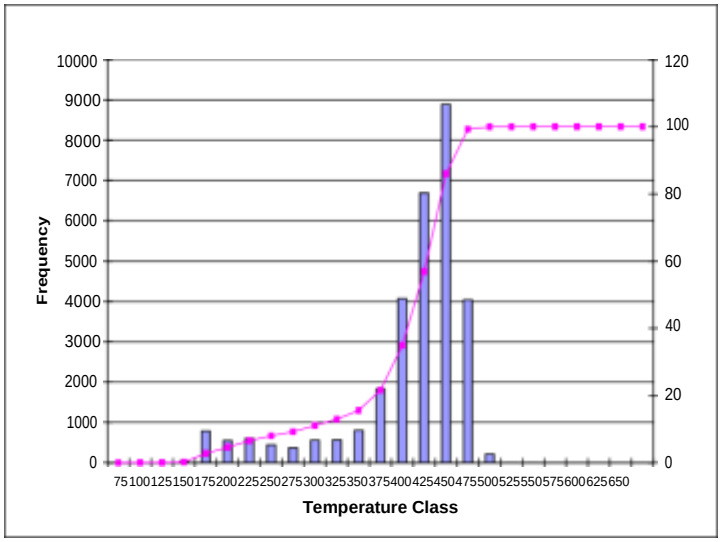

Figure 21: Simple temperature frequency distribution for data logged at 1 second intervals. Vertical bars show the number of observed temperatures in each temperature range. For example, the bar associated with the range 387.5 to 412.5°C temperatures in this range occurred just over 4000 times. The red points and line show the cumulative number of observations as a function of temperature as a percentage of total observations. For example, approximately 20% of the observations are <375°C.

An example of a simple frequency distribution for these same temperature data is shown in Figure 21. The frequency distribution, however, must be interpreted cautiously. One cannot conclude, for example, that because 60% of the observations are above 400 °C that these are exclusively the result of a number of continuous periods above this temperature. If this result is assumed, it could falsely lead believing that a passive DPF (using a catalyst) could be effectively regenerated by such temperatures. The flaw in reaching this conclusion is that the number of times the temperature is >400°C says nothing about the length of time the temperature stays above 400°C for each episode. That is, 4000 measurements in the range of 400°C ± 12.5°C could represent a single episode containing a continuous 4000 seconds or it could represent 4000 different episodes where >400°C occurred for only 1 second, or it could represent anything in between these two extremes. It is known that successful passive regeneration of some DPF require a significantly prolonged episode of exhaust temperatures >400°C. The simple frequency distribution fails to give the information critical in assessing the duty cycle for passive regeneration.

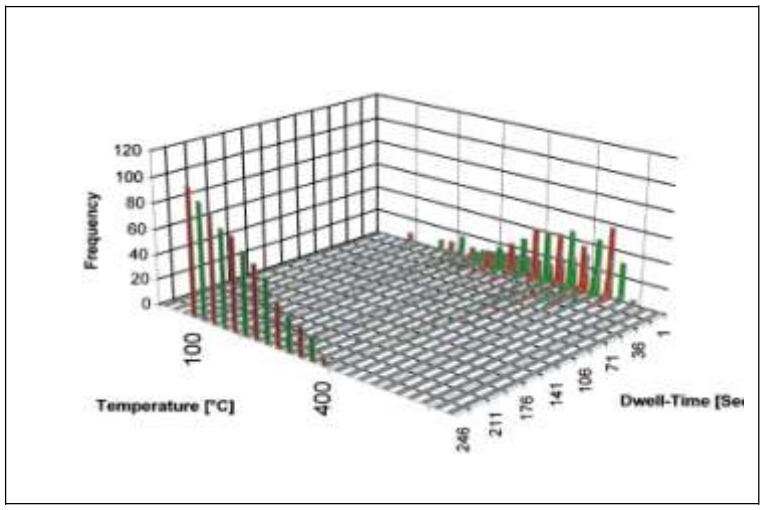

Figure 22: Temperature and dwell time frequency distribution for LHD #445 using 1 second data collection interval.

A. Mayer, during his work with VERT work, developed an additional way to analyze the data by including the determination and presentation of the dwell time, or number of consecutive times, the exhaust spent within a given temperature range. The dwell time frequency distribution is presented as a three-dimensional diagram, where the third dimension is the dwell time added to the previous simple temperature frequency distribution, as shown in Figure 22.

This graph allows one to see that the highest temperatures are usually associated with very short dwell times (on the order of tens of seconds) and that such dwell times would be insufficient to overcome the thermal inertia of the filter medium and to sustain these temperatures for the time necessary to ignite and completely burn the collected soot. An improved diagram, Figure 68, was developed for data interpretation after DPF systems had been installed.

5.6 Results

The duty cycle monitoring results for the selected vehicles during April-September 2000 are shown in Table 5 and Table 6.

Table 5: Exhaust temperatures of test vehicles obtained from duty-cycle monitoring, logged every second.

Vehicle #	Vehicle description	Hours	T1 ^{o}C Mean	T1 ^{o}C Max/Min	T2 ^{o}C Mean
735	26 ton Truck	27.3	233	477/78	223
820	LHD	183.3	313	498/51	313
2180	Tractor	294.0	159	543/57	147
621	Tractor	363.8	No data	No data	No data
362	LDH	453.2	366	465/135	364
445	LHD	592.1	341	468/66	338

Table 6: Exhaust temperatures of test vehicles obtained from duty-cycle monitoring, peak temperature for 60, 1-sec samples logged every 60 sec.

Vehicle #	Vehicle description	Hours	T1 ^{o}C Mean	T1 ^{o}C Max/Min	T2 ^{o}C Mean
735	26 ton Truck	27.3	No Data	No Data	No Data
820	LHD	183.3	329	615/54	328
2180	Tractor	294.0	192	609/51	178
621	Tractor	363.8	203	606/54	178
362	LHD	453.2	370	549/57	378
445	LHD	592.1	382	579/60	356

5.7 Conclusions

(1) The low hours on truck #735 was due to general maintenance problems with this truck. The truck was taken out of service by the mine in the summer of 2000 and no substitute vehicle was available.
(2) Passive DPFs using a catalyst to reduce soot ignition temperature might be successfully used on the LHDs, but detailed examination of the data show that the exhaust temperature variation is large and dwell times are limited, either of which may limit the successful use of passive DPF systems.
(3) Tractors definitely need active DPF systems.
(4) Alarms on backpressure are highly recommended.

6. Selection of Filter Systems

The vehicles selected for DPF system testing, initially included three LHDs, one heavy duty truck and two light-duty tractors. More than fifty manufacturers worldwide offer DPF systems capable of filtering DPM, but this number was reduced significantly by application of several service and performance criteria. In selecting DPF systems for testing, consideration was given to each candidate system's expected reliability, the technical and operational viability under the duty cycle of the vehicle, and effect on noxious gaseous emissions. Important also was reliability shown through experience elsewhere and technical support of the DPF system manufacturer. In addition, the Stobie tests were able to take into consideration its companion DEEP project at Brunswick mine where testing using two LHDs and two trucks was already underway.

6.1 Criteria for initial selections of DPFs

Long term successful operation of a DPF system requires timely regeneration, whether passive or active, be guaranteed. The probability of successful regeneration depends on the method used for regeneration and the compatibility of that method with mine facilities and operation. Factors affecting success and applicability are shown in Table 7.

The strategy employed for selecting DPFs for the Stobie project relied on two principal types of information:

- The experience gained during extensive testing of many systems in Europe by VERT.
- The types of DPFs under test at Brunswick mine because duplication of effort was to be avoided.

Table 7: Critical factors affecting success or application of various DPF regeneration methods.

Regeneration method	Passive (P) or Active (A)	Implementation complexity	Fuel quality	Secondary Emissions (NO_2)	Regeneration Rate	Duty Cycle (Exhaust Temp)	External Mains Power / Air	Additive dosage	Cost	Dependability	Operating logistics
No catalyst	P					XXX					
Noble metal catalyst wash-coat on filter (1)	P		X	XX	X	X					
Base metal catalyst wash-coat on filter (2)	P				X	XX					
Fuel-Borne Catalyst (FBC).	P	X			X	XX		X	X		X
Full exhaust flow fuel burner (in service operation)	A	XXX		X					XX	X	
Fuel burner (idle operation)	A	XX		X	X				XX	X	X
On-board electric heaters (off-service operation) (3)	A	XX					X		XX	X	XX
Off-board oven/kiln/vacuum (DPF swap) (4)	A	X					X		XX	X	XX

Notes: The number of Xs signifies the importance of the factor.

(1) Noble metals, e.g., platinum, reduce ignition temperature the greatest, but tend to increase NO_2 by catalytic oxidation of NO; catalyst effectiveness is reduced by fuel sulfur content and ideally requires fuel with less than 15ppm sulfur.

(2) Base metals are less effective in reducing ignition temperature but have no secondary emissions (NO_2).

(3) Electric heating elements, located on engine side of filter element, are integral to DPF. Regeneration requires substantial electric power which must be supplied from mine and a small air flow. The regeneration control system can be either on-board (imposes space requirement and susceptibility to damage) or off-board and located in convenient and ventilated spot in mine. Initial secondary emissions may be CO and organic vapor before soot ignites completely.

(4) Suitable for small DPF systems. DPF (canister containing filter element) can be removed from vehicle and exchanged for a freshly regenerated DPF. DPF exchange can be quick. DPF is regenerated in a specially designed oven, usually electric, equipped with a vacuum and control circuitry.

6.1.1 VERT Criteria

VERT published (VERT, 2004) results of DPF system testing that met certain broadly accepted criteria. These criteria were:

- Filtration of >95% (new and at 2000 hours service), and EC in the exhaust reduced by >90% when averaged over four operating conditions of the ISO 8178 test cycle.

- No increase in CO, chained hydrocarbons, NOx, dioxins, furans, polycyclic aromatic hydrocarbons and nitro-poly-aromatic hydrocarbons during DPF operation and/or regeneration.

- Opacity of exhaust of <5% during free (no load on engine) acceleration.

- With engine at full speed (maximum exhaust flow), the exhaust backpressures should be
  - For new filter: <50 mbar
  - For operating (containing soot) filter: < 200 mbar (alarm)

- For fuel additives, dosing should be automatic with an interrupt if filter ruptures.

- Muffling capacity is to be equivalent to muffler that is being replaced by the DPF.

- The life expectancy of the DPF system is >5000 hours. Useable hours until ash cleaning was expected to be > 2000 hours.

- Labeling of serial number and manufacturing date must be clearly visible and legible even after prolonged use. Also, flow direction through the DPF canister must be indicated by an arrow and reverse mounting should be prevented by design.

The candidates meeting VERT criteria are listed in Table 8.

6.1.2 Criteria from duty cycle monitoring

For heavy duty vehicles - LHDs: Even though passive DPF systems were favored because of the lack of attention they required, the duty cycle information showed the time spent (dwell time) by the exhaust at soot ignition temperatures was so variable that passive regeneration could not be guaranteed except for possibly one LHD. Thus, except for one DPF system, all others incorporated electric heaters for manual regeneration.

For light duty vehicles - Tractors: The duty cycle data clearly showed exhaust temperatures too low for any passive DPF; active DPF systems were the only viable candidates.

Table 8: Candidate DPF systems meeting VERT criteria. Those marked with an (X) were under test at Brunswick mine.

Heavy Duty - LHDs	Light Duty - Tractors
Engine Control Systems (ECS) Combifilter	ECS-3M Omega
Engelhard DPX2	Diesel Control Limited (DCL) Titan
Oberland-Mangold (X)	Greentop
Diesel Control Limited (X)	
Johnson-Matthey (JM)	
Deutz	
HJS	
HUSS	

6.2 DPF systems selected for testing and selection rationale

Deutz — Chosen for the #735 Truck
Reasons: With the truck having a Deutz engine, it was thought that matching a Deutz DPF system with a Deutz engine was wise. The Deutz DPF has been well-proven in Europe. Deutz DPFs were not tested in Brunswick. Of the various means of regeneration, the Deutz system used a fuel burner in the full exhaust flow ahead of the DPF. The Stobie project team believed that this type of system should be tested.
Deutz, however, chose not to participate in the project.

Johnson-Matthey — Chosen for the #820 LHD
Reasons: The JM DPF system uses a FBC to achieve passive regeneration. Other DPF systems using a FBC were under test at Brunswick, and the JM system was viewed as a competitive system in terms of reliability and operational viability. With the risk of unsuccessful passive regeneration possible, electric heaters were incorporated into the DPF to provide a method of active regeneration should that be necessary.

Oberland-Mangold — Chosen for the #445 LHD
Reasons: This system has a knitted glass fiber filtration medium, which is significantly different than the cordierite/silicon carbide ceramic wall-flow media. It depends on a FBC for passive regeneration. A similar system was under test on a truck at Brunswick and it was thought beneficial to get a comparison on an LHD for the same kind of system.

Engelhard — Chosen for the #362 LHD
Reasons: This passive DPF system uses a noble metal catalytic wash-coat on the cordierite wall-flow filter medium. It appeared to be competitive with similar catalytic coatings under test at Brunswick. The Stobie team

was aware that such catalysts on DPFs can increase exhaust NO_2 concentrations.

ECS-3M — Chosen for the #2180 Tractor
Reasons: This system was seen to be a leading candidate for active systems for light duty vehicles. Additionally the ceramic fiber filter media was unique.

Greentop — Chosen for the #621 Tractor
Reasons: This system has proven to be reliable in Europe and is another leading candidate for active systems.

6.2.1. Vehicle problems

During the project a number of the initial vehicles became unavailable for the following reasons:

#735 Truck: was retired from the Stobie fleet prior to PFS installation; no suitable replacement truck was available.

#445 LHD: was retired by Stobie mine after 2 years of testing.

#621 Tractor: was used infrequently; an identical tractor (#017) was substituted in order to gain more DPF service time.

#2180 Tractor: was replaced by #3013 after about three years because of higher than normal maintenance and concomitant infrequent use

#213 LHD: was buried by a run of ore on 8 November 2004, and was damaged.

#820 LHD: completed testing after 2.5 years; the two DPFs were removed.

Second choices for DPF systems to test were made as a result of operational problems encountered with the first choices. These were:

ECS/Combifilter — Chosen for #445 LHD and #213 LHD
Reasons: to replace poorly performing Oberland-Mangold DPF. The active ECS system tested by Stobie used electric heaters for regeneration instead of a passive ECS Cattrap that used a catalytic wash-coat being tested at Brunswick mines.

ECS/Combifilter — Chosen for #2180 Tractor and #3013 Tractor
Reasons: to replace ECS/3M Omega system after 3M announced its decision to stop production of the Omega line.

DCL-Titan — Chosen for #621 Tractor and #017 Tractor

Reason: to substitute for Greentop, who could not supply their DPF systems under the terms and conditions requested by Stobie.

Arvin-Meritor Chosen for #111 LHD
Reason: to substitute for the Deutz burner active DPF system that was to be installed on #735 Truck. Since a truck was not available at Stobie, an active DPF system by Arvin-Meritor, which also used a fuel burner, was installed on an LHD.

6.2.2 DPF system-vehicle combinations tested

The final configurations of the DPF systems and the vehicles are given in Table 9.

Table 9: Final DPF system-vehicle pairings tested

PFS System Model	Johnson-Matthey DPF 201	Oberland Mangold	ECS/CombifilterS18	ECS/Combifilter S18	Engelhard DPX2	Arvin-Meritor.	ECS-3M Omega	ECS/Combifilter S	DCL Titan
Vehicle #	#820	#445	#445	#213	#362	#111	#2180	#2180 → #3013	#621 → #017
Vehicle type Engine	LHD Deutz (dual exhaust)	LHD DDEC60	LHD DDEC60	LHD DDEC60	LHD DDEC60	LHD DDEC60	Tractor Kubota	Tractor Kubota	Tractor Kubota
Type of DPF	Pass.+act.	Passive	Active	Active	Passive	Active	Active	Active	Active
Filter medium	(a)SiC (b)cordierite	Knitted glass	SiC	SiC	Cordierite	Cordierite	Ceramic fiber	SiC	SiC
Catalyst	Fuel borne	Fuel borne	----------	----------	Filter wash-coat	----------	----------	----------	----------
Active. Regen.	On board electric	----------	On board electric	On board electric	----------	Fuel burner	On board electric	On board electric	Off board electric

7. DPFs: Descriptions and Installations

7.1 Oberland-Mangold

The Oberland-Mangold (O-M) DPF system uses a deep bed filter element made of knitted glass fibers compressed between two perforated tubes to form cartridges. The required number of cartridges is assembled into a filter assembly as shown in Figure 24. The number of cartridges to be included in the DPF was determined by O-M using information on the diesel engine type, age and duty cycle. The unit was mounted on LHD #445 with DDEC 60 engine, Figure 23.

Figure 24: O-M housing containing eight filter cartridges.

Figure 23: O-M filter as installed on LHD #445.

The O-M DPF system used a FBC to promote passive regeneration. As part of the installation procedure, the engine was run for 3-4 hours using 1.27 L of the FBC for 376-379 L of diesel fuel, to fully coat the filter fibers with the platinum-based catalyst. Under normal operation the FBC was dosed automatically from a 12 L addition tank by means of a dosing control module, components of which are shown in Figure 25. A metal frame and guard was used to secure the FBC dosing system to the LHD chassis.

Figure 25: O-M FBC dosing components. Left: overall system; Upper right: electronic dosing control; Lower right: dosing pump.

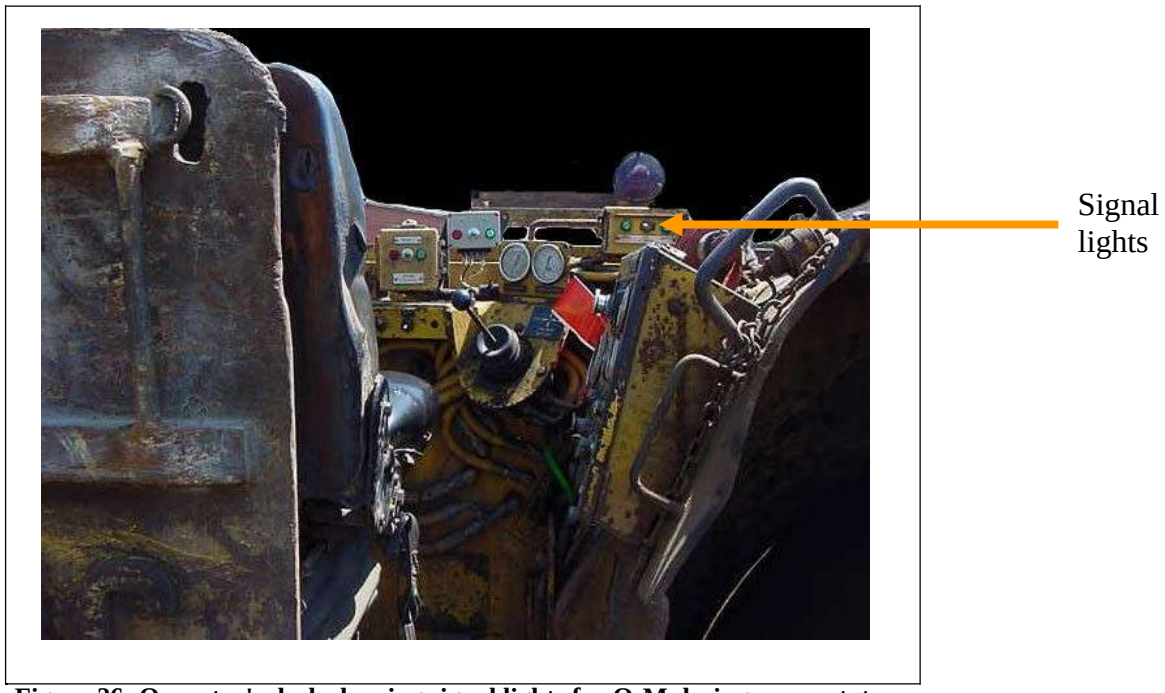

Figure 26: Operator's dash showing signal lights for O-M dosing pump status.

Special FBC dosing pump status lights were added to the dash, as shown in Figure 26 so that action could be taken by the operator should the pump fail. Additional DPF system alert signals that signified DPF plugging were hard-wired to the existing “engine problem” lights on the dash.

The O-M DPF installation, including the fuel additive dosing system, was started for LHD #445 on 18 June 2001 and completed on 22 June 2001. Vale’s Maintenance Dept. trained the heavy-duty equipment mechanics on the O-M system. Manuals for the operation of the DPF system were compiled by Vale’s Training Dept.

7.2 Johnson Matthey

JM manufactures a variety of DPF systems that operate on different principles. The DPF system selected for LHD #820 (Deutz V-12 engine) was a configuration of two JM DPF systems: the DPFiS (fuel additive) and DPFi (electrical heating) systems. This LHD was used in clean up activities and experienced brief periods of heavy loads and extended periods of light loads. Duty cycle monitoring confirmed that exhaust temperatures and associated temperature dwell times might not achieve reliable passive regeneration. Therefore, an active regeneration method using on-board electrical heating was incorporated into the system.

Because the #820 LHD had the dual exhaust systems to accommodate the V-12 Deutz engine, two identical DPFs (JM-DPFi201) with SiC wall-flow filter media were installed on the vehicle, one for each exhaust. After considerable testing, the driver's side DPF showed a minor separation of the filter medium with the canister. This separation was initially not influencing the DPM filtration performance; it continued in operation for an additional 723 hours. Eventually, the separation became more severe, and at 2138 hours this DPF was replaced by a new DPF using a cordierite wall-flow filter. Following the special tests in the summer of 2004, the off-driver side SiC DPF was also replaced with a cordierite DPF.

The DPF system was modular consisting of stainless steel canisters connected with V-clamps and gaskets for easy assembly and servicing. A diffusion plate at the inlet spread the incoming exhaust flow over the face of the filter element. The heating element stage, Type EC-B/Ca, shown in Figure 27, consisted of electric heating elements with connections for heater power and air supply. The air flow during regeneration assisted in obtaining the optimum heat distribution to the filter's mass, and provided the air needed for soot combustion.

Figure 27: Heating element at the bottom of the JM DPF system.

The DPFs were installed vertically, using vibration-reducing mountings, on each side of the engine in place of the mufflers, as shown for one side in Figure 28.

Figure 28: One of two JM filters mounted on either side of the dual exhaust Deutz V-12 engine.

Figure 29: Automatic FBC dosing equipment (left) and backpressure monitoring display on dash (right).

The FBC was cerium-based (EOLYS™) from Rhodia and stored in an on-board reservoir. The dosing of the FBC was done automatically with every refueling using an automatic dosing system, DOSY 200, supplied by JM, Figure 29 (left). The amount of FBC used was set to reduce the soot ignition temperature to 400 °C (752 °F).

Monitoring of backpressure was not only done using the normal data loggers described in Chapter 5, but additionally used the JM PIO210 monitoring system, Figure 29 (right), which was mounted on the vehicle's dashboard. A line of green, yellow, and red LEDs indicated a progression of increasing backpressure. A "red" signal indicated that the DPF had to be electrically regenerated.

The electric regeneration control station for the JM DPF system was located outside the 2400 Level garage in Stobie mine. The vehicle was brought to the station where a specific procedure was followed each time. The components of the station are shown in Figure 30. Power to the DPF heater was provided via a 230V connector, Figure 31. Air for regeneration was provided using a quick disconnect from the mine's compressed air lines, Figure 31. The JM control box provided a timed sequence for the heater coil to attain 600^{o}C and monitored the progress of regeneration by means of air pressure measurement. The system turned off and displayed a light on the panel automatically when the pressure reading of the filter attained a pre-set low value. Regeneration typically lasted 1-2 hours.

Figure 30: JM electric regeneration control display panel (on left) and interior (on right).

Figure 31: Air line with moisture removal and pressure gauge (left). The electrical connector (blue) and air line to its left (right).

7.3 ECS/3M Omega

The ECS/3M Omega DPF system was installed on Kubota tractor #2180 on 4 Sept 2001. The system consisted of cartridges containing 3M ceramic fibers located within a cylindrical housing, which was mounted horizontally on the left front fender of the tractor, Figure 32.

The system had an exhaust backpressure monitoring system to monitor filter soot loading. The display, shown in Figure 33, has two sets of indicators: one contained a linear set of four LEDs that indicated backpressure, the other contained a single LED alarm light and audible alarm to indicate system failure or DPF plugging.

The regeneration station for the system was inside the 1800 Level garage, Figure 34. This station controlled the timed air flow and power to the heating element. The 60 minute regeneration was to be conducted after each shift.

Figure 32: ECS/3M Omega filter mounted on tractor #2180. The yellow cage was to prevent operator contact with hot surfaces. The red box on the fender is a protective casing containing the power connector for electrical regeneration.

Figure 33: Omega dash display

Figure 34: ECS/3M Omega regeneration station

7.4 ECS Combifilter

Because a 3M decision to cease production of ceramic fiber filters rendered the ECS/3M Omega system obsolete, an ECS Combifilter was installed on tractor #2180 on 6 May 2002.

Figure 35 shows the ECS Combifilter mounted horizontally on the front fender of the #2180 tractor. The DPF consisted of a SiC wall-flow filter element with the addition of an electric heating coil built into the intake end of the DPF housing. The filter was sized to collect soot for a single 8-hour shift, and immediately thereafter was to be connected to the regeneration control station located inside the 1800 Level garage, Figure 34. The regeneration period under these conditions was about 60 minutes.

Tractor #2180 continued to have general maintenance problems due to its age. To increase the accumulation rate of operating hours on the ECS Combifilter, it was transferred to a new Kubota tractor #3013 during 12-19 July 2004 where it was installed exactly as it had been on tractor #2180.

Figure 35: ECS Combifilter, left: as received; right: mounted on vehicle #2180.

7.5 Engelhard DPX2

The Engelhard DPX2 DPF system, Figure 36, was installed on LHD #362 (DDEC 60 engine) on 10 June 2001. This system was fully passive utilizing a cordierite wall-flow filter with a wash-coat of a platinum-based catalyst.

The installed system is shown in Figure 37, which also shows the dash-mounted backpressure indicator with yellow (warning) and red light displays.

Figure 36: Engelhard DPX2 DPF system

Figure 37: Engelhard DPX2 DPF as installed with insulation (left) and backpressure monitor on dash (right).

7.6 DCL Titan

The DCL Titan DPF system was installed on Kubota tractor #621 on 3 February 2002. During July 2004 it was transferred to an identical Kubota tractor #017 so that additional operating time would accumulate more quickly.

The DPF, shown in Figure 38, was a SiC wall-flow filter contained in a stainless steel cylinder. It was mounted between inlet and outlet caps joined by gasketed flanges and quick disconnect clamps that facilitated its removal for regeneration.

Figure 38: DCL Titan DPF, side view on the left and end view on the right. The side view shows the two end caps connected to the main canister by quick disconnect clamps.

The DPF assembly was mounted horizontally on the front fender, Figure 39, and covered with a metal box to prevent operators coming into contact with its hot surfaces.

Figure 39: Views of DCL Titan mounted on the Kubota fender. Lower photograph shows the protective box.

Figure 40: DCL backpressure monitor mounted on dash.

A backpressure monitoring unit, Figure 40, supplied by DCL, was mounted on the dash of the vehicle. A green light indicated normal operation; a yellow light indicated a backpressure of about 125 mbar as a warning that the filter was becoming loaded; and a red light indicated that the filter needed to be regenerated.

The regeneration control station was located inside the 1800 Level garage. Instead of plugging an on-board system into the power station, as was done for most of the DPF systems being tested at Stobie, the DCL Titan filter was removed from the vehicle and placed on top of the electric heating element within a cylindrical "cooker," Figure 41. The cooker was permanently connected to a wall-mounted power control panel, Figure 42. The control panel provided a timed regeneration cycle which typically lasted 1-2 hours. Natural convection supplied the air for soot combustion. After the heating cycle was completed, the filter was allowed to cool to room temperature before removing it from the cooker.

Two identical DCL Titan DPFs were used for this tractor so that one DPF could be used on the operating vehicle while its companion DPF was being regenerated.

Figure 41: Regeneration "cooker" for DCL Titan DPFs: side view (left) and top view showing heater elements (right).

Figure 42: DCL Titan DPF regeneration station with a DPF placed in the cooker and cooker control panel (upper right).

7.7 Dual ECS/Combifilters

Two ECS S18 Combifilters were installed on LHD #213 on 17 Feb 2003 to operate in parallel on the single exhaust from the DDEC 60 engine. The dual DPFs were mounted vertically side by side. The Combifilter DPF used the SiC wall-flow filter. Each filter canister contained electric heating elements at the bottom (inlet) of its housing.

The filters were sized to collect soot over two working shifts with active electrical heating regeneration performed each day. The dual filters operated in parallel. Two DPFs were used instead of one larger DPF due to spatial considerations, Figure 43 and Figure 44.

Figure 43: Top view of installed ECS Combifilters

Figure 44: Side view of Combifilters (left) and backpressure monitor on dash (right).

Backpressure monitoring was carried out by the DPF system. A dash-mounted, red LED indicated high exhaust backpressure and the need for regeneration, Figure 44 (right). A green "test" button was located next to the LED.

The regeneration station, shown in Figure 45, was initially located at the 3000 Level garage. However, due to inconsistent regeneration, the cause of which appeared to be inconvenient location of Level 3000, the station was moved to Level 3400 truck bay. The regeneration unit consisted of two identical control panels, power cables and connectors, Figure 46, and compressed air supplies, Figure 47, that were hooked up to each DPF. A 70-minute heating cycle was generally used followed by a 20-minute cool down period. The control panel showed each heating coil current in amperes and heating time remaining.

Figure 45: Regeneration control station for the DPF system using dual ECS Combifilters.

Figure 46: Regeneration control panel for one of the ECS Combifilters (left) and power cables connectors (right).

Figure 47: Compressed air connection.

CombiClean™ Off-board Regeneration System

Vale purchased an ECS CombiClean™ regeneration system independently of the DEEP Stobie project, because the company had decided to purchase an ECS CatTrap DPF for one of its LHDs. The CatTrap DPF, which did not incorporate integral electric heating within the DPF itself, required it to be removed from the vehicle and placed in a CombiClean regeneration system for off-board regeneration. The CombiClean is similar to, but much more sophisticated than, the DCL "cooker" mentioned previously.

However, due to periodic problems encountered with the ECS regeneration station used for the ECS Combifilters in the Stobie tests, the Stobie team decided to use the CombiClean off-board regeneration on these Combifilters as a substitute. The CombiClean was very effective in returning the Combifilter DPFs to a clean state. In the latter stages of the Stobie tests, the ECS Combifilter was periodically cleaned by the CombiClean system even if the Combifilter's on-board heaters were working. The Stobie team decided to use the CombiClean regeneration system to clean the DCL Titan DPF (on a tractor) during the last few months of testing.

The CombiClean system consisted of the following components: two base units containing the electric heater and DPF mounting flanges, a vacuum system, a compressed air system, and a control panel. The system is shown in Figure 48.

Figure 48: The ECS CombiClean™ DPF regeneration system, consisting of two heating compartments. Below what is shown is a shop type vacuum system (see Figure 50) used in conjunction with compressed air jet at the beginning of the regeneration process to remove the bulk of soot and ash.

The loaded filters were carried to the CombiClean system and were securely mounted to the top of a heater unit using a gasket seal and clamp, Figure 49. Care was taken to orient the DPF so that the direction of exhaust flow through the DPF when mounted on the vehicle corresponded to the upward direction when the DPF was mounted on the CombiClean. The DPF was first cleaned by sweeping a jet of compressed air across the top of the exposed filter element while simultaneously operating the vacuum which provided a high reverse air flow so that residual soot and ash could be removed from the engine side of the filter The control panel switch, Figure 50, was then used to activate the upward flow of combustion air and the heater. Lights on the control panel signified when the regeneration was complete.

Figure 49: Mounting a loaded DPF on the CombiClean heater (left) and securing it with gasket and clamp (right).

Figure 50: The CombiClean control panel (left), access for sweeping compressed air across the outlet side of the DPF filter element (middle) and vacuum system valve (right).

7.8 Arvin Meritor

Arvin Meritor manufacturers an active DPF system which uses an automatically controlled fuel burner followed by a cordierite wall-flow filter, Figure 51, and a diesel oxidation catalyst to reduce CO and organic emissions. The fuel burner was activated when the sensed exhaust backpressure exceeded a pre-set level that indicated when regeneration was needed. The regeneration burner regulated the diesel fuel and combustion air to raise the exhaust temperature to 650 °C for typically eight minutes while the vehicle was performing its normal activities.

Figure 51: Arvin-Meritor PFS (horizontal position).

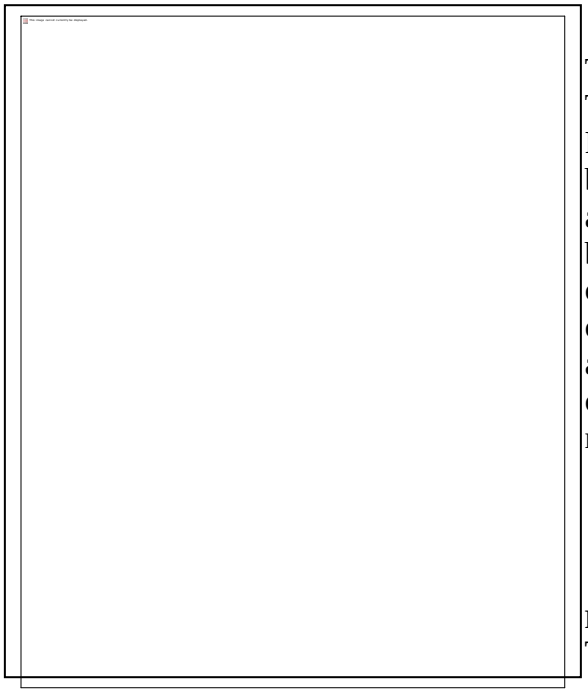

Two identical units were installed in parallel on a Toro LHD #111 (DDEC 60 engine) on 4 Jun 2004, Figure 52. These systems were mounted vertically because of special restrictions and extensive alteration of the exhaust pipe was necessary. The burners were located in the top sections of each DPF canister, Figure 53, with the bottom sections containing the cordierite filter element. Compressed air was provided for the burners using an air compressor and air drier provided by the manufacturer, Figure 54.

Figure 52: Vertically mounted dual Arvin-Meritor DPFs on Toro #111 LHD.

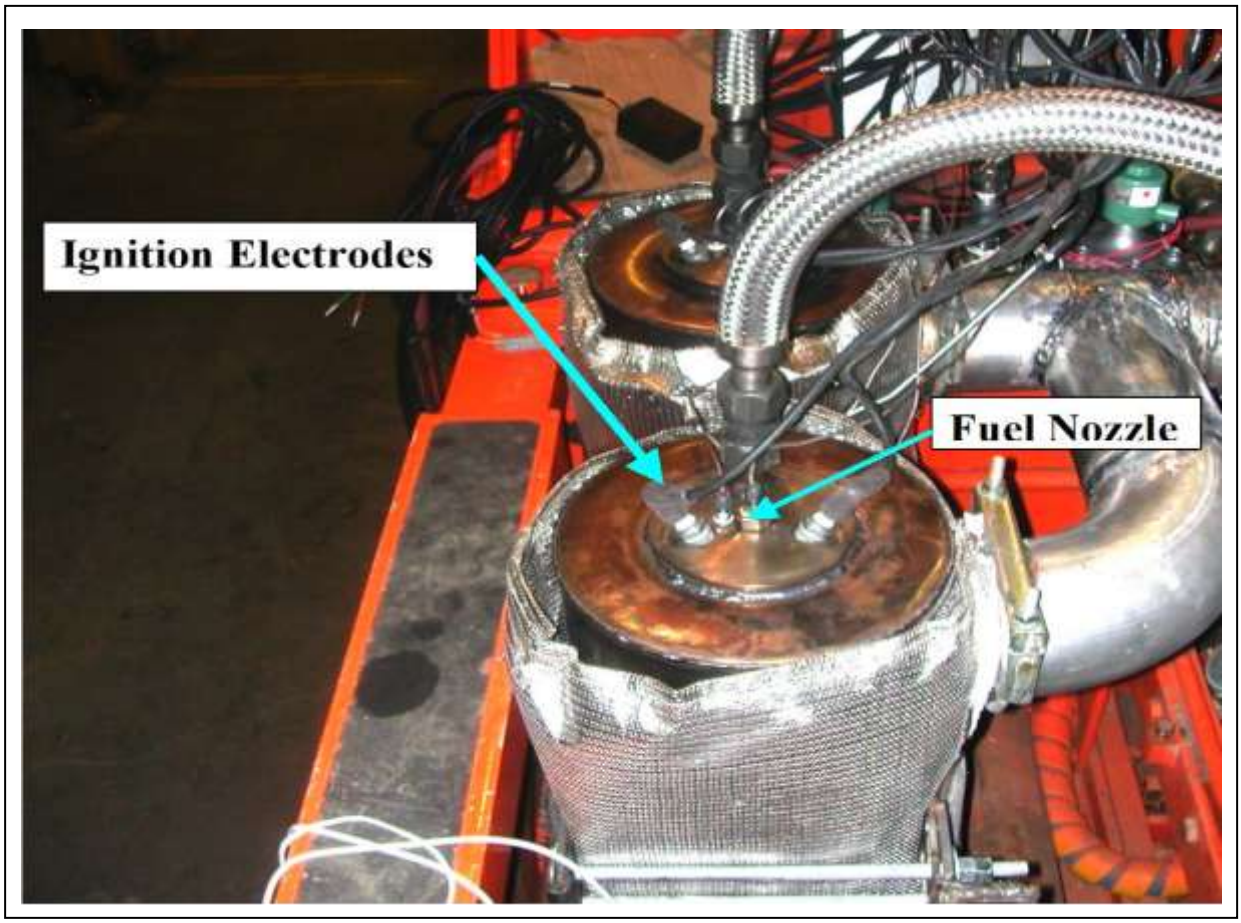

Figure 53: Close up view of the top of the Arvin-Meritor DPFs showing the burner components. Also shown is the alteration done to the exhaust pipe in order to install the exhaust gases so that they entered the tops of the DPFs in parallel. The flexible hoses coming out of the top of the units are the burner fuel lines.

Figure 54: Air drier for burner

The burner had its own diesel fuel tank, fuel filter, fuel pump (with shutoff valve), a fuel-air mixing unit and an atomizer. Flexible, high pressure fuel lines (3/8 in diameter) were employed. The combustion air was supplied through flexible stainless steel (1 in diameter) hose to the burner, Figure 53. The combustion air source was a compressed air tank located on the vehicle. Pressure sensors and pressure regulators controlled the combustion air, which was also filtered and pumped. The vehicle's on-board batteries supplied power to the air and fuel pumps and to the 40,000 volt fuel igniter. A lamp was used to indicate when the backpressure after regeneration was unacceptably high due to non-soot ash build-up.

8. Methods for Testing DPF Performance

8.1 Special Emission Testing

Three comprehensive DPF system performance tests based upon exhaust emission measurements were carried out jointly by the Stobie project team and NIOSH diesel research scientists during the Stobie project:

- 16-19 July 2001
- 25-31 May 2002
- 7-11 June 2004

The work was performed as in-kind contributions by A. Bugarski and G. Schnakenberg, scientists from the Pittsburgh Research Laboratory of NIOSH, and D. Wilson of ECOM America (Gainesville, Georgia). The Stobie team acknowledges with gratitude the services provided by these individuals in all aspects of the performance measurements on the DPF systems. Copies of the special test reports are included as Appendix E on the CD ROM.

The measurement methodologies were consistent for the three test sessions so that direct comparisons could be made as a function of the operating time for each DPF system. The test method specified four repeatable engine modes -- three steady state engine loadings and one transient condition -- to provide consistent exhaust emissions across the test sessions. Most measurements were made upstream and downstream of the DPF. The exhaust parameters measured were the following:

- Particulate number and size distributions;
- DPM concentration based on photoelectric aerosol analyzer measurements;
- Gaseous components (NO, NO_2, CO, CO_2, and O_2);
- Opacities;
- Smoke Numbers.

Test sessions were held at the Frood surface shop so that there would be convenient access to the instruments being used. Each vehicle was taken out of production for a day and driven to the shop. The general procedure was to chock the wheels, set the service brake, locate exhaust pipe ports for upstream sampling, instruct the vehicle operator of the test procedure and warm up the engine. Emissions sampling was performed at three steady state engine modes (combination of power and rpm) and one transient mode as described below:

- Low idle (LI) - transmission in neutral, engine at normal idle speed;
- High idle (HI) - transmission in neutral, vehicle accelerator pedal held fully depressed;
- Torque converter stall (TCS) - applicable for LHDs only, transmission engaged in highest gear, accelerator pedal fully depressed. TCS places a realistic and reproducible load on the engine that is needed to provide consistent raw exhaust emissions under load where DPM concentrations are high. The duration of TCS is, of necessity, relatively short, less than a minute, since all the power developed by the engine is dissipated in the torque converter as heat which can quickly overheat and damage the converter.
- Snap acceleration - transmission in neutral, engine at idle, then on cue from the instrument operator the vehicle operator fully depresses the accelerator pedal as quickly

as possible, holds it there for a few seconds until engine speed is stable and releases it. Several of these snaps may be run and averaged. The effective load on the engine is the inertia of the flywheel.

Engine speed for all engine test conditions was measured using an AVL DiSpeed 490, which senses fuel injection pulses via a clamp on transducer and interprets the results as RPM.

8.1.1 Filter Efficiency Measurements

The efficiency of a DPF to remove soot particles (DPM) or gaseous exhaust components was obtained by taking measurements upstream and downstream of the DPF (or, in some cases, with and without the DPF) and calculating the efficiency using the following formula:

$$\text{Efficiency (in \%)} = 100 \times \left\{ \frac{(\text{Measurement})_{up} - (\text{Measurement})_{down}}{(\text{Measurement})_{up}} \right\} \qquad \text{[Equation 1]}$$

:

PAS 2000

The photoelectric aerosol analyzer (PAS 2000) was used as one measurement of the soot (DPM) concentrations for the steady state engine modes[β]. The PAS 2000, shown in Figure 55, developed by Matter Engineering (Wohlen, Switzerland) and

Figure 55: PAS 2000 photoelectric aerosol analyzer (on the right) with the dilution equipment on the left.

marketed by EcoChem (League City, Texas). The PAS is based on the detection of the ionized particles. Soot particles in diesel exhaust are typically elemental carbon (EC) particles with a layer of PAH adsorbed on their surfaces. When exposed to ultra-violet light, the PAH become ionized, resulting in positively charging the soot particle to which it is attached. The PAS exposes the sample stream to UV light and detects the flow of these charged particles as an electric current, which is proportional to the total particle surface area. Other work has shown a

[β] The PAS 2000 was unsuitable for measuring the transients produced during snap acceleration.

good correlation between the current measured and the concentration of EC. However, because particle size distributions affect the correlation between mass concentration of EC and the PAS current, and these distributions may be different upstream and downstream of a filter, the filter efficiencies so-measured are considered to be only estimates of the true DPM efficiency of the DPF.

The DPM particle concentration of the raw exhaust was too high for a direct measurement by the PAS 2000. The exhaust was therefore diluted using a spinning disk system from Matter Engineering, Model MD19-2E, Figure 55. Two heated sampling lines were used, one connected to the port upstream and the other placed in the exhaust stream downstream of the DPF (see Figure 59). The diluter was configured to allow quick switching between upstream and downstream sampling locations. The sampling lines were heated to 150 °F to prevent condensation of semi-volatile organics. The dilution ratios had to be adjusted occasionally for differences in soot concentrations over the various engine conditions being used, but all measurements were normalized to the dilution ratio of the measurement.

Total aerosol concentration

The number concentrations and size distributions of particles between 10-392 nm were measured using a Scanning Mobility Particle Sizer (SMPS) from TSI Inc. (St.Paul, Minnesota), shown in

Figure 56. The SMPS was configured with a Model 3080L electrostatic classifier and a Model 3025A condensation particle counter (CPC). The sample and sheath air flows were maintained at 0.6 L/min and 6.0 L/min, respectively. At these flow conditions the instrument measures only aerosols with electrical mobility diameters ($_{50}d_{em}$) below 480nm. The CPC was operated in high-flow mode to minimize diffusion losses. The measurements were performed from the exhaust port located upstream and the exhaust stream downstream of the DPF systems (see Figure 59). In order to keep the aerosol concentrations below upper the measurement range of the SMPS, the exhaust was diluted using the spinning disk diluter described previously.

Identical dilution settings were used for measurements performed at upstream and downstream locations.

Figure 56: Scanning Mobility Particle Sizer.

The SMPS selectively passed aerosol in 10-392 nm mobility diameters, and the CPC particle counter optically counted each particle. Over about one minute the classifier scanned through the full range of mobility diameters. Size distributions were collected for specified engine conditions; an example of the display is shown in Figure 57. To obtain total aerosol, all sizes were summed. Efficiencies were calculated using Equation 1.

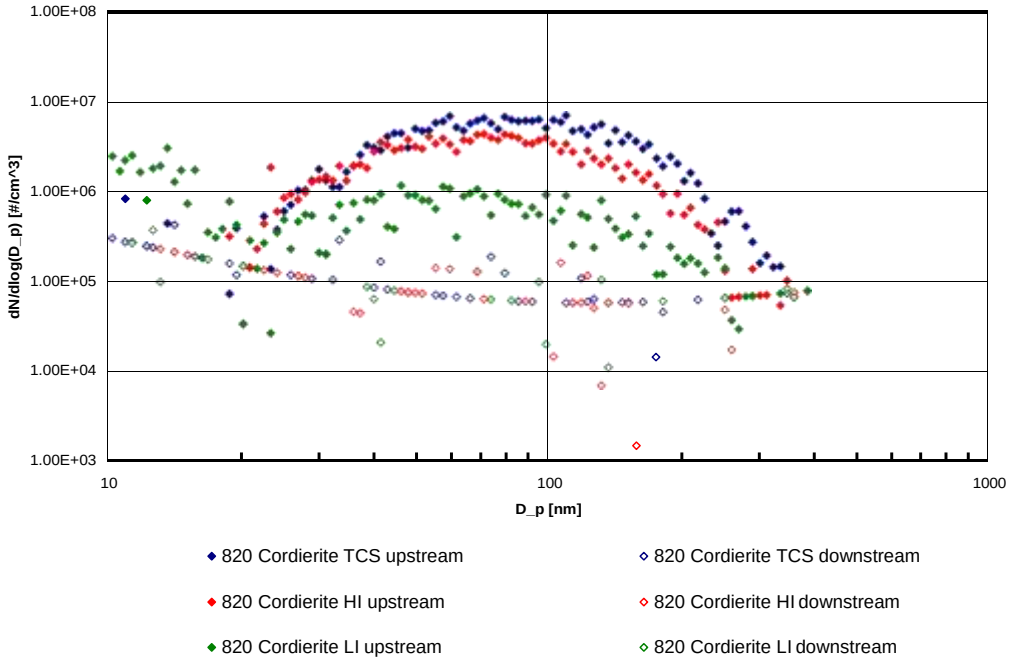

Figure 57: Example of exhaust t particle size distributions collected over various engine conditions. Filled points are upstream of the DPF and open points are downstream. Both axes are logarithmic. Data are from NIOSH tests June 2004 for LHD #820 Left with a Johnson Matthey DPF with cordierite filter element.

When interpreting the results of the number concentrations and size distributions, one should take into consideration that the accuracy of the SMPS measurements and corresponding calculations might be somewhat affected by the following: (1) the results are based on a limited number of measurements; (2) reliable SMPS measurements require operating the engine at steady-state conditions for at least 60 seconds. Although this is achieved easily for LI and HI, it was quite challenging to make measurements under TCS conditions where the length of the test is limited by the possibility of the torque converter fluid becoming overheated; (3) relatively high dilution of the filtered exhaust resulted in extremely low aerosol concentrations downstream of the filter. In many instances in the tests run in 2002 and 2004, the size distributions downstream of the DPF resemble a "sagging clothes line" which is evident in Figure 57. Efficiency estimates based upon this data may be in error. The data are contained in the NIOSH report of test results in Appendix E.

Gaseous Components

The concentrations of the noxious target gases CO, NO, and NO_2, as well as CO_2 and O_2 were measured using ECOM KL and ECOM AC Plus portable analyzers from ECOM America (Gainesville, Georgia) shown in Figure 58. Two ECOM units were employed for the special tests with NIOSH because of the interest in comparing the results. Because only the ECOM-AC Plus

was used for routine testing by the Stobie personnel, this report primarily uses ECOM-AC measurements rather than the ECOM-KL used by NIOSH. Calibration of the ECOM-AC was done periodically.

Figure 58: **ECOM-KL gas analyzer (left) and the AVL Dicom 4000 (right)**

Special probes, examples of which are shown in Figure 59, were used for conducting ECOM measurements.

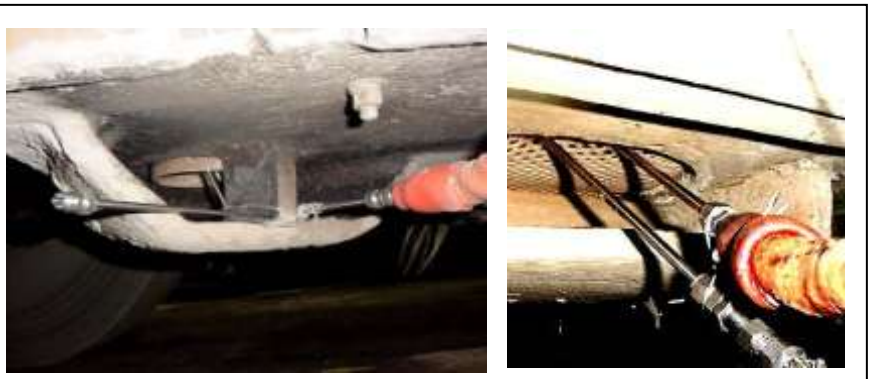

Figure 59: Probes for making ECOM measurements located in vehicle exhaust outlet after DPF.

8.1.2 Smoke Numbers

Both ECOM gas analyzers are equipped to collect soot samples for Bacharach smoke number determination. For the LHD's these are collected at TCS test condition; for the tractors smoke samples were collected during HI test condition. To collect a smoke sample, the ECOM drew 1.6 L of exhaust through a filter paper that was clamped in the sampling probe, Figure 60. All of the sampled volume passed through a 6 mm diameter spot of the filter, Figure 60. ECOM supplied shade of gray scale (Bosch/Bacharach smoke number scale) consisting of a card with ten circles varying from white (smoke number = 0) to black (smoke number = 9)). The center of each circle was open so the sampled spot could be placed behind the gray shaded circle for visual comparison. Smoke spots that appeared to be between two shades of gray were given a half

integer value. If possible, three measurements were made and averaged. The approximately one minute sampling time pushed the temperature limits of a safe TCS.

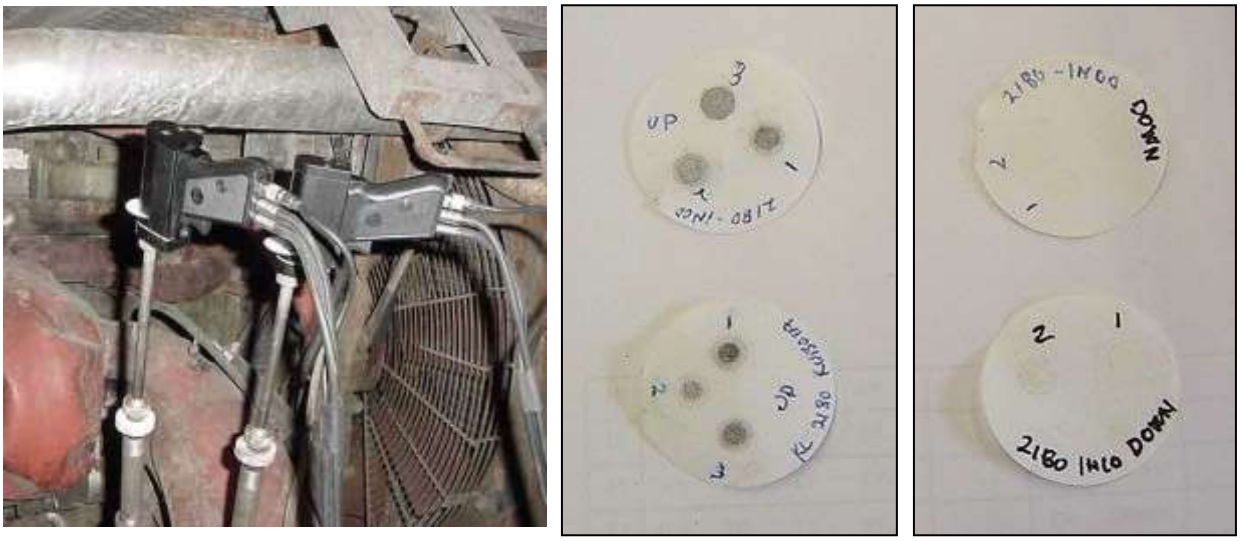

Figure 60: ECOM probes for gas sampling and holding filters for smoke numbers measurements (left). Examples of filters upstream (middle) and downstream (right).

8.1.3 Opacity

The AVL DiCom 4000 was used to measure exhaust opacity. The measurement is based on light transmission through the exhaust stream. The engine performed a snap acceleration while the AVL instrument detected the rpm increase and started the measurement. Once the instrument detected a steady high engine speed, it displayed the peak rpm and the opacity in percent. The following DPF opacities are generally recognized in assessing DPF performance:

- 0-5% good DPF performance
- 5-10% marginal DPF performance
- >15% unacceptable DPF performance.

Figure 61: Equipment and crew set up in the Frood shop for conducting comprehensive testing.

Figure 62: Crew taking special measurements (A. Bugarski top left, G. Schnakenberg top right, vehicle operator bottom left, and J. Stachulak and G. Schnakenberg bottom right).

8.1.4 Engine backpressure

For some of the special testing, a Magnehelic™ differential pressure gauge from Dwyer Instruments (Michigan City, Indiana) was used to measure exhaust backpressure. The gauge was connected to a port located just upstream of the DPF.

8.2 Routine Testing

All vehicles were periodically brought into the underground maintenance shop for routine maintenance. During the time when the vehicles were undergoing such examination, the Stobie DEEP team also performed testing on the DPF systems. The plan was to conduct such routine tests at least every 250 vehicle operating hours. Due to convenience, often the routine testing was done more frequently.

The routine tests used the ECOM AC Plus instrument described previously. The measurements obtained were smoke numbers and gas concentrations of CO, NO, NO_2 and O_2 both upstream and downstream of the DPF. The ECOM calculated CO_2 concentration using O_2 measured and the fuel type (diesel #2).

8.3 Data Logger Data Evaluation

Data from the data loggers was downloaded weekly and sent via e-mail to A. Mayer in Switzerland for analysis. For each DPF, these data files were joined to make a single complete data set for that DPF. For some of the longer tests, the complete data sets were split into calendar year periods. The analysis and treatment procedures for the DPF test data were the same as described in Chapter 5 for duty cycle monitoring. An example of such a data set is shown in Figure 63 for #820 LHD (left side). In this figure the horizontal axis is the operating time (not real time), and the small black crosses along the axis indicate the individual data file. The start date for each sub-file is the only instance for which a calendar date and time exists. For the operational data, however, the calendar time is not the preferred way of displaying data, because there were many periods where the vehicle was not operating. Consequently, the operating time was selected as the most appropriate way to view the data as a function of time. Appendix C, on a CD-ROM, contains all of the data files and related analysis and comments for each DPF system, organized in folders by DPF system and vehicle #. All of the files mentioned below can be found in Appendix C within the appropriate DPF-vehicle folder; e.g., "JohnsonMatthey-820L."

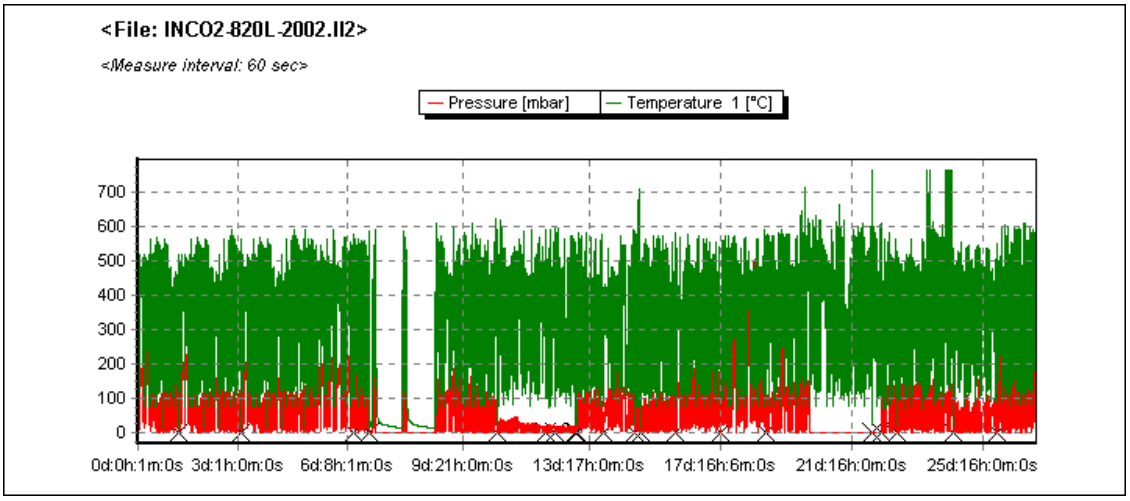

Figure 63: Example of the display of pressure and temperature data as a function of vehicle operating time.

For each DPF tested, the exhaust and temperature data was segmented into shorter periods and plotted to form a contiguous set of individual "data-zoom" files (e.g., "INCO2-820L-zoom03.xls") so that the data could be investigated in detail. The full set of zooms appears as graphs/charts in a single file (e.g., "INCO2-820L-16 Zooms.doc"). A circle containing a number may appear on a zoom graph, as exemplified in Figure 64. It signifies an event of significance requiring a comment. The comments for the all events are in a single *.doc file (e.g., "Events820L.doc").

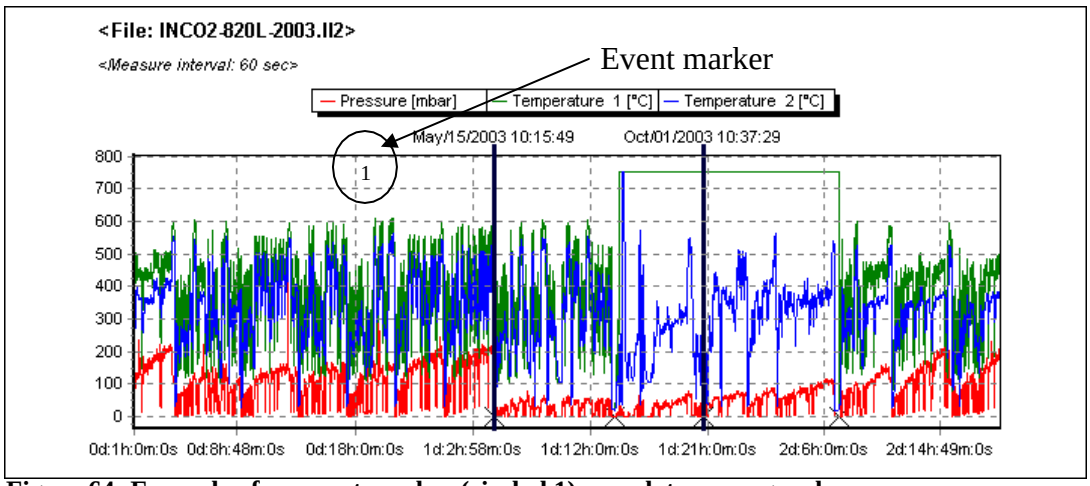

Figure 64: Example of an event marker (circled 1) on a data zoom graph.

Each zoom was analyzed to produce variety of useful statistical summaries and these are presented as a separate PDF file for each zoom (e.g., "zoom 03_INCO2-820L.pdf") shown in Figure 65. This single-page file contains the following items:

- A graph of the exhaust temperature and backpressure for the entire zoom period at top left;
- A pie chart, Figure 66, that shows the percentage of pressure readings that were normal (green at < 150 mbar), alert mode (yellow at > 150< 200 mbar), and alarm mode (red at > 200 mbar).
- A Episode Frequency (bubble) diagram of exhaust temperature upstream of the DPF, Figure 68, for the entire zoom period;
- A table of descriptive statistics of the temperature and pressure data for the entire zoom period at the bottom. The data from this table, assembled for all the zooms, are presented for each DPF in Chapter 9. They are also used to generate the trend charts, Figure 69; and
- Several graphs associated only with the two smaller zoom periods (zoom 1 and zoom 2) designated by boxes appearing in the top zoom graph for the entire period.
    - Temperature and pressure over the small zoom periods;
    - Temperature histogram and frequency distribution for each of the two zoom periods, Figure 67.

Additionally for each DPF system, there are "super" zoom data summary pages, with contents and format as above, but covering a period of a year (e.g., "INCO4-213-TOT-2003.pdf").

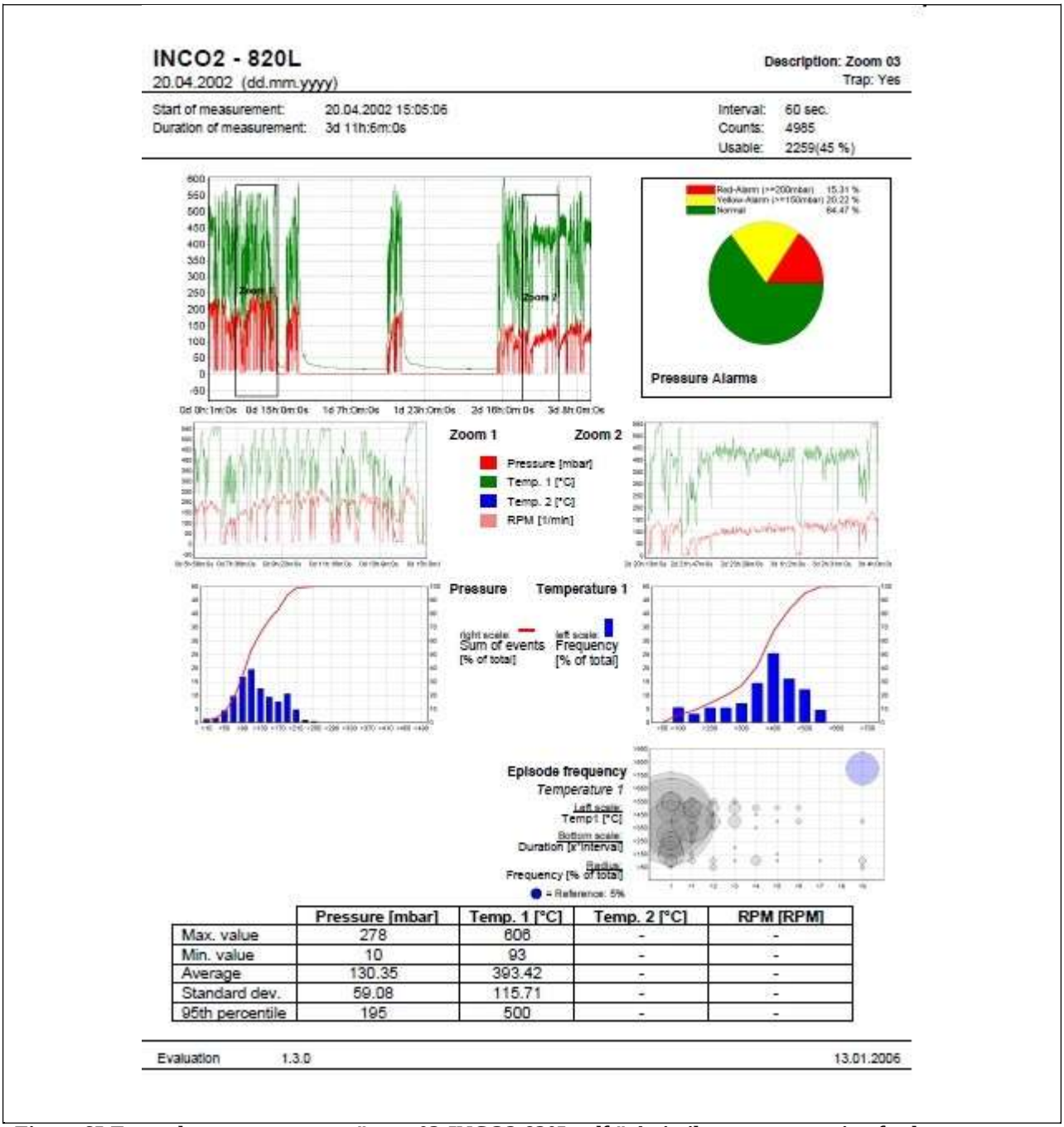

	Pressure [mbar]	Temp. 1 [°C]	Temp. 2 [°C]	RPM [RPM]
Max. value	278	606	-	-
Min. value	10	93	-	-
Average	130.35	393.42	-	-
Standard dev.	59.08	115.71	-	-
95th percentile	195	500	-	-

Figure 65 Example zoom summary, "zoom03-INCO2-820L.pdf." A similar summary exists for longer periods, e.g., a calendar year "INCO2-820l-2003.pdf."

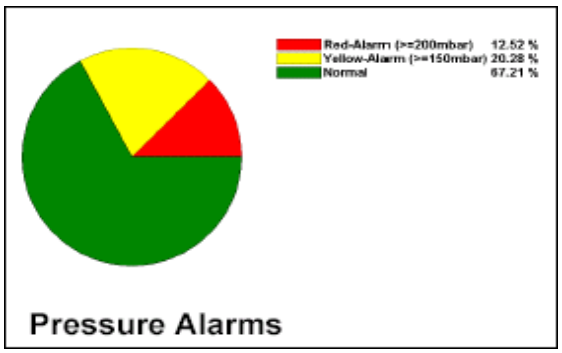

Figure 66: Example of a pie chart showing percentage of pressures exceeding alert and alarm levels.

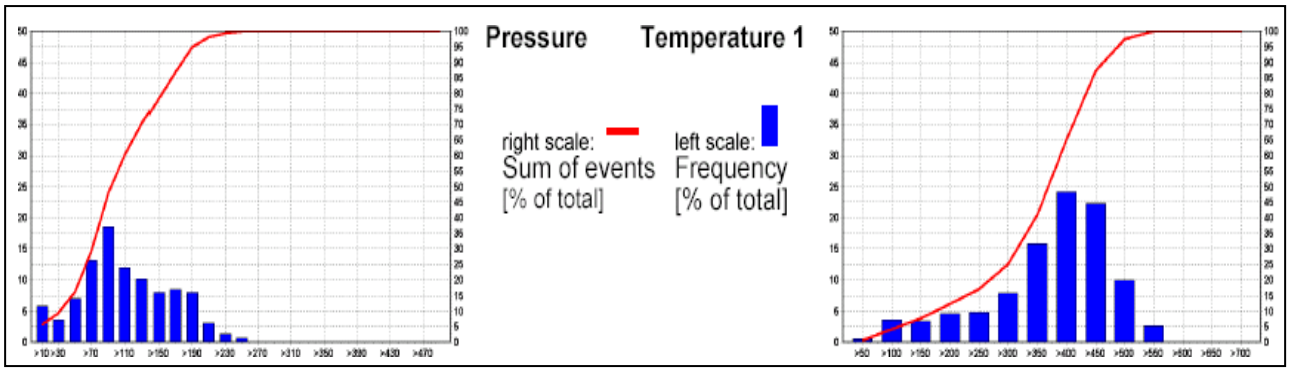

Figure 67: Examples of frequency distributions for pressure and temperature that appear on a zoom data page. These correspond to the smaller zoomed in data defined by boxes on the larger zoom graph.

The Episode frequency graph for the zoom, Figure 68, is an alternative method of representing the 3-dimensional dwell time diagram described earlier in Chapter 5. These "bubble diagrams" were believed to be easier to understand. Consider the example shown in Figure 68. Note that the temperature range is on the vertical axis (not horizontal as in Figure 67), and if it were a histogram, the bars representing temperature frequency would be horizontal. However, in the bubble diagram, the diameter of a circle, centered vertically on the temperature, represents the frequency attribute of the data. (Note that in Figure 68, the temperature increments (bin sizes) are 50 °C but are labeled every 100 °C.) The horizontal position of the center of the circle represents the temperature along the horizontal axis whose scale is the dwell time expressed as integer multiples of the sampling period. For example, if a data set was collected using 60-sec intervals[φ], then the integers on the horizontal axis refer to the number of 60-sec periods, and the label "1" represents data with dwell times of 1 minute or less, ">1" represents data with a dwell time of >1 to 2 minutes (>60s to 120 s), and so on. Thus, the diameter of a circle centered on >400 (between >350 and >450) on the vertical axis, and on >1 on the horizontal axis represents the relative number of temperature data points which are within a temperature of >400 to 450 °C for 2 consecutive sampling periods (a dwell of 2 minutes). The red circle labeled as point A in Figure 68 shows this data bubble. Lastly, the size/diameter of the circle represents the *relative* frequency of the data as a percent of the total number of data points, or equivalently, of the total time of the zoom. At the upper right of each diagram is a shaded circle whose size represents 5% of the time and can be used as a reference.

When the temperature data contains many points which vary rapidly, most of the circles will fall to the left of the diagram. If a temperature is steady for a couple of minutes or more and that occurs frequently, then the bubble at the temperature will be more to the right. In Figure 68 it is fairly easy to see that, for most of the time, the temperature stays within a narrow range (50 °C) for less than 120 seconds. There are a few points at greater than 120 seconds duration (i.e. >2 and higher), but the circles are relatively small indicating only relatively few times when consecutive temperatures stay within 50 °C for more than two minutes.

At the bottom of each data-zoom summary page is a table of statistics (minimum, maximum, average, standard deviation, and 95th percentile) for critical parameters (often backpressure and DPF inlet exhaust temperatures were the only reliable measurements). These

[φ] Note that the data collection interval for each data set is defined at the top right corner of each summary data page in Appendix C.

summary statistics for the individual zooms can be collected and displayed to show trends in the parameters for the DPF as a function of time. Examples of such trend plots are shown for vehicle #820 (left side DPF) in Figure 69. All trend plots appear as a PDF file (e.g., "Trend INCO2-820L.pdf") in Appendix C in folder JohnsonMatthey-820L. Selected trend plots are shown for specific DPFs in Chapter 9.

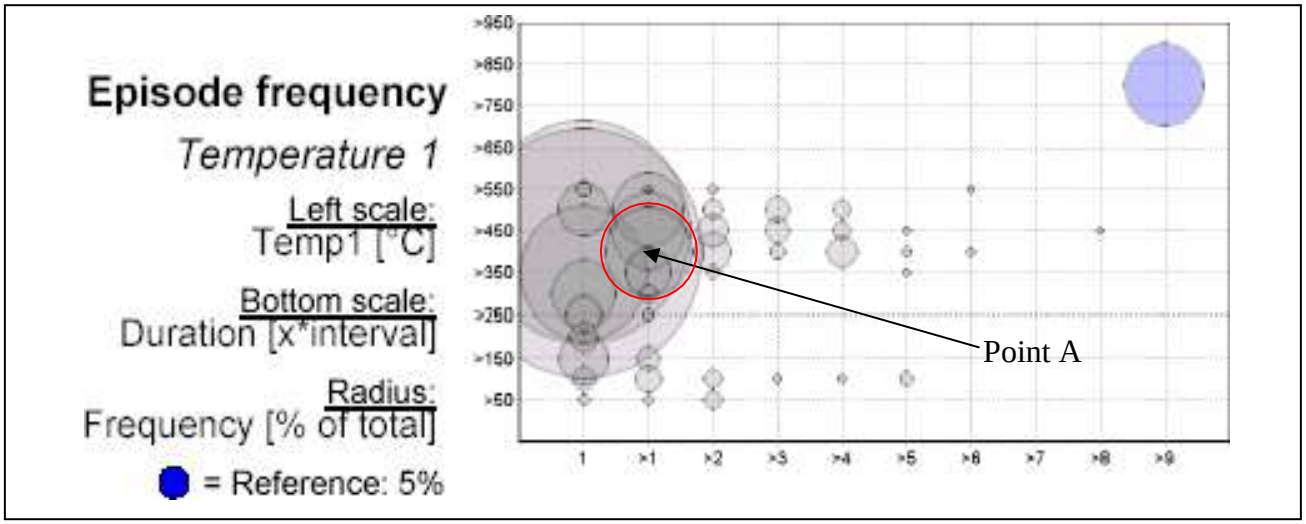

Figure 68: Example of a frequency distribution of temperature durations.

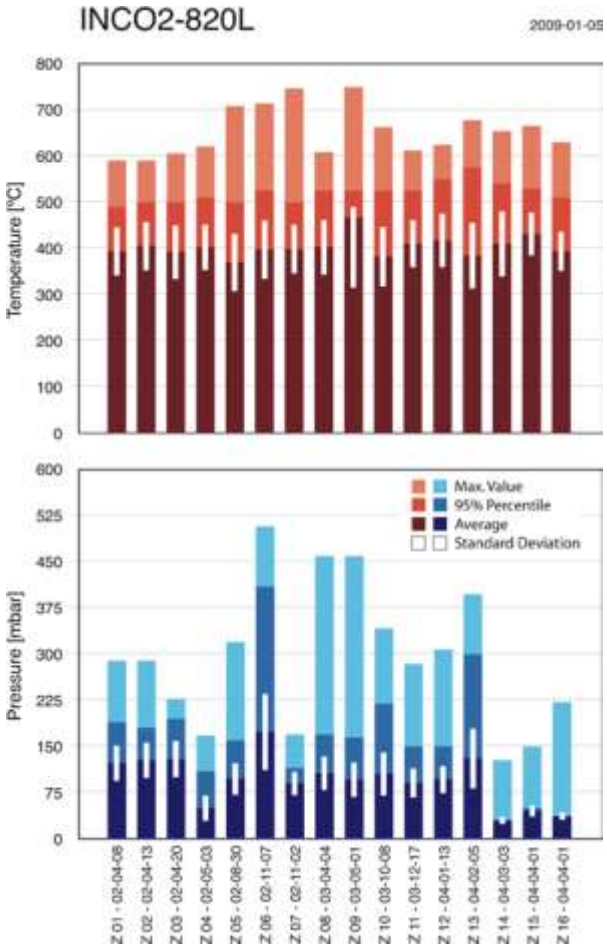

Figure 69: Example of trend plots constructed from the statistics of the zoom data covering the entire useable data set. In this case the data from vehicle #820 (left side) are represented by 16 zoom data files covering the DPF operation from April 2002 to April 2004. Each zoom is plotted in sequence from left to right on the horizontal axis. The vertical white lines in each zoom represent one standard deviation, σ centered on the average. The colour code is shown at the top right of the bottom diagram.

9. Performances of DPF systems

The performance of each DPF will be discussed in this chapter; relevant comparisons of certain systems will be made in Chapter 10. A number of performance criteria were established and evaluated for the DPFs, namely: particle number reduction and the effects on particle size distributions that were obtained in special NIOSH tests; reduction of specific exhaust gases and smoke numbers that were obtained by routine testing by Vale carried out about every 250 hours (as part of routine vehicle maintenance activities); ease of installation and maintenance of a system; and effective operation of the system. The results obtained for each of these criteria will be discussed for each DPF tested. In general, for a DPF exhibiting adequate DPM reduction, the downstream smoke numbers should be 2 or below, and opacity less than 5%.

An overall history of the testing at Stobie is shown in Figure 70, where the DPFs and their respective vehicles are listed across the top and time in months is listed down the rows from May 2001 to January 2005. The events are coded as follows: Green indicates DPF installation; red indicates DPF removal; yellow indicates that a potential problem was noted; blue indicates the NIOSH special tests (three in total); light blue indicates routine ECOM testing by Vale; and, purple indicates IH DPM monitoring. Details are provided below.

Fuel and lubrication oil:

The fuel used for all diesel units was Shell's Low-sulfur Diesel Fuel CP-34 containing 350 ppm S. The lubrication oil used for all engines was Esso's XD-3™ Extra.

Terminology:

Some of the terminology used in the text and tables need explanation. References to "temperature" and "backpressure" imply that they are for the engine exhaust in the vicinity and upstream (engine side) of the DPF. "Engine speed" refers to the engine mode and speed as described earlier in the testing protocol. "Hour meter" refers to the time indicated by the vehicle's hour meter that accumulated vehicle operating time. "Sm No." refers to the smoke number obtained by ECOM sampling, and when presented as two numbers, the table entry is in the form of upstream/downstream. "PAS" refers to the results of the PAS 2000 instrument that measures total DPM particles. "EC" (only done for special tests of July 2001) refers to elemental carbon determined by NIOSH method 5040 (Chapter 11). "#" refers to total particle number as obtained by the SMPS. DPF efficiencies in filtering DPM differ for PAS, EC or # because these methods measure different aspects of the DPM. "Opacity" refers to the obscuration of light by the diesel exhaust "smoke" and is obtained only for Snap Acceleration engine test mode. The target gases are obvious, with the critical ones being CO, NO and NO_2. "σ" indicates one standard deviation.

THIS PAGE INTENTIONALLY LEFT BLANK

Figure 70: History of major events in the Stobie project (overleaf)

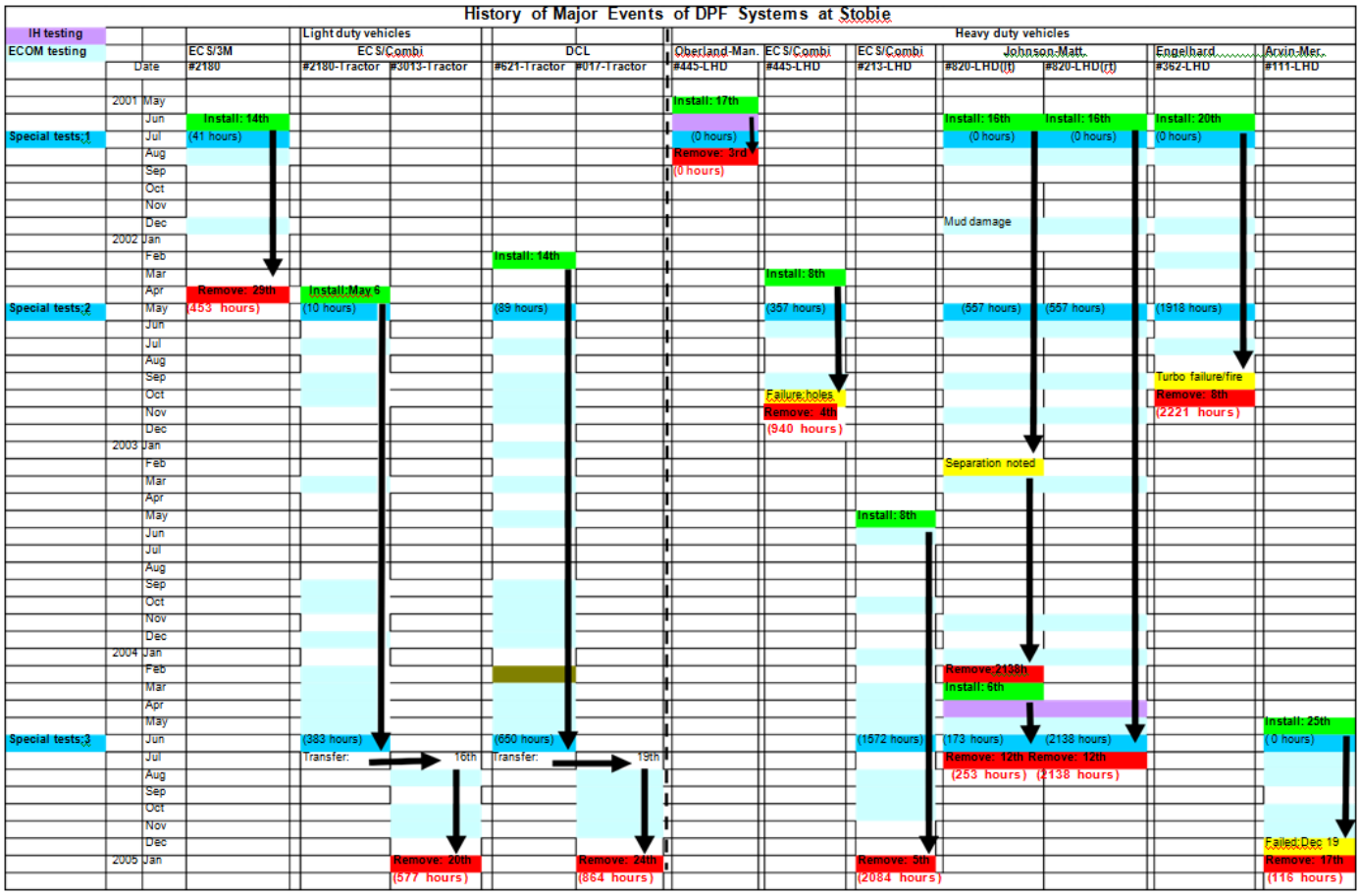
History of Major Events of DPF Systems at Stobie
IH testing
ECOM testing
Light duty vehicles
Heavy duty vehicles
EC S/3M
EC S/Combi
DCL
Oberland-Man.
EC S/Combi
EC S/Combi
Johnson-Matt.
Engelhard
Arvin-Mer.
Date
#2180
#2180-Tractor
#3013-Tractor
#621-Tractor
#017-Tractor
#445-LHD
#445-LHD
#213-LHD
#820-LHD(lt)
#820-LHD(rt)
#362-LHD
#111-LHD
2001 May
Jun
Jul
Aug
Sep
Oct
Nov
Dec
2002 Jan
Feb
Mar
Apr
May
Jun
Jul
Aug
Sep
Oct
Nov
Dec
2003 Jan
Feb
Mar
Apr
May
Jun
Jul
Aug
Sep
Oct
Nov
Dec
2004 Jan
Feb
Mar
Apr
May
Jun
Jul
Aug
Sep
Oct
Nov
Dec
2005 Jan
Special tests;1
Special tests;2
Special tests;3
Install: 14th
(41 hours)
Remove: 29th
(453 hours)
Install: May 6
(10 hours)
(383 hours)
Transfer:
16th
Remove: 20th
(577 hours)
Install: 14th
(89 hours)
(650 hours)
Transfer:
19th
Remove: 24th
(864 hours)
Install: 17th
(0 hours)
Remove: 3rd
(0 hours)
Install: 8th
(357 hours)
Failure:holes
Remove: 4th
(940 hours)
Install: 8th
(1572 hours)
Remove: 5th
(2084 hours)
Install: 16th
(0 hours)
Mud damage
(557 hours)
Separation noted
Remove:2138h
Install: 6th
(173 hours)
Remove: 12th
(253 hours)
Install: 16th
(0 hours)
(557 hours)
(2138 hours)
Remove: 12th
(2138 hours)
Install: 20th
(0 hours)
(1918 hours)
Turbo failure/fire
Remove: 8th
(2221 hours)
Install: 25th
(0 hours)
Failed:Dec 19
Remove: 17th
(116 hours)

9.1 Oberland-Mangold System

Special tests with NIOSH

The O-M DPF system uses a knitted fiber filter element and a FBC and was installed on LHD #445 with a DDEC60 engine. Shortly after the O-M system was installed, Stobie project team and NIOSH conducted the first special test in July 2001. Table 10 relates the very disappointing findings.

Table 10: Results of the special test for the Oberland-Mangold DPF on LHD #445.

Engine		Efficiency (%), eq [1]		Smoke No.[a]	Opacity %	Downstream				
Temp.	Speed[b]	PAS	EC			%		ppm		
0 hrs						O_2	CO_2	CO	NO	NO_2
warm	HI	13.6								
warm	TCS	2.8		7/5.5						
warm	TCS	19.3	39.8		15.2					
warm	TCS	44.5	47.4		14.2					
warm	TCS	17.5			18.2					
warm	Snap A		66.5							
cold	LI					15.7	3.8	85	810	39
cold	TCS					9.2	8.6	337	603	17

a: upstream/downstream

b: HI=High idle; LI= Low idle; TCS= Torque converter stall; Snap A= Snap acceleration

No upstream measurements, other than a smoke number, were made because of the extremely poor filtration efficiencies, which ranged from 2.8% to 65.5%. The downstream smoke number was very high at 5.5, which showed significant soot was coming through the filter.

This system was deemed to have failed and was removed from service and returned to Oberland-Mangold. No statistical analysis of the data collected was performed.

9.2 ECS/ 3M Omega System
on Tractor #2180

The ECS/3M is an active DPF system which uses a catalyzed ceramic fiber filter with integral electric heater for regeneration. It was installed on the Kubota tractor #2180 on 14 June 2001 and was removed on 29April 2002 after compiling 453 operating hours.

Routine Tests

Two routine tests were carried out on the ECS/3M Omega system (see the light blue months shown in July and December 2001 in Figure 70) with results shown in Table 11.

Table 11: Results of routine tests of the ECS/3M Omega DPF on tractor #2180.

Date	Hour Meter	Upstream						Downstream				
mm/dd/yy	(h)	Smk No.	CO (ppm)	NO (ppm)	NO_2 (ppm)	O_2 (%)	T (^oF)	Sm No.	CO (ppm)	NO (ppm)	NO_2 (ppm)	O_2 (%)
8/17/01	2540	9	193	173	44	16.1		3.5	233	165		15.7
12/7/01	2805	6	232	166	58	15.3	218	2.0	238	154	43	15.5

Note: Temperature readings may not represent true steady state conditions.

The filter showed marginal performance in that the downstream smoke numbers were not as low as desired. No significant increases in target gases downstream were observed.

Special tests with NIOSH

In July 2001, the system was tested for filtration efficiency shortly after it had been installed; results are shown in Table 12.

Table 12: Results of the special test of ECS/3M Omega DPF on tractor #2180.

									Downstream				
Engine	Efficiency (%), eq [1]						Smoke No.[a]	Opacity %	%		ppm		
Speed[b]	PAS	EC	O_2	CO	NO	NO_2			O_2	CO_2	CO	NO	NO_2
41 hrs													
HI	77	94.4	2	-21	5	32	9/3.5		15.7		233	165	30
HI	88.3												
HI	84.3												
HI	83.5												
Snap A		91.4						4.2-5.8					

a: upstream/downstream

b: HI=High idle; LI= Low idle; TCS= Torque converter stall; Snap A= Snap acceleration

Note: a negative number in efficiency means downstream was greater than upstream.

The filter had marginal filtration efficiency ranging from 77-94% for DPM depending upon method of measurement and engine mode. The downstream smoke number was fairly high at 3.5 and the opacity was marginal at about 5%. Surprisingly, the CO showed an increase of 21% and the NO_2 showed a decrease of 32%, both relative to their upstream values. As these results were the opposite of what would be expected from a catalyzed DPF, the results were double-checked and were verified as correct.

Even though this filter had marginal performance, it remained in service for nearly a year and accumulated 453 operating hours. It was removed in April 2002 only because 3M had announced its business decision to cease manufacturing the ceramic fibers employed in the filter. Because this DPF became obsolete, it was removed so that another relevant candidate DPF could be tested on tractor #2180.

Other comments

The operators of tractor #2180 were inconsistent in their regeneration practices due likely to a lack of habit of "plugging it in," i.e., connecting it to the regeneration control system.

Some problems were experienced with the transformer for electrical regeneration and the ECS/3M Omega controller required a wiring harness replacement, but the DPF was not employed long enough for definitive predictions to be made about the robustness of this system. These issues, however, become irrelevant because the system is no longer manufactured.

Statistical analyses of data for the ECS/3M filter are given in Appendix C in the ECSOmega-2180 folder, but are not discussed here because this system has become obsolete.

9.3 ECS/Combifilter
on Tractors #2180 and #3013

The ECS/Combifilter, an active DPF using a SiC wall flow filter and integral electric heater, was installed on tractor #2180 in April 2002, following the removal of the ECS/3M system (see above). This filter operated for more than two years on tractor #2180 and then was transferred to tractor #3013 (an identical tractor) to accumulate more operating hours. The system remained on #3013 until the end of the project in January 2005. This system accumulated 577 operating hours.

Table 13: Results of the routine tests of ECS Combifilter DPF on Tractors #2180 and #3013.

Date	Hour Meter	Upstream						Downstream				
mm/dd/yy	(h)	Sm No.	CO (ppm)	NO (ppm)	NO2 (ppm)	O2 (%)	T (°F)	Sm No.	CO (ppm)	NO (ppm)	NO2 (ppm)	O2 (%)
7/4/02	2976	4	299	127	39	15.6	428	1				
7/11/02	2979	8	268	136	39	15.6	408	2	290	145	24	16
7/25/02	2988	6	105	346	11	13.2	177	0	330	143	61	15.6
9/4/02	3011	6	296	123	54	16	454	0	320	112	54	16.1
10/4/02	3039	5	306	131	44	15.8	489	1	309	134	31	16
10/31/02	3044	7	303	161	48	16	293	1	235	185	46	16.6
3/20/03	3114	6	346	141	53	15.4	441	1	340	150	36	15.8
9/26/03	3172	7	365	102	54	15.4	469	1	362	120	38	16
10/29/03	3198	7	407	87	50	15.9	423	1	363	92	47	16.2
12/4/03	3228	7	360	133	46	15.9	465	1	332	119	52	16.6
12/27/03	3235	8	328	158	56	15.2	451	0	310	160	43	15.6
2/5/04	3256	7	297	158	50	15.4	439	1	304	170	35	15.9
3/11/04	3275	7	277	155	45	15.3	291	1	286	145	42	15.7
4/2/04	3282	6	270	107	51	16.1	445	1	272	121	32	16.4
5/5/04	3294	7	319	62	39	17.2	378	2	323	82	39	16.4
8/10/04	10	9	402	103	63	15.9	218	2	408	181	13	16.
10/6/04	95	6	268	166	50	15.6	480	0.5	269	150	46	16.4
11/5/04	134	6	273	181	54	15.4	584	1	293	150	55	16.4
Average		6.6	305	143	47		407	1	314	139	41	

Note: Temperature readings may not represent true steady state conditions. See Table 15 for better data.

Routine tests

Eighteen routine tests of the DPF system were carried out. The smoke numbers and target gas analyses for each test are shown in Table 13. The smoke numbers showed reasonable filter efficiency with an average of 6.6 upstream and 1.0 downstream. As shown in Figure 71, no trends in smoke numbers were observed. There appeared to be no significant change in the target gas concentrations between upstream and downstream values. As can also be seen in Figure 71, which plots gas analyses as a function of operating time, no trends were observed.

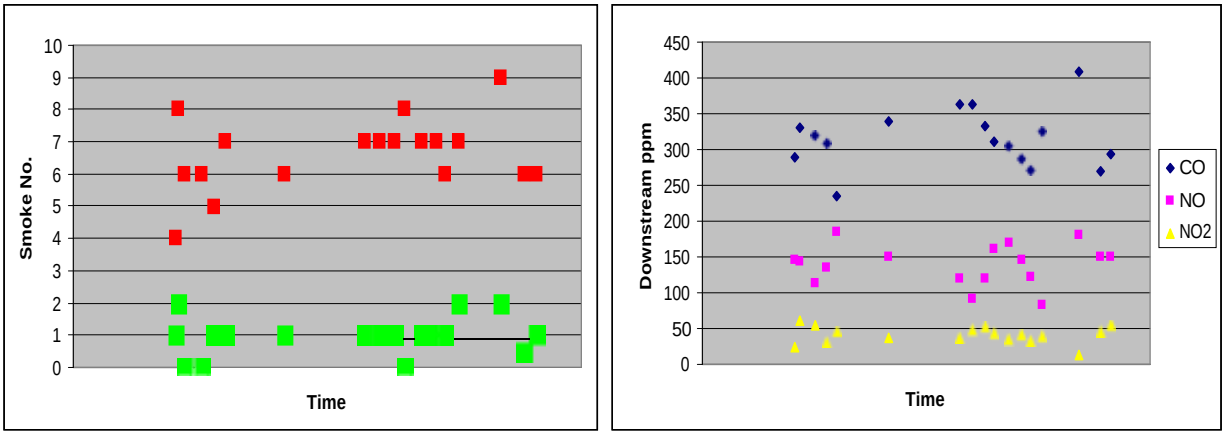

Figure 71: Results of routine testing of ECS/Combifilter DPF on Tractors #2180 and #3013 over its operating time. Left: Smoke numbers as a function of operating hours (red data are upstream and green data are downstream of DPF). Right: Target gas concentrations (in ppm) downstream of the DPF.

Special tests with NIOSH

Two special tests were carried out on the ECS/Combifilter installed on tractor #2180, one in May 2002 and the other in June 2004. These two tests bracket the routine testing done on this system while it was installed on tractor #2180. Just after the June 2004 special tests, the system was transferred to tractor #3013 to acquire more operating hours.

The May 2002 and June 2004 special test results are shown in Table 14.

Table 14: Results of two special tests of ECS/Combifilter DPF on Tractors #2180 and #3013.

								Upstream	Downstream					
Engine	Efficiency (%), eq [1]						Smoke No.[a]	Opacity %	Opacity %	%		ppm		
Speed[b]	PAS	#	O_2	CO	NO	NO_2				O_2	CO_2	CO	NO	NO_2
May 2002- 6 h														
HI	99.9	99.7	2	-6	5	10	6.5/0			15.2	4.3	370	88	80
LI	99.9	99.7		2	-3	20				17.5	2.7	135	182	66
Snap A								40.0	0.23					
Jun 2004- 366 h														
HI	99.9	99.9		14	-105	47	8.5/0				4.0	375	315	38
LI				-3	-44	73					2.3	153	204	18
Snap A								44.7	0.0					

a: upstream/downstream

b: HI=High idle; LI= Low idle; TCS= Torque converter stall; Snap A= Snap acceleration; #=number of particles

Note: a negative number in efficiency means downstream was greater than upstream.

These results showed excellent DPF efficiencies, very low opacity in downstream exhaust, and marginal changes in target gas concentrations between upstream and downstream. The largest change was observed for NO and NO_2. NO_2 decreased between upstream and downstream and NO increased. This is due to conversion of some of the NO_2 to NO by the carbon soot collected on the filter.

Size distribution

The size distribution measurements in May 2002, shown in Figure 72, were carried out for HI and LI engine operating modes.

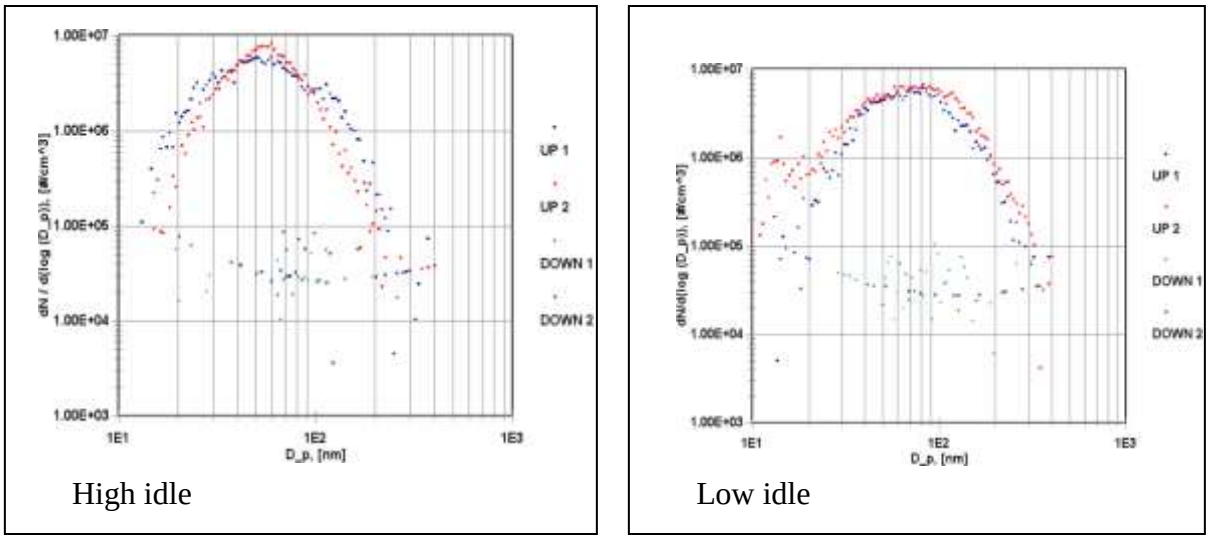

Figure 72: Particle size distributions at HI and LI for tractor #2180. The upstream size distributions are the arched red and blue dots; the downstream size distributions after the ECS/Combifilter DPF are those falling below 1.00 E+06 line and may be subject to instrument error (see Chapter 8).

The upstream (raw exhaust from the Kubota engine) distributions are both single modal, but differ between the HI and LI conditions. The LI condition generated particles with larger mean electrical mobility diameters (larger "size") and somewhat lower concentrations. As would be expected due to all test tractors (#2180, #3013, #621, and #017) being virtually identical, they all generated very similar upstream, engine out, size distributions.

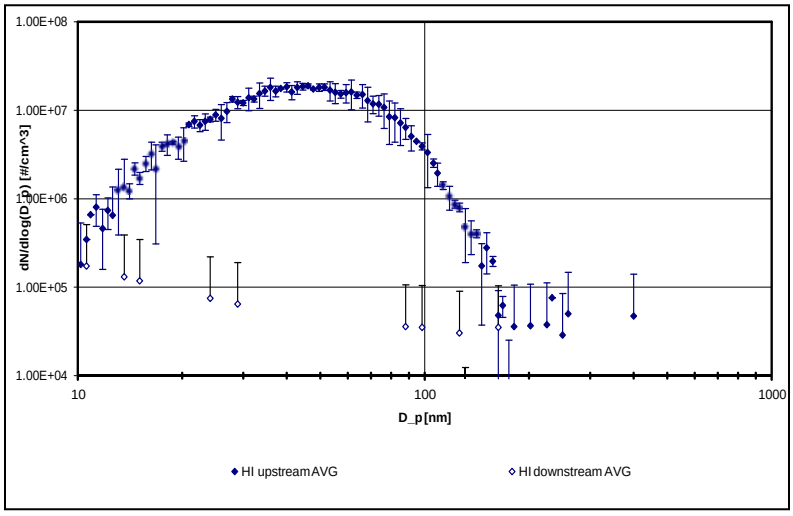

Figure 73: Average size distributions for tractor #2180 with the ECS/Combifilter DPF, June 2004 tests.

The size distribution measured in Jun 2004 for the HI condition is shown in Figure 73, where average particle counts were obtained from several scans. Clearly the downstream particle concentrations are a factor of 10 to 100 lower than the upstream concentrations, although as cautioned in Chapter 8, the measurements downstream of the DPF may be compromised.

.

Statistical analyses

The temperature and pressure data collected for tractor #2180 (Jan 2002 to May 2004) are contained in Appendix C in the ECSCombi-2180 folder. This entire period was split into 12 sections (called zooms) and the statistics for each zoom period are given in Table 15. The trend of exhaust temperature and backpressure over the 12 zooms is given in Figure 74.

Table 15: Statistical data for ECS/Combifilter on tractor #2180.

Zoom No.	Calendar start	Pressure (mbar)					Temperature (°C)				
		Min.	Ave.	Max.	95%	σ	Min.	Ave.	Max.	95%	σ
1 (a)	Jan 2002	10	75	256	190	60	84	264	528	475	136
2 (a)	Jan 2002	10	107	320	260	84	93	358	726	575	158
3	9 Aug 2002	10	44	86	50	17	156	415	750	600	139
4	27 Sep 2002	10	57	108	70	24	75	313	696	500	143
5	30 Apr 2003	10	45	96	55	18	90	264(b)	750	500	145
6	19 Sep 2003	10	70	168	120	39	93	337	747	500	144
7	10 Oct 2003	10	53	94	60	22	60	346	744	480	129
8	30 Oct 2003	10	57	140	70	25	81	341	744	500	140
9	28 Nov 2003	10	55	140	75	26	81	322	744	500	143
10	15 Jan 2004	10	56	152	90	34	51	266	651	475	149
11	22 Jan 2004	10	36	122	80	30	66	179	612	485	132
12	2 Apr 2004	10	52	276	80	34	51	231	678	475	144

a: Zooms 1 and 2 were for data when the ECS/3M filter was on tractor #2180.

b: Value here and in trend should be 319

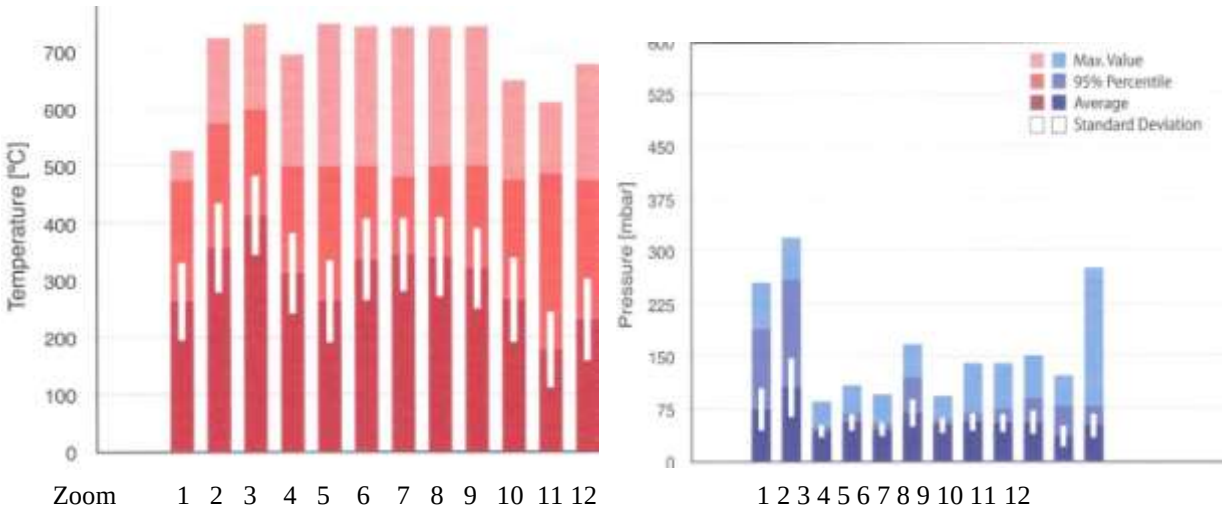

Figure 74: Exhaust temperature (left) and backpressure trend over 12 zooms for ECS/Combifilter DPF on tractor #2180.

The best integral period upon which to judge the statistics of the ECS/Combifilter DPF on tractor #2180 covers the calendar period from 30 April 2003 to June 2004 (263 operational hours to 383 operational hours). This integral period, covering zooms 5 to 12, had backpressure and temperature statistics shown in Table 16.

The frequency distributions for pressure and temperature over this integral period are shown in Figure 75. The episodic temperature (temperature durations) frequency distribution is shown in Figure 76. For the nearly 15,000 useable pressure data collected (at 60 sec intervals), Figure 77 shows the fractions of the backpressure that were normal, alert mode (yellow), and alarm mode (red). It can be seen that the backpressure on this filter was generally well behaved.

Table 16: Integral performance data of ECS/Combifilter on tractor #2180 (03 Apr 03 to Jun 04)

	Pressure (mbar)				Temperature (^{o}C)			
Location	Min.	Ave.	Max.	95%ile	Min.	Ave.	Max.	95%ile
inlet side	10	55	510	87	51	293	750	485
outlet side					3	270	765	400

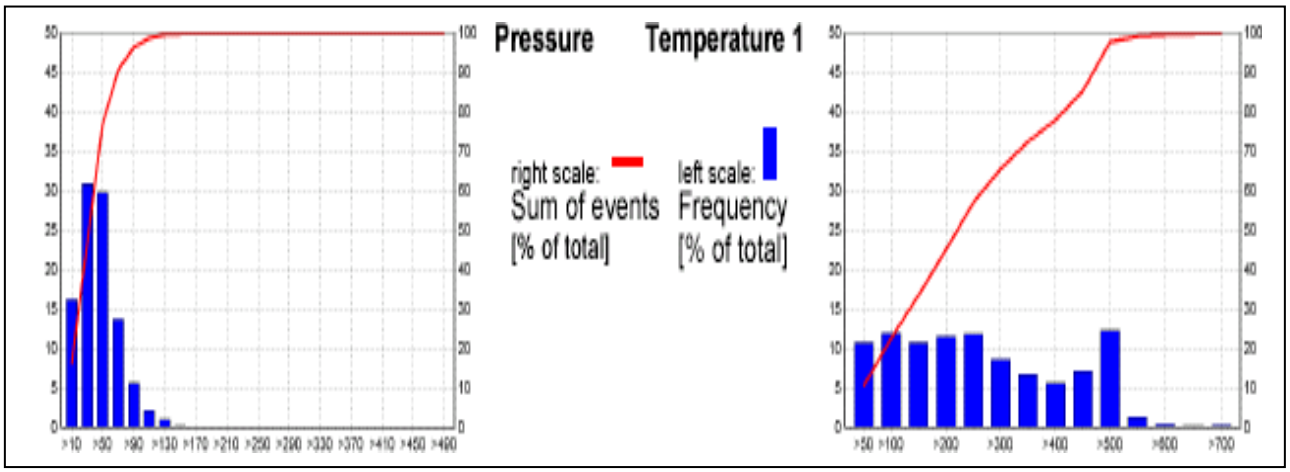

Figure 75: Frequency distributions of backpressure and temperature for ECS/Combifilter DPF on tractor #2180.

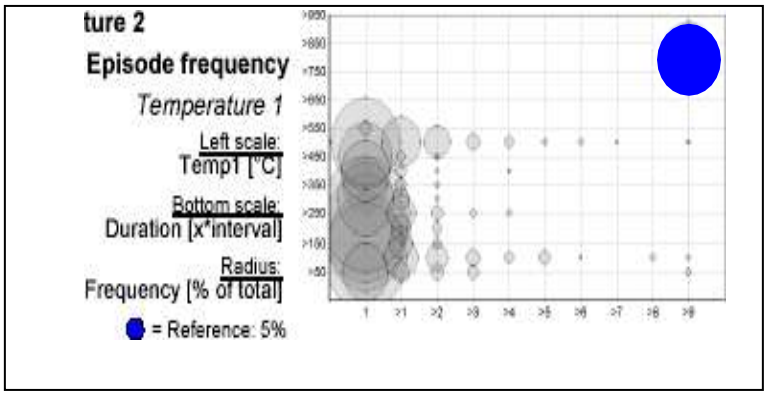

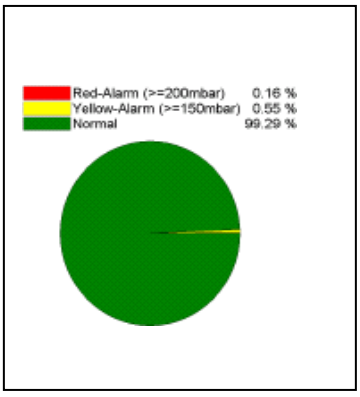

Figure 76: Episodic temperature-duration frequency, tractor #2180.

Figure 77: Backpressure pie chart.

9.4 DCL Titan

on Tractors #621 and #017

The DCL Titan, an active DPF system using a SiC wall flow filter and an off board regeneration apparatus, was installed on tractor #621 in February 2002 and operated for more than two calendar years (see Figure 70). Because of the limited use #621 was getting, the system was transferred to an identical Kubota tractor, #017, where it remained for the remainder of the project. Overall, the DCL Titan DPF system had almost three years of testing.

It must be noted, as previously explained in Chapter 7, that the system consisted of a single DPF unit, but that two identical DPFs were used alternately. That is, when one DPF was being regenerated off-board, the other DPF was being used on the vehicle. The DPFs were switched after every shift.

Routine tests

The two DPFs used for this system during the project were individually identified for routine testing of smoke numbers and gas analyses. Results are given in Table 17.

Table 17: Results of the routine tests of DCL Titan DPFs on tractor #621 and #017.

DPF1594

Date	Hour Meter(h)	Upstream					Downstream			
		SmNo.	CO(ppm)	NO(ppm)	NO2(ppm)	T(°F)	SmNo.	CO(ppm)	NO(ppm)	NO2(ppm)
7/31/02	578	7	271	124	26	159	1	323	127	60
9/4/02	603	6	271	140	56	452	1	280	147	46
10/3/02	642	8	226	194	34	491	3	235	181	33
11/1/02	690	8	194	254	40	487	1	209	195	37
5/2/03	866	7	252	192	43	495	1	261	178	39
9/26/03	935	7	288	176	50	477	1	219	136	35
11/25/03	952	7	260	194	40	549	1	265	169	42
2/5/04	1006	7	162	243	31	653	1	170	191	33
4/2/04	1025	7	218	175	39	511	1	197	141	15
5/7/04	1044	6	195	175	36	484	1	216	185	21
8/10/04	119	7	269	148	54		1	265	149	39
10/6/04	175	6	246	167	54	454	1	244	158	42
11/4/04	226	7	279	154	54	536	1	252	141	40
Average		7	241	180	43	479	1.0	241	161	37

DPF1593

9/4/02	604	2	286	140	52	460	0	268	143	45
1/30/03	794	7	117	141	41	483	1	195	202	34
3/12/03	826	6	228	225	40	465	1	243	190	31
10/27/03	944	6	210	204	43	355	1	209	191	41
12/27/03	976	6	212	219	41	541	1	220	199	41
3/1/04	1015	7	199	218	37	946	1	218	191	29
9/17/04	172	6	220	167	48	504	2	207	154	44
Average		6	210	188	43	536	1.0	223	181	38

Note: Temperatures may not represent steady state conditions. See Table 19 for better data.

DPF 1594 experienced 13 routine tests, while DPF 1593 had 7 tests. Of the 13 tests performed on DPF 1594, 10 of the tests were done while the DPF was on tractor #621 and 3 of the tests (the three last rows in the table) were done while the DPF was on tractor #017. Similarly, for the 7 tests done on DPF 1593, 6 tests were done while the DPF was on #621 and 1 test (the last row in the table) was done while the DPF was on tractor #017.

There did not appear to be significant differences in smoke numbers or target gas concentrations between the two DPFs (as judged by the similarity of average values). Also, when smoke numbers were plotted as a function of time, as shown in Figure 78, no significant trends were apparent.

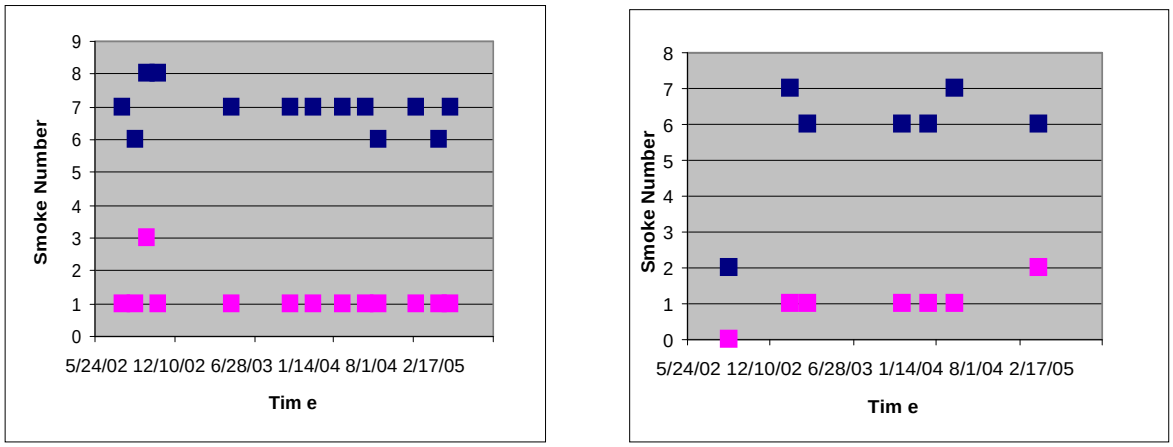

Figure 78: Smoke numbers for DCL DPF #1594 (left) and #1593 (right) on tractor #621 and #017.

The plots of downstream gas concentrations for both DCL DPFs are shown in Figure 79. No trends are apparent. An apparently higher average NO concentration for filter #1593 is likely within analytical uncertainty.

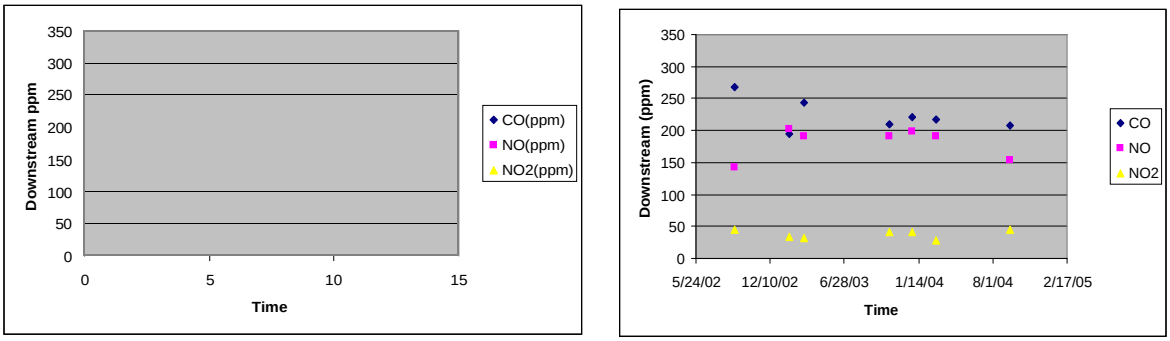

Figure 79: Target gas concentrations downstream of DCL DPF #1594 (left) and #1593 (right) on tractor #621 and #017.

Special tests with NIOSH

Two special tests were conducted: the first in May 2002; the second in June 2004. Results of these tests are given in Table 18. Excellent soot filtration efficiencies were found for both tests. Likewise, downstream smoke numbers and opacities were also good. Some marginally higher NO was observed downstream (relative to upstream) in the 2004 tests, and this is due to some small amount of conversion of NO_2 to NO by the soot on the filter.

Table 18: Results of the special tests of DCL-Titan on DPF on tractor #621.

Engine Speed[b]	Efficiency (%), eq [1]						Smoke No.[a]	Upstream Opacity %	Downstream Opacity %	Downstream %		Downstream ppm		
	PAS	#	O_2	CO	NO	NO_2				O_2	CO_2	CO	NO	NO_2
May 2002 - 89 h														
HI	99.8	99.8		-1	8	7	6/0.5			16.2	3.6	312	116	84
LI	99.9	99.3		4	13	9				18	2.2	122	211	70
Snap A								33.5	0.3					
Jun 2004 - 650 h														
HI	99.9	97.5		11	-15	19	5.5/1				4.6	375	101	48
LI				0	-13	42					2.2	153	154	43
Snap A								37.9	0.0					

a: upstream/downstream

b: HI=High idle; LI= Low idle; TCS= Torque converter stall; Snap A= Snap acceleration; #=number of particles

Note: a negative number in efficiency means downstream was greater than upstream.

Size distribution

The size distributions of particles were measured by NIOSH during special testing of June 2004. Both the upstream (engine out exhaust of the Kubota engine) and the size distributions downstream of the DCL Titan DPF during HI are shown in Figure 80. Each point on the distribution was the result of many measurements, and the average values are represented as points with uncertainty bars being ±1 standard deviation. The upstream particle size distribution is representative of particulate coming from a light duty engine running at HI. Effective removal of particulate by the DPF is seen across all particle sizes. The size distribution downstream of the DPF may be somewhat compromised as indicated in Chapter 8.

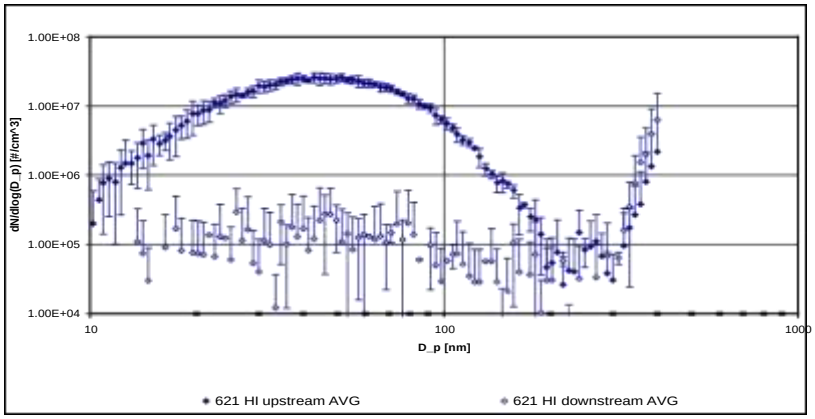

Figure 80: Particle size distribution of upstream (engine out) and downstream of DCL Titan DPF during HI of tractor #621. The downstream size distributions for >200 nanometer have spurious electronic signals and are to be ignored.

Statistical analyses

Exhaust temperature and backpressure data for the DCL Titan DPF on tractor #621 for the period Mar 2002 to June 2004 are contained in Appendix C in the DCL-621 folder. This period was split into 8 zooms, the statistics for which are given in Table 19. The DCL Titan filter was transferred to tractor #017 in Jul 2004 to get a faster accumulation of hours. The data collected on #017 for 4 zoom periods are given in Table 20. Table 19and Table 20 give the entire history.

Table 19: Statistical data for DCL Titan DPF on tractor #621.

Zoom No.	Calendar start	Pressure (mbar)					Temperature (°C)				
		Min.	Ave.	Max.	95%	σ	Min.	Ave.	Max.	95%	σ
1	8 Apr 2002	10	46	104	50	19	75	298	477	425	102
2	13 Apr 2002	10	48	262	60	26	72	279	501	425	110
3	27 Apr 2002	10	64	168	100	34	84	300	555	450	124
4	14 Nov 2002	10	64	484	80	44	87	326	726	450	116
5	31 Jan 003	10	61	156	90	34	51	280	588	475	140
6	4 Dec 2003	10	70	160	110	37	63	305	561	485	136
7	12 Feb 2003	10	71	186	110	39	51	281	558	475	131
8	7 May 2004	10	71	218	135	48	66	266	723	480	142

Table 20: Statistical data for DCL Titan DPF on tractor #017.

Zoom No.	Calendar start	Pressure (mbar)					Temperature (°C)				
		Min.	Ave.	Max.	95%	σ	Min.	Ave.	Max.	95%	σ
1	10 Aug 2004	10	170	414	290	95	93	316	615	535	153
2	10 Aug 2004	38	339	502	490	170	108	317	681	550	152
3	11 Aug 2004	10	135	404	230	80	99	297	615	500	137
4	19 Aug 2004	16	143	400	270	82	66	226	597	430	115

Trends of temperature and backpressure with time for this DPF are shown in Figure 81. This figure contains the statistics over the 8 zooms of #621 and the 4 zooms of #017. It can be seen that the backpressures were generally well-behaved while on #621 (except for a maximum value of nearly 500 mbar, which indicates that regeneration was necessary), but the backpressures were somewhat higher when the filter was installed on #017.
An explanation of the higher backpressures on #017 may be due to a combination of:

- During the week of 17 July 2004 when the DCL unit was installed on #017, most of the DEEP team was on vacation and training about regeneration was very limited;
- During early Aug 2004 it was found that the DCL regeneration station was not completing its cycle. It was sent to DCL for repair.
- A major rock burst on the main ramp for level 3400 prevented tractor #017 from returning to be regenerated.

During these periods it was requested that the DCL filter be regenerated using the CombiClean unit located on the surface. It is highly likely that the DCL filter experienced poorer regeneration during this period, and the higher backpressure may have resulted.

The best integral performance data for the DCL Titan filter is on tractor #621 from 31 Jan 2003 until its transfer. For this integral period the statistics are given in Table 21. The pressure and temperature frequency distributions are shown in Figure 82 and the episodic temperature-duration frequency is shown in Figure 83. The fraction of time the backpressure was normal is shown in Figure 84.

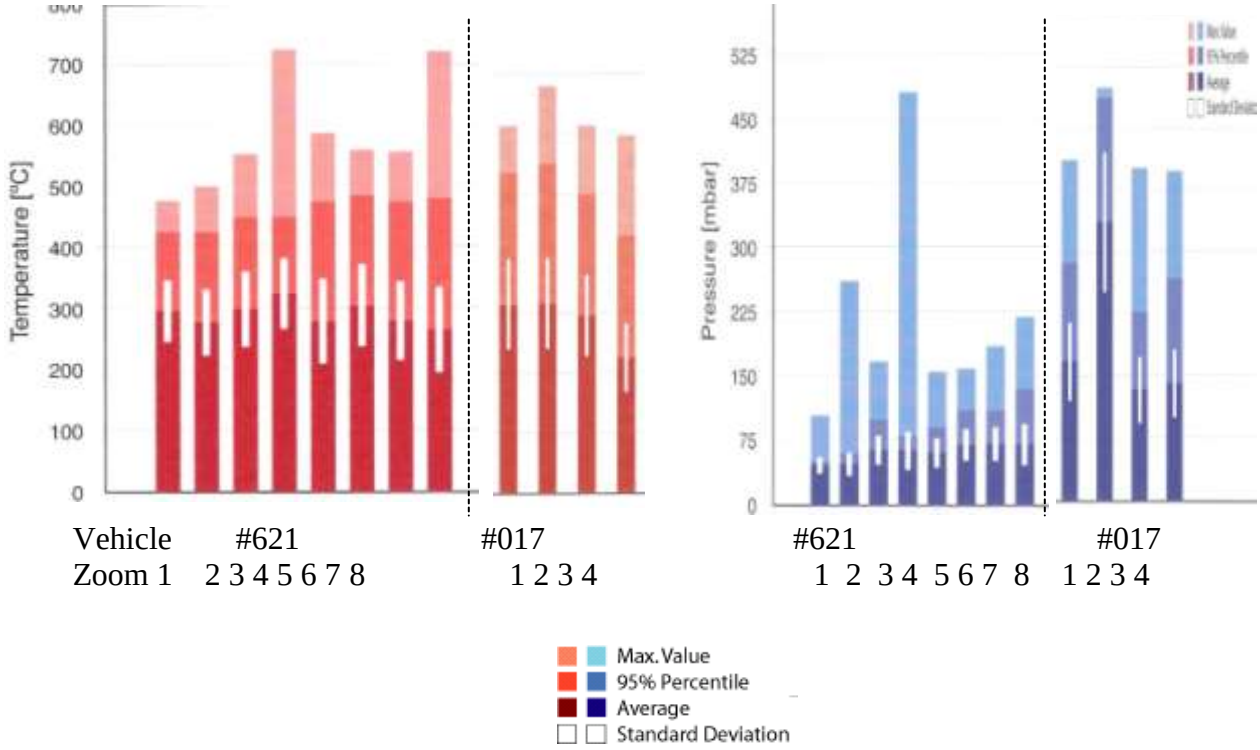

Figure 81: Trend of temperature (left) and backpressure for DCL Titan DPF on tractors #621 and #017

Table 21: Integral statistics for DCL Titan on tractor #621 (21 Jan 2003 to 19 Jul 2004).

Location	Pressure (mbar)				Temperature (°C)			
	Min.	Ave.	Max.	95%ile	Min.	Ave.	Max.	95%ile
inlet side	10	68	510	110	54	276	726	481
outlet side					3	251	765	392

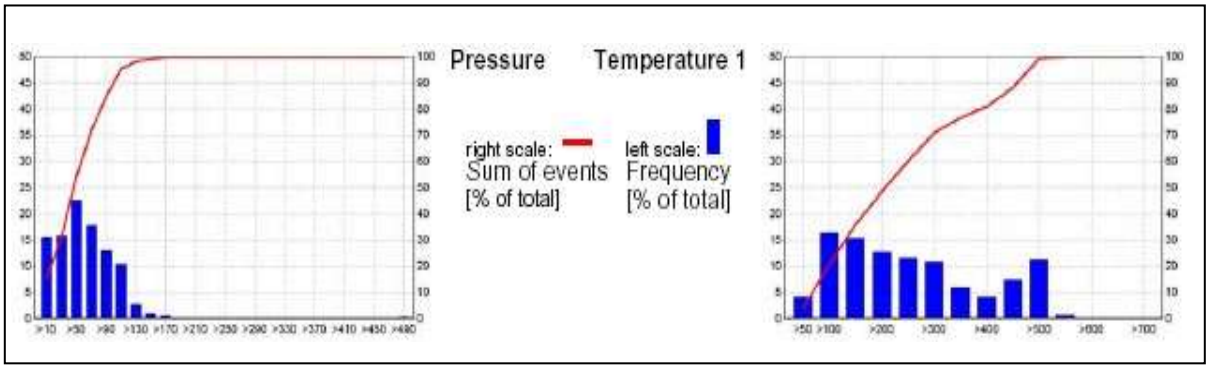

Figure 82: Pressure and temperature frequency distributions for DCL Titan filter on tractor #621.

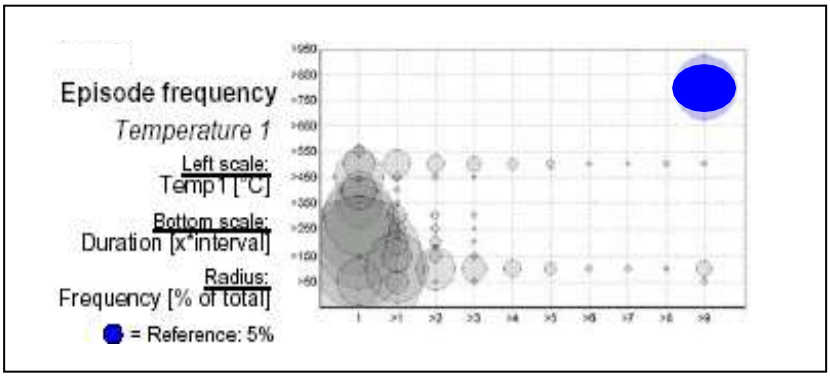

Figure 83: Episodic temperature-duration frequency tractor #621.

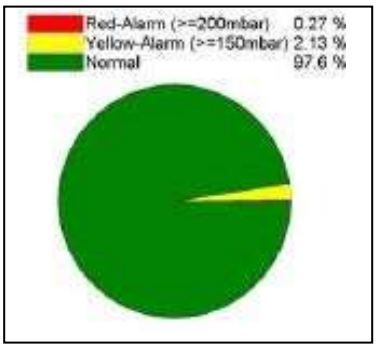

Figure 84: Exhaust backpressure pie chart for DCL Titan on tractor #621.

9.5 ECS/Combifilter (first) on LHD #445

After the failure of the Oberland-Mangold system on LHD #445, the Stobie project team decided to install an ECS/Combifilter on LHD #445. The ECS/Combifilter is a passive DPF using a SiC wall flow filter and an integral heater for regeneration. This DPF was installed during April 2002. Three routine tests were conducted to measure smoke numbers and target gas concentrations, and one special test by NIOSH was carried out on the system in May 2002 shortly after its installation.

Special test (May 2002)

Table 22: Results of the special tests of ECS/Combifilter DPF on LHD #445.

Engine Speed[b]	Efficiency (%), eq [1]						Smoke No.[a]	Upstream % Opacity	Downstream % Opacity	Downstream %		Downstream ppm		
	PAS	#	O_2	CO	NO	NO_2				O_2	CO_2	CO	NO	NO_2
TCS	94.8	99.6		-104	-41	63				9.4	8.6	224	688	13
HI	92.9	--		22	-30	60	7.8/5.7	35.3	1.6	13.4	5.6	98	553	12
LI	93.0	93.6		-9	-8	75				16.3	3.9	93	858	34

a: upstream/downstream

b: HI=High idle; LI= Low idle; TCS= Torque converter stall; Snap A= Snap acceleration; #=number of particles

Note: a negative number in efficiency means downstream was greater than upstream.

The notable points about the special tests results were:

(a) The upstream exhaust from #445 had the highest PAS readings and highest number of particles (#) of all of the vehicles tested (see Figure 117, Figure 118 and the NIOSH report 2002 in Appendix E, Table 2 and Table 3). This is because LHD #445 has a very high fuelling rate and higher power output compared to other LHDs being tested.
(b) Downstream particulate concentrations were higher than expected (ibid); the PAS measured efficiencies fell between 92-94% as shown in Table 22 above.
(c) Smoke numbers were very high and the opacity was higher than expected.
(d) The unusual increase in downstream CO (as denoted by the negative efficiency number) was likely caused by some filtered soot burning (regeneration) during the test at TCS, the engine mode that produces high exhaust temperatures.
(e) Backpressure was noted to exceed 150 mbar under the TCS condition.

The special test indicated that this system was not performing as expected, even after only a short operational life. Concerns about vehicle operator attention to regular active regeneration (plugging the unit into the regeneration station power supply) were discussed (see below).

Routine tests

Three routine tests were carried out on this system, and the results are shown in Table 23. By September 2002 the system was showing extremely high smoke numbers, and it was obvious that regeneration was not occurring.

Table 23: Results of routine tests of ECS/Combifilter DPF on LHD #445.

Date	Hour Meter(h)	Upstream					Downstream			
		SmNo.	CO(ppm)	NO(ppm)	NO2(ppm)	T(^{o}F)	SmNo.	CO(ppm)	NO(ppm)	NO2(ppm)
6/27/02	281	7	154	542	12	851	1			
9/11/02	540	8	70	558	11	805	6	89	562	7
9/15/02	444	7	90	606	14	939	7	114	648	6

Note: Temperatures may not represent steady state conditions.

Regeneration problems

The Stobie project team investigated the possible reasons why regenerations were not being performed routinely. They learned that the regeneration station, located on level 3000, was not the best location for regeneration because of the distance between it and operating location of the LHD #445. This situation created extra effort in conducting the regeneration with the result that the DPF was becoming more and more blocked with soot. Backpressure readings became unacceptably high, and it was decided to clean the filter manually using the CombiClean system.

Damage to the ECS/Combifilter

When the DPF was cleaned of the built up soot, it became obvious that significant damage to the filter element had occurred which compromised its integrity.

The failure of the ECS/Combifilter on LHD #445 was due to a number of reasons. The first obvious reason was the logistical difficulties that the operators experienced in doing routine regeneration of the system. If systems that rely on active regeneration are not provided with a good and easily conducted regeneration program, then it should not be surprising when such a system fails. While the Stobie team thought it had adequately communicated the need for regeneration to the vehicle operators, an unforeseen problem associated with ease of access to the regeneration station prevented the vehicle operators from fulfilling regeneration in a regular fashion.

The second reason for failure of this system was caused by the regeneration system itself. This was only clearly established after another ECS/Combifilter was installed on LHD #213. At the beginning of operation on LHD #213, the ECS DPF also showed some indications of less than adequate regeneration (e.g., higher than expected backpressure). After consultation with ECS engineers it was determined that adjustments to the regeneration station were required, namely, that the air flow had to be decreased to prevent excessive cooling of the filter element during regeneration, and that both the temperature and duration of the heating had to be increased. Upon making these adjustments the ECS CombiClean regeneration system performed well.

Statistical analyses

Statistical data on this filter are contained in Appendix C in the ECSCombi-445 folder. Owing to its failure due to poor regeneration practice, no further analysis of these data is given here.

9.6 ECS/Combifilter (second)
on LHD #213

Dual ECS/Combifilters acting in parallel were installed on LHD #213 on 14 Feb 2003. Because of the previous failure of routine regeneration of the same type of DPF on LHD #445, the Stobie team made an extra effort to educate vehicle operators about the importance of their role and actions regarding regeneration. In addition, the off-board ECS regeneration station was moved from Level 3000 to Level 3400 so that its location was more convenient to LHD #213. All of these efforts were rewarded with excellent service of the unit over more than 1.5 years until LHD #213 was buried by a run of ore and was removed from further testing near the end of 2004.

Routine tests

Fourteen routine tests of this system were carried out, and the results are shown in Table 24. The smoke numbers showed good filter efficiency with an average upstream value of 7.1 and an average downstream number of 1.0 (see also Figure 85).

Table 24: Results of routine tests of ECS/Combifilter DPF on LHD #213.

		Upstream						Downstream				
Date	Hour Meter (h)	Sm No.	CO (ppm)	NO (ppm)	NO_2 (ppm)	O_2 (%)	T (^oF)	Sm No.	CO (ppm)	NO (ppm)	NO_2 (ppm)	O_2 (%)
5/7/03	390	7	135	634	19	10.5	790	0.5	110	525	10	11.3
5/25/03	546.8	7	108	1269	48	10.3	764	1	107	473	9	11.2
10/30/03	721.3	6	98	581	26	14.3	593	0.5	88	586	12	14.4
1/5/04	970.6	8	116	1375	48	10.8	739	2	106	642	14	11.7
1/29/04	1173.1	8	131	1253	32	10.4	764	0	143	815	18	11.4
3/6/04	1376.8	7	113	1037	28	10.7	492	1	120	698	21	11.9
3/17/04	1462	7						1				
4/8/04	1661.5	7	77	1043	30	11.6	707	1	86	466	7	12.2
4/15/04	1688	7	83	463	12	11.7	639	2	77	443	6	12.3
5/4/05	1855	8	87	518	16	11.2	740	1	90	497	6	12
6/7/04	1968	8	107	467	26	14.7	501	0	117	445	3	11.2
8/19/04	274	7	84	477	26	14.8	903	3	75	474	4	14.8
9/13/04	314	7	57	639	24	13.8	634	1	62	460	9	15.1
10/1/04	425.3	6	84	502	27	14.6	700	1	71	501	10	15.4
Average		7.1	98	789	28	12.3	690	1	96	540	10	13

Note: Temperatures may not represent steady state conditions. See Table 26 for better data.

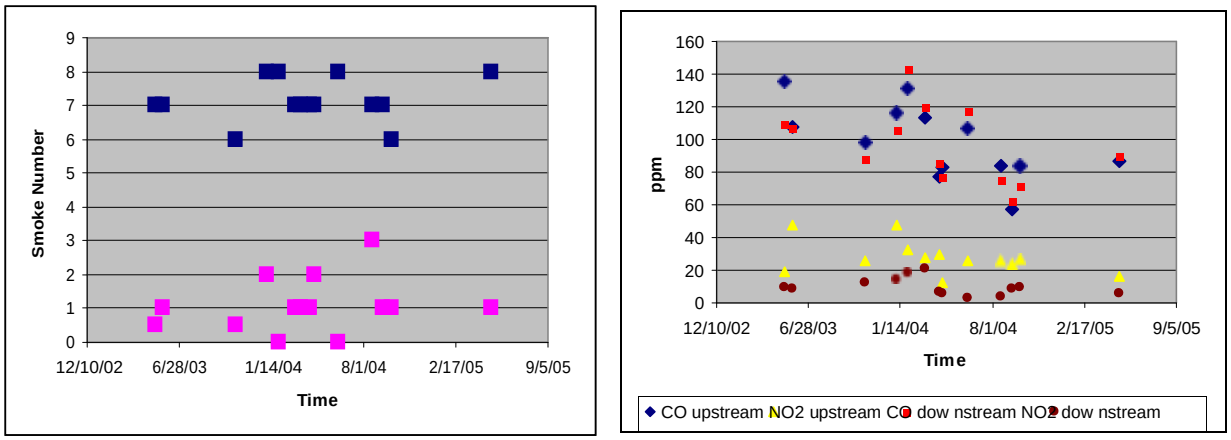

Figure 85: Smoke numbers (left) and target gas concentrations for the ECS/Combifilter DPF on LHD #213.

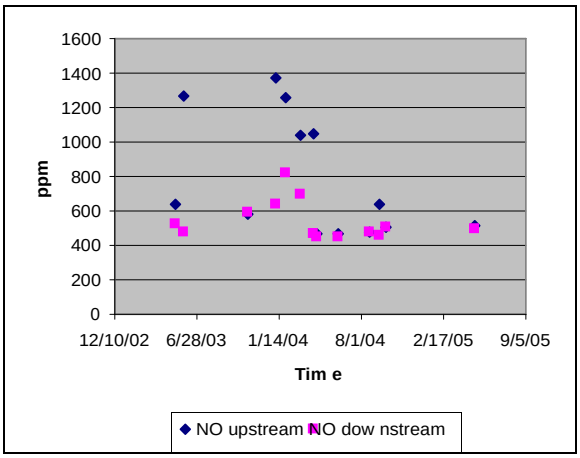

Upstream and downstream CO concentrations (Figure 85) may have decreased with time. This may have been related to changing engine conditions. NO_2 concentrations are relatively low. NO concentrations, shown separately in Figure 86, were high from this engine (upstream) and were reduced by the ECS/Combifilter DPF. Although considerable scatter exists, the upstream NO concentrations may also be decreasing with time.

Figure 86: NO concentrations for ECS on tractor #213.

An example of routine operation of this system is shown in Figure 87. The horizontal axis is time and covers about 52 hours between 11:40AM, 30 April and 3:40 PM, 2 May. The green line shows the upstream temperature, blue shows the downstream temperature, and red shows the backpressure. During the period shown, the backpressure slowly increased from about 60 to about 100 mbar.

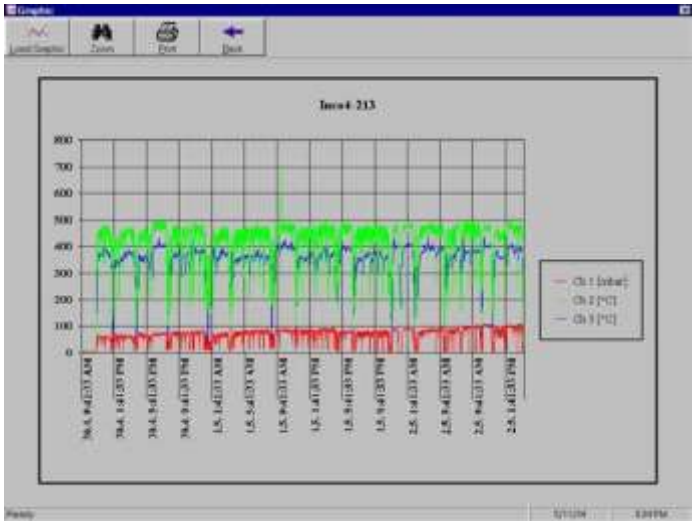

Figure 87: Routine data logging for vehicle #213 over a 52 hour period April 30-May 2, 2004.

Special test

One special test was conducted on this system in June 2004. The NIOSH test report can be found in Appendix E. Summary results are given in Table 25. In general, excellent soot removal efficiencies were observed with smoke numbers at HI being 8.5 and 0 upstream and downstream, respectively. The only numbers that are worth noting in this table are the significant reductions in downstream NO_2 under all engine conditions tested.

Table 25: Results of special test of ECS/Combifilter DPF on LHD #213.

								Upstream	Downstream					
Engine Speed[b]	Efficiency (%), eq [1]						Smoke No.[a]	% Opacity	% Opacity	%		ppm		
	PAS	#	O_2	CO	NO	NO_2				O_2	CO_2	CO	NO	NO_2
HI	99.8	98.9		3	3	61	8.5/0				4.6	112	369	5
LI				4	4	81					2.1	116	355	7
TCS	99.9	91.2		-23	12	36					7.7	169	376	7
Snap A								45	0.4					

a: upstream/downstream

b: HI=High idle; LI= Low idle; TCS= Torque converter stall; Snap A= Snap acceleration; #=number of particles

Note: a negative number in efficiency means downstream was greater than upstream.

Size distribution

Figure 88 shows the particle size distribution was measured for LHD #213 for torque converter stall and high idle engine conditions. Data for the TCS, since it presents a real load on the engine, are more representative of real world conditions and in this case provide fairly reliable downstream measurements.

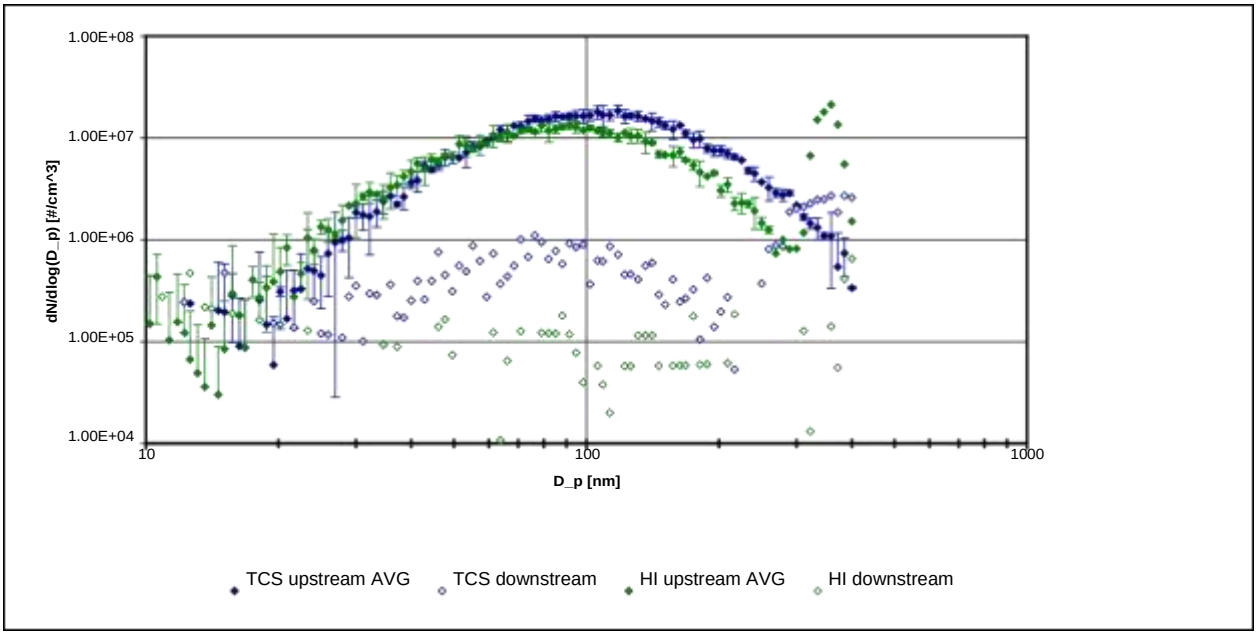

Figure 88: Size distributions for LHD #213; upstream TCS (solid blue) and HI (solid green) are compared to the distributions (open blue and open green, respectively) after the ECS/Combifilter DPF. The high readings in the coarsest particle region (far right) for the solid green and open blue points are due to spurious electronic signals and should be ignored as should the open green data for HI where measurements have questionable validity.

Accident with LHD #213

On 8 November 2004, LHD #213 was partially buried in a muck pile. The vehicle sustained significant damage when it rolled onto its right side and had to be pulled out of the muck. Photos showing the damaged unit after it had been towed to the garage at 2400 Level are shown in Figure 89. The ECS DPF system and the data logger on LHD #213 still worked, but the system was not put back into operation because LHD #213 was too damaged, and it was impractical to relocate the filter system to another LHD because the project testing was due to end within months.

Showing damaged vehicle electrical box.

Showing cracked and open top of engine block.

Showing position of ECS/Combifilters.

Figure 89: Damage to LHD #213 from mucking accident. Refer to Figure 43 and Figure 44 to see the installed positions of the dual ECS/Combifilter DPFs on this vehicle.

Statistical analyses

Temperature and pressure data for the ECS/Combifilter DPF on LHD #213 are contained in Appendix C under the ECSCombi-213 folder. A total of 15 zoom periods covered the entire history of this DPF on LHD #213. The statistical analyses for these 15 periods are given in Table 26. Trends of temperature and backpressure are shown in Figure 90. One can see that the average backpressure was much improved from the earlier ECS/Combifilter DPF (on LHD #445) due to increased attention to regeneration. In fact, the trend is downward over the 15 periods showing improved regeneration practice with time. The temperature trend is fairly stable with averages over the 15 periods of about 400 ^{o}C. This relatively low exhaust temperature on an LHD points out the need for active regeneration when no noble metal catalyst is present on the filter element.

Table 26: Statistical data for ECS/Combifilter on LHD #213 over 15 zoom periods.

Zoom No.	Calendar start	Pressure (mbar)					Temperature (^{o}C)				
		Min.	Ave.	Max.	95%	σ	Min.	Ave.	Max.	95%	σ
1 (a)	14 Feb 02	10	96	418	130	72	102	448	750	600	72
2	10 Oct 03	10	90	158	100	29	102	425	540	450	69
3	30 Oct 03	10	105	212	130	39	114	403	642	435	65
4	12 Dec 03	10	100	200	130	38	99	402	561	430	66
5	22 Dec 03	10	100	156	110	31	96	409	552	450	66
6	29 Jan 04	10	90	160	110	34	96	399	513	435	66
7	14 Feb 04	10	93	218	120	38	96	394	528	425	74
8 (b)	27 Feb 04	10	85	152	100	32	123	403	714	450	63
9	17 Mar 04	10	59	138	70	19	99	417	513	435	45
10	27 Mar 04	10	56	122	50	14	99	423	633	450	46
11	8 Apr 04	10	67	130	85	23	123	432	570	450	48
12	18 Apr 04	10	52	90	50	13	114	423	513	445	44
13	12 May 04	10	55	110	60	17	129	433	708	450	51
14	23 May 04	10	54	116	50	16	129	432	708	450	55
15	25 Jun 04	10	55	116	50	19	69	458	747	525	84

a: The tabular date and data above for zoom 1 do not match the data for zoom 1 in trends charts below. Zoom 1 date in the trend chart is 30 April 2003.
b: Ave pressure of 85 mbar is inconsistent with trend chart below. Data are from PDF summary in Appendix C.

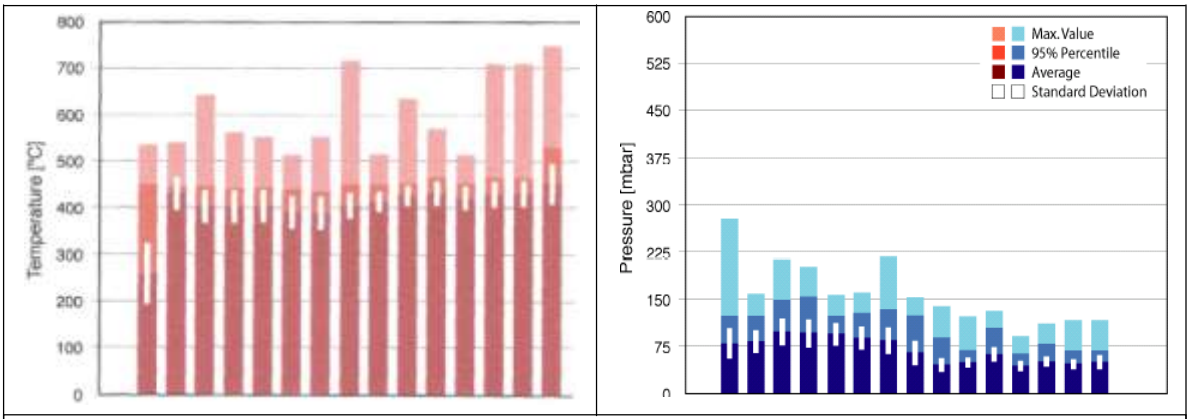

Figure 90:Trend of temperature (left) and backpressure (right) for ECS/Combifilters on LHD #213

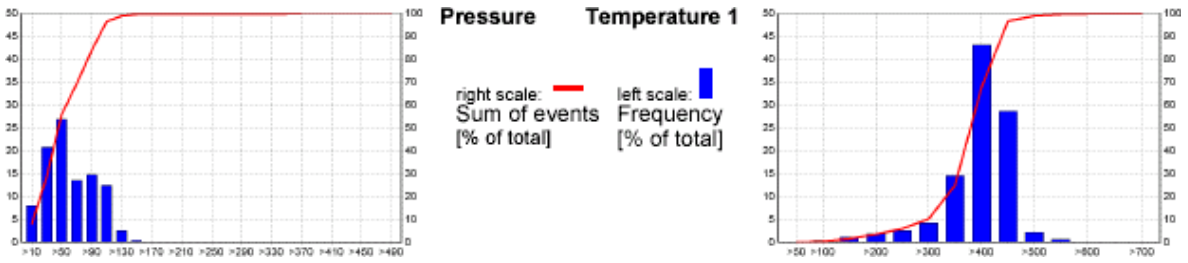

Figure 91: Frequency distributions of temperature and backpressure for LHD #213.

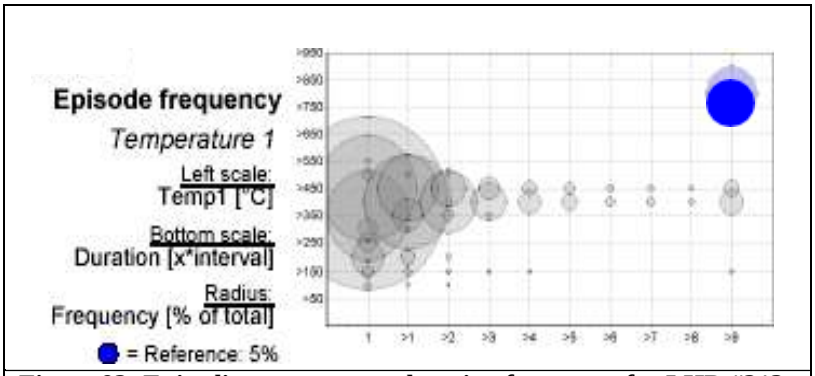

Figure 92: Episodic temperature-duration frequency for LHD #213

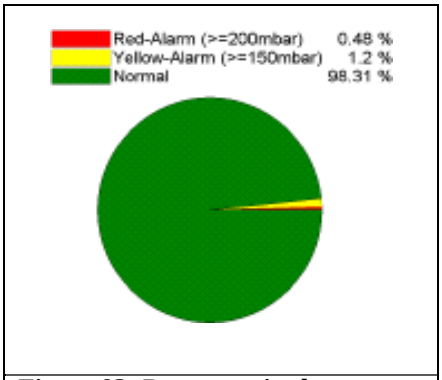

Figure 93: Pressure pie chart.

Table 27: Integral statistics for ECS/Combifilter on LHD #213.

	Pressure (mbar)				Temperature (°C)			
Location	Min.	Ave.	Max.	95%ile	Min.	Ave.	Max.	95%ile
inlet side	10	80	510	109	72	419	750	448
outlet side					3	345	567	380

The integral statistics, covering 30 April 2003 to 19 August 2004, are given in Table 27.

The frequency distributions of both temperature and backpressure over the DPF's life are shown in Figure 91, and the episodic frequencies at temperature are shown in Figure 92. These data clearly show that the temperature-durations were limited to <450°C, < 2 minutes; this temperature-duration would not be adequate by itself to passively ignite and burn the soot on the uncatalyzed filter. Recognition of this fact is an important finding for LHD-DPF selection.

As would be expected from the improved regeneration practice, the fraction of normal backpressure, shown in Figure 93, was very good.

Concluding comments on ECS/Combifilter

The ECS/Combifilter, an active DPF using an uncatalyzed SiC wall flow filter and integral electric heating element, performed very well for heavy duty LHD service. It was gratifying for the Stobie team to see this system perform well after the poor experience with an identical DPF when regeneration was not carried out routinely. This experience shows the importance of training operators and having an operational system that assures regeneration. Without such attention, active systems like this one are bound to fail. With good attention to regeneration, this system worked well.

9.7 ngelhard
on LHD #362

The Engelhard DPF, a passive system utilizing a noble metal catalyst wash coat on the cordierite wall flow filter element, was installed on LHD #362 with a DDEC60 engine on 20 June 2001. The system operated for more than a year with good performance, including surviving an accident where mud penetrated into the filter from the discharge side. In September 2002 a fire occurred on the vehicle. The fire was associated with failure of the engine's turbo, which sprayed oil over the hot engine and adjacent surfaces which ignited the oil. This incident caused the Engelhard DPF to be removed. It had accumulated 2221 operating hours.

Routine tests

Ten routine tests of this system were carried out and the data are displayed in Table 28. The smoke numbers showed very good filter soot removal efficiency, averaging about 7 upstream and <1 downstream. Smoke numbers as a function of time are shown in Figure 94.

Table 28: Results of routine tests of Engelhard DPF on LHD #362.

Date	Hour Meter	Upstream						Downstream				
			CO	NO	NO2	O2	T		CO	NO	NO2	O2
mm/dd/yy	(h)	Sm No.	(ppm)	(ppm)	(ppm)	(%)	(°F)	Sm No.	(ppm)	(ppm)	(ppm)	(%)
7/18/01	7892	8	82	572	26	7.8		0.5	10	470	60	7.9
12/6/01	8670	7.5	76	526	16	11.2	691	1	0	521	66	11.5
12/30/01	93	7.5	73	973	54	11.2	578	1	0	524	60	11.9
2/1/02	345	7	75	630	22	11.2	470	0	22	1099	40	11.7
5/23/02	1011	7	93	1313	61	10.7	628	1	0	1154	77	11.6
7/4/02	1156	9	98	479	13	10.8		0				
7/18/02	1191	3	79	557	30	14.2	526	1	11	541	22	14.4
8/7/02	1268	7	69	584	32	14.8	517	0	0	596	18	15.3
9/14/02	1581	7	99	542	11	10.7	520	1	16	630	16	11.3
9/18/02	1585	7.5	91	553	19	10.8	733	0	0	490	29	11.4
Average		7.1	84	673	28	11.3	583	0.6	7	669	43	11.9

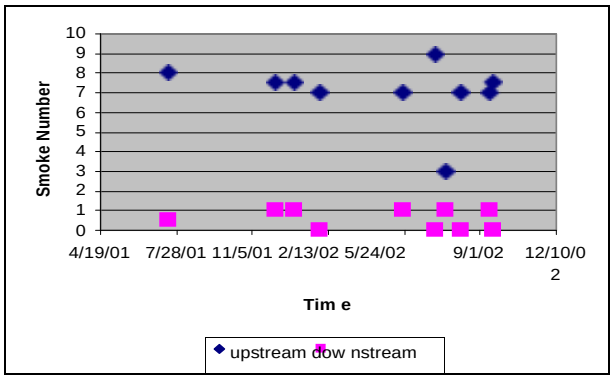

Figure 94: Smoke numbers for LHD #362 before and after the Engelhard DPF.

One smoke number of 3 (upstream) appears to be anomalous. It is suspected that the measurement may have been conducted prior to the engine condition having been stable. If this number is removed, the upstream average smoke number becomes 7.5.

Gas concentrations are shown in Figure 95. CO concentration downstream of the Engelhard DPF was very low, which is consistent with the filter having a catalytic coating that assists in oxidizing CO to CO_2. It also appears that the NO_2 was somewhat

lower during the latter periods of testing, but no reason exists for this behaviour. Likewise, there seems to be considerable scatter among the NO results for both upstream and downstream.

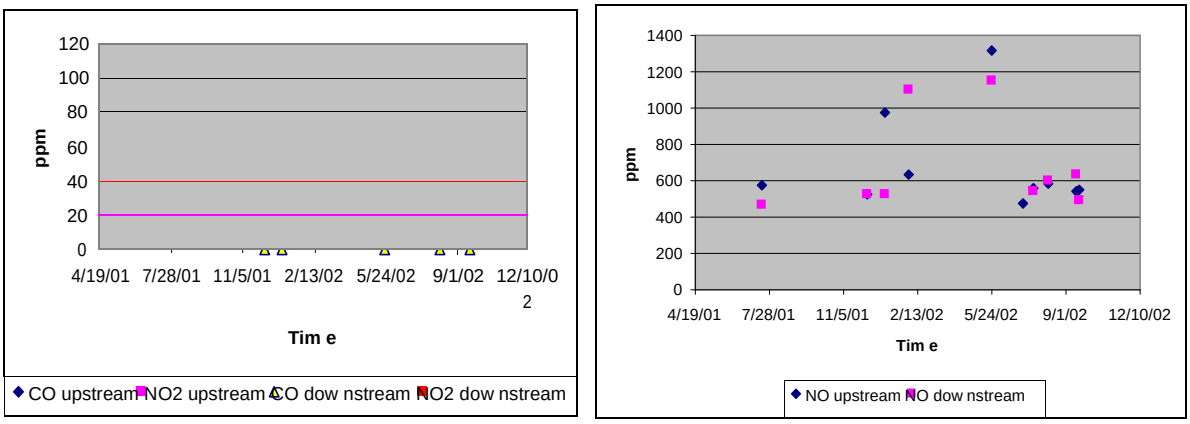

Figure 95: Target gas concentrations for the Engelhard DPF on LHD #362.

Special tests with NIOSH

Two special tests with NIOSH were carried out on this system, one in July 2001 shortly after the system was installed, and the other in May 2002 when the system had accumulated 1918 operating hours. The full reports of the tests are in Appendix E. Summary results of these two tests are given in Table 29. Of note is the high removal of CO by the Engelhard DPF. This was expected because of the catalytic coating present. The noble metal catalyst also increases the downstream NO_2 concentrations, in some cases substantially, as expected.

Table 29: Results of special tests of Engelhard DPF on LHD #362.

								Upstream	Downstream					
Engine Speed[a]	Efficiency (%), eq [1]						Smoke No.[a]	% Opacity	% Opacity	%		ppm		
July 2001 - 0 h														
	PAS	EC	O_2	CO	NO	NO_2				O_2	CO_2	CO	NO	NO_2
HI	99.7			98	-800	-81				9.9		2	421	58
TCS	99.6						8/0.5		0.2	7.9		10	470	60
TCS		98.8		80	18	-130								
TCS		100												
TCS		99.5												
Snap A		99.4												
May 2002 - 1918 h														
	PAS	#	O_2	CO	NO	NO_2				O_2	CO_2	CO	NO	NO_2
TCS	100	97		90	-1	-55	9/0	35.9	0.4	10.7	7.7	12	495	53
HI	100	95.1		91	2	1				14.2	5.1	9	506	50
LI	99.6			83	10	-12				17.6	2.5	25	492	85

a: upstream/downstream

b: HI=High idle; LI= Low idle; TCS= Torque converter stall; Snap A= Snap acceleration; #=number of particles

Note: a negative number in efficiency means downstream was greater than upstream.

Size distribution

During the special tests on May 2002, NIOSH measured the size distributions upstream (raw exhaust of Deutz engine) for three different engine conditions as shown in Figure 96 (left). TCS and HI conditions showed similar upstream distribution; LI showed particle counts more than an order of magnitude lower. Figure 96 (right) shows upstream and downstream distributions for torque converter stalls. Two replicate upstream distributions are shown in red and blue, while three replicate downstream distributions are shown in yellow, green and black. The TCS data downstream of the DPF appears in this case to be minimally compromised by the caveats noted in Chapter 8.

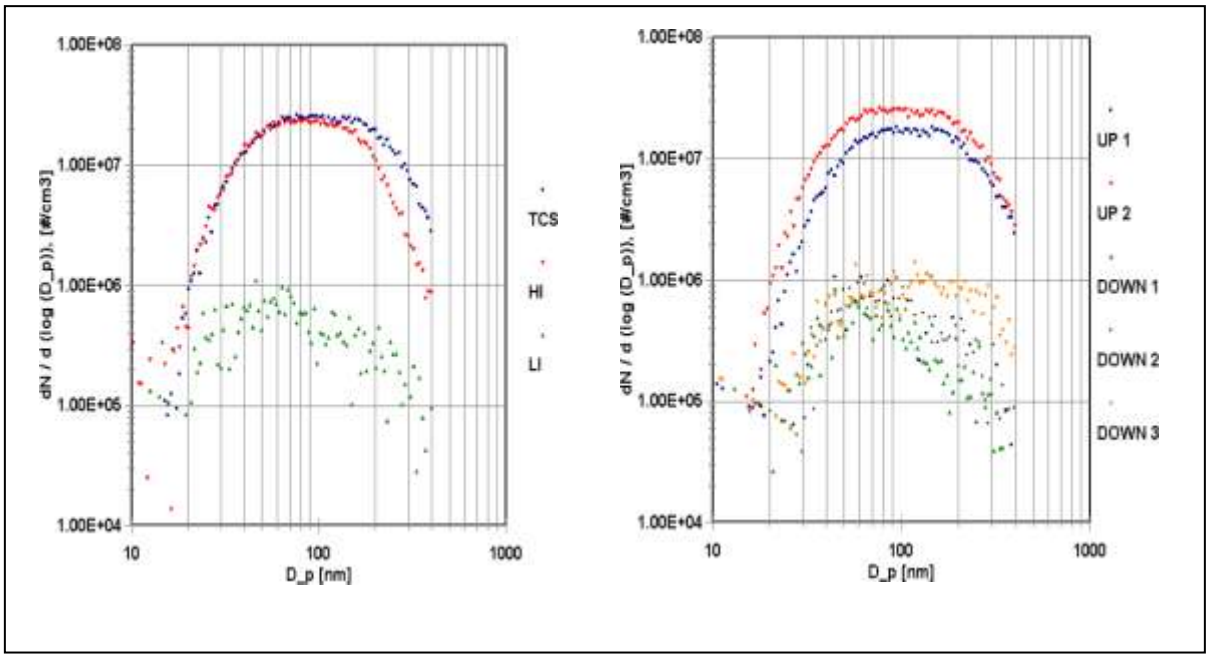

Figure 96: Left: Exhaust particle size distributions upstream of Engelhard DPF on LHD #362 for three engine conditions; Right: Size distributions upstream and downstream of the DPF for TCS.

Statistical analyses

The data for the Engelhard DPF on LHD #362 are contained in Appendix C under Engelhard-362 folder. A total of 16 zoom periods covered the entire history of this filter (from Aug 2001 to its removal in Oct 2002 when the engine's turbo failed). Statistics for each of the zooms are given in Table 30 and integral statistics for the complete history are given in Table 31. The trends of temperature and backpressure are shown in Figure 97.

Frequency distributions of pressure and temperature are shown in Figure 98. As observed with other LHDs, the temperature distribution clearly shows temperatures <500 ^{o}C. The episodic temperature duration frequencies are shown in Figure 99 and look very similar to other LHDs in this project.

As shown in Figure 100, which is a pie chart showing the fraction of normal backpressure, it is clear that this filter suffered relatively high backpressures for sustained periods, but its filtration efficiency (see above) remained excellent.

Table 30: Statistical data for Engelhard DPF on LHD #362 over 16 zoom periods.

Zoom No.	Calendar start	Pressure (mbar)					Temperature (°C)				
		Min.	Ave.	Max.	95%	σ	Min.	Ave.	Max.	95%	σ
1	03 Oct 01	10	298	508	470	148	57	450	627	535	103
2	09 Nov 01	10	139	236	160	33	204	434	534	450	42
3	12 Nov 01	10	156	228	180	39	141	442	735	450	48
4	04 Dec 01	10	158	242	190	40	165	441	540	450	47
5	17 Dec 01	10	174	464	200	48	162	441	579	450	52
6	11 Jan 02	10	151	220	175	37	195	438	528	450	46
7	19 Jan 02	10	154	228	180	38	192	444	531	450	48
8	01 Feb 02	10	155	248	190	46	198	448	600	475	54
9	05 Feb 02	10	132	198	155	41	165	439	567	475	61
10	09 Feb 02	10	150	370	200	48	177	466	570	500	57
11	14 Feb 02	10	154	248	190	42	156	452	600	475	51
12	18 Feb 02	10	148	250	200	48	171	439	570	450	52
13	13 Apr 02	10	190	306	235	58	189	451	564	480	62
14	17 Apr 02	10	202	326	260	76	129	450	600	500	85
15	18 Jul 02	10	201	322	250	80	117	460	711	500	95
16	10 Aug 02	10	197	508	220	63	99	481	573	500	79

Table 31: Integral statistics for Engelhard on LHD #362.

Location	Pressure (mbar)				Temperature (°C)			
	Min.	Ave.	Max.	95%ile	Min.	Ave.	Max.	95%ile
inlet side	10	168	510	229	102	449	738	488

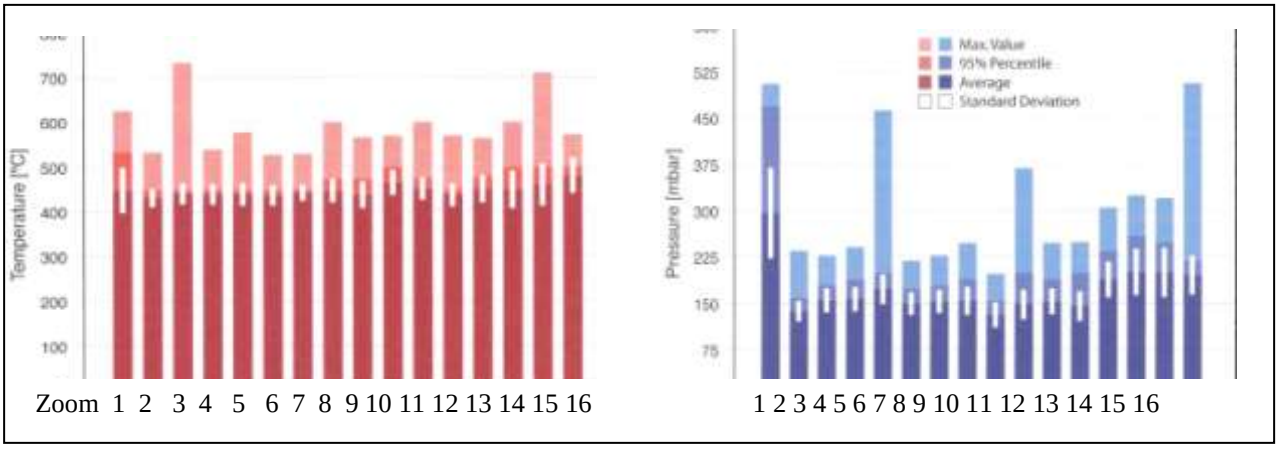

Figure 97: Trend of temperature (left) and backpressure (right) for Engelhard on LHD #362.

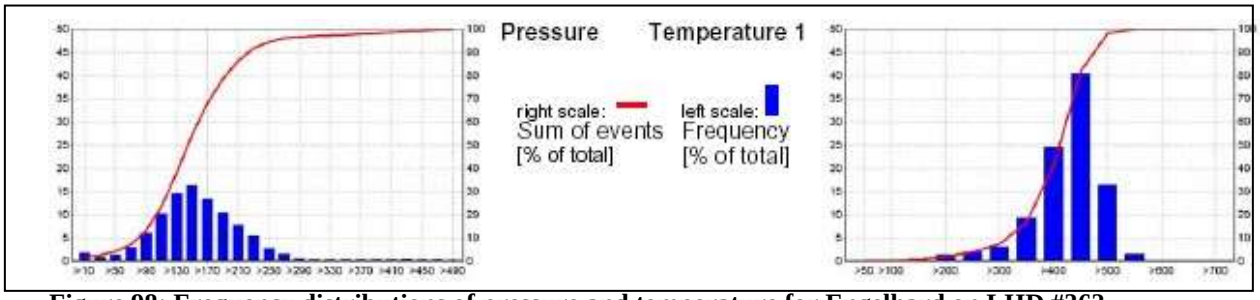

Figure 98: Frequency distributions of pressure and temperature for Engelhard on LHD #362.

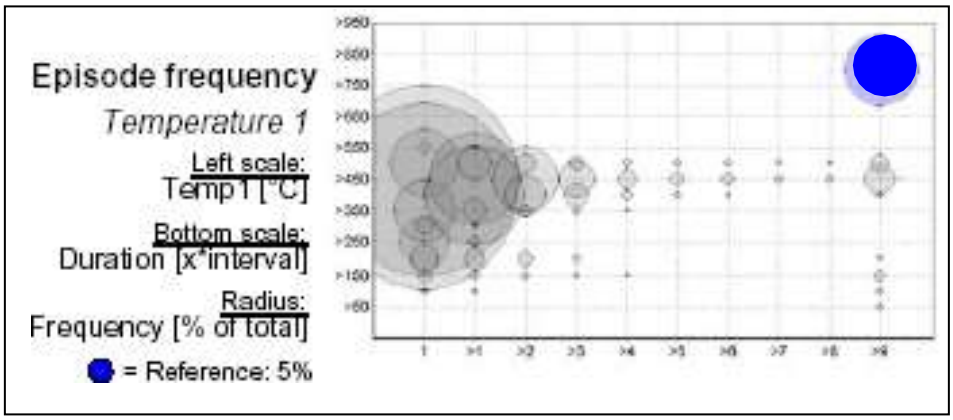

Figure 99: Episodic temperature duration frequencies for Engelhard on LHD #362.

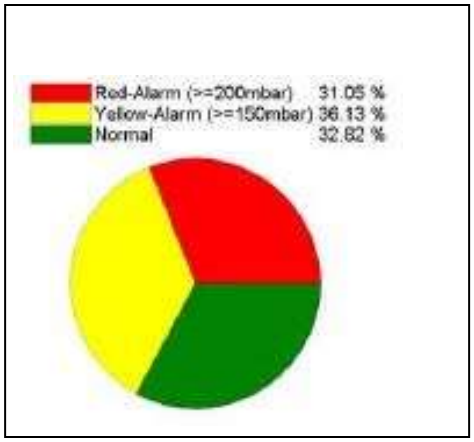

Figure 100: Backpressure pie chart for Engelhard on LHD #362

9.8 Johnson Matthey
on LHD #820

LHD #820 used a V-12 Deutz engine with dual exhausts, and therefore two independent Johnson Matthey DPFs were installed on 16 June 2001. Each initially used SiC wall flow filter elements in conjunction with a FBC to achieve passive regeneration. Additionally, each was equipped with an electric heating element to perform active regeneration should that be necessary. The two DPFs are referred to as "left side" and "right side" from the vantage point of the driver. Alternatively, the left side could be termed the "driver's side" while the right side could be termed the "off-driver's side." Both routine tests and special tests were carried out on each filter. Since the filters perform independently of each other, their performances are presented and discussed separately.

9.8.1 Johnson Matthey
(left/driver's side)

Routine tests

Thirteen routine tests were performed on the left DPF. Results are given in Table 32. While this DPF generally showed acceptable smoke numbers downstream (averaging 1.5) compared to upstream (averaging 7.0), there were several periods of high backpressure caused by lack of sufficient regeneration. Lower than expected upstream gas temperatures (averaging 566 ^{o}C) were insufficient to ignite and completely burn the soot on the filter element to achieve passive regeneration. Since the amount of FBC added to the fuel was targeted to achieve ignition of the soot at 750^{o}F (400 ^{o}C), it is clear that this temperature was not attained for considerable

Table 32: Results of routine tests of Johnson Matthey DPF (left side) on LHD #820.

Date	Hour Meter	Upstream						Downstream				
	(h)	Sm No.	CO (ppm)	NO (ppm)	NO2 (ppm)	O2 (%)	T (^{o}F)	Sm. No.	CO (ppm)	NO (ppm)	NO2 (ppm)	O2 (%)
7/17/01	6086	6.5	115	480	15	9.3		0	115	534	10	9.1
1/3/02	6292						689	9+	0	517	20	9.6
6/28/02	6748	4	162	493	10	9.4		0				
9/30/02	6887	7	111	609	10	8.3	925	1	111	609	10	8.3
11/27/02	7097	8	153	337	33	14.7	351	1	134	354	24	14.8
2/3/03	7322	7	169	580	9	9	414	4	131	601	6	9
2/20/03	7390	9	112	440	11	8.1	479	4	84	485	6	8.5
3/26/03	7578	8	134	557	9	8.5	542	1	103	546	3	8.9
11/27/03	7916	6	128	610	6	7.8	687	1	107	589	3	8.8
1/26/04	8105	7	174	555	22	10.3	487	4	128	610	11	10.9
3/11/04	138	7	116	522	20	10.8	584	2	107	548	13	11
SiC DPF replaced 31 March 2004 with a cordierite DPF												
4/14/04	234	7	159	487	27	11.1	445	1	141	528	10	11.2
6/14/04	385		46	194	2	16.2	621	--	26	170	2	17.2
Average		7.0	132	489	15	10.3	566	1.5	99	508	10	10.6

periods of time during the test. As this possibility had been foreseen, the Johnson Matthey DPF also had the capability of being regenerated by electrical heating. The fact that periods of high

backpressure occurred indicates that electrical regeneration was not practiced as routinely as was necessary. One such period is shown in Figure 101, where temperature (green) and backpressure traces (red) are shown over a 17 hour period in late Sep 2002. It can be seen that the red backpressure on the right side filter (the left side behaved similarly) continues to increase over this time, despite the downtime of the vehicle in the middle of the period.

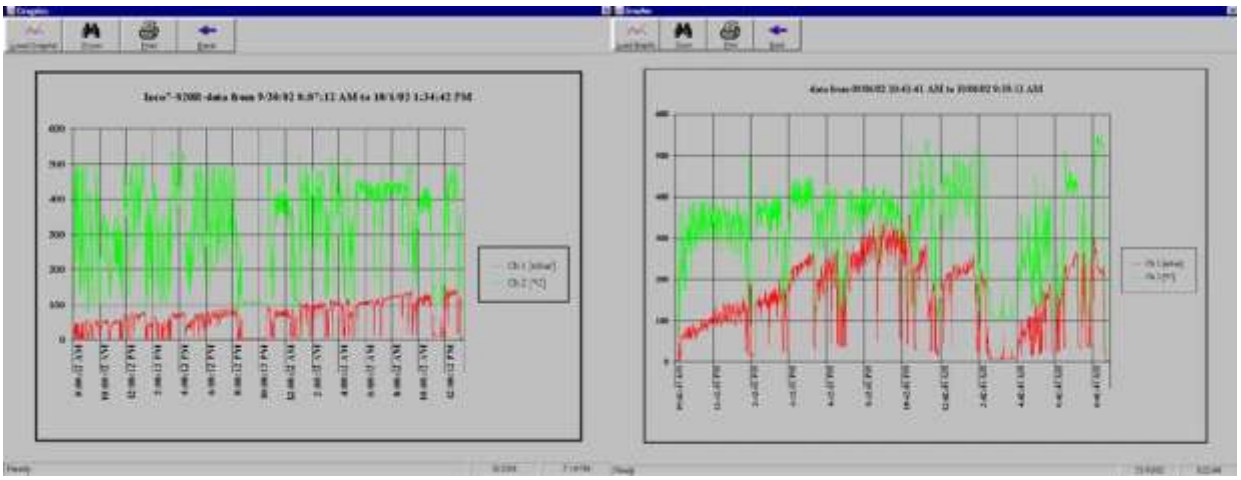

(a) **(b)**

Figure 101: Temperature (green) and backpressure (red) traces over (a) a 17 hour period in late Sep 2002 and (b) a one month period in late Sep 2002 for Johnson-Matthey DPF on vehicle #820 (right side).

It should be noted that specific high downstream smoke numbers (Table 32) in early 2003 were associated with the appearance of a noticeable crack between the filter element and its metal canister. This separation is shown in Figure 102. After consultation with Johnson Matthey technicians, the Stobie team decided to continue operation of the left side DPF, but to watch it closely. In early 2004 it became apparent that the crack was growing, and it then was decided to remove the left side DPF (at 2138 total operating hours). It was replaced with a new cordierite filter from Johnson Matthey (installed on the left side on 31 Mar 2004) and the LHD #820 was returned to production until the test was concluded in July 2004.

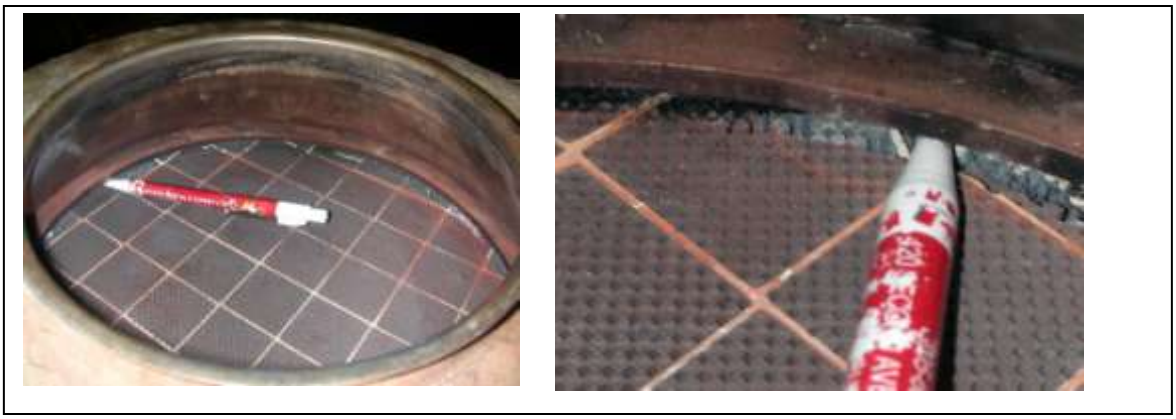

Figure 102: Separation of the Johnson Matthey filter (left side) in February, 2003. This DPF remained in service until March, 2004, when the separation had worsened and DPF efficiency was decreasing.

Smoke numbers as a function of time for the routine tests are shown in Figure 103. CO, NO and NO_2 concentrations from the routine tests are shown in Figure 104. Considerable scatter in these data exist, but no discernable trends with time are evident.

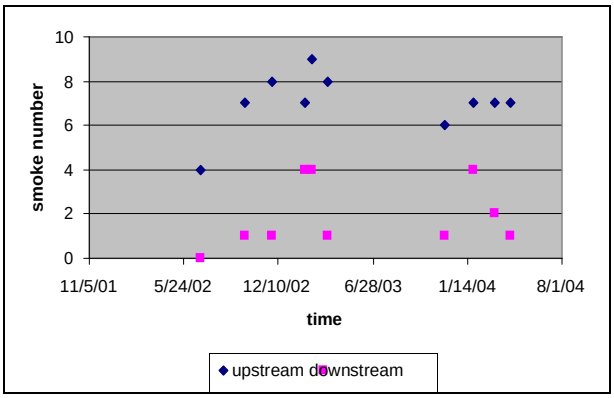

Figure 103: Smoke numbers for Johnson Matthey (left) on LHD #820.

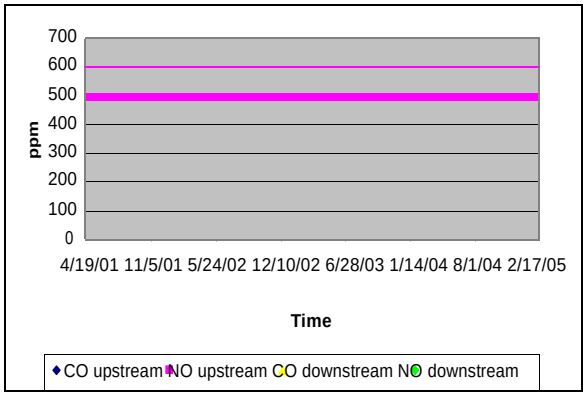

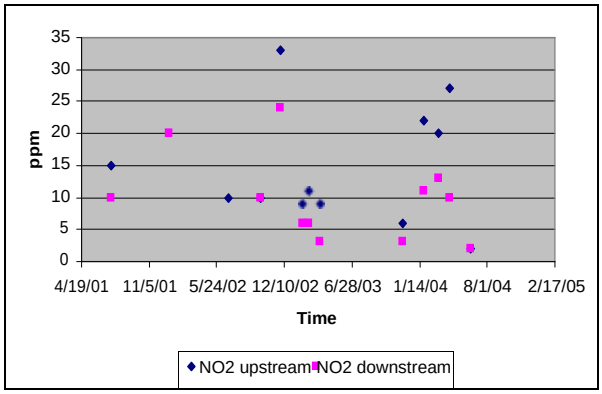

Figure 104: Target gas concentrations for Johnson Matthey DPF on left side of LHD #820.

Special tests with NIOSH

The Johnson Matthey DPF on the left side of the vehicle was tested in July 2001 just after it was installed and again in May 2002 with 424 operating hours. NIOSH test reports can be found in Appendix E. The original SiC DPF was removed from the left side after 2057 operating hours because of a noticeable separation between the filter element and the canister. A replacement Johnson Matthey DPF made of cordierite was installed on 31 March 2004, and this DPF underwent special tests with NIOSH in June 2004 after 173 hours of operation.

The special test results (see Table 33) show very good soot filtration efficiencies under all engine conditions. Both CO and NO_2 reductions were significant, and the downstream NO_2 concentrations were low.

Table 33: Results of special tests of Johnson Matthey DPF on the left side of LHD #820.

								Upstream	Downstream					
Engine Speed[a]	Efficiency (%), eq [1]						Smoke No.[a]	%Opacity	%Opacity	%		ppm		
July 2001 - 0 hrs														
	PAS	EC	O_2	CO	NO	NO_2				O_2	CO_2	CO	NO	NO_2
HI	99.9			0	-20	75				15.6		99	300	5
LI				13	-10	47				18.6		62	207	8
TCS	100	97.6			-11	33	6.5/0			9.1		115	534	10
Snap A		95.1												
May 2002 - 424 h														
	PAS	#	O_2	CO	NO	NO_2				O_2	CO_2	CO	NO	NO_2
TCS	100	99.1		50	-2	50	8.8/0	7.8	0.1	6.5	7.7	185	364	6
HI	99.8	98.8		30	8	65				13.9		50	297	6
LI	99.8	97.2		92	-1	79				17.5		5	199	6
June/04 – 173 h														
TCS	99.9	98.7		-25	1		-/0.5	8.9	0			178	460	
HI	99.8	96.3		8	-4							84	315	
LI		84.5		4	-6							56	204	

a: upstream/downstream

b: HI=High idle; LI= Low idle; TCS= Torque converter stall; Snap A= Snap acceleration; #=number of particles

Note: a negative number in efficiency means downstream was greater than upstream.

The inlet end and the discharge end of the Johnson Matthey filter before regeneration is shown in Figure 105. Clearly the inlet end is blackened with soot, as expected. The discharge end of the same filter is clean.

Figure 105: The inlet side (left) and discharge side (right) of the Johnson Matthey DPF on left of LHD #820.

Size distribution

The size distributions for the TCS, HI and LI engine conditions for the exhaust of the Deutz V-12 engine upstream of the DPF are shown in Figure 106 (left). All distributions appear to be bi-modal with increasing amounts of the smaller size fractions occurring as one goes from TCS to HI to LI. The right side of Figure 106 compares the size distribution for two runs of the SMPS upstream to three runs downstream of the DPF at TCS engine mode which is considered more representative of the real world. The measurements downstream appear fairly decent given the caveats on downstream size distribution measurements listed in Chapter 8. The size distributions for the cordierite filter element, which replaced the SiC element, can be seen in Figure 57.

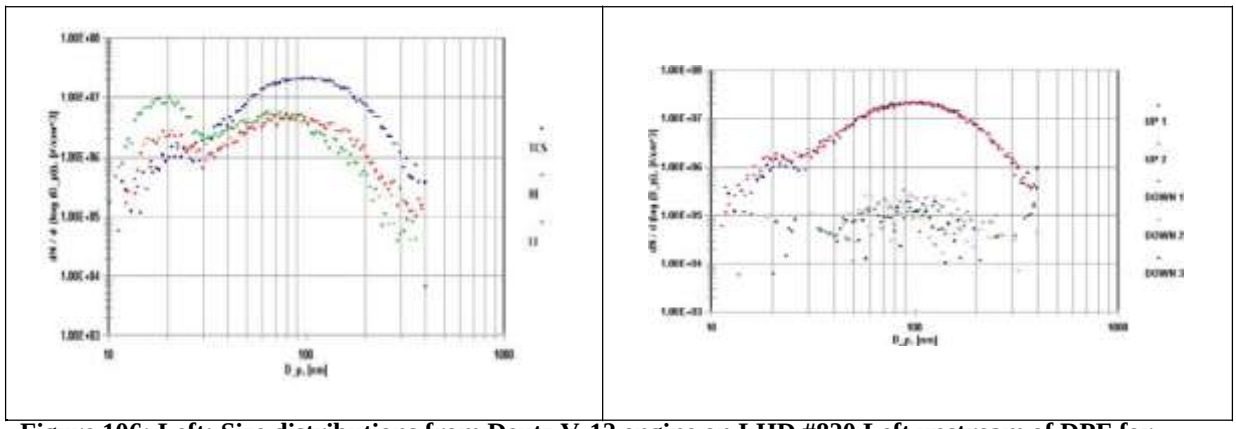

Figure 106: Left: Size distributions from Deutz V-12 engine on LHD #820 Left upstream of DPF for TCS, HI and LI: Right: Upstream and downstream particle size distributions at TCS showing effect of the Johnson Matthey DPF.

Statistical analyses

The data from the JM filter on LHD #820 Left is contained in Appendix C in the JohnsonMatthey-820L folder. The entire history of this filter is given in 16 zoom periods, as summarized in Table 34. Trends of temperature and backpressure for the 16 zoom periods are shown in Figure 107. It can be seen that the average temperature was fairly constant at around 400 ^{o}C. The pressure trend was more variable, but the average was generally well-behaved. There were high pressures observed regularly, and these indicate that more attention to regeneration was necessary.

Table 34: Statistical data for Johnson Matthey on LHD #820 Left over 16 zoom periods.

Zoom No.	Calendar start	Pressure (mbar)					Temperature (^{o}C)				
		Min.	Ave.	Max.	95%	σ	Min.	Ave.	Max.	95%	σ.
1	08 Apr 02	10	124	290	190	58	75	395	591	490	104
2	13 Apr 02	10	128	290	180	57	60	406	591	500	105
3	20 Apr 02	10	130	228	195	59	93	393	606	500	116
4	03 May 02	10	50	168	110	41	84	403	621	510	99
5	30 Aug 02	10	98	320	160	52	75	370	708	500	124
6	07 Nov 02	10	174	508	410	124	75	398	714	525	127
7	30 Nov 02	10	90	170	115	38	96	399	747	500	106
8	04 Apr 03	10	107	460	170	54	108	403	609	525	119
9	01 May 03	10	96	460	165	56	108	467	750	525	175
10	08 Oct 03	10	106	342	220	70	87	383	663	525	129
11	17 Dec 03	10	91	284	150	47	84	410	612	525	103
12	12 Jan 04	10	97	308	150	44	81	418	624	550	116
13	05 Feb 04	10	131	398	300	97	54	384	678	575	142
14	03 Mar 04	10	30	128	20	11	51	410	654	540	141
15	01 Apr 04	10	46	150	50	18	135	431	666	530	93
16	16 Apr 04	10	37	222	20	13	135	395	630	510	85

Note: Highlighted values do not match the values shown in the trend chart, Figure 107

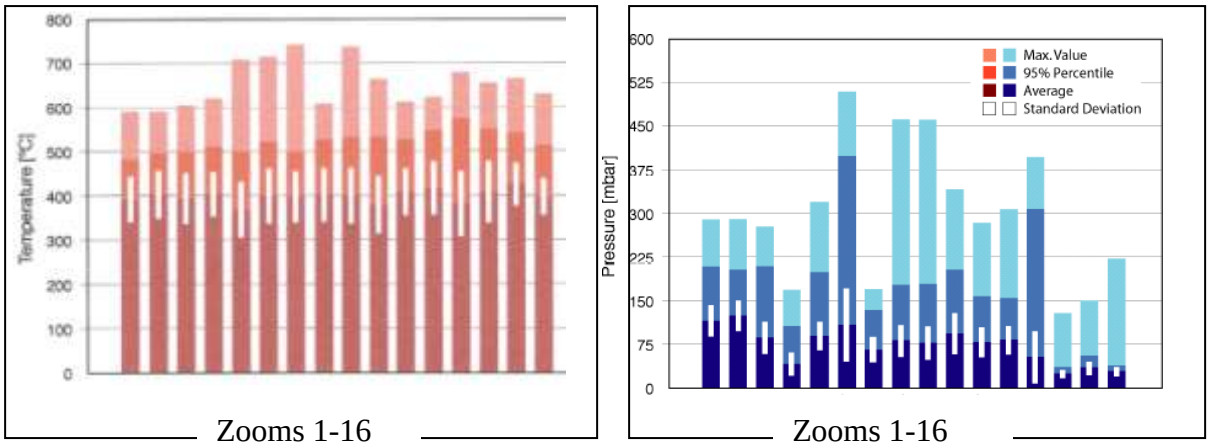

Figure 107: Trend of temperature (left) and backpressure (right) for JM on LHD#820.

Integral statistics across calendar years 2003-2004 are given in Table 35. The pressure and temperature frequencies for this integral period are shown in Figure 108. The episodic temperature duration frequencies are shown in Figure 109, and the fraction of normal pressure is shown in the pie chart in Figure 110.

Table 35: Integral statistics for the year 2003 for JM on LHD #820 (left side).

Location	Pressure (mbar)				Temperature (°C)			
	Min.	Ave.	Max.	95%ile	Min.	Ave.	Max.	95%ile
inlet side	10	80	510	172	51	406	681	538
outlet side					3	333	765	474

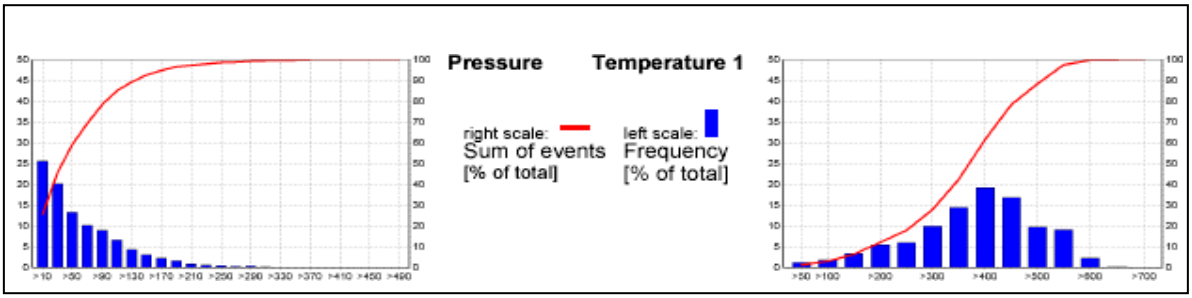

Figure 108: Pressure and temperature frequency distributions for JM on LHD #820 (left).

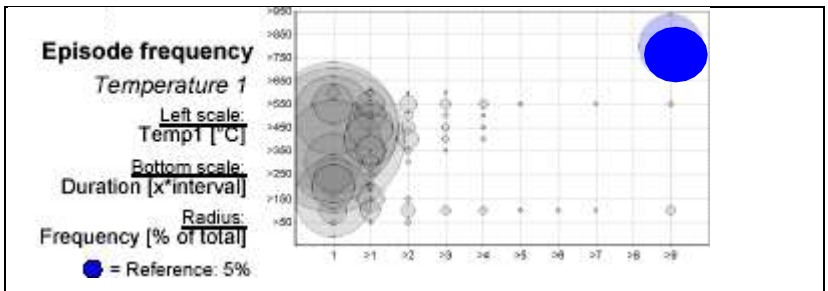

Figure 109: Temperature duration frequency distribution.

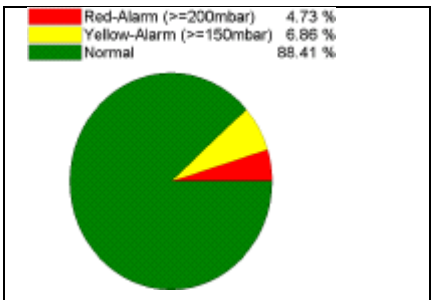

Figure 110: Pressure pie chart

9.8.2 Johnson Matthey
on LHD #820 right side

A Johnson Matthey DPF, installed on the right side (off driver side) of LHD #820 on 16 June 2001, operated a total of 2343 hours until its removal on 12 Jul 2004. It was one of the most successful systems tested.

Routine tests

Thirteen routine tests were conducted on the right side, and results are given in Table 36. The upstream and downstream smoke numbers averaged 6.3 and 1.6, respectively. However, if the 9+ downstream smoke number is considered anomalous, then the smoke number average downstream is reduced to 0.9.

Table 36: Results of routine tests of Johnson Matthey (right side) on LHD #820.

		Upstream						Downstream				
Date	Hour Meter	Sm No.	CO	NO	NO2	O2	T	Sm No.	CO	NO	NO2	O2
	(h)		(ppm)	(ppm)	(ppm)	(%)	(^{o}F)		(ppm)	(ppm)	(ppm)	(%)
7/17/01	6086	6	133	398	22	9.3		0	130	435	10	9.4
1/3/02	6292						654	9+	8	485	47	9.5
6/28/02	6748	5	63	549	11	9.6		0				
9/30/02	6887	6	96	599	7	8.5	565	2	79	600	5	9
11/27/02	7097	7	135	308	27	14.5	329	2	122	313	22	14.9
2/3/03	7322	7	77	564	10	9.2	584	1	72	578	6	9.1
2/20/03	7390	7	110	373	15	9.1	433	1	87	396	5	8.5
3/26/03	7578	8	80	524	8	8.5	535	1	71	560	3	9
11/27/03	7916	6	148	498	6	9	512	0	84	499	4	10
1/26/04	8105	7	71	550	22	11.2	479	1	69	540	15	11.5
3/11/04	138	6	129	500	19	10.8	452	1	99	511	9	11.6
4/14/04	234	7	96	501	13	11.2	517	2	103	517	6	11.4
6/14/04	385	4	20	144	0	17.6	664	1	10	155	0	17.8
Average		6.3	96	459	13	10.7	520	1.6	78	466	11	11.0

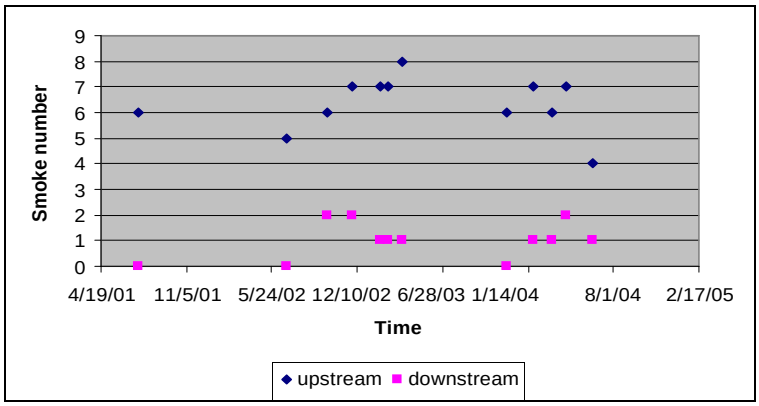

Figure 111: Smoke numbers for Johnson Matthey (right side).

.

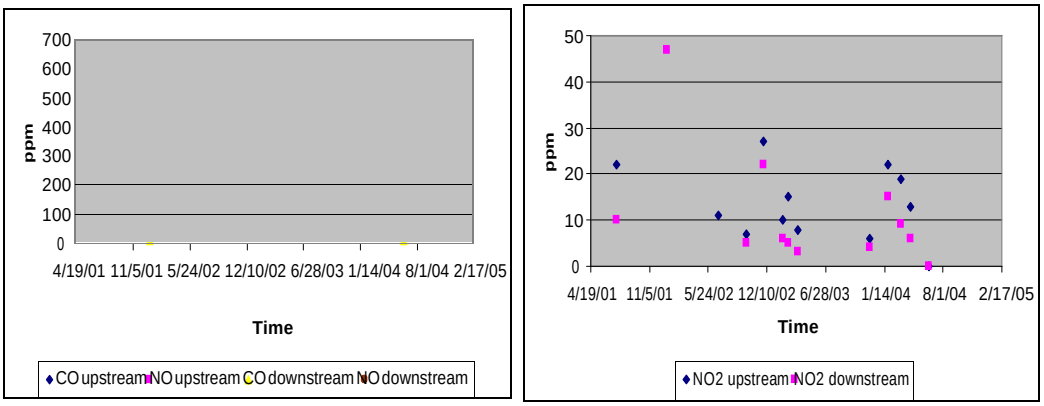

Figure 112: Target gas concentrations for Johnson Matthey DPF on right side of LHD #820.

Smoke numbers as a function of time are shown in Figure 111 (the 9+ anomalous downstream reading is not shown). No trends are evident. Target gas concentrations are shown in Figure 112. No trends are evident.

Special tests with NIOSH

Three special tests were conducted on the Johnson Matthey (right side) filter and results are summarized in Table 37. NIOSH test reports can be found in Appendix E.

Table 37: Results of special tests of Johnson-Matthey DPF on the right side of LHD #820.

								Upstream	Downstream					
Engine Speed[b]	Efficiency (%), eq [1]						Smoke No.[a]	%Opacity	%Opacity	%		ppm		
July 2001 - 0 h														
	PAS	EC	O_2	CO	NO	NO_2				O_2	CO_2	CO	NO	NO_2
HI										15.9		110	263	10
LI				12	-37	92				18.8		75	240	2
TCS	99.9	98.3		2	-9	55	6.0/0			9.4		130	435	10
Snap A		97.8		17	-27	88								
May 2002 - 424 h														
	PAS	#	O_2	CO	NO	NO_2				O_2	CO_2	CO	NO	NO_2
HI	99.9	98.7		15	-21	82				15.4		120	235	8
LI	99.9	97.2		16	-27	56				18.3	2.0	137	149	31
TCS	99.9	98.1		7	-8	71	7.0/0			8.9	9.0	92	457	9
June 2004 – 173 h														
HI	99.8	98.1				65					4.5			7.7
LI		96.9				67					2.1			9.7
TCS	99.9	97.8				55					10.1			6.7

a: upstream/downstream

b: HI=High idle; LI= Low idle; TCS= Torque converter stall; Snap A= Snap acceleration; #=number of particles

Note: a negative number in efficiency means downstream was greater than upstream.

The soot removal efficiencies were very good for all periods. Good NO_2 reductions were achieved.

Size distributions

Size distributions for the Johnson Matthey filter on LHD #820 (right side) are provided in the NIOSH reports to Vale in Appendix E.

Statistical analyses

Data for the Johnson Matthey filter on LHD #820 (right side) are in Appendix C under the JohnsonMatthey-820R folder. This filter behaved very similarly to the Johnson Matthey filter on the left side (see above). The reader is referred to Appendix C for more details.

9.9 Arvin-eritor
on LHD #111

The Arvin-Meritor DPF system is an active system using an automatically activated fuel burner to increase exhaust gas temperatures prior to entering the cordierite filter element. It was installed on 7 May 2004 late in the Stobie project in order to study the performance of a system using an active burner-assisted regeneration. Such a system was originally planned by the project team to be placed on a truck, but the truck was retired from service just prior to installation. Consequently, when it became possible to test a burner-activated system through Arvin-Meritor, the Stobie team decided to proceed with it on an LHD.

Considerable effort was expended by the Stobie team and by Arvin-Meritor personnel in doing the necessary safety checks before this system would be permitted underground. Additional effort was expended in installing the various components of the system, as described earlier in Chapter 7. It was with great optimism that the system was put into operation. It was very disappointing that the system did not perform well. In November 2004 it was removed from operation.

Routine tests

Four routine tests were carried out on this system and results are summarized in Table 38. Results even in mid-August 2004 showed relatively high smoke numbers downstream of the DPF, indicating that DPF efficiency for soot removal was being adversely affected. Trends as a function of time of these tests are given in Figure 113 and Figure 114. The cause of the high of NO concentrations in Feb 2004 is not known. If those readings are anomalous, then no trend of NO was evident. In the case of CO upstream, there appears to be an increasing trend, while NO_2 upstream shows a decreasing trend. These data show a likely poisoning of the Diesel Oxidation Catalyst placed downstream of the soot filter in Arvin-Meritor's system (see further discussion below).

Table 38: Results of routine tests of Arvin-Meritor DPF on LHD #111.

		Upstream						Downstream				
Date	Hour Meter	Sm No.	CO	NO	NO2	O2	T	Sm No.	CO	NO	NO2	O2
	(h)		(ppm)	(ppm)	(ppm)	(%)	(^{o}F)		(ppm)	(ppm)	(ppm)	(%)
2/6/04	1478	5	21	1333	66	11.7	646	1	25	1232	39	12.5
8/12/04	3382	7	51	481	18	14.8	602	3	53	407	49	15.4
11/5/04	4148	7	54	492	27	14.9	624	3	10	437	30	15.4

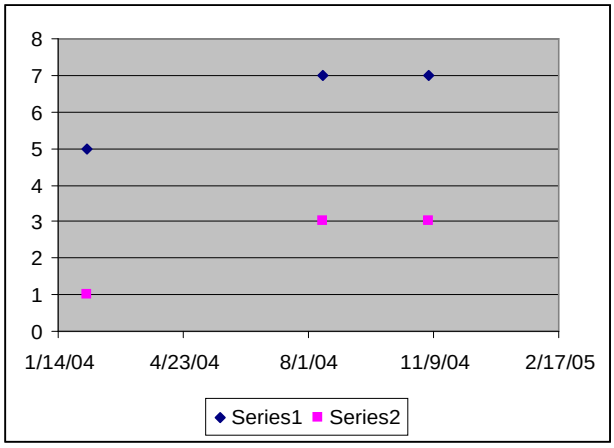

Figure 113: Smoke numbers for Arvin-Meritor DPF on LHD #111. Series 1 is upstream; series 2 is downstream.

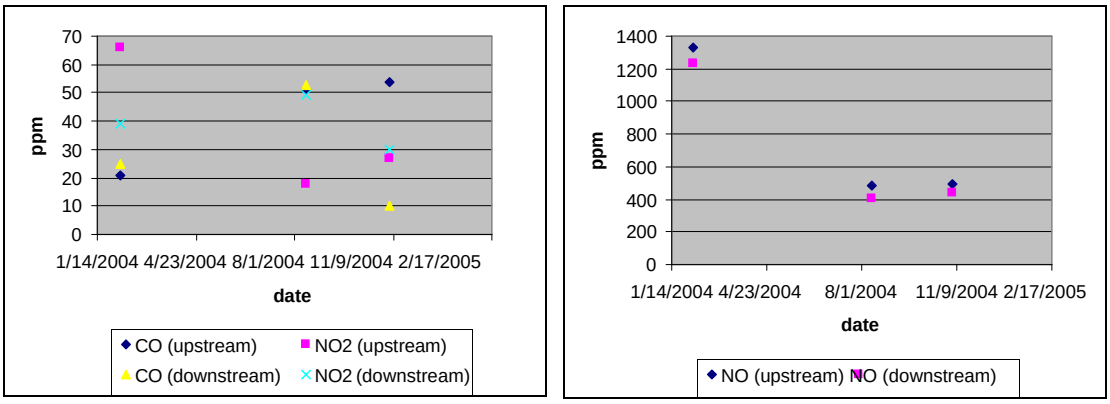

Figure 114: Target gas concentrations for Arvin Meritor DPF on LHD #111.

Special test

One special test in June 2004 was conducted soon after the system was installed. The full NIOSH test report is in Appendix E. Summary results are shown in Table 39. It is clear that soot filtration efficiencies were good immediately after installation. The high CO reduction efficiency is due to Arvin-Meritor's use of a Diesel Oxidation Catalyst downstream of the DPF. The DOC is designed to control CO and HC emissions during the regeneration using the fuel burner. This DOC, which oxidizes NO to NO_2, is also responsible for the reduction of NO and the significant increase in NO_2 between upstream and downstream.

Table 39: Results of the June 2004 special test of Arvin-Meritor on LHD #111.

0 hrs.

								Upstream	Downstream					
Engine Speed[b]	Efficiency (%), eq [1]						Smoke No.[a]	%Opacity	%Opacity	%		ppm		
	PAS	#	O_2	CO	NO	NO_2				O_2	CO_2	CO	NO	NO_2
HI	99.8	96.8		98	50	-432					4.4	1	211	147
LI		95.6		100	74	-496					2.3	0	120	273
TCS	99.9	98.1		92	21	-324	6.2/1				6.6	4	386	95
Snap A								23.6	0.4					

Size distribution

Since this was removed from service after only a short time of operation, size distribution data obtained by NIOSH in June 2004 are not presented here. They can be found in the NIOSH test report in Appendix E.

Statistical analyses

Data collected for this system are located in Appendix C under the ArvinMeritor-111 folder. Since the period of operation was short, no details are presented here.

Overall conclusion

The Arvin-Meritor system experienced considerable problems with the software used to control the burner cycling. This problem, combined with the apparent decrease in filter efficiencies, caused the system to be removed from further testing.

10. Comparisons of DPF Systems

In this chapter, the effectiveness of reducing DPM in the exhaust and the effects on target gas concentrations of the various DPF systems are compared. Table 40 lists these DPF systems and the vehicles selected for comparison. All of these systems were available for the special tests conducted jointly by the Stobie project team and NIOSH in May 2002. NIOSH scientists were responsible for obtaining particle measurements related to the DPM in the engine exhaust. The target exhaust gases were measured by both teams with the Stobie team using the ECOM AC and NIOSH using the ECOM KL. It must be noted that the upstream (before DPF) and downstream (after DPF) measurements of the exhaust components were measured in separate "runs" of the TCS engine mode separated by periods of HI and LI between the TCS runs to cool the torque converter. Thus, although the engine conditions were the same, exhaust and DPF temperatures, state of regeneration, etc. may not have been identical for both runs. This can affect the comparison between up and downstream gas concentrations. The data presented in this chapter are contained in the draft report by NIOSH scientists, A. Bugarski and G. Schnakenberg, to Vale of the DPF efficiency tests conducted from 25 - 31 May, 2002, available from Vale and is included in Appendix E on CD rom.

Table 40: DPF systems and vehicles.

Vehicle ID	Engine	DPF manuf.	Filter Element	Regeneration Class	Regeneration Method
LHD #820 Left & Right	Deutz V-12 Dual exhaust	Johnson-Matthey	SiC wall flow	Passive / Active	FBC / Electric on board
LHD #445	DDEC 60	ECS/Combifilter 2 parallel	SiC	Active	Electric on board
LHD #362	DDEC 60	Engelhard	Cordierite Wall flow	Passive	Catalyst wash coat
Tractors #2180/ #3013	Kubota	ECS/Combifilter	SiC wall flow	Active	Electric on board
Tractors #621/ #017	Kubota	DCL Titan	SiC wall flow	Active	Electric off board (swap)

10.1 Particle Concentrations

The DPM or soot concentration in the diesel engine exhaust and the efficiency of the DPF to reduce the DPM concentration can be determined using several methods. These were discussed in Chapter 8. The most meaningful and pragmatic of these methods are Bosh/Bacharach Smoke Number and exhaust opacity under snap acceleration. NIOSH and Vale each possessed instrumentation to measure smoke numbers (the ECOM models) and opacity (the AVL DiSmoke 4000). Particle numbers and size their distribution obtained by the SMPS and the particle numbers by the PAS method are informative but not critical for successful DPF deployment. Only NIOSH had the instrumentation to measure particle size distributions and total particles.

With the exception of LHD #362, which used a cordierite wall flow filter element, all the DPF filter elements were SiC wall flow elements and could be expected to exhibit similar performance.

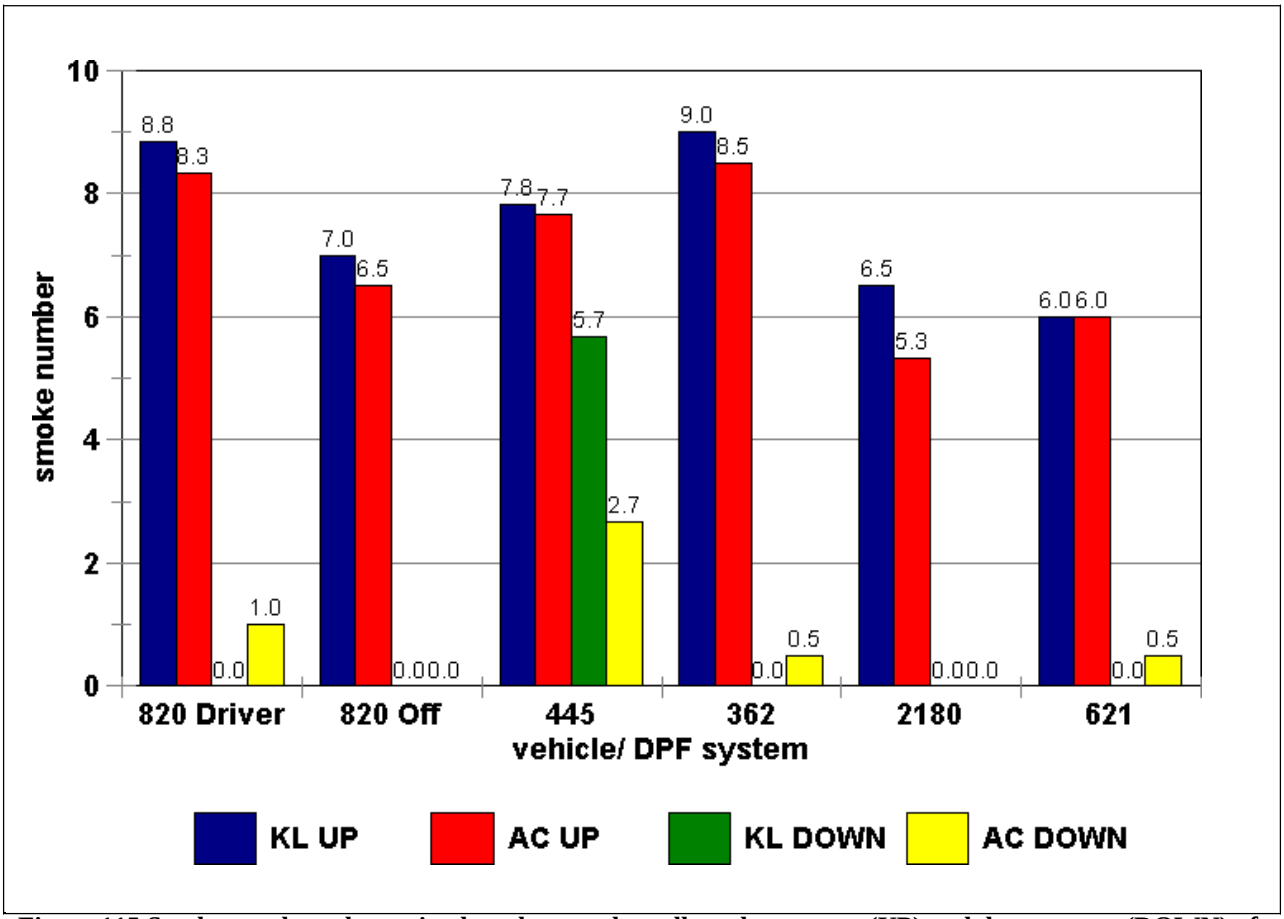

Figure 115 Smoke numbers determined on the samples collected upstream (UP) and downstream (DOWN) of the DPF systems as measured by the ECOM KL (KL) and ECOM AC Plus (AC)

Figure 115 shows the smoke number results obtained by the Stobie team using the ECOM AC and the NIOSH team using ECOM KL. Smoke numbers are obtained with the engine operating in TCS mode. The high downstream (after DPF) smoke number for LHD #455 (with the ECS/Combifilter DPFs configured in parallel) should be considered as cause for investigating whether the DPF has become defective. Based upon smoke number results, all DPFs, but the ECS/Combifilter on LHS#445, are performing well.

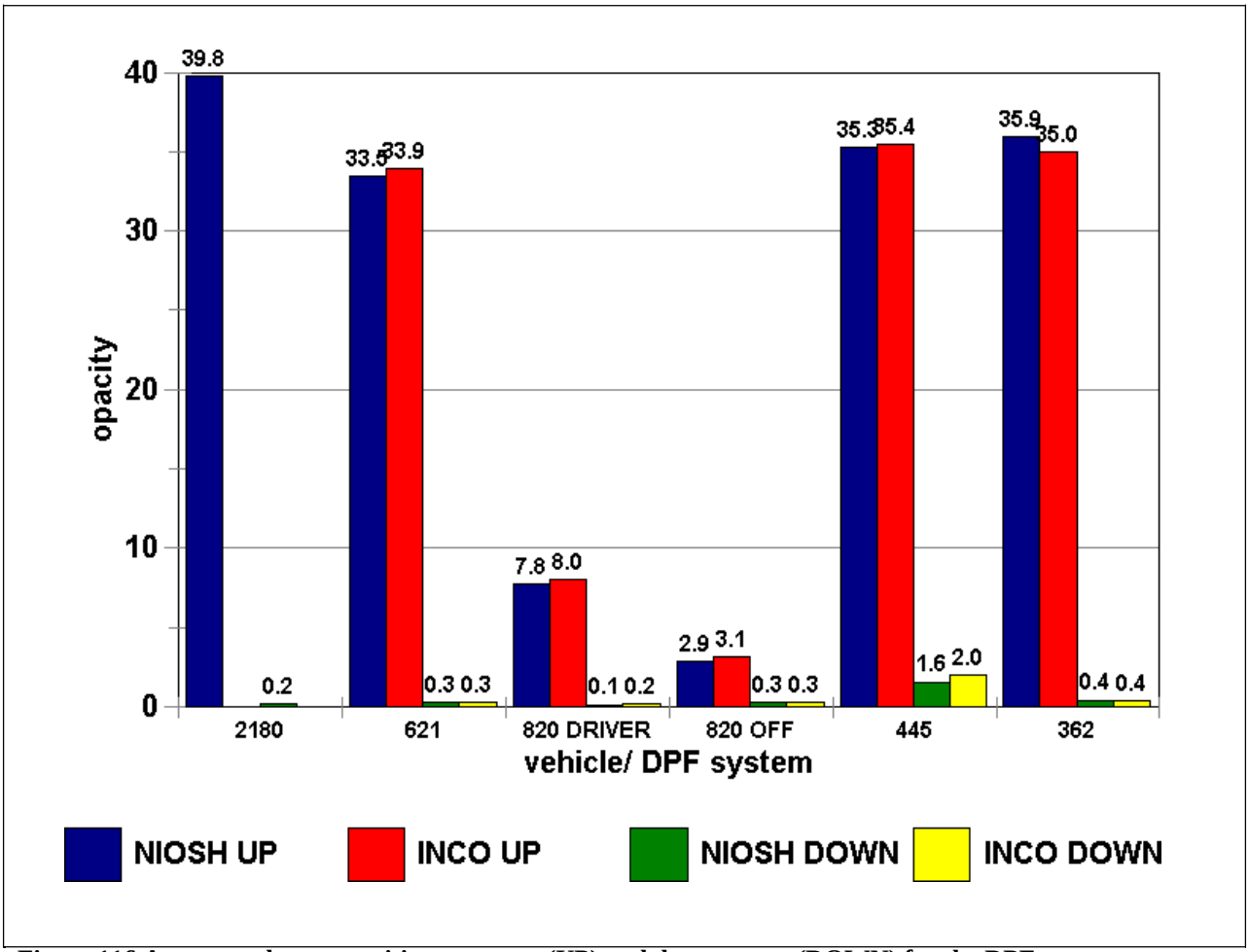

Figure 116 Average exhaust opacities upstream (UP) and downstream (DOWN) for the DPF systems measured using NIOSH and Vale instruments, both AVL DiSmoke 4000.

Figure 116 shows the results of exhaust opacity measurements made by NIOSH and Vale. These measurements are made while the engine is undergoing rapid (snap) acceleration from idle to maximum speed with no load on the engine other than the inertial load of the flywheel and other rotating masses. The transmission is in neutral. As with the smoke numbers, the downstream exhaust the opacity of LHD #445 is somewhat high but still below the 5% benchmark for being concerned with filter efficiency. The Deutz V-12 engine of LHD #820 showed the lowest engine out opacity under snap acceleration of all of the engines tested, yet this is in contrast with the smoke number results measured at constant speed full load (TCS).

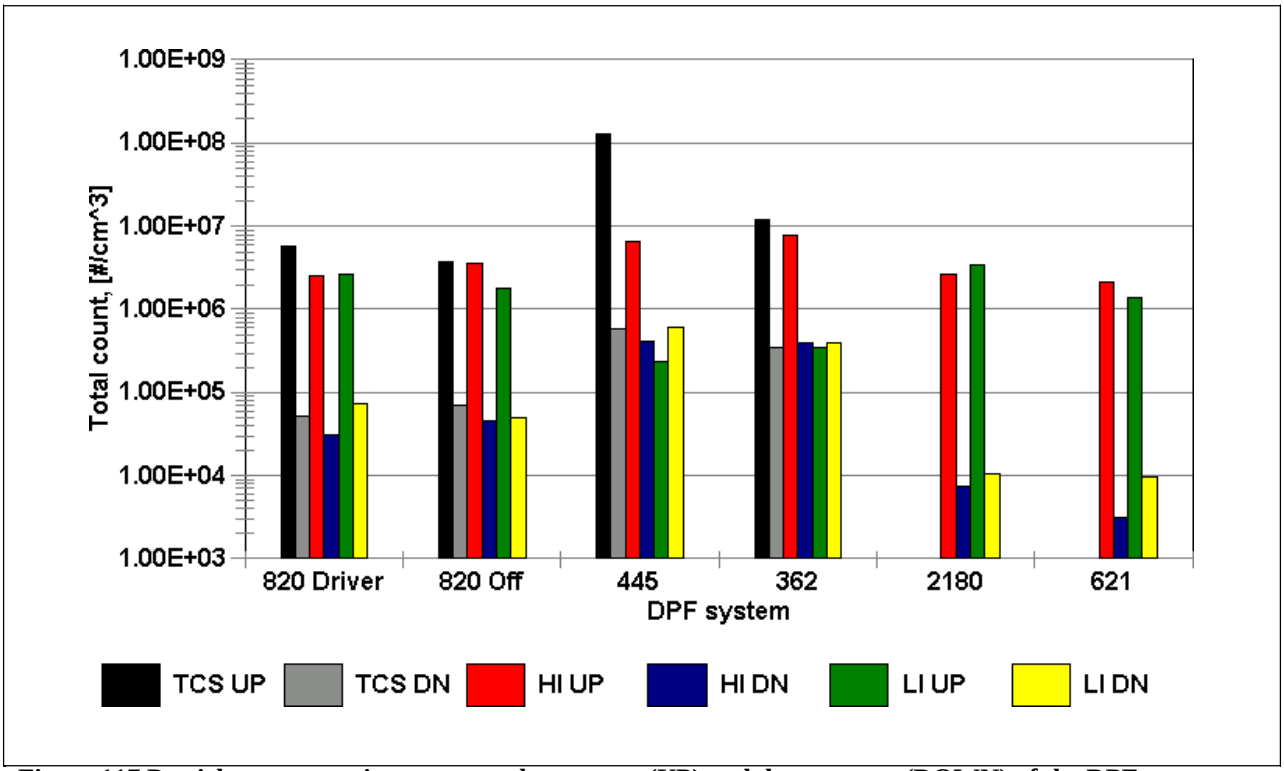

Figure 117 Particle concentrations measured upstream (UP) and downstream (DOWN) of the DPF systems under various steady state engine operating conditions.

Figure 117 shows the results from the aerosol number concentration measurements performed by NIOSH using the SMPS instrumentation as described in Chapter 8. The measurements were made with the engine operating in each of the three steady state modes: TCS, HI and LI. In this figure the vertical axis is logarithmic and each major division represents a factor of a hundred in particle number. Note that only for the TCS test condition does LHD #445 show exceptional total particle numbers relative to the other vehicles. This demonstrates a) that the vehicle engine for #445 was being fueled at a higher fueling rate (higher maximum fuel-air ratio) than the others, and (b) that TCS is a crucial diagnostic test condition.

All filter efficiencies for particle number reduction are in the range of 97 to 99% as noted for the respective DPFs in Chapter 9. The only exception is for LHD #445 and #362 at HI, where efficiencies were 94 and 95% respectively. The light duty tractors with the ECS/Combifilter and DCL Titan DPF showed the lowest number concentration after the DPF.

The particle number measurements made by the PAS 2000, described in Chapter 8, are shown in Figure 118. The vertical scale is logarithmic which must be accounted for in interpreting the relative heights of the bars. Again as with the SMPS, LHD #445 showed the highest particles in the upstream exhaust of all of the engines under TCS conditions. It is also clear that the DPF was much less efficient at removing the DPM as measured by the PAS 2000 than any other DPF tested at this time.

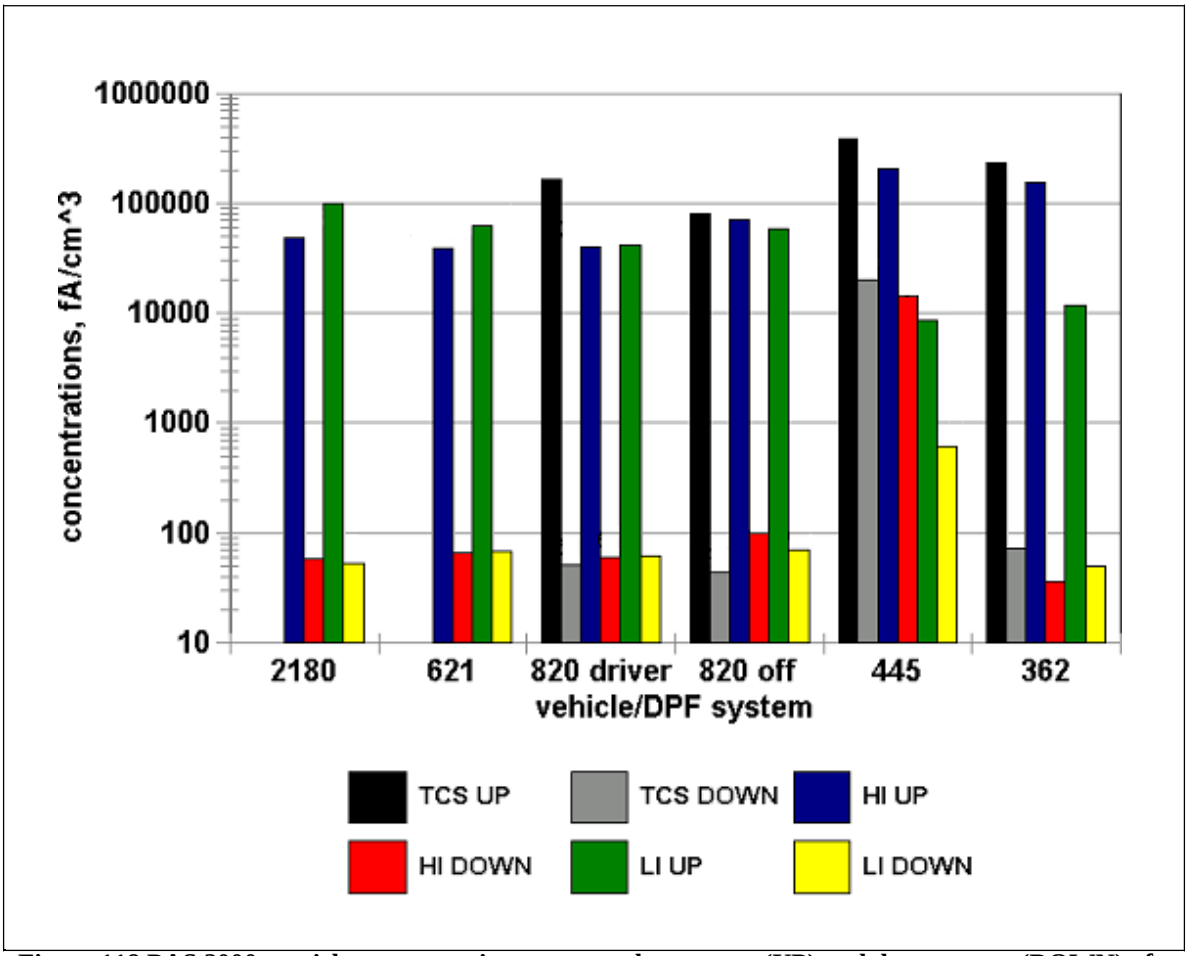

Figure 118 PAS 2000 particle concentrations measured upstream (UP) and downstream (DOWN) of the DPF systems under various steady state engine operating conditions..

10.2 Target gas concentrations

Figure 119 shows CO concentrations under three different engine modes: TCS, HI, and LI. The measurements showed that concentrations of CO downstream of the Engelhard DPF were reduced by more than 89.5 % at TCS and HI conditions. The results showed an unexpected increase in CO concentration downstream of ECS/Combifilter DPF at TCS condition. It can be speculated that the high exhaust temperatures of the TCS engine mode caused DPF regeneration during measurements which increased the CO. The Johnson-Matthey DPF installed on the driver's (left) side of Deutz engine on LHD #820 reduced the exhaust CO concentrations by up to 91.7 % depending on engine operating mode. Surprisingly, the J-M DPF installed on the off driver's side (right) of Deutz engine was not nearly as efficient as the one on driver side in removal of CO. The other DPFs did not exhibit significant effects on the CO concentrations which is consistent with non-catalyzed DPF systems.

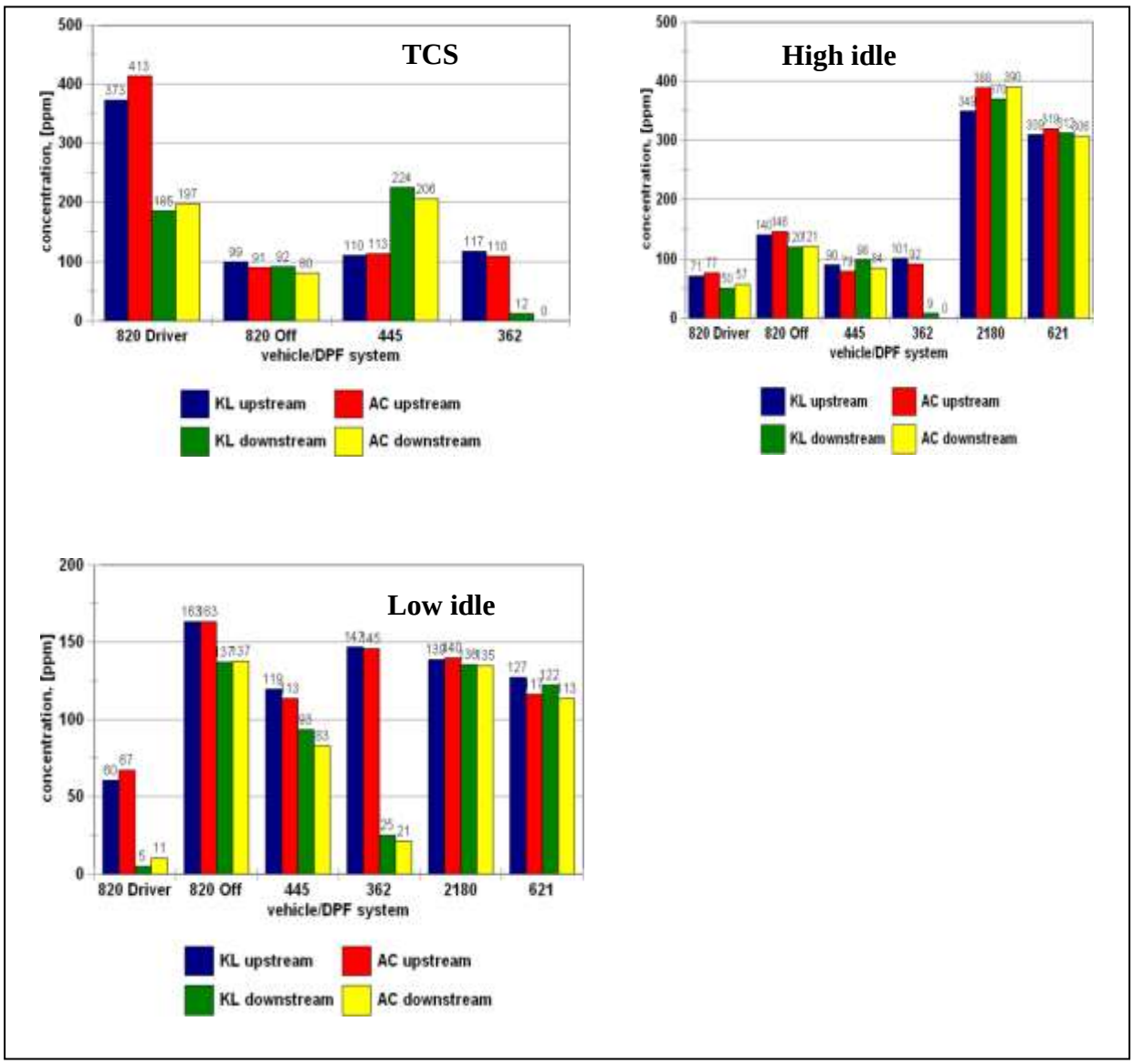

Figure 119: CO concentrations upstream and downstream of DPFs for various engine conditions. KL and AC refer to models of the ECOM exhaust gas analyzers used for the measurements.

NO concentrations for TSC, HI and LI conditions are compared in Figure 120. Only the ECS/Combifilter DPF on LHD #445 significantly (40%) increased NO concentrations.

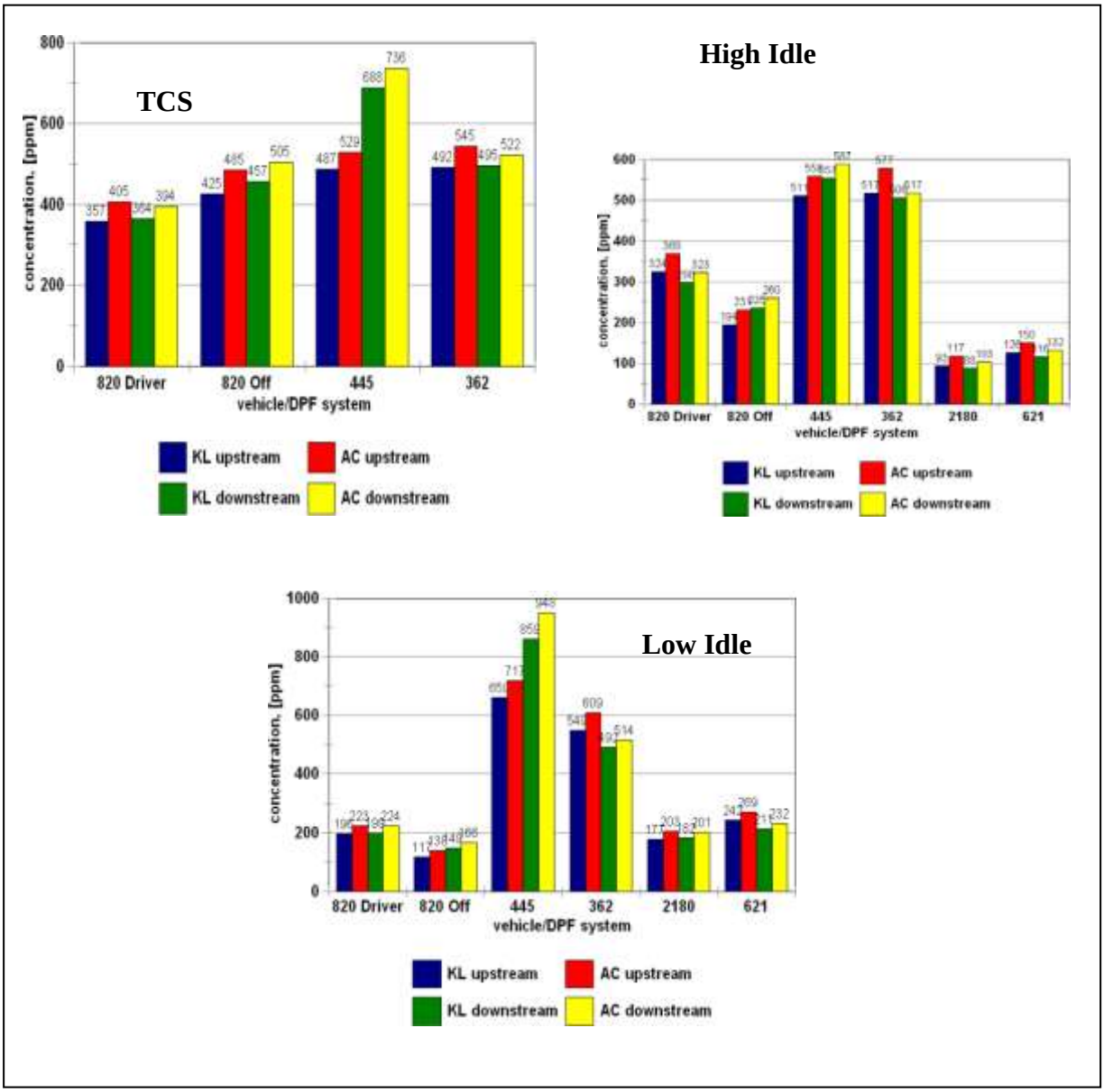

Figure 120: Concentrations of NO upstream and downstream for the DPF systems for various engine conditions. KL and AC refer to models of the ECOM exhaust gas analyzers used for the measurements.

NO_2 concentrations for various engine conditions are shown in Figure 121. Only the Engelhard DPF on LHD #362 showed increases in downstream NO_2 under TCS and low idle conditions. This increase of NO_2 was expected as the effect of the use of a noble metal catalyst to promote regeneration.

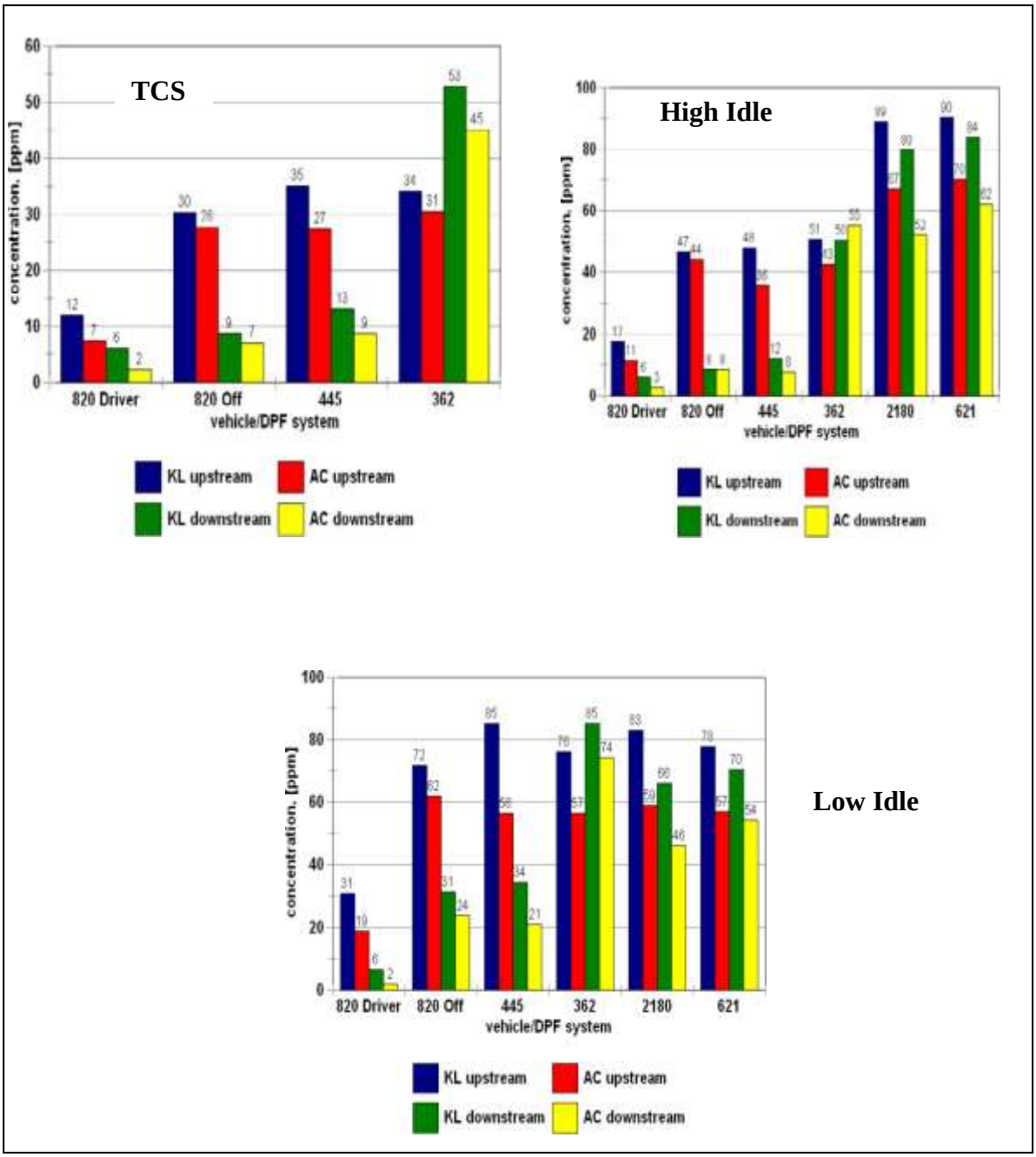

Figure 121: Comparisons of NO_2 concentrations for the DPF systems for various engine conditions. KL and AC refer to models of the ECOM exhaust gas analyzers used for the measurements.

11. Industrial Hygiene Measurements

11.1 Introduction

Conditions for performing and interpreting industrial hygiene measurements for the Stobie Project were less than ideal because the diesel units and DPF systems being tested were not operating in special test areas where ventilation rate and incidental contamination of the incoming air from other vehicles could be controlled. Because all the units tested were part of normal operations within the mine, the presence of other non-test vehicles was possible. Accordingly, even though IH measurements were conducted and neighbouring vehicles were noted, the results obtained must be interpreted as having the possibility of interference from non-filtered diesel vehicles.

The procedures were carried out by personnel trained in performing IH measurements as part of ventilation monitoring. Certain test vehicles were operated without their DPF installed to give a baseline; these vehicles were then subjected to similar tests with the DPF installed. Generally the IH work was conducted during day shift with the samples being representative of conditions on that shift.

11.2 Analysis of soot in mine air

There exist several methods to analyze for DPM in mine air. The two methods relevant to the Stobie project were the RCD method and the Thermal-optical method, the essentials of which are given below.

11.2.1 The RCD method

The Respirable Combustible Dust (RCD) method was developed in Canada (Hews and Rutherford, 1973; Rutherford and Elliot, 1977; Maskery, 1978) and has been routinely used by the mining industry in Canada to estimate DPM. Respirable dust in mining operations can come from mineral dusts, oil mists from pneumatic equipment and diesels. This is schematically shown in Figure 122.

All of the respirable aerosol is collected by passing mine air at a controlled and known flow rate through a cyclone to reject coarse aerosol and then through a 25 or 37 mm diameter silver membrane having a 0.8 µm pore size (alternatively, a pre-fired glass fiber filter can be used), which collects the respirable particulate. The amount (mass) of material collected is determined by weighing the membrane before and after collection.

The silver membrane is then subjected to a controlled combustion at 400 ^{o}C for up to two hours which burns off all of the carbon containing mass. The amount of mass lost is taken to be the respirable combustible dust (RCD). A factor is available to correct for the expected loss of the membrane itself.

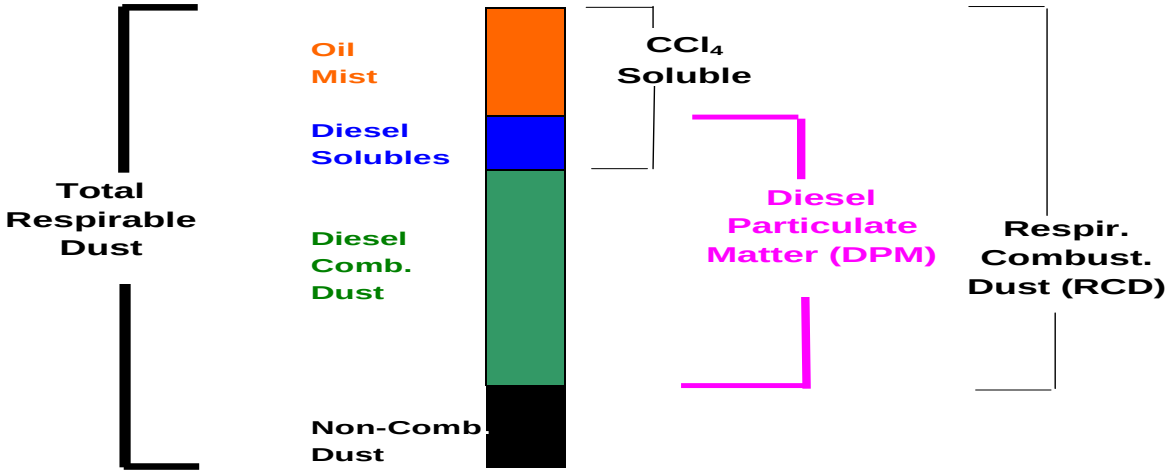
Total Respirable Dust
Oil Mist
Diesel Solubles
Diesel Comb. Dust
Non-Comb. Dust
CCl4 Soluble
Diesel Particulate Matter (DPM)
Respir. Combust. Dust (RCD)

Figure 122: Schematic diagram showing the relationships between components of total respirable dust.

It is important to recognize that the RCD method analyzes the sampled respirable material for all organic (carbon containing) matter which includes not only DPM but such materials as oil mists from pneumatic equipment. Generally DPM is assumed to be approximately two-thirds of the RCD under typical mining conditions.

11.2.2 The Thermal-Optical Method

Unlike the RCD method, the thermal optical method distinguishes between hydrocarbons (HC) and elemental carbon (EC). While also not able to analyze DPM per se (because HCs from diesels cannot be separated from the HCs from oil aerosols from other sources such as pneumatic equipment), the EC portion of the analysis is a very good indicator of the major portion of DPM. Because the method is able to detect very small amounts of EC with high precision, this method is now the basis for new occupational exposure limits.

NIOSH in the U.S. developed a sensitive method (NIOSH Analytical Method 5040) for determining the HC and EC components of an air sample deposited on a quartz filter (Birch and Cary, 1996; NIOSH, 2003). The sampling of air is conducted using a similar technique as used in the RCD method, except that the sample filter material is pre-combusted ultra-pure quartz. A specific sized portion of the loaded filter is punched for analysis and inserted into a special apparatus designed for the purpose.

As a preliminary step, the sample is placed into the apparatus and oriented so that a laser beam shines through it, and the filter's transmittance is monitored by a photodiode detector. During the first stage of analysis, oxygen free helium flows over the sample which is heated in four steps to 900^{o}C. During this heating, During the first stage of analysis, oxygen free helium flows over the sample which is heated in four steps to 900^{o}C. During this heating, mineral carbonates will decompose to evolve carbon dioxide and the HCs (from DPM or from oils) will volatilize and are oxidized to carbon dioxide as they pass through granular manganese dioxide at 870^{o}C. All of the carbon dioxide is then catalytically converted to methane, which is subsequently quantitatively measured by a flame ionization detector (FID). A small portion of the HCs present in the sample may pyrolyze to form a carbon "char." This char can be detected by a reduction in the transmittance of the laser beam shining through the sample.

The temperature is then reduced to 525^{o}C, and a 2% oxygen-helium mixture flows over the sample, which again is heated in four steps to 900^{o}C. In the presence of oxygen the EC and char burn to form carbon dioxide. Any char that was formed in the first stage HC removal is corrected for by allowing the laser transmittance to regain its pre-first-stage value before beginning to integrate the EC signal from the FID.

The method is calibrated by injecting a known volume of methane into the oven assembly. Excellent reproducibility has been obtained by NIOSH and other laboratories.

11.3 Specific procedures

Typically ten air samples were taken for a test vehicle on an IH day. The distribution of samplers was as follows:

- 3 for RCD analysis using a 25mm silver membrane and a pumping rate of 1.7 L/min with a cyclone ahead of the sampler. These samplers were located in a basket just behind the vehicle operator;
- 3 for EC analysis using a 37mm filter and a pumping rate of 2 L/min with a cyclone and an impactor size selector ahead of the sampler. These samplers were also located in a basket (the same as the one for the RCD samplers) just behind the vehicle operator;
- 2 for EC analysis located to sample the incoming air entering the area;
- 2 for EC analysis located to sample the outgoing air from the area.

Flow rates on the pumps were set at the beginning of the shift and were checked for the same setting at the end of the sampling period. The flows were calibrated with a Gillian Flow Calibrator. All results reported had constant flow rates over the sampling periods.

Generally the samplers on the vehicle were started at 8:30AM, then the samplers for incoming air were started at 9:15AM, the samplers for the outgoing were started at 9:25AM. The IH personnel recorded the work being performed by the vehicle and the occurrence of any other diesel vehicles nearby. The outgoing air and incoming air supply samplers were typically stopped at a little before 3 PM, and the vehicle basket samplers stopped just after 3 PM.

Air flow measurements in the area were also taken.

11.4 Results

Table 41 shows the IH results for #2180 tractor with and without the ECS Combifilter DPF. The first comment that can be made about the data is that the EC concentration in the incoming air was very low. The EC samples taken at the vehicle without the DPF installed averaged 0.08 mg/m^3, but its accuracy suffers from a short 1.33 hr sampling time. With the ECS/Combifilter DPF installed, the EC samples averaged 0.05 mg/m^3. Additionally, the prevailing ventilation rates for the without and with DPF conditions were substantially different, and additional DPM was contributed by other diesel traffic as noted. If these factors are taken into account, it is not evident from the data that the known low EC emissions from the DPF equipped tractor caused a measureable effect on DPM concentration at the tractor operator location. As expected, the outgoing air showed a minor increase in soot over the supply air. The DPM in all samples was below the detection limit for the RCD method.

Table 41: IH sampling results for tractor #2180 without and with ECS/Combifilter DPF.

Date	Duty	Ventilation (CFM)	Sampling time (h)	DPM (mg/m^3)			
				Incoming Air EC	At vehicle RCD	At vehicle EC	Outgoing Air EC
WITHOUT DPF							
6/25/01	Per.Car	58810	1.33	0.02	<0.13	0.07	0.09
"	"	"	"	0.01	<0.13	0.11	0.08
"	"	"	"	0.01	<0.13	0.07	0.08
Average	"	"	"			0.08	
Average*	**Note 1.**	**50000**				**0.10**	
WITH DPF							
3/31/04	Per.Car	94000	3.3	0.01	<0.14	0.04	0.02
"	"	"	"	0.04	<0.12	0.06	0.007
"	"	"	"	--	<0.15	0.06	--
Average	"	"	"			0.05	
Average*	**Note 2.**	**50000**				**0.10**	
4/01/04	Per.Car	99500	3.0	0.008	<0.15	0.05	0.08
"	"	"	"	0.00	<0.15	0.04	0.08
"	"	"	"	--	<0.15	0.05	--
Average	"	"	"			0.05	
Average*	**Note 2.**	**50000**				**0.09**	

Notes:
Per.Car means Personnel Carrier
* Average of the triplicate EC samples at operator when corrected (normalized) to a ventilation rate of 50000 CFM. Normalization was applied to the unrounded EC average.
1. Secondary and passing equipment in the area.
2. Many passing diesel vehicles on the ramp which significantly contributed DPM and overwhelming any reductions from the DPF on the tractor.

The results for #621 tractor with the DCL Titan DPF are given in Table 42. They show undetectable EC in the incoming ventilation air. For the samples taken on the vehicle, the "without" DPF EC had an average of 0.10 mg/m^3 and the "with" DPF had an average of 0.03 mg/m^3, which shows good EC reduction by the DPF even at the very low EC concentrations yielded by the engine. Correcting for the differing prevailing ventilation rates among the tests had little effect on the results. The outgoing air EC, when testing the "without" condition, was somewhat higher than the outgoing air for the "with" condition; this may have been caused by noticeably more nearby diesel equipment operating during the Feb 2002 testing. For the most part the RCD measurements were consistent with the EC measurements; the only significant departure between these results was for one sample of RCD on 2/26/02 that showed 0.25 mg RCD/m^3. No reason for this high reading is known.

Table 42: IH sampling results for Tractor #621 with and without DCL Titan DPF.

Date	Duty	Ventilation (CFM	Sampling time (h)	DPM (mg/m^3)			
				Incoming Air EC	At vehicle RCD	EC	Outgoing Air EC
WITHOUT DPF							
2/25/02	Per.Car	39700	2.3	0.00	<0.3	0.13	0.11
"	"	"	"	0.00	<0.3	0.09	0.07
"	"	"	"	--	<0.3	0.10	--
Average	"	"	"			0.11	
Average*	**Note 1.**	**50000**				**0.08**	
2/26/02	Per.Car	44000	3.9	0.00	0.13	0.11	0.11
"	"	"	"	0.00	0.18	0.10	0.10
"	"	"	"	--	0.25	0.09	--
Average	"	"	"			0.10	
Average*	**Note 2.**	**50000**				**0.09**	
WITH DPF							
3/26/04	Per.Car	56700	4.1	0.00	<0.12	0.03	0.01
"	"	"	"	0.00	<0.12	0.02	0.009
"	"	"	"	--	<0.12	0.03	--
Average	"	"	"			0.03	
Average*	**Note 3.**	**50000**				**0.03**	
3/29/04	Per.Car	64500	3.6	0.00	<0.14	0.04	0.00
"	"	"	3.6	0.00	<0.14	0.04	0.00
"	"	"	"	--	<0.14	0.04	--
Average	"	"	"			0.04	
Average*	**Note 3.**	**50000**				**0.05**	

Notes:
Per.Car means Personnel Carrier
* Average of the triplicate EC samples at operator and then corrected (normalized) to a ventilation rate of 50000 CFM. Normalization was applied to the unrounded EC average.
1. Secondary and passing equipment
2. Secondary equipment and two scoops
3. Diesels passing by on ramp

The IH data for LHD #820 with the Johnson-Matthey DPF are shown in Table 43. The table indicates that the EC concentration in the incoming air was very low for all sampling periods. During the first period of sampling on 7/5/01 (8-4 shift) the EC concentration at the vehicle was higher than for the second period (12-8 shift). This is likely due to the presence of additional nearby diesel equipment during the 8-4 shift. The data indicate that using the DPF significantly reduced the normalized EC concentrations at the vehicle from an average of 0.16 mg/m^3 to 0.04 mg/m^3. The RCD results at the vehicle were, for the most part, consistent with the EC readings, but, as noted previously, the limit of detection and precision of the RCD method was inferior to the NIOSH 5040 method for EC. The outgoing air for all periods was, as expected, marginally higher in DPM than the incoming air.

The data indicate that the Johnson-Matthey DPFs were probably reducing soot emissions for this LHD.

Table 43: IH sampling results for LHD #820 LHD with and without Johnson Matthey DPFs.

Date	Duty (buckets)	Ventilation (CFM)	Sampling time (h)	DPM (mg/m^3)			
				Incoming Air EC	At vehicle RCD	At vehicle EC	Outgoing Air EC
WITHOUT DPF							
7/5/01	Tram(10)	86700	3.3	0.01	0.17	0.12	0.04
"	"	"	"	0.00	0.20	0.12	0.05
"	"	"	"	0.00	0.28	0.13	0.05
Average	"	"	"			0.12	
Average*		**50000**				**0.21**	
7/5/01	Tram(17)	82200	3.2	0.00	<0.15	0.08	0.10
"	"	"	"	0.00	<0.15	0.07	0.10
"	"	"	"	0.00	<0.15	0.05	0.10
Average	"	"	"			0.07	
Average*		**50000**				**0.11**	
WITH DPF							
3/17/04	Muck(5)	30300	4.0	0.00	<0.12	0.04	0.04
"	"	"	"	0.00	<0.12	0.05	0.04
"	"	"	"	--	0.17	0.04	--
Average	"	"	"			0.04	
Average*		**50000**				**0.03**	
3/18/04	Tram(5)	66900	4.1	0.007	<0.12	0.04	0.05
"	"	"	"	0.003	0.14	0.04	0.04
"	"	"	"	--	<0.12	0.04	--
Average	"	"	"			0.04	
Average*		**50000**				**0.05**	

Notes:
Tram (10) means carrying 10 buckets over the sampling period.
* Average of the triplicate EC samples at vehicle and then corrected (normalized) to a ventilation rate of 50000 CFM. Normalization was applied to the unrounded EC average.

The results shown in Table 44 for LHD #213 with and without ECS/Combifilter DPFs indicate a significant reduction in EC concentration when the ECS/Combifilter DPF was used. The results for the "without" filter operation showed fairly high RCD with the comparable EC, being from one-third to one-fourth of the RCD. This difference between the RCD and EC may be explained by the higher than normal oil mist (source of hydrocarbons but not EC) from pneumatic tools in use in the area. These oil aerosols are measured by the RCD and reported as a carbon mass, whereas the NIOSH 5040 method separately measures organic (oils) carbon and EC.

The data indicate that the ECS/Combifilter DPFs were effectively reducing soot emissions for this LHD.

Table 44: IH sampling results for LHD #213 with and without ECS Combifilter DPFs.

Date	Duty (buckets)	Ventilation (CFM)	Sampling time (h)	DPM (mg/m^3)			
				Incoming Air EC	At vehicle RCD	At vehicle EC	Outgoing Air EC
WITHOUT DPF							
4/2/05	Tram(60)	24500	6.7		0.35	0.045	
"	"	"	"		0.35	0.119	
"	"	"	"		0.25	0.109	
Average**	"	"	"			0.114	
Average*		**50000**				**0.056**	
4/3/05	Tram(60)	39750	7.5		0.39	0.109	
"	"	"	"		0.39	0.107	
"	"	"	"		0.33	0.118	
Average	"	"	"			0.111	
Average*		**50000**				**0.089**	
WITH DPF							
3/23/04	Tram(30)	62600	4.3	0.00	<0.12	0.005	0.002
"	"	"	"	0.00	<0.12	0.005	0.005
"	"	"	"	--	<0.12	0.004	--
Average	"	"	"			0.005	
Average*		**50000**				**0.006**	
3/24/04	Tram(50)	63500	4.3	0.001	<0.14	0.01	0.006
"	"	"	"	0.002	<0.14	0.01	0.008
"	"	"	"	--	<0.14	0.01	--
Average	"	"	"			0.01	
Average*	**"**	**50000**				**0.01**	

Notes:
Tram (10) means carrying 10 buckets over the sampling period.
* Average of the triplicate EC samples at vehicle and then corrected (normalized) to a ventilation rate of 50000 CFM. Normalization was applied to the unrounded EC average.
** The EC sample of 0.045 was not used in computing the average because it was significantly lower than the other two sample values.

12. ASH RESIDUE ANALYSES

Ash samples were collected from several DPFs after regeneration. These samples were submitted for chemical analysis and morphology to the J.Roy Gordon Research Laboratory in Mississauga.

12.1 Analytical techniques

Carbon content of the ash was determined on an as-received sample by combustion using a Leco instrument.

Elements Cu, Ni, Co, Fe, Ca, Al, Mg, Si, As, Pb, Zn, Mn, Cr, P, B, Ag, Au, Ba, Be, Bi, Cd, Ce, Ga, Ge, Hf, Hg, In, La, Li, Mo, Nb, Nd, Pd, Pr, Pt, Re, Rh, Ru, Sb, Se, Sn, Sr, Ta, Te, Th, Ti, Tl, U, V, W, Zr, Na, K, Rb, Cs, Sc, Y, Sm, Eu, Gd, Tb, Dy, Ho, Er, Tm and Yb were analyzed by complete digestion followed by Inductively Coupled Plasma-Mass Spectrometry (ICP-MS) on the resulting solution. Digestion was accomplished by weighing a known amount of the sample and digesting it with 1 volume of nitric acid plus 2 volumes of hydrochloric acid at 95^{o}C for one hour. After cooling to room temperature the solution was diluted to 50mL with ultrapure de-ionized water and centrifuged. To 0.5mL of the resulting solution, 200µL of nitric acid was added and then diluted to 10mL with ultrapure de-ionized water. The ICP/MS unit was a Perkin-Elmer Sciex Elan DRC2 model.

Elements Fe, Ca, S, Zn and P were obtained by complete digestion of a known weight of the sample followed by conventional ICP analysis.

Carbonate analysis was done by boiling a weighed amount of the sample in sulfuric acid. The evolved gas was trapped, its volume measured and then the gas was passed through a caustic scrubber several times, each time returning to the volume measuring chamber. The change in volume after scrubbing is calculated as carbon dioxide and converted to carbonate in the original sample.

Low magnification optical images were taken using a Wild Leitz M8 Zoom Stereomicroscope. SEM secondary electron images at 100X magnification were obtained using a JEOL 6400 Scanning Electron Microscope with a tungsten filament, for which the ash particulate was placed on an aluminum stub using two sided sticky tape and sputtered with gold-platinum to achieve a conducting surface. Higher resolution secondary electron images were done using an Hitachi S5200 cold field emission Scanning Electron Microscope.

12.2 1st Sampling Trial

It should be understood that obtaining samples of ash that accumulates inside the DPF filter media after regeneration is not a simple matter. The Stobie team tried to accomplish this initially by using compressed air jet on the outlet side of the filter a completely regenerated filter to blow the ash from the inlet side into a special clean collection can.

The procedure used to attempt this sampling was limited to DPFs that fit onto the ECS CombiClean regenerating station described previously in Chapter 7 because this unit allowed the best chance of capturing ash into a special can that attached to the unit. DPFs from DCL, ECS and Arvin-Meritor were regenerated as per normal procedure (note that for regeneration the filters are inverted so that the filters' intakes were next to the electrical heating element at the bottom of the holder). Initially the soot-laden filters were cleaned of soot from around the flanges as much as possible. Then the filters were put through their normal regeneration. Finally, the vacuum was turned on and air was blown from the top (reverse from the way the filter operated during soot filtration) to blow out the ash that had resulted from the soot burning.

The problem encountered was that considerable unburned soot was also blown out. This soot probably resulted from non-uniform regeneration temperatures where portions of the wall flow filter cells containing soot did not reach adequate ignition temperatures. Figure 123 shows the ECS/Combifilter DiC wall flow element after seven "cookings" and then being tapped on the table.

The black material on the table resembles very fine pencil lead and obviously the material comes directly out of the honeycomb cells in the filter. Since this material is black, one would assume that it is unburned soot. Any white ash that would be in this material would be overwhelmed by the amount of black soot.

Despite these problems, the samples were examined to see what could be learned.

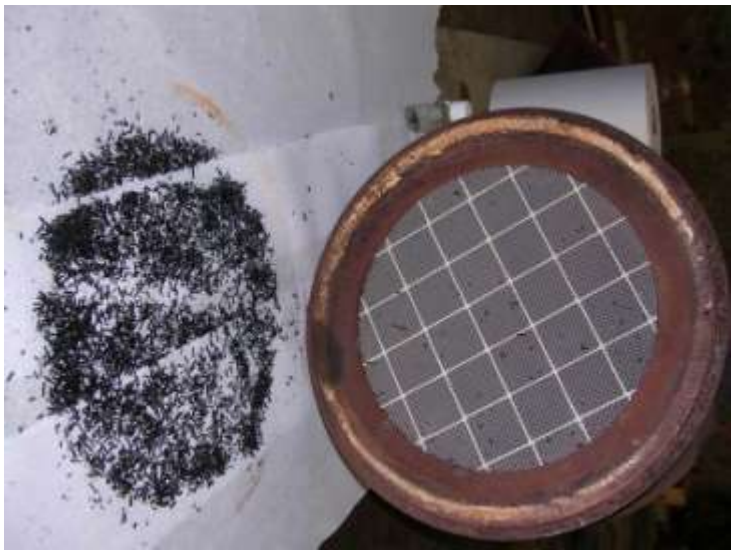

Figure 123: Material falling out of the ECS filter after seven regeneration cookings

12.2.1 1st Sampling trial results

Five ash samples were examined and assigned identification numbers:

Ash from the DCL Titan DPF on #017 Tractor; Lab ID.# 76937
Ash from the ECS/Combifilter DPF on #3013 Tractor; Lab ID.# 76938 Ash from the ECS/Combifilter DPF (a) on #213 LHD; Lab ID.# 76939 Ash from the ECS/Combifilter DPF (b) on #213 LHD; Lab ID.# 76940 Ash from the Arvin-Meritor DPF on #111 LHD Lab ID.# 76943

Bulk chemical analyses of the samples are given in Table 45. It should be noted that one of the samples listed in the Table (Lab ID.# 76942) has no results because of insufficient sample mass available; another sample (Lab ID.# 76941) came from a filter that Vale was operating outside the Stobie Project.

The first thing that is evident is that the carbon analyses for all samples are generally high, and this is undoubtedly due to the contamination of the ash samples by unburned soot (see above).

The optical and scanning electron microscope images are complex because of the unburned soot contamination. In some of the photographs the distinction between soot and ash is evident. However, in the highest magnification photographs it is not clear whether the agglomerated particles are unburned soot (many of them probably are) or are ash that has taken the same agglomerated morphology as the parent soot. Because of the similarity of most of the samples, a typical high carbon sample of ash from the DCL Titan DPF is shown below. Another sample containing the lowest amount of carbon, from the ECS/Combifilter DPF, is also shown.

Table 45: Bulk chemical analyses of selected ash samples.

INCO

Report of Analysis

Inco Technical Services Limited **Research and Development**

Description:	Analysis of Diesel Particulates
Project #:	Analysis of Diesel Particulates
Date:	SP1-3174 55609

LIMS ID	06-03-17 14:08	C	CO3	Fe	Ca	S	Zn	P	Cu (MS)	Ni (MS)	Co (MS)	Fe (MS)	Ca (MS)	Al (MS)	Mg (MS)	Si (MS)
		%	%	%	%	%	%	%	µg/g	µg/g	µg/g	µg/g	µg/g	µg/g	µg/g	µg/g
76937	Stobie 017 tractor DCL	63.0	<0.5	4.79	6.54	2.20	3.80	3.67	900	370	20.6	>10000	>10000	1600	1930	2620
76938	Stobie 3013 Tractor ECS	11.0	<0.5	3.70	21.5	4.70	7.32	11.0	1716	540	17.7	>10000	>10000	3250	6900	2780
76939	Stobie 213 Trap #1 ECS	68.0	<0.5	11.1	3.19	2.10	1.84	1.61	8826	1230	45.7	>10000	>10000	3270	3030	1600
76940	Stobie 213 Trap #2 ECS	74.0	<0.5	5.62	0.66	0.90	0.48	0.32	3766	840	46.9	>10000	6600	2510	1600	1540
76941	107 2934.5 HRS	31.0	<0.5	17.2	11.9	3.80	5.31	5.81	2105	1090	45.3	>10000	>10000	3400	8690	4140
76942	111 Before	nes	nes	nes	nes	nes	nes	nes	nes	nes	nes	nes	nes	nes	nes	nes
76943	111 After	41	<0.5	6.59	10.6	7.00	4.19	3.46	1200	2190	41.3	>10000	>10000	2470	4440	2690

		As (MS)	Pb (MS)	Zn (MS)	Mn (MS)	Cr (MS)	P (MS)	B (MS)	Ag (MS)	Au (MS)	Ba (MS)	Be (MS)	Bi (MS)	Cd (MS)	Ce (MS)	Ga (MS)
		µg/g	µg/g	µg/g	µg/g	µg/g	µg/g	µg/g	µg/g	µg/g	µg/g	µg/g	µg/g	µg/g	µg/g	µg/g
76937	Stobie 017 tractor DCL	7.84	64.8	>10000	31.2	149	>10000	<5	0.87	2.5	33.8	<0.5	0.205	11.07	2.81	1.02
76938	Stobie 3013 Tractor ECS	32.7	643	>10000	152	278	>10000	<5	0.4	0.9	81.7					
76939	Stobie 213 Trap #1 ECS	12.2	159	>10000	61.2	385	>10000	<5	0.86	0.8	30.3	<0.5	1.65	10.24	6.81	1.29
76940	Stobie 213 Trap #2 ECS	4.33	54.6	4840	29.7	173	3200	<5	0.45	<0.5	46.6	<0.5	0.67	8.19	4.35	0.9
76941	107 2934.5 HRS	92	614	>10000	164	314	>10000	<5	0.5	<0.5	66.2	<0.5	6.11	10.38	7.28	1.72
76942	111 Before	nes	nes	nes	nes	nes	nes	nes	nes	nes	nes	nes	nes	nes	nes	nes
76943	111 After	6.13	183	>10000	59	1317	>10000	<5	3.49	<0.5	68.2	<0.5	0.53	6.63	5.05	1.24

		Ge (MS)	Hf (MS)	Hg (MS)	In (MS)	La (MS)	Li (MS)	Mo (MS)	Nb (MS)	Nd (MS)	Pd (MS)	Pr (MS)	Pt (MS)	Re (MS)	Rh (MS)	Ru (MS)
		µg/g	µg/g	µg/g	µg/g	µg/g	µg/g	µg/g	µg/g	µg/g	µg/g	µg/g	µg/g	µg/g	µg/g	µg/g
76937	Stobie 017 tractor DCL	<1	0.02	<0.05	0.012	1.32	4.97	84.3	0.36	1	0.9	0.24	0.3	<0.005	<0.2	<0.2
76938	Stobie 3013 Tractor ECS		0.07	<0.05	0.031	4.83	7.22	44.9	3.51	1.67	1.9	0.42	1.4	<0.005	<0.1	<0.1
76939	Stobie 213 Trap #1 ECS	<1	0.02	<0.05	0.023	2.54	4.44	54.1	1.15	1.9	0.7	0.46	<0.1	<0.005	0.1	<0.1
76940	Stobie 213 Trap #2 ECS	<1	0.11	<0.05	0.035	1.88	2.71	23.5	0.74	1.42	1.5	0.35	<0.1	<0.005	<0.1	<0.1
76941	107 2934.5 HRS	<1	0.05	<0.05	0.037	3.74	12.46	61.2	3.97	2.87	3.5	0.87	0.7	0.007	<0.1	<0.1
76942	111 Before	nes	nes	nes	nes	nes	nes	nes	nes	nes	nes	nes	nes	nes	nes	nes
76943	111 After	<1	0.03	<0.05	0.014	2.43	14.55	36.4	1.74	1.92	0.7	0.41	<0.2	0.009	<0.2	<0.2

		Sb (MS)	Se (MS)	Sn (MS)	Sr (MS)	Ta (MS)	Te (MS)	Th (MS)	Ti (MS)	Tl (MS)	U (MS)	V (MS)	W (MS)	Zr (MS)	Na (MS)	K (MS)
		µg/g	µg/g	µg/g	µg/g	µg/g	µg/g	µg/g	µg/g	µg/g	µg/g	µg/g	µg/g	µg/g	µg/g	µg/g
76937	Stobie 017 tractor DCL	4.35	3.69	52.6	27.2	0.01	<0.05	0.33	91	<0.05	0.416	41.3	6.2	0.74	2000	522
76938	Stobie 3013 Tractor ECS	3.65	2.93	48.8	79.1	0.01	0.2	0.43	164	<0.05	0.915	2973	37.1	3.53	3100	1211
76939	Stobie 213 Trap #1 ECS	1.41	0.9	20.6	17.4	<0.01	0.19	0.29	94	<0.05	0.388	200	26.7	0.64	3200	741
76940	Stobie 213 Trap #2 ECS	0.48	0.75	7.02	7.85	<0.01	0.11	0.31	164	<0.05	0.202	16.3	5.57	2.94	1400	807
76941	107 2934.5 HRS	6.17	4.94	71.4	45.6	0.01	0.58	0.69	160	<0.05	0.633	3594	65.3	2.33	8800	3348
76942	111 Before	nes	nes	nes	nes	nes	nes	nes	nes	nes	nes	nes	nes	nes	nes	nes
76943	111 After	2.46	2.62	31.9	57.9	<0.01	0.19	0.58	143	<0.05	0.579	35.5	28.6	0.87	6500	794

		Rb (MS)	Cs (MS)	Sc (MS)	Y (MS)	Sm (MS)	Eu (MS)	Gd (MS)	Tb (MS)	Dy (MS)	Ho (MS)	Er (MS)	Tm (MS)	Yb (MS)
		µg/g	µg/g	µg/g	µg/g	µg/g	µg/g	µg/g	µg/g	µg/g	µg/g	µg/g	µg/g	µg/g
76937	Stobie 017 tractor DCL	1.89	0.059	0.8	1.15	0.19	0.03	0.19	0.03	0.14	0.02	0.06	0.01	0.04
76938	Stobie 3013 Tractor ECS	1.71	0.505	1	1.61	0.35	0.07	0.63	0.05	0.24	0.04	0.11	0.02	0.13
76939	Stobie 213 Trap #1 ECS	2.45	0.151	0.6	1.91	0.36	0.06	0.35	0.05	0.29	0.05	0.13	0.02	0.07
76940	Stobie 213 Trap #2 ECS	2.81	0.167	0.7	1.11	0.22	0.04	0.29	0.03	0.19	0.02	0.07	0.01	0.05
76941	107 2934.5 HRS	3.07	0.674	1.3	2.26	0.55	0.11	0.49	0.07	0.37	0.07	0.19	0.02	0.18
76942	111 Before	nes	nes	nes	nes	nes	nes	nes	nes	nes	nes	nes	nes	nes
76943	111 After	3.24	0.218	1.3	1.47	0.35	0.08	0.29	0.04	0.23	0.03	0.12	0.01	0.11

Ash from DCL Titan on Tractor #017

(high carbon content)

Wide field
Low magnification
2000 µm scale at lower right

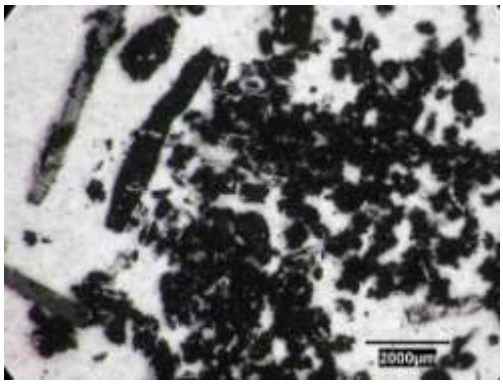

Wide field
100X magnification
100 µm scale at lower center

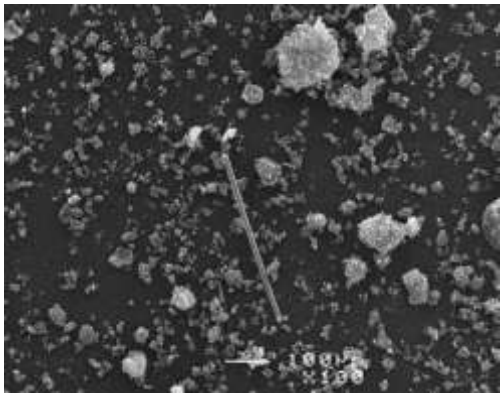

Typical particle agglomerate
SEM image
500 nm scale at lower right

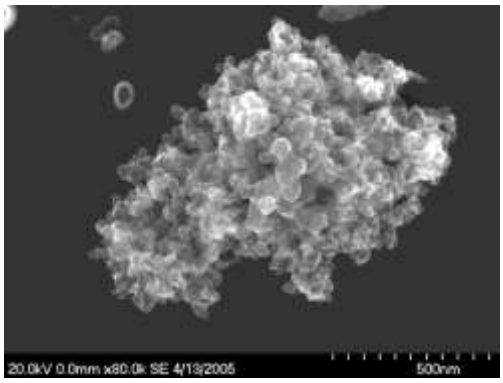

Another agglomerate
SEM image
200 nm scale at lower right

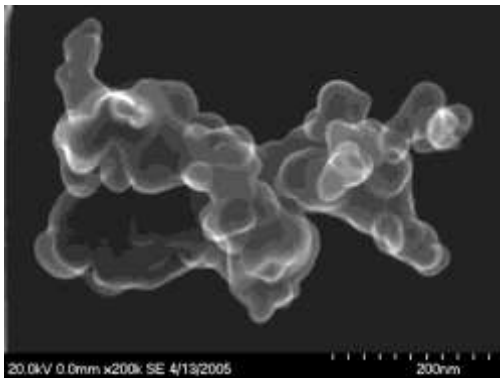

Figure 124: Photos of ash particles from DCL DPF.

Ash from ECS/Combifilter on Tractor #3013

(low carbon content)

Wide field
Low magnification
2000 µm scale at lower right

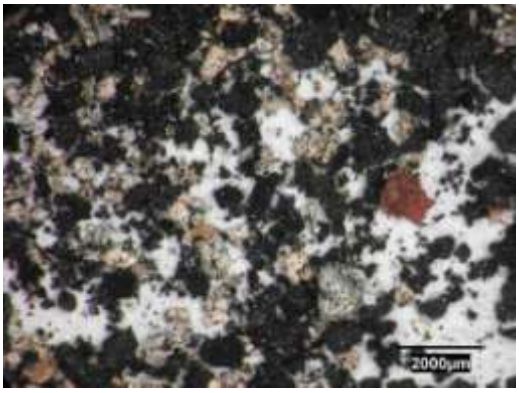

Wide field
100X magnification
100 µm scale at lower center

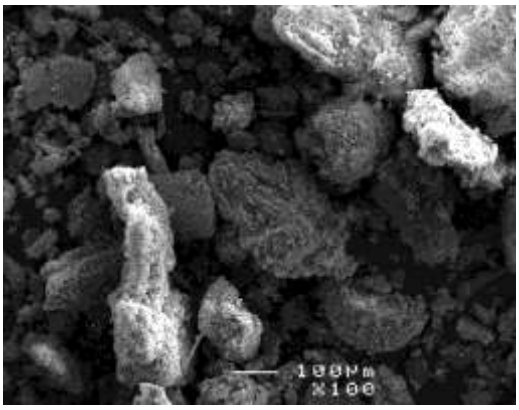

Typical particle agglomerate
SEM image
500 nm scale at lower right

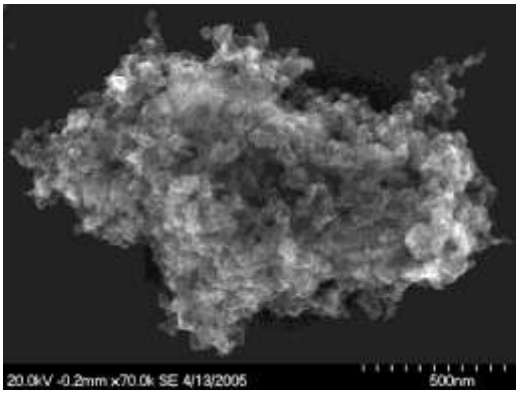

Another agglomerate
SEM image
500 nm scale at lower right

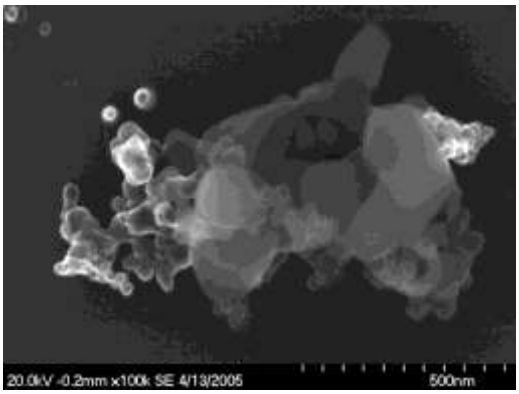

Figure 125: Photos of particles from ECS DPF.

12.3 2nd Sampling trial

A second sampling of ash trial was carried out on the ECS/Combifilter DPF on tractor #3013. An attempt was made to minimize the amount of unburned soot by handling the filter with great care as it was put into the CombiClean oven chamber. Then the cooking was carried out for seven consecutive periods without removing the filter from the oven. The filter was then carefully removed so as not to jar loose any unburned soot. When the inside of the oven was examined, as shown in Figure 126, a fine white dust was visible on horizontal surfaces. Samples of this dust were removed using an eyedropper and were combined into a single ash sample.

Figure 126: Inside of oven after seven "cookings" of the ECS DPF.

12.3.1 2nd Sampling trial results

Chemical analyses of two samples are shown in Table 46. Sample #95294 was the ash sample recovered by the eyedropper from the oven. Sample #95295 was the material blown out of the regenerated filter.

Table 46: Bulk chemical analyses of 2nd sampling trial.

ITSL#	Sample Description	C	S	Cu	Ni	Co	Fe	Ca	Al	Mg	Si	As	Pb
		%	%	%	%	%	%	%	%	%	%	%	%
95294	Combi clean station ash	nes	6.93	0.24	0.27	<0.02	12.4	17.6	0.39	0.46	3.58	<0.02	0.06
95295	Combi station/trap soot	71.2	0.44	0.02	<0.02	<0.02	10.7	1.13	0.09	0.02	0.18	<0.02	<0.02
		Zn	Mn	Cr	P	B	Ag	Au	Ba	Be	Bi	Cd	Ce
		%	%	%	%	µg/g	µg/g	µg/g	µg/g	µg/g	µg/g	µg/g	µg/g
95294	Combi clean station ash	9.99	0.25	0.32	9.15	40	5	63	49	<1	1.1	32	14
95295	Combi station/trap soot	0.55	<0.02	<0.02	0.40	7	0.2	3.3	3	<0.2	<0.1	2	0.6
		Ga	Ge	Hf	Hg	In	Ir	La	Li	Mo	Nb	Nd	Pd
		µg/g	µg/g	µg/g	µg/g	µg/g	µg/g	µg/g	µg/g	µg/g	µg/g	µg/g	µg/g
95294	Combi clean station ash	<5	N/A	<5	3	<0.5	4	4	134	700	<5	<5	20
95295	Combi station/trap soot	<1	N/A	<1	<0.2	<0.1	0.3	0.3	2	46.5	<1	<1	0.7
		Pr	Pt	Re	Rh	Ru	Sb	Se	Sn	Sr	Ta	Te	Th
		µg/g	µg/g	µg/g	µg/g	µg/g	µg/g	µg/g	µg/g	µg/g	µg/g	µg/g	µg/g
95294	Combi clean station ash	<5	3	<0.5	<1	<1	9	9	451	57	<5	1	<5
95295	Combi station/trap soot	<1	0.3	<0.1	<0.2	<0.2	0.6	2	22.7	3	<1	<0.2	<1
		Ti	Tl	U	V	W	Zr	Na	K	Rb	Cs	Sc	Y
		µg/g	µg/g	µg/g	µg/g	µg/g	µg/g	µg/g	µg/g	µg/g	µg/g	µg/g	µg/g
95294	Combi clean station ash	350	<5	1	839	240	10	8780	1600	<5	<5	17	9
95295	Combi station/trap soot	56	<1	0.1	40	13	<1	521	80	<1	<1	1	<1
		Sm	Eu	Gd	Tb	Dy	Ho	Er	Tm	Yb			
		µg/g	µg/g	µg/g	µg/g	µg/g	µg/g	µg/g	µg/g	µg/g			
95294	Combi clean station ash	<5	<5	<5	<5	<5	<5	<5	<5	<5			
95295	Combi station/trap soot	<1	<1	<1	<1	<1	<1	<1	<1	<1			

There was insufficient sample of the white ash to analyze for carbon content, but visually there existed very little soot in it. The other sample, clearly black in colour, had obviously been contaminated by unburned soot and contained 71% carbon by weight.

Only the "clean" ash sample, #95295, was examined further.

XRD Results:

The ash sample gave a weak and diffuse XRD pattern. This made it very difficult to properly identify certain phases, but possible phases of calcium phosphate [$Ca(PO_3)_2$], calcium iron phosphate [$Ca_{19}Fe_2(PO_4)_{14}$], anhydrite [$CaSO_4$] and hematite [Fe_2O_3] were suggested.

SEM Results:

The ash sample was sprinkled on a stub mount and placed in the SEM to attempt to identify the compounds present. Figure 127 shows the sample with 10 μm shown as the bright horizontal line.

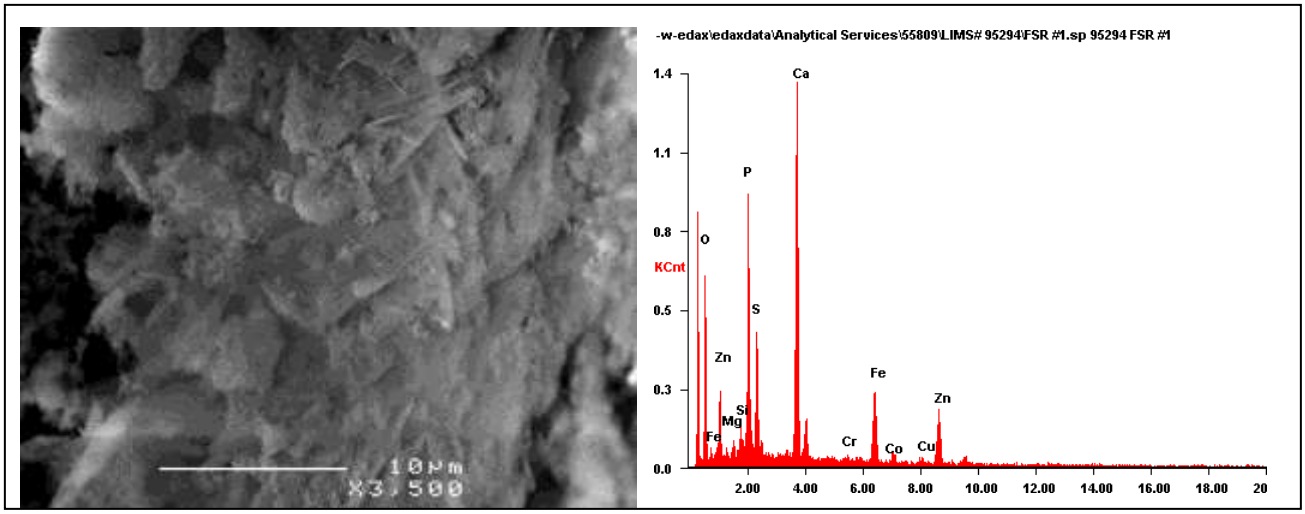

Figure 127: Scanning electron microscope backscatter image of ash sample (left) and x-ray spectrum of a large area of the sample (right) for ECS/Combifilter removed from tractor #3013 .

Clearly this sample has morphology very different from the 1st sampling trial samples. Very little of the typical agglomerates of diesel soot were present in this ash. The x-ray spectrum of a fairly large area of the sample is shown in the right side of Figure 127. It shows the presence of oxygen, iron, zinc, magnesium, silicon, calcium, chromium, cobalt and copper.

Additional detailed portions of the sample were focused on, as identified in Figure 128 and Figure 129, and x-ray spectra obtained. These analyzes confirm the crude identifications seen by x-ray diffraction, namely, that the sample contains significant quantities of complex phosphates and sulfates of calcium and iron, and that some iron oxides and zinc oxide are likely also present.

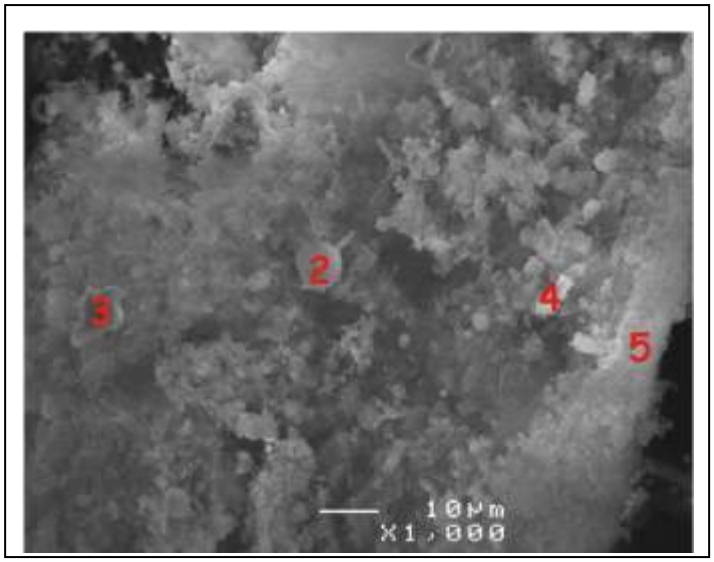

Figure 128: Ash particles, indicated by red numbers, for which specific x-ray spectra were obtained, shown below.

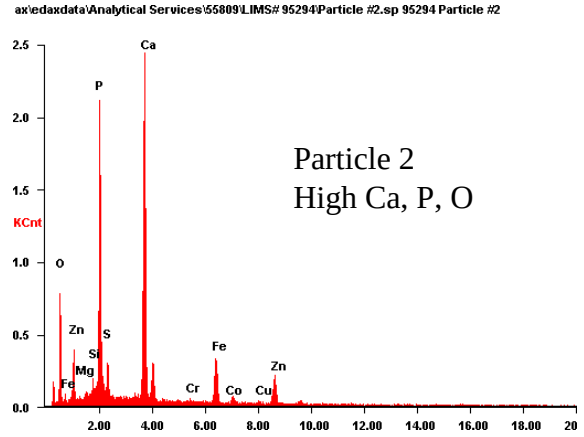

Particle 2
High Ca, P, O

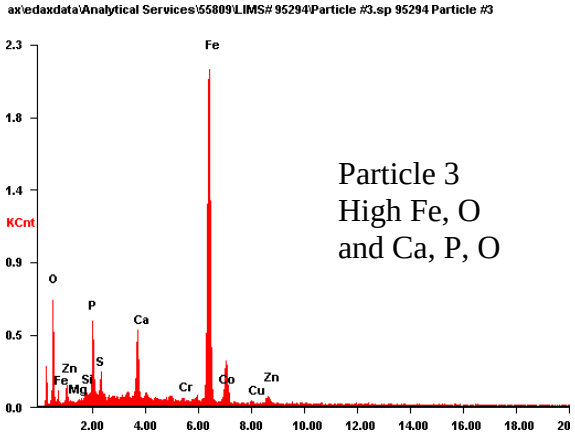

Particle 3
High Fe, O
and Ca, P, O

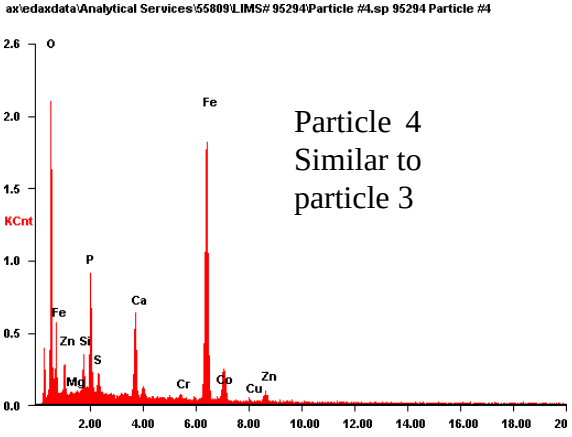

Particle 4
Similar to
particle 3

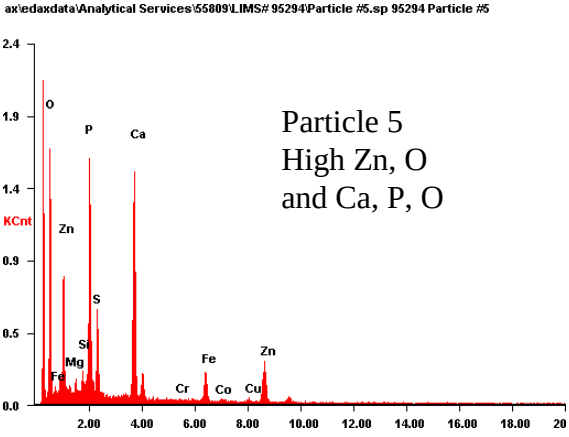

Particle 5
High Zn, O
and Ca, P, O

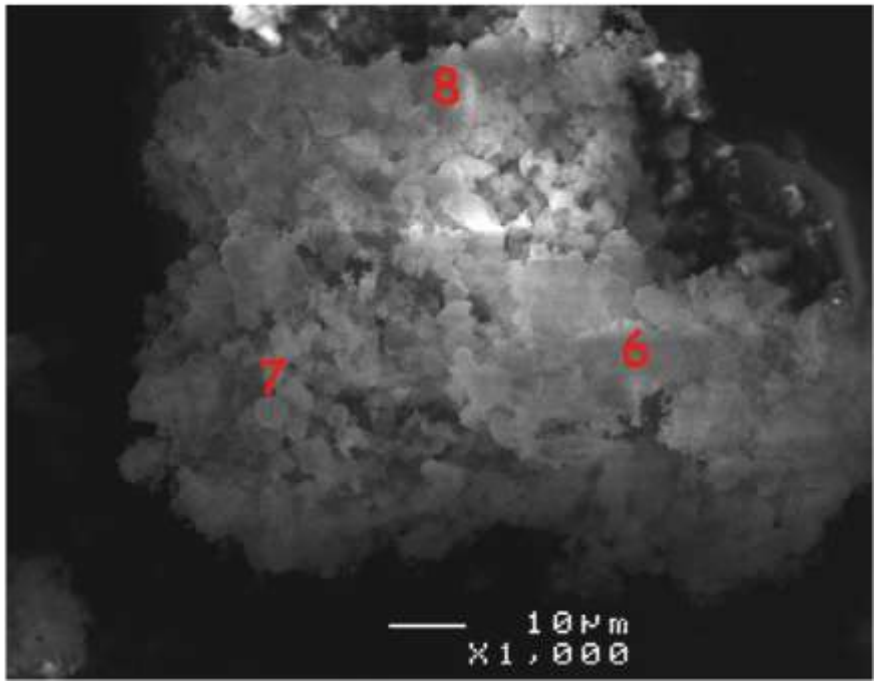

Figure 129: An agglomerate consisting of many small particles. Three areas highlighted by the red numbers were specifically analyzed and each x-ray spectrum is shown below.

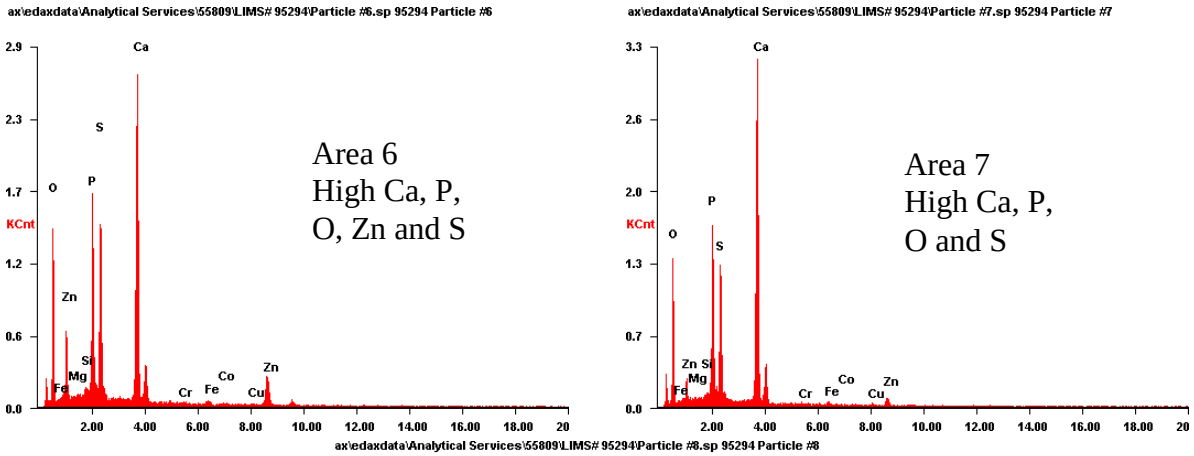

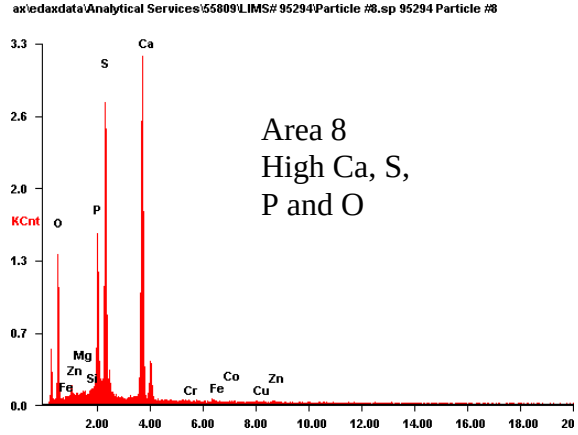

13. Post-Testing Efficiencies and Analyses

At the completion of the in-mine testing six DPFs were evaluated by the Diesel Emission Research Laboratory of CANMET-MMSC in Ottawa by means of:

- Emission testing using engine dynamometers;
- Characterizations of emitted DPM for soluble organic fractions, sulfate and PAHs;
- Inspections of the DPFs and filter elements for internal and external damage.

The entire CANMET Report is contained in Appendix D and readers are referred to it for details.

13.1 Filters

The filters provided to CANMET and their tests on them are listed in Table 47.

Table 47: Tests run on filters at CANMET.

Filter	Test No.	CANMET I.D.	Vehicle No.	Vehicle Type
None	1	Baseline-heavy duty		
Johnson Matthey	2	HD820	820	LHD
ECS	3	HD213-A	213	LHD
ECS	4	HD213-B	213	LHD
None	5	Baseline-light duty		
ECS	6	LD612	612	Tractor
DCS Titan	7	LD2180	2180	Tractor
Engelhard (a)	None	I362	362	LHD

a: The Engelhard was oil soaked due to turbo failure and fire and was not suitable for testing.

13.2 Experimental procedures

Two diesel engines were used in the laboratory testing. A Liebherr D914T engine was used for those DPFs installed on LHDs at Stobie and a Kubota V3300 TE engine was used for the DPFs installed on the tractors. Figure 131 shows a filter connected to an engine at CANMET. The fuel used contained 0.033 wt% sulfur.

The Schenck Pegasus Corporation AC dynamometer used at CANMET, shown in Figure 130, is extremely rugged and can be controlled by a DC 6000 controller with high accuracy.

Raw diesel exhaust gas concentrations were measured by a California Analytical Instruments Company unit shown in Figure 132. This unit included a gas sampling and conditioning system, emission analyzers, a 64 point gas divider for calibration, and an NOx efficiency tester.

The mass of DPM emitted from the engine was sampled and measured gravimetrically using a Sierra BG-2/3 Particulate Partial Flow Sampling System. The samples were collected on Palliflex T60A20 Teflon-coated glass fiber filters.

Particle size distributions were obtained using a Scanning Mobility Particle Sizer (SMPS) similar to the one described in Chapter 8. A NanoMet sampler (similar to that used to dilute raw exhaust samples by NIOSH as discussed in Chapter 8) was used with a photoelectric aerosol sensor (PAS) to obtain information about the EC portion of DPM.

Smoke opacity was measured with a Bosch RT 100 meter according to the SAC J1667 snap acceleration test protocol.

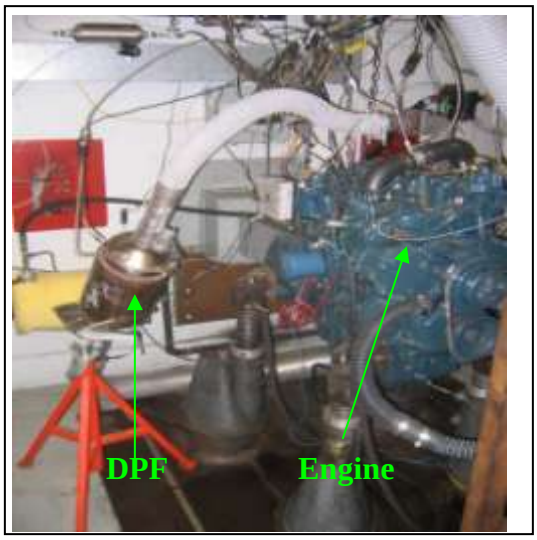

Figure 131**: Filter being tested..**

Figure 130: Dynamometer

Figure 132: Raw gas analysis unit.

Table 48: ISO 8178-C1, 8-mode diesel engine emissions test conditions of RPM and load.

Mode #	1	2	3	4	5	6	7	8
Engine Speed	Rated Speed				Intermediate Speed			Low idle
Torque, %	100	75	50	10	100	75	50	0
Weight factor	0.15	0.15	0.15	0.1	0.1	0.1	0.1	0.15

The test cycles used were:

- 7-modes per ISO-8178-C1 specifications. The integrated values for each parameter were obtained by using the weights assigned for each mode (see Table 48);
- 3-modes (full torque converter stall, high idle without load and low idle without load);
- Snap acceleration.

Analysis of DPM samples for an individual mode was impossible due to insufficient sample mass. Since DPM sampling for each mode used two filters, each 8 mode test resulted in 16 filters. These were combined into one sample to obtain the soluble organic fraction, PAHs and sulfate.

Inspections of each DPF were done visually and by X-ray prior to laboratory testing. Additional inspections were done by borescope and sometimes destructive inspections following the laboratory testing. The borescope was purchased from the Karl Stortz Industrial Group. It used fiber-optic light to illuminate the internal channels of the ceramic monolith filters.

13.3 Results

The 8-mode conditions for all DPF tests were within 1% of the engine baseline data thus verifying that the various modes run were being replicated very well. Therefore, any changes in engine emissions with a DPF in place were attributed to the DPF. The emissions reduction data for the 5 DPF tests (relative to the baselines) are given in Table 49.

Table 49: Emissions reductions for integrated 8-mode tests.

	HD820 Johnson Matthey	HD213A ECS/Combi (used in parallel; tested separately)	HD213B filters	LD2180 ECS Combi S5	LD621 DCL Titan
CO_2	-0.3%	0.9%	-0.2%	0.1%	-1.3%
CO	8%	-3%	-4%	-7%	1%
NO_2	67%	38%	63%	44%	44%
NO	2%	1%	1%	-3%	-5%
THC	28%	8%	16%	15%	18%
DPM (Mass)	89%	85%	93%	94%	95%

Note: HD refers to Heavy Duty (LHD) and LD refers to Light Duty (tractors)

The DPF filtration efficiencies based on numbers of DPM particles and based upon PAS are presented in Table 50.

Table 50: DPF filtration efficiencies determined from particle number by SMPS and PAS

	Efficiencies based on numbers of particles						Efficiencies based on PAS				
Modes	**HD820 JM**	**HD213A ECS**	**HD213B ECS**	**LD2180 ECS**	**LD621 DCL**		**HD820 JM**	**HD213A ECS**	**HD213B ECS**	**LD2180 ECS**	**LD621 DCL**
1	99.0%	91.8%	99.5%	100.0%	99.7%		95.5%	93.7%	99.8%	73.4%	89.6%
2	99.5%	91.9%	99.7%	100.0%	99.7%		90.8%	77.6%	99.3%	80.4%	88.5%
3	99.0%	94.7%	99.9%	100.0%	99.7%		90.6%	80.1%	99.5%	82.4%	88.4%
4	99.0%	96.0%	99.9%	100.0%	99.5%		65.6%	34.9%	96.5%	85.9%	90.6%
5	98.7%	95.7%	99.9%	100.0%	99.0%		79.1%	70.8%	98.5%	84.5%	89.5%
6	98.8%	94.6%	99.9%	100.0%	98.8%		56.0%	35.3%	96.0%	83.9%	88.7%
7	99.2%	96.8%	99.9%	100.0%	98.8%		55.9%	33.3%	94.8%	83.7%	88.3%
8 (LI)	94.4%	83.7%	99.7%	99.4%	87.4%		47.5%	19.6%	93.0%	84.0%	88.3%
TCS	98.6%	95.9%	99.9%	100.0%	99.1%		81.8%	78.4%	98.8%	72.5%	87.7%
HI	99.2%	95.9%	99.9%	100.0%	99.3%		93.1%	96.2%	99.7%	52.6%	87.5%
Average (8-mode)	98.4%	93.2%	99.8%	99.9%	97.8%		72.6%	55.7%	97.2%	82.3%	89.0%

The filters which collected the DPM from the engine exhaust, with and without DPF in place, were analyzed for sulfate, soluble organic fraction, and PAHs. Results are given in Table 51.

Table 51: Analyses of mass and percent reductions for components of DPM in engine exhaust filter samples.

Sample	Baseline No DPF	HD820 JM	HD213A ECS	HD213B ECS	Baseline No DPF	LD2180 ECS	LD621 DCL	Blank filter
SO_4, µg	275	182	193	155	200	230	214	<MQL
Reduction in SO_4	--	34%	30%	44%	--	- 15%	- 7%	--
SOF, mg	3.65	2.04	2.71	2.54	1.53	1.72	1.03	1.03
Reduction in SOF	**--**	44%	26%	30%	--	12%	33%	**--**
PAH, ng	2775	478	830	313	2716	273	336	100
Reduction in PAH	**--**	83%	70%	89%	--	90%	88%	**--**

Note: HD refers to Heavy Duty (LHD) and LD refers to Light Duty (tractors)

13.4 Inspections of DPFs

Johnson Matthey (from LHD #820): This DPF had a large dent in the outer shell (Figure 133, left), but the inner filter canister was undamaged (Figure 133, right). The mat used to hold the SiC wall flow filter tightly against its canister had severely degraded (Figure 134) and this likely allowed some exhaust (and thus DPM) to flow along the outside of the filter between it and the canister. It is also likely that the degradation of this mat resulted in the filter element separating from the inlet and outlet retaining rings (Figure 135) and the concomitant soot bypass that was evident at this point (Figure 136).

Figure 133: Johnson Matthey outer shell dent (right) and undamaged inner canister (left).

Figure 134: Degradation of mat holding J-M filter element in place.

Figure 135: Separation of SiC filter from canister ring (top of photo).

Figure 136: Blackened soot shadow at points of monolith separation indicating unfiltered exhaust bypassing filter.

ECS/Combifilters (from LHD #213): These SiC DPFs had been used in dual mode (parallel configuration) on LHD #213. The outlet sides of the filter element had some surface damage. At certain points (see Figure 137(a)) the ceramic bonding the individual SiC blocks together was missing to depths of 10-20 cm, but no evidence of soot blowthrough appeared at these points.
Soot blowthrough was noted on the outlet side face in some areas (see Figure 137(b)).

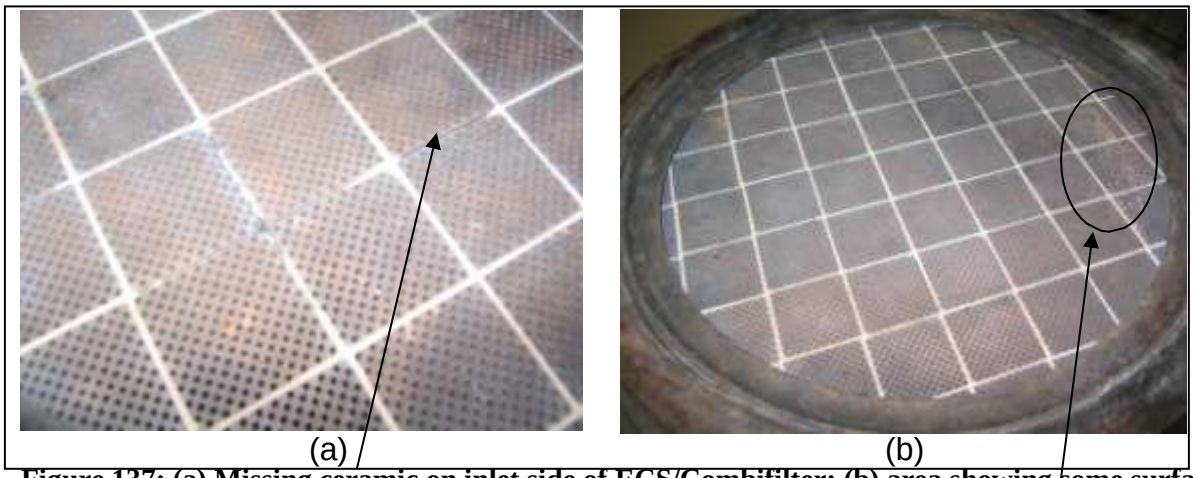

Figure 137: (a) Missing ceramic on inlet side of ECS/Combifilter; (b) area showing some surface abrasion.

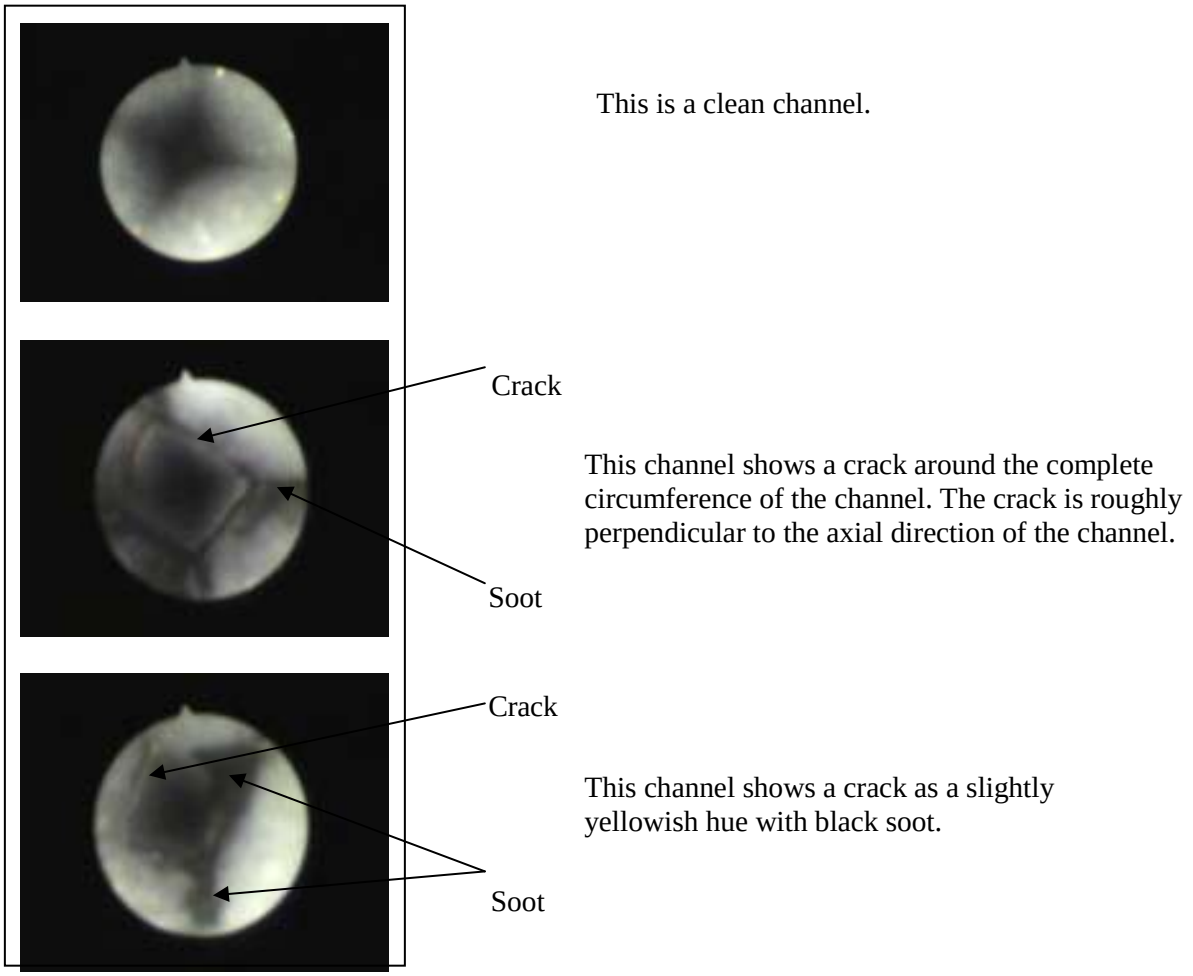

Figure 138: Borescope photographs of channels on the outlet side of the ECS/Combifilter.

Following the 8-mode tests of these DPFs, several of the channels in the blowthrough areas were investigated with the borescope, as shown in Figure 138. Several cracks were seen roughly perpendicular to the axial direction of the channels on the discharge side. It is surmised that these cracks were caused by differences in thermal expansion between these cells and neighbouring cells. This could occur if soot is not uniformly distributed among the inlet side channels. If soot is ignited in some channels, causing them to heat significantly, but soot is absent from neighbouring channels, which are relatively cooler, then thermal expansion stresses can be generated. This kind of stress might be expected from SiC wall flow filter, because it is not a single monolithic honeycomb as is the cordierite element, but is comprised of smaller monolithic blocks cemented together with refractory paste (see Figure 137). Thus heat is not conducted as uniformly throughout the entire filter as it is in a single honeycomb monolith such as those made of cordierite. This differential heating causes the stress.

ECS Combifilter S5 (from tractor #2180): The SiC filter element of this DPF appeared to be structurally sound with no surface damage and no cracking. Some of the spider support welds had broken off the face ring (see Figure 139) and there was a very small amount of DPM blowthrough evident. With a simple re-welding of the spider support, this unit could have gone on operating.

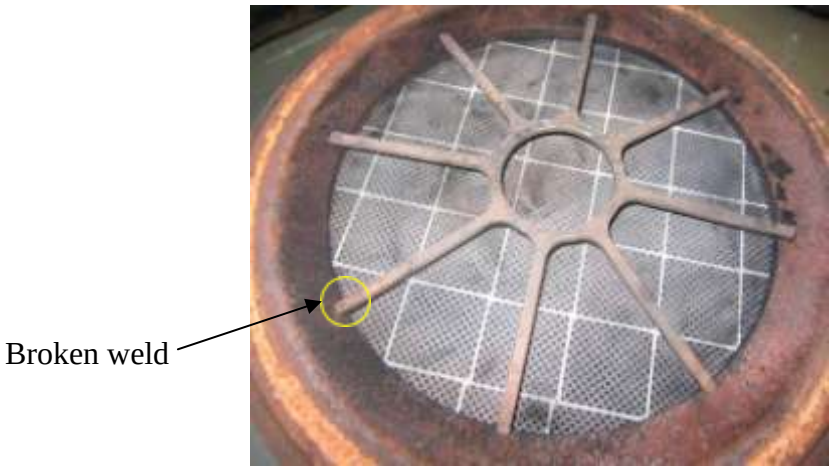

Figure 139: Welds for the spider support were broken.

DCL Titan (from tractor #621): The DPF inlet side had a few surface abrasions. Some of the SiC filter blocks were cracked where they contacted the retaining ring. This may have resulted from vibration. The discharge side of this filter, shown in Figure 140, showed evidence of DPM blow through (< 50 cells) in one block section.

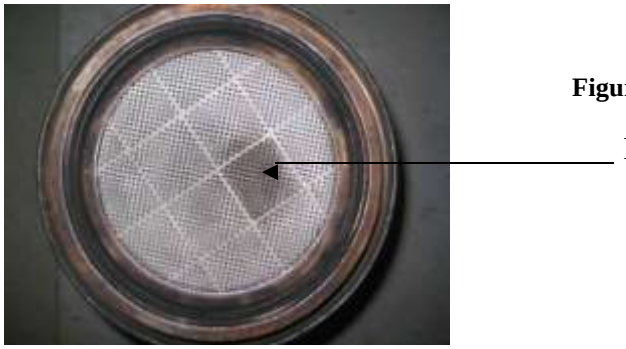

Figure 140: Soot blowthrough on the discharge side of the DCL DPF.

A particular cell in the area of the blowthrough seen in Figure 141 was investigated by positioning the borescope at various depths along the length of a single honeycomb cell. Photographs of these positions are shown in Figure 141 going from left to right from discharge side to inlet end of the filter. It is clear that the soot accumulation increases nearest the inlet side and this may indicate that the end caps at the inlet end of the discharge channels were leaking. While not evident in the blowthrough zone because of the large amount of soot obscuring the view of the wall, several nearby cleaner cells were seen to have minor cracks, as shown in Figure
142. Although the blowthrough is quite evident, its effect is minimal as evidenced by the DPF filtration efficiencies for this DCL Titan DPF, Table 50.

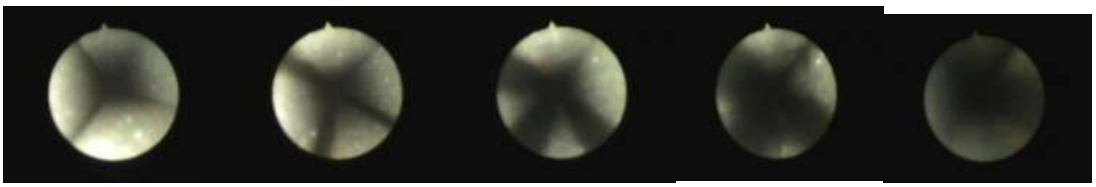

Figure 141: Images along the length of a cell showing blowthrough in the DCL filter. Left to right the images go from the inlet side to the discharge side.

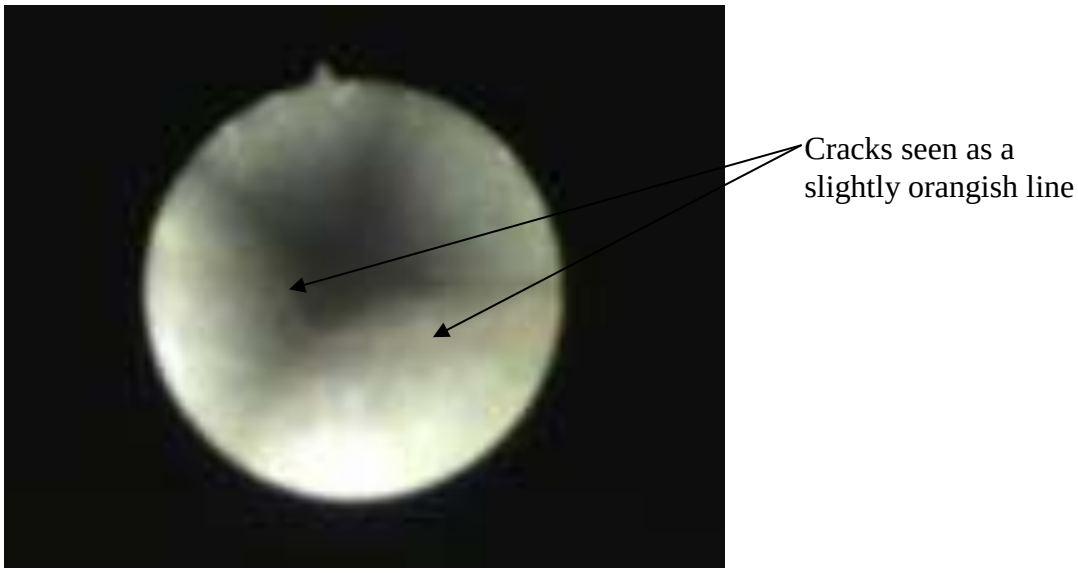

Figure 142: Minor cracks in the wall of a cell in the DCL filter.

Engelhard (from LHD#362): This unit was not found suitable for bench testing because excessive oil had entered the inlet from a turbocharger failure, which had occurred during the field testing at Stobie. The filter, cut open as shown in

Figure **143** showed the oil contamination to be extensive.

Figure 143: Engelhard filter showing the extent of oil contamination it suffered from the turbocharger failure on LHD #362.

14. Project Management

14.1 Team Construction

Since the DPF testing project at Stobie was to be performed while the host vehicles carried out their normal production duties, the associated production people were formed into a Stobie team. All the team members took on these project responsibilities as additional duties to their normal job. This additional work caused some problems with time constraints and personal priorities. There was, however, no other way to conduct the project at Stobie. The personal dedication of the personnel on the Stobie project to spending extra time on the project when it was necessary contributed significantly toward minimizing disruptions in the project schedule.

Going into the project, the team recognized the potential difficulties with the primary technical consultant, A. Mayer, being located in Switzerland, but the Stobie team believed that his technical expertise was essential for a successful project. For that reason, Mayer visited Stobie and met with the project team several times, and these visits were well justified. Extensive use was made of the internet for sending large quantities of raw data logging files, and this worked fairly well. While overall Mayer's expertise was effectively applied to the project, some technical challenges would have been more efficiently solved by more opportunity for face-to- face meetings with him.

14.2 Team Communications

Regular team meetings were an important part of the project. Initially scheduled every two weeks, these meetings became weekly in response to a need for better team communications during last half of the project. Minutes of all meetings were recorded and archived by the team's secretary.

14.3 Data records

The data logger files are organized in a relatively straightforward manner by identifying the vehicle, the DPF and the time period. However, what was not as straightforward was recording the vehicle/DPF status. The creation of log books for each DPF solved part of this problem. Daily operating sheets were instigated so that vehicle operators could report what had happened during each shift. All of this information is archived on a Vale Sudbury server. Of course, one of the consequences of recording such data is that a team member had to be designated to review the reports and cross reference events with the logged data.

14.4 Training and communicating with operators

The Vale Training Department undertook responsibility for packaging information about each DPF and communicating with relevant Vale personnel. Training manuals exist as a result of these actions, and they may be reviewed by outside parties, if desired.

One of the most critical and difficult part of the project was getting vehicle operators to take responsibility for routinely performing the active regeneration required of certain DPF systems. To some operators this was likely to be viewed as yet another thing for them to have to do, and in some cases the importance of regeneration was not realized. Owing to good operator feedback, the team learned that some DPF regeneration was not being carried out because of the difficulty in getting the vehicle to the inconveniently located regeneration station at the end of a shift. Based on this feedback, the project team relocated the regenerating stations to a more favorable location which was essential to getting more routine regeneration.

Another challenge was to limit the operation of the test vehicles to those operators who had undergone the necessary training in the DPF for their vehicle. This was easier for the LHD vehicles than for the tractors because an LHD tends to be driven by a small team of operators, whereas the tractors are used in a collective mode by anybody needing transportation. Putting labels on LHDs, informing operators not to use the vehicle unless trained in the DPF, worked fairly well. However, similar labels on tractors were not effective because often a test tractor was the only one available, and mine operation took precedence over this project.

14.5 Limited vehicle use

The hit and miss use of certain tractors meant that some operating hours fell short of expectations. This was sometimes caused by the perception that some tractors were prone to problems (problems not associated with the project), and some tractors required more general vehicle-engine maintenance than others. Thus, towards the later part of the project, DPFs were moved to another identical tractor so that operating hours could be accumulated more rapidly.

14.6 Managing change

Vale has found it beneficial to manage change in operating environments. Usually this includes a complete review of what is being changed, the development of a strategy for how to communicate the need for the change, and monitoring of the acceptance of change. All of the DPFs and associated equipment (regenerating stations) were subjected to management of change analysis before being taken underground. In some cases a more extensive program of systematic hazard review was necessary. This kind of work took more effort than the team initially forecast.

14.7 Technical knowledge transfer

There exist several types of technical transfer.

(a) Within the Stobie mine: Extensive interactions between mine personnel and the Stobie project team took place throughout the four years of testing. In addition, A. Mayer and his data logging expert, P. Nöthiger, were brought over from Europe for several weeks at a time to transfer their knowledge to the Stobie team and mining personnel.

(b) Within the DEEP membership: Two major workshops were held on site at Stobie for members of DEEP. The first of these in November 2000 was related to the duty cycle monitoring results and the criteria for selecting DPFs for the Stobie project; the second in July 2004 reviewed results of the Stobie project in a general way. The presentations from both of these workshops are included in the Appendices to this report.

(c) Within the mining community: Presentations on the Stobie project status and results were given every year from 2001 through 2006 at the Mining Diesel Emission Conference (MDEC) held in Markham, Ontario. Organized by CANMET staff, these conferences aim to keep stakeholders in diesel emission issues aware of developments throughout the world. Usually attended by more than 100 people from Canada and the United States, MDEC has experienced expanded interest from Europe and Africa. As part of DEEP's technology transfer initiative, J. Stachulak, project principal investigator, made presentations about the Stobie project at four regional workshops held in mining centres across Canada: at Marathon, Ontario in Sep 2003, at Val d'Or, Quebec in Oct 2003, at Saskatoon, Saskatchewan in Oct 2003 and at Bathurst, New Brunswick in May 2004.
Combined, these workshops attracted 133 underground and open pit mining personnel.

(d) International: The Stobie project has also been presented at the following international technical conferences by the project's principal investigator:

- **a.** Mine Expo 2000 in Las Vegas, Nevada;
- **b.** 6th International Symposium on Ventilation for Contaminant Control in 2000 in Helsinki, Finland;
- **c.** 7th International Mine Ventilation Congress in 2001 in Cracow, Poland;
- **d.** Mine Health and Safety Conference in April 2002 in Sudbury, Ontario;
- **e.** National Institute for Occupational Safety and Health Diesel Workshop in February 2003 in Cincinnati, Ohio;
- **f.** The Society of Mining Engineers Annual Conference in 2003 in Cincinnati, Ohio;
- **g.** The Caterpillar Engine Conference/Workshop held in February 2004 in Peoria, Illinois;
- **h.** 8th International Mine Ventilation Congress in July 2005 in Brisbane, Australia.
- **i.** 1st Global Forum in Mineral Technology in November 2008 held in Vale, Belo Horizonte, Brazil;
- **j.** Ninth International Mine Ventilation Congress, in November 2009 held in New Delhi, India;
- **k.** 13th United States/North American Mine Ventilation Symposium in June 2010 held in Sudbury, Ontario, Canada.

(e) On-going: The Stobie team intends to continue its technology transfer across Vale's other mines in Ontario and Manitoba and to assist, where requested, other mining companies in implementing DPF technology to existing or new diesel equipment.

14.8 Budget and expenditures

The budget for the project was originally of $467,124. Due to adjustments during the project, the final budget was $419,962 from two sources:

DEEP consortium	$319,962
Ontario WSIB	$100,000

Vale's in-kind contributions are difficult to quantify accurately, but an estimate can be made by accounting for employee hours spent on the project and for the non-budgeted equipment expenditures directly associated with the project. The employee hours spent on the project are summarized below:

	Person-hours
Site preparation and project planning	470
DPF installation and maintenance	6540
Data logger installation and downloading	290
Technology transfer	1190
Meetings and communications	9840
Training operators/mechanics	730
Performance testing	710
External interfacing and training	410
Reporting	1846
Project management	5700
Total	27700

The line item "Meetings and Communications" consists of 333 meetings of the core Stobie team.

It is estimated that Vale's personnel cost >$2.3 million. Excluded from this amount are the contributions of personnel and equipment from supporting companies (engine manufacturers, control equipment manufacturers, etc.) and from assisting agencies (NIOSH, other scientists).

It is estimated that the complete Stobie project had a total cost, inclusive of cash and in- kind contributions, of around $3 million.

15. Conclusions and Recommendations

The Stobie Project was successful in meeting its objectives.

- It tested eight state-of-technology diesel particulate filter systems on nine vehicles operating in underground production mode.
- Both heavy duty and light duty vehicles were used in the tests.
- Extensive duty cycle monitoring was conducted so that DPF system characteristics could be chosen to properly match the real-world engine performance.
- In a number of the systems, operational time with high DPM filtration efficiencies exceeded 2000 hours.
- Exhaust analyses were carried out routinely on all systems, and special more comprehensive analyses were carried out three times.
- Industrial hygiene measurements of airborne DPM made with and without a DPF installed.
- Post-test analyses were conducted on certain DPFs.

15.1 General conclusions

(1) Both heavy duty and light duty vehicles in underground mining operations can be retrofitted with high efficiency Diesel Particulate Filter (DPF) systems that effectively remove DPM from the vehicle exhaust.

(2) Making the effort to correctly match the duty cycle of an *individual* vehicle as reflected by engine exhaust temperature profiles with an appropriate DPF is essential for a retrofitting program to be successful.

a. This matching must be done to correctly size the DPF so that an acceptable soot collection period is obtained. Too small a DPF will result in loading the filter too quickly and/or high exhaust backpressure and will negatively impact on vehicle productivity. Too large a DPF will result in cramped space for the DPF on the vehicle, and this could negatively impact safe use of the vehicle and ease of its maintenance.

b. This matching must be done to obtain the optimum method of regeneration of the DPF. The optimum method of regeneration must take into account issues such as the complexity of the regeneration system, the period of time needed for regeneration, maintenance of components of the regeneration system, ease of installation and use, and cost.

(3) Proper communication with vehicle operators is essential. The presence of a DPF means an increase in the exhaust backpressure of the engine. Operators must be instructed on the interpretation of and the appropriate action to be taken in response to novel dashboard status indicators for the DPF to avoid serious harm to the DPF and/or the engine.

(4) Simple, but effective, dashboard indicators of the DPF status, usually related to exhaust backpressure, are essential to successful DPF operation.

(5) All of the systems tested required more close attention than desired, although there was a wide variation in the amount of attention needed. Ideally, a DPF would be invisible to a vehicle's operator and almost invisible to the maintenance department. That is, people would go about their jobs in a conventional manner and would not need to pay attention to the DPF or its regeneration. This was clearly NOT the case for any of the DPFs being tested in the Stobie project. This remains a critical issue in any successful program for retrofitting or for installing DPFS as OEMs.

(6) The increased emission of noxious gases is often a consequence using a DPF. There is a minimal increase in CO and HC emissions during initial stage of regeneration which is of little consequence when it occurs passively in production, but a minimal ventilation needs to be present at the location of off-duty regeneration station. Some passive DPFs employ a noble metal catalyst which increases the NO_2 concentration in the exhaust. While there may exist ways to control such emissions, system complexity (by adding on components) is undesirable.

(7) An emissions-based maintenance component of an overall vehicle/engine maintenance program is essential. Proper functioning of a DPF should be evaluated as part of routine maintenance. Training of maintenance personnel in the specifics of each DPF is essential.

15.2 Specific conclusions for heavy duty (LHD) vehicles

Engelhard:

This was a passive DPF system using a noble metal catalyst wash coat on the cordierite wall flow filter. It was of low complexity and required relatively little attention. Filtration efficiency for soot was high, but backpressures readings exceeding 300mbar were observed occasionally to last for extended periods. It is not known what role, if any, these high backpressures may have played in the turbo failure (and subsequent fire) after 2221 hours of operation. Because of the catalytic properties of the filter's wash coat, the increased emission of NO_2 was expected and observed. The system was robust and survived an accidental circumstance in which mud penetrated the discharge side of the filter.

Johnson-Matthey:

This DPF system was designed as a passive system with active electric regeneration as backup. It used a SiC wall flow filter. It was somewhat complex because of the need to meter the fuel-borne catalyst. The need for and subsequent use of an auxiliary electrical heater for regeneration turned out to be essential for the particular LHD on which the system was installed. This was due to the unconventional and highly variable duty cycle (exhaust temperatures were not reliably high enough to initiate passive regeneration) of LHD #820's use at Stobie Mine. The system had excellent soot filtration efficiency throughout the tests, and, as expected, no increase in NO_2 emissions was observed. After over 1000 hours one of the filter elements became slightly separated from its canister, but filtration efficiencies still were good. Only after another 900 hours did the separation increase to the point where filtration efficiency was compromised. The companion filter (dual exhaust system) operated well without incident for nearly 2400 hours. The electrical regeneration components showed less than desired reliability.

ECS/Combifilter:

This is an active DPF system using a SiC wall flow filter with integral electric heaters for off- duty regeneration. It showed excellent performance as long as operators were attentive to its regeneration. The first system installed on an LHD failed because of lack of necessary regeneration. Another system was installed on another LHD with significant communication with the vehicle operators, and this system performed well until the project's conclusion (over 2000 hours). The filter was robust when properly regenerated. The electrical regeneration system worked well.

Oberland-Mangold:

This was designed to be a passive DPF system using a fuel borne catalyst. The filter element used knitted glass fiber assembled into a cartridge several of which were packaged into a filter canister. This system was relatively complex due to the pumping system of the fuel-borne catalyst, and the performance of the system was a disappointment. The Stobie team had spent considerable resources to get the system properly installed. Two maintenance people from Stobie had gone to Germany for a week of intensive training at the Oberland-Mangold facility. Despite these efforts, the system showed undesirable soot emissions from the tailpipe right away and it had to be removed from further testing.

Arvin-Meritor

This is an active DPF system with a cordierite filter element. It employed an active exhaust manifold burner for regeneration. As it was the only in-situ burner equipped DPF system tested in the Stobie project, much time and effort were made by both Arvin-Meritor and Vale personnel to install it and educate Vale maintenance people about its operation. Stobie mechanics spent a week in Columbus, Indiana, to learn about the system. It was, therefore, very disappointing when this system failed to give good filtration efficiencies from the beginning of its service. The Stobie team concluded that the system was too complex and was not as fully developed as needed for this kind of field trial.

15.3 Specific conclusions for light duty vehicles

ECS/Combifilter

This is an active DPF system using a SiC wall flow filter with integral electric heaters for off- duty regeneration. This DPF system, sized for the tractor's engine, gave excellent soot removal efficiencies throughout the nearly three years of testing on a tractor used for personnel transportation within Stobie mine. NO_2 concentrations were slightly decreased downstream of the filter. The short regeneration time (60 minutes) by electrical heating fit nicely into the scheduled use of the vehicle. It was essential that good communication be established with prospective users of the vehicle because of the active attention these users had to have for regenerating the DPF after each shift. It was found that restricting the number of drivers to only a few led to more responsibility being taken by each of the drivers for the vehicle. With more drivers there was a tendency to "let the next guy take care of it," and this can lead to difficulties with the DPF. Given appropriate attention to active regeneration by the operators, this system is a good fit for light duty vehicles.

DCL Titan

This is an active DPF system using a SiC wall flow element. Regeneration was performed by removing the DPF and placing it into a special regeneration oven. Two DPFs were used alternatively on a single tractor. This DPF was very compact and was very easy to use, regenerate and service. The anticipated challenge associated with changing DPFs alternately was not realized due to the quick-disconnect flanges and ease of removing and installing DPFs.

Excellent soot filtration efficiencies were present throughout the nearly three years of operation of the DPF. The regeneration station worked well. No NO_2 increase was seen (nor expected) downstream of the DPF. The same comment about the need for operator attention to regeneration that was made above is applicable here as well and, as long as that occurs, this system is a good fit for light duty vehicles.

ECS/3M

This DPF system was only tested for eight months and showed marginal soot removal effectiveness. It was removed from the testing program because 3M announced they would cease production of the glass fiber filter medium. It is no longer a candidate for light duty vehicle service.

15.4 General recommendations

Several technical issues arose during the Stobie DPF testing program. These were solved, some quickly with little effort, and others with considerable time and effort. To help prevent others from encountering the same problems and struggling through them, the Stobie team offers the following recommendations to mines interested in either testing DPFs or installing them on existing on new diesel equipment.

(a) Making periodic exhaust gas and soot number measurements at the tailpipe of a vehicle using the ECOM analyzer are a very good way to determine the status of a DPF. These measurements are most effectively carried out by skilled mechanics during scheduled vehicle maintenance. It is relatively easy but imperative to include these procedures in the routine maintenance performed as part of the normal vehicle servicing.

(b) The use of data loggers prior to DPF installation and selection is essential for successful DPF operation; they are recommended for use when installing proven DPFs (unless they come from the manufacturer as an integral part of the DPF system being installed). When data loggers are needed for testing, then it is important to buy from a local supplier so that their maintenance and troubleshooting can be handled in a timely fashion. The specifications for the data loggers should not deviate much from those used in this study.

(c) While it is obvious that the DPFs must be sized and operated in coordination with the duty cycle and planned use of the diesel vehicle, it is less obvious, but very important, that close attention should be given to the design, specifications and installations of auxiliary equipment to the DPFs. Such equipment includes electrical circuits, fuses, heating elements, timers, air flow controllers associated with electrical regeneration. In other types of regeneration, such as fuel-borne catalysts and burner-assisted exhaust heating, the special equipment required needs attention to ensure that it meets Canadian standards for safety, that consumables can be purchased easily and that maintenance is straight-forward.

(d) Equipment suppliers must be contracted to have an on-going service commitment for their units.

(e) Heat wrapping of exhaust pipes (and the DPF where possible) was found to be effective in improving DPF performances.

(f) The use of welding gloves when handling DPFs or in plugging in units for electrical regeneration was found to be advantageous.

(g) The use of metal electrical connectors (instead of the supplied plastic connectors) was found to improve their ruggedness, resulting in less attention to breakage or shorting.

(h) Using shock absorbing mounts were found to be advantageous to the longevity of the installed DPFs.

(i) Mounting DPFs high enough on an LHD was found to be beneficial in limiting the amount of mud/water that can enter the bottom (often containing an electrical heater) of the housing. Sometimes electrical connections in these locations can become compromised. As an alternative to mounting the DPF higher, it is also possible to design and install a cover that does the job of both heat dissipation (when the heater is on) as well as protection. Another option is to redesign these DPFs so that the electrical heater is not carried with the filter canister, but can be quickly snapped into place when regeneration is needed.

(j) Care should be taken when installing the DPF and associated exhaust pipes to stay well away from fire suppression actuators located on the vehicle. The Stobie test had one incident in which an activator was initiated due to its close proximity to the new routing of the exhaust pipe.

(k) It was found beneficial to redesign electronic control modules (ECMs) on electronically-controlled engines so that an engine can be ramped down if excessive exhaust backpressure is detected.

(l) It was found beneficial to substitute the mine's compressed air supply for compressed air modules on DPF systems requiring air for regeneration. Air compressors and air pumps provided in the regeneration control units were found to require excessive maintenance. Attention should also be given to removing moisture from the mine air line. This can be done easily with conventional water separators.

(m) It was found necessary to adjust the air supply during regeneration on some units. Excessive air can cause excessive cooling with the result that combustion temperatures are not met or are not maintained long enough to accomplish regeneration. Originally set airflow criteria supplied with some units were found to need adjustment.

(n) Long exhaust pipes and additional bends are to be minimized for optimum performance.

References

American Conference of Governmental Industrial Hygienists. (1995). *TLV and BEI Booklet*. Cincinnati, OH: ACGIH.

Birch, E. and Cary. (1996). Elemental carbon-based method of occupational monitoring of particulate diesel emissions: Methodology and exposure issues. *Analyst, 121,* 1183-1190.

Bugarski, A.D., Schnakenberg Jr G.H., Noll J.D., Mischler S.E., Patts L.D., Hummer J.A. and Vanderslice S.E.. (2006a) Effectiveness of selected diesel particulate matter control technologies for underground mining applications—Isolated zone study, 2003. U.S. Department of Health and Human Services, DHHS (NIOSH) Publication No. 2006-126, Report of Investigations 9667. Centers for Disease Control and Prevention. Atlanta, GA, USA.

Bugarski, A.D., Schnakenberg Jr G.H., Noll J.D., Mischler S.E., Patts L.D. and Hummer J.A. (2006b). Effectiveness of selected diesel particulate matter control technologies for underground mining applications—Isolated zone study, 2004. U.S. Department of Health and Human Services, DHHS (NIOSH) Publication No. 2006-138, Report of Investigations 9668. Centers for Disease Control and Prevention. Atlanta, GA, USA.

Burtscher, H. (2005). Physical characterization of particulate emissions from diesel engines: a review. *J. Aerosol Science, 36* (7), 896-932.

Dainty, E.D., Mogan, J.P., Lawson, A., and Mitchell, E.W. (1985). The status of total diesel exhaust filter development for underground mines. Presented at the XXIst International Conference of Safety in Mines Research Institutes, Sydney, Australia.

Health Effects Institute's Diesel Working Group. (1995, April). Diesel exhaust: A critical analysis of emissions, exposure and health effects. Health Effects Institute.

Hews, C. and Rutherford, J.G. (1973). Trackless mining. Underground Diesel Seminar, Johannesburg, South Africa.

International Agency for Research on Cancer (IARC). (1989). Monograph on the Evaluation of Carcinogenic Risks to Humans, No. 46, Diesel and Gasoline Engine Exhausts and Some Nitroarenes. IARC: Lyons, France.

Kittlelson, D. (1998). Engines and nanoparticles: A Review. *J. Aerosol Science, 29* (5/6), 575- 588.

Maskery, D. (1978) Respirable combustible dust Inco method No. 1H011A. Inco Limited, Sudbury, Ontario, Canada,

McGinn, S. (2004). Final Report of Investigation: Noranda Inc. Brunswick mine diesel particulate filter field study. Diesel Emissions Evaluation Program, CAMIRO: Sudbury, Ontario, Canada. From http://www.deep.org

McKinnon, D.L. et al. (1989, September). Diesel particulate filter underground trial at Brunswick Mining and Smelting No. 12 Mine. SAE Paper 891846.

Mines Safety and Health Administration (MSHA). (2005). Diesel particulate matter exposure of underground metal and non-metal miners, Final Rule. Federal Register, Vol. 70 (107), 30CFR Part 57, 32868.

National Institute for Occupational Safety and Health (NIOSH). (1988, August) Carcinogenic effects of exposure to diesel exhaust. NIOSH Current Intelligence Bulletin 50. DHHS (NIOSH), Publication No. 88-116, Centers for Disease Control and Prevention. Atlanta, GA, USA.

National Institute for Occupational Safety and Health (NIOSH). (2003). Diesel Particulate Matter (as Elemental Carbon) 5040. *NIOSH Manual of analytical methods (NMAM), 4th edition.* DHHS (NIOSH) Publication 94-113 (August, 1994), 1st Supplement Publication 96-135, 2nd Supplement Publication 98-119, 3rd Supplement 2003-154. Schlecht, P.C. & O'Connor, P.F. (pfo1@cdc.gov), Eds.

Occupational Health and Safety Act – R.R.O 1990, Reg. 854, Mining and Mining Plants, Ontario, Canada (http://www.e-laws.gov.on.ca/html/regs/english/elaws_regs_900854_e.htm#BK9)

Rutherford, J.G. and Elliot, W.T. (1977). Monitoring the workroom environment: the Inco program. 46th annual MAPAQ meeting, Toronto, Ontario, Canada.

Schnakenberg, G., and A. Bugarski. (2002, August). Review of technology available to the underground mining industry for control of diesel emissions. DHHS (NIOSH) Publication 2002-154. NIOSH Information Circular 9462.Centers for Disease Control and Prevention. Atlanta, GA, USA. (http://www.cdc.gov/niosh/mining/pubs/pubreference/outputid28.htm)

VERT Filter List: Tested and approved particulate-trap systems for retrofitting diesel engines, edited by A. Mayer, (2004). Published by the Swiss Agency for the Environment, Forests, Landscape: Luzern, Switzerland.

VERT, Final Report, 29.2.2000, Available from SUVA (Swiss National Accident Insurance Organization) Luzern (http://www.suva.ch)

VERT Report: results of a 4 year European joint project: curtailing emissions of diesel engines in tunnel sites, A. Mayer. (1997, May). Report W11/12/97 VERT/SUVA/AUVA/TBG/BUWAL.

World Health Organization (WHO). (1996). Environmental Health Criterion 171: Diesel Fuel and Exhaust Emissions. World Health Organization: Geneva, Switzerland.

Additional references not specifically cited in the Report, but relevant to the Stobie project and to current state-of-the-art technologies.

Bugarski, A. D. and Schnakenberg, G. H. (2002). Evaluation of diesel particulate filter systems at Inco Stobie Mine. Proceedings of 8th Mining Diesel Emissions Conference, Markam, Ontario, October 28–31.

Cantrell, B. and Stachulak, J.S. (1996). Inco-University of Minnesota aerosol measurement comparisons. Presented at the Canadian Ad-hoc Diesel Committee Proceedings, Toronto, 1996

Current monitoring and control technologies-DPM/RCD and air quality monitoring in mines. ibid.

Conard, B.R; Stachulak, J.S. (2000, June). Underground evaluation of diesel particulate filter systems at Inco Stobie mine. Proceedings of the 6-th International Symposium on Ventilation for Contaminant Control, Helsinki Finland.

Schnakenberg, G.H., and Bugarski, A.D. (2004). Evaluation of diesel particulate filter systems at INCO's Stobie Mine - June 2004 Study. Presented at MDEC, Markham, Ontario, Canada. October 13-16. Proceedings of 10th Mining Diesel Emissions Conference (MDEC), Markham, Ontario, Canada, October13-16.

Stachulak, Jozef S, Hensel Volker.(2010., June). Successful application of DPF system at Vale Inco's Creighton mine. Proceedings of 13th United States/North American Mine Ventilation Symposium, Sudbury, Ontario, Canada.

Stachulak, J.S, Conard, B.R, Gangal, M.K. (2009, November). Experience and evaluation of innovative diesel particulate filter systems at Vale Inco. Proceedings of Ninth International Mine Ventilation Congress, New Delhi, India.

Stachulak, Jozef S. (2008, November). Impact of Stobie research on Vale Inco's international search to curtail diesel emission. Proceedings of 1st Global Forum in Mineral Technology at Vale, Belo Horizonte, Brazil.

Stachulak, J. S, Conard, B.R. (2008, June). Vale Inco's international search to curtail diesel emission. Proceedings of the 12th US/North American Ventilation Symposium, Reno, Nevada, USA.

Stachulak, J.S, Conard, B.R, Bugarski, A.D and Schnakenberg, G.H. (2006, June). DEEP project of diesel particulate filters at Inco's Stobie Mine. Proceedings of the 11th US/North American Ventilation Symposium, Pen State Univ. USA.

Stachulak, J. (2000 - 2007). DPF- Diesel Particulate Filter System Project. Proceedings of MDEC for 2000 – 2007.

Stachulak, J.S, Conard, B.R, Bugarski, A.D and Schnakenberg, G.H. (2005, June). Long term evaluation of diesel particulate filter systems at Inco's Stobie Mine. Proceedings of the International Mine Ventilation Congress, Brisbane, Australia.

Stachulak, J.S. (Various). DEEP-Sponsored Diesel Emission/DPF system. Workshops Proceedings: Marathon, Ontario, Sept 16, 2003; Val D'Or, Quebec, Oct 6, 2003; Saskatoon, Saskatchewan, Oct 19, 2003;Bathurst, N. B. May 4, 2004

Stachulak, J.S. (2003, March). Diesel emission control strategy. Proceedings of NIOSH Diesel Workshop, Salt Lake City, Utah, USA.

Stachulak, J.S. (2003, February & March). Inco diesel trap project. Proceedings of NIOSH Diesel Workshop, Cincinnati, Feb, 2003 Ohio and Salt Lake City, Utah, Mar, 2003

Stachulak, J. and Conard, B.R. (2001, June). Diesel emission control strategy: underground evaluation of particulate system at Inco's Stobie Mine. Proceedings of the 7th International Mine Ventilation Congress, Cracow, Poland.

Stachulak, Jozef S. and Conard, B.R. (1997). Diesel emissions control strategy at Inco. Presented at the 6th International Mine Ventilation Congress, Pittsburgh, USA.

Stachulak, J., Dainty, E.D., McPherson, Malcolm J. (1990, 1991). The phenomenon of dust deposition in exhaust ventilation shafts at Inco Mines. Presented at the International Conference on Occupational Health and Safety in the Mineral Industry, Pert, Western Australia, Sept 10 -14, 1990, and published in the *Journal of the mine Ventilation of South Africa*, Vol. 44, No. 11 pp183 - 195, 1991.